EIDESSTATTLICHE ERKLÄRUNG

Ich erkläre an Eides statt, dass ich die vorliegende Arbeit selbstständig verfasst, andere als die angegebenen Quellen/Hilfsmittel nicht benutzt, und die den benutzten Quellen wörtlich und inhaltlich entnommenen Stellen als solche kenntlich gemacht habe. Das in TUGRAZonline hochgeladene Textdokument ist mit der vorliegenden Dissertation identisch.

11. 11. 2015
Datum

Simone Strasser
Unterschrift

SIMONE STRASSER, DIPL.-ING. BSC

*Ligno*POLY

CHEMICAL MODIFICATIONS OF WHEAT STRAW LIGNIN

DOCTORAL THESIS
DISSERTATION

zur Erlangung des akademischen Grades
einer Doktorin der technischen Wissenschaften
eingereicht an der

Technischen Universität Graz

Betreuer
Assoc.Prof. Dipl.-Ing. Dr.techn. Christian Slugovc
Institut für chemische Technologie von Materialien

Graz, November 2015

TU Graz

ACKNOWLEDGEMENT

Herewith I would like to express my profound gratitude to all who helped me completing this work and who accompanied me during my doctoral studies.

First I want to thank Christian Slugovc for the great supervision during my work on the doctoral thesis and for sharing his excellent knowledge with me. I highly appreciate the support in various issues, the countless helpful pieces of advice and enlightening discussions. Furthermore, I am very grateful for the opportunity to attend international conferences and meetings.

I also want to thank Ortwin Ertl from Annikki GmbH for interesting discussions and insights in the working environment apart from university. My sincere thanks go to Alexander Dybov for the cooperation during project periods and for providing lignin samples as well as GPC analyses.

I would like to acknowledge the extremely valuable work of Alexander Eibel with respect to lignin. I owe particular thanks to Birgit Ehmann who excellently assisted and supported me in many hours of laboratory work. I also want to thank Isabel Hanghofer and Angelina Eder for their skillful synthetic work related to the substances presented in Chapter 5. Moreover, I express my thanks to Kathrin Bohnemann for experienced laboratory work.

My gratitude goes to Petra Kaschnitz for recording special NMR measurements and for many useful and instructive conversations in terms of NMR spectroscopy. In addition, I want to thank Josephine Hobisch for STA and GPC measurements, Monika Filzwieser for elemental analyses as well as Adriana Kovalcik for DMA analyses.

Of course I want to thank all my colleagues at ICTM for assisting me in every need, for spending many pleasurable hours together and for an inspiring working environment day by day. Special thanks go to the members of the Slugovc group for supporting and helping me in many questions and for sharing data and experience. Apart from that, I want to particularly emphasize the 'writing room colleagues' who made the daily work routine funny and pleasant. I am especially greatful to Katharina Gallas for uncounted amusing hours and always understanding at a glance how I feel. I would like to extend very warm thanks to Christina Wappl for being a supportive, patient, sympathetic but also critical associate.

I express my heartfelt gratitude to Fabian for being at my side all the time, for his loving attention, for his support, for giving me the feeling of security and for keeping up good spirits during stressful, challenging times.

My sincere thank is owed to my family for being with me and for their faith and trust in me. Furthermore I want to particularly thank Fabian's family for their support and participation in my concerns.

This work deals with different approaches towards higher value adding to lignin. The highly complex biopolymer lignin consists of phenylpropanoid units connected via different interunit linkages. A wheat straw lignin from an *Organosolv* process was characterized using quantitative ^{31}P NMR and ^{13}C-^1H HSQC NMR as well as ATR-FTIR spectroscopy, elemental analysis, simultaneous thermal analysis and size exclusion chromatography. In order to obtain organosoluble lignin derivatives, different possible modification methods of the lignin hydroxyl groups (aliphatic as well as phenolic) were tested.

First of all, the hydroxyl groups were esterified with fatty acid chlorides in the presence of triethylamine as a base. More than half of the hydroxyl groups could be modified using this protocol. The obtained ligninesters are well soluble in non-polar organic media. Yet the separation of remaining free fatty acids constitutes a challenge.

The ligninesters were then used as soluble filler or reactive component in polydicyclopentadiene (PDCPD), a crosslinked thermoset produced by ring opening metathesis polymerization (ROMP). It was found, that the ligninesters predominantly act as a plasticizer, downgrading the mechanical characteristics of neat PDCPD.

In another approach, bicomponent thin films with trimethylsilyl cellulose (TMSC) were produced by spin coating solutions containing ligninester and TMSC in different ratios on silica wafers. Homogeneous and smooth films could only be reached with palmitoyl functionalized lignin. The morphology and wettability of these blend films were investigated by atomic force microscopy and static water contact angle measurements. Additionally, the adsorption of proteins on the composite films was studied.

Second, D,L-lactide and ε-caprolactone were grafted onto lignin (functioning as a macroinitiator) via ring opening polymerization (ROP), mediated by *N*-centered nucleophiles. The length of the graft chains is adjustable by the ratio of lignin and ROP monomer. The reaction proceeds at elevated temperatures without any solvent and thus this protocol closer meets the criteria of *green* synthesis compared to the esterification with fatty acid chlorides. The resulting ligningrafts are well soluble in chloroform. A drawback of this protocol is the homopolymer formation as side product.

Amongst several other modification reactions, the oxa-Michael addition of divinyl sulfone and various alcohols was extensively investigated as a promising model reaction for future lignin functionalization. The main advantage of this method over the esterification is the introduction of a non-hydrolyzable ether bond. In some preliminary attempts, polymeric networks were obtained upon reacting lignin as a polyol with divinyl sulfone.

ZUSAMMENFASSUNG

Diese Arbeit befasst sich mit verschiedenen Ansätzen zur Wertsteigerung von Lignin. Das hochkomplexe Biopolymer Lignin besteht aus Phenylpropanoid-Einheiten, die über verschiedene Verknüpfungen verbunden sind. Das *Organosolv*-Weizenstrohlignin wurde mittels ^{31}P NMR- und ^{13}C-^{1}H HSQC NMR-, sowie ATR-FTIR-Spektroskopie, Elementaranalyse, simultaner thermischer Analyse und Gelpermeationschromatographie charakterisiert. Mit dem Ziel, in organischen Medien lösliche Ligninderivate zu erhalten, wurden verschiedene Modifizierungsmethoden der im Lignin vorhandenen Hydroxygruppen (sowohl aliphatische als auch phenolische) getestet.

Als Erstes wurden die Hydroxygruppen in Anwesenheit von Triethylamin als Base mit Fettsäurechloriden verestert. Anhand dieses Protokolls konnten mehr als die Hälfte der im Lignin vorhandenen Hydroxygruppen modifiziert werden. Die erhaltenen Ligninester sind gut in apolaren organischen Medien löslich. Die Entfernung der im Produkt verbleibenden freien Fettsäuren stellen jedoch ein Problem dar.

Die Ligninester wurden als löslicher Füllstoff sowie als reaktive Komponente in Polydicyclopentadien (PDCPD), einem vernetzten, mittels ringöffnender Metathese-polymerisation (ROMP) hergestellten Duromer, eingesetzt. Es wurde festgestellt, dass die Ligninester hauptsächlich als Weichmacher wirken und die mechanischen Eigenschaften von PDCPD erheblich verschlechtern.

In einem weiteren Ansatz wurden Zweikomponenten-Dünnschichtfilme aus Ligninestern und Trimethylsilylcellulose (TMSC) in verschiedenen Verhältnissen mittels Spin-Coating auf Siliciumwafern hergestellt. Homogene Filme konnten nur mit palmitoyl-funktionalisiertem Lignin erreicht werden. Die Morphologie und Benetzbarkeit dieser Zweikomponenten-Filme wurden mittels Rasterkraftmikroskopie und Kontaktwinkel-messungen untersucht. Außerdem wurde die unspezifische Adsorption von Proteinen an den Oberflächen untersucht.

Als Zweites wurden D,L-Lactid und ε-Caprolacton mittels ringöffnender Polymerisation (ROP) mithilfe von *N*-zentrierten Nucleophilen an Lignin (agiert als Macroinitiator) „gegraftet". Die Länge des Polyester-„Grafts" ist über das Verhältnis von Lignin zu ROP-Monomer einstellbar. Die Reaktion verläuft bei höheren Temperaturen ohne Lösungsmittel und erfüllt somit die Ansprüche einer *grünen* Synthese eher als die Veresterung mit Fettsäurechloriden. Die entstehenden Ligningrafts sind gut in Chloroform löslich. Nachteil dieser Methode ist die Bildung von Homopolymeren als Nebenprodukt.

Neben einigen neuen Modifizierungsmethoden wurde im Speziellen die oxa-Michael-Addition von Divinylsulfon und verschiedenen Alkoholen als vielversprechende Modellreaktion für zukünftige Ligninmodifizierungen eingehend untersucht. Hauptvorteil der Methode gegenüber der Veresterung ist die Einführung einer nicht hydrolysierbaren Etherbindung. In Vorversuchen wurden zudem polymere Materialien aus der Reaktion von Lignin als Polyol und Divinylsulfon erhalten.

The following work was accomplished within two FFG funded projects on the application of lignin or lignin derivatives, respectively, in polymeric materials. The consortium of both projects consists of two academic research groups and one corporate partner located in Graz, Austria:

- Annikki GmbH (Mag. Ortwin Ertl, Dr. Alexander Dybov)
- Institute of Applied Synthesic Chemistry, TU Vienna (Prof. Simone Knaus)
- Institute for Chemistry and Technology of Materials, TU Graz (Prof. Christian Slugovc)

The work was based on previous studies in the framework of a *FFG*-funded project (*Biomimetischer Lignocellulose-Aufschluss,* 830107/14233SCK/SAI), where modifications of low molecular weight wheat straw lignin have already been performed. The focus of this follow-up project (*Lignin-basierende Polymermaterialen*, 838900) is the substitution of petrochemical components in polymers by using tailor-made fractions of the biogenic compound lignin without losing typical material properties. By covalent cross-linking of lignin with thermosets, e.g. polyurethanes or polydicyclopentadiene, innovative materials featuring high market potential should be developed.

The project comprises several work packages (WPs) whereas most of the herein presented work is located in one of them: WP2 aimed at the development of chemical modification methods for the lignins obtained from WP1 (Annikki GmbH). Thus, a cheap and sustainable esterification protocol should be established and the obtained lignin derivatives should be used as component in duroplastic polymers.

This contribution is composed of several parts that are all linked through the motivation of higher value adding to lignin. The main focus was laid on the modification of lignin to obtain a cheap, tailored material for the application in polymeric materials. Ideally, it should be suitable as comonomer for the ring opening metathesis polymerization of dicyclopentadiene. We tried to meet the requirements by esterification of the hydroxyl groups present in lignin and searched for a *green* method that is feasible for industrial processes.

After a general introduction about the biopolymer lignin and different pulping processes, current approaches to utilize unmodified lignins will be described. Chapter 2 is about lignin characterization and common methods are delineated exemplarily based on *Annikki* wheat straw lignin. After that, an overview of modification methods and the state of the art regarding the application of lignin derivatives is given. The next part deals with the modification of *Annikki* lignin, predominantely by esterification. The characteristics as well as the utilization of the obtained ligninesters are described in chapters 3 and 4. Experimental details are given at the end of each section, together with standard operating procedures (SOPs).

Chapter 5 describes novel approaches for the modification of lignin apart from the esterification, where a hydrolysable moiety is introduced. Thus, an excursus in the Oxa-Michael addition reaction as well as in the according polymerization method is given.

CONTENT

1 INTRODUCTION

1.1 GENERAL ASPECTS

Currently there is a rethink with regard to the depletion of fossil fuels, and many attempts are made to reasonably use waste or byproducts of existing processes and substitute valuable resources. Renewable resources are also applied to a greater extent, but during processing also byproducts accrue which could be used. First and foremost, easily accessible and simply processible resources are used at the moment, such as fatty acids or ethanol obtained from various plants. Unfortunately, the utilization of such renewable resources is often concurring with foodstuff or agricultural areas.[1] This is not the case for lignin. Lignin is not only a waste product accruing in paper and pulp industries, but can also be selectively extracted from agricultural waste products like straw or other annual plants. Thus it concurs neither direct nor indirect with foodstuff, which makes lignin an exceptionally valuable resource.

Lignin is, apart from cellulose and fats, the second most abundant natural material and is incorporated in the cell wall of all vascular plants. The lignin content varies between 15 and 40 %, depending on nature, age and habitat of the plant. Lignin acts as sealing compound and thus plays a key role for the water transport through the cell wall. Plants are reinforced by the adhesive properties of lignin, providing strength and stability. Furthermore, lignin protects the plant against microorganisms. The highly complex structure of lignin features a variety of functional groups, complicating the accurate characterization as well as the processing of the natural resource. A number of pulping processes is already available, yielding lignins with diverse characteristics.

The possibility to use the abundantly available natural resource lignin for the manufacturing of polymer materials has been investigated for decades. The necessity to substitute fossil resources by renewable materials and sustainable concepts recently intensified the ongoing research in this field. Taking part in the rethinking process in economy and industry, all aspects have to be taken into account and not only the fact that a resource is renewable itself. Hence, it is an important task of the research and science community not only to recognize materials of high potential, but also develop processing methods to obtain valuable resources and products. *Green* materials are readily available yet *green* processing to the final application is still demanded.

1.2 LIGNIN

Lignin (latin *lignum* 'wood') is the second most abundant naturally occurring substance apart from cellulose and natural oils. It is found as one of the three main components of vascular plants besides cellulose and hemicelluloses. The lignin content in woody stems of aborescent hardwoods and softwoods varies between 15 and 40 %, depending on the species, tissue, growth conditions and age of the plant. In general, however, softwoods feature the highest lignin content over hardwoods and annual plants (Table 1).

Lignin meets three essential tasks in the wooden tissue: First, it acts as water sealant and controls the transport of water, nutritients and metabolites through the conducting xylem. The hydrophobic lignin is able to decrease the permeation of water across the cell walls comprising cellulose fibers and amorphous hemicelluloses. Second, lignin confers rigidity to the cell walls. Together with hemicelluloses it functions as permanent glue between cells and thus gives the woody stems their well-known strength and impact resistance. Third, lignin protects plants against biological attacks by hampering the penetration of destructive enzymes. Lignin is largely concentrated between adjacent cell walls and at the cell corners (~ 70 %). The content across the secondary cell walls is notedly lower (~ 20 %), but nevertheless most lignin is found herein as the secondary cell wall occupies the largest volume in the wood cells.[2,3]

Table 1. Lignin content of selected plants.[4]

Plant species	Lignin content / %
Softwoods	
Normal wood	25–33
Compression wood	34–41
Norway spruce	27
Monterey pine	27
Scots pine	26
Hardwoods	
Temperature zone	18–25
Tropical zone	20–32
Tension wood	16–20
European birch	19
European beech	24
American red oak	22
Annual plants	
Bamboo	20–24
Bagasse	18–20
Wheat straw	17–18
Rape straw	19–22
Flax shives	22

Lignin is a complex biopolymer built up by chemical polymerization of three main structural moieties, p-coumaryl (4-hydroxycinnamyl)-, coniferyl (4-hydroxy-3-methoxycinnamyl)- and sinapyl (3,5-dimethoxy-4-hydroxycinnamyl)-alcohols via enzymatically generated radicals. Incorporated into the lignin polymer, these monolignols produce the p-hydroxyphenyl (H), guiaiacyl (G) and syringyl (S) phenylpropanoid lignin units which differ in the degree of methoxy substitution at the phenyl ring (Figure 1). The monolignols are synthesized via phenylpropanoid and monolignol-specific biosynthetic routes from phenylalanine, which is derived from the shikimate biosynthesis, a seven stage metabolic route used by plants.[5,6]

Oxidases or peroxidases initiate the polymerization of the phenylpropanoid units, whereas the detailed mechanism still remains undisclosed. A combination of free radicals, generated by enzymatic dehydrogenation is considered as the key reaction, either under enzymatic control or in a random combinatorial mechanism. The lignin subunits are connected via several types of carbon-carbon or carbon-oxygen bonds, whereas the most prevalent interunit linkage is an ether bond between a p-hydroxy moiety and the β-carbon of a propenyl group (β-O-4'). The presence of little amounts of α-O-4' linkages is also reported, but it is very likely that those are formed during pulping and don't exist in native lignin. Other characteristic interunit linkages, albeit less commonly occurring, are β-1' (1,2-diarylpropane), β-β (resinols), 5-5' (biphenyl), 4-O-5' (diaryl ethers) and β-5' (phenylcoumarans) bonds (Figure 2). Lignin comprises hydrophilic as well as hydrophobic moieties, but due to the three-dimensional chemical structure, the hydrophobic character is more pronounced in the original appearance.[1,4,7]
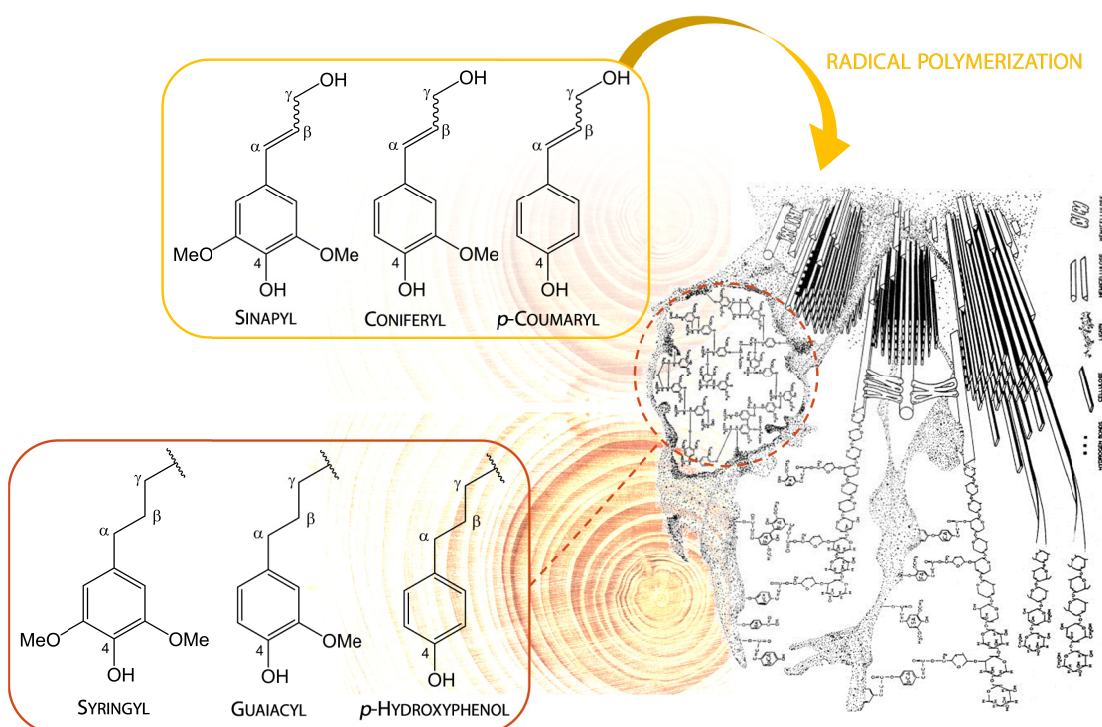
Figure 1. Main structural moieties of Lignin.
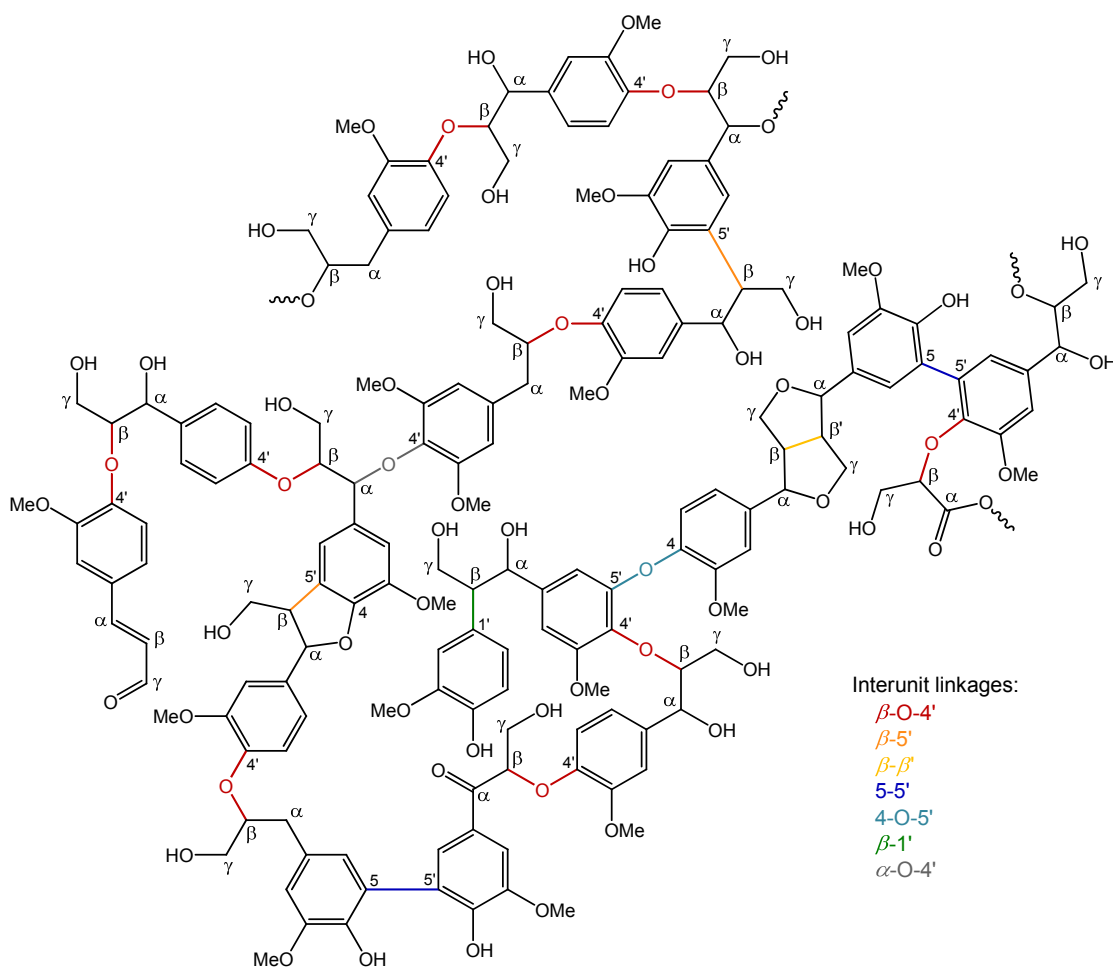
Figure 2. Schematic section of lignin structure (softwood).[4]

The composition of the three main building blocks of lignin strongly depends on the botanical origin. Softwoods comprise mainly guaiacyl units (G-lignins), whereas hardwoods consist of guaiacyl and syringyl units (GS-lignins). Annual plants (e.g. straw, grasses) feature a greatly varying composition of all three main building blocks and can contain up to 33 % *p*-hydroxyphenyl units (GSH lignins). Correspondingly, hardwood lignins exhibit the highest, and grass lignins the lowest amount of methoxy groups. The degree of substitution not only affects the constitution of lignin, but also determines the level of crosslinking and as a consequence the rigidity of the structure. Softwood lignin is more condensed than hardwood lignin, indicated by increased amounts of 5,5'-biphenyl linkages. [1,3,4]

The isolation and characterization of lignin in its native form is not feasible due to its thight connection to cellulose and hemicellulose in the secondary cell walls. Thus, the extraction of lignin from lignocellulosic materials is always accompanied with the degradation of the biopolymer. Accordingly, structure and properties of the isolated lignin strongly depend on the isolation conditions.[3] An overview of the most important pulping methods and the characteristics of the obtained lignins is given in section 1.2.1.

Lignin is available as (waste) product from various pulping processes of plant feed stocks and hence a valuable renewable resource.[1] Despite its widespread availability, high-value industrial applications of lignin are still hardly established.[8] The reason for this is the highly complex structure of lignin which varies according to type, origin and age of the used plants as well as to the pulping process. Thus the accurate characterization and further processing of this valuable natural resource are rather challenging.

Considering the depletion of fossil fuels and the need to find a substitute, the high-value adding of lignin is obvious as it is an extant natural resource. The most important advantages of lignin are the unrestricted cheap availability and the non-competition with foodstuffs or agricultural areas.

1.2.1 LIGNIN PULPING PROCESSES

The use of wood for the production of pulp for paper manufacturing was initiated in the 1840s with the development of mechanichal pulping by F. G. Keller. Based on these early works, nowadays lignin is extracted from lignocellulosic materials in various pulping processes which are briefly depicted in the following (Table 2). Lignin pulping goes hand in hand with the degradation of the biopolymer, yielding fragments of lower molecular weights featuring significantly altered physicochemical properties compared to native lignin in its initial surrounding. Aside from the origin of lignin, the pulping process sustainably influences the characteristics of the technical lignins obtained, whereas most delignification processes proceed either acid or base catalyzed.[1] Besides the few dominating pulping processes (*Kraft*, *Sulfite* and *Soda* process), a variety of pulping methods exists which don't have any industrial impact.

Generally, it can be distinguished between sulfur-containing and sulfur-free pulps or lignins respectively.[4] Characteristic parameters of lignins obtained from various pulping processes are listed in Table 3.

Table 2. Overview of lignin pulping processes.[4]

Process	Chemicals	Raw materials	Product
sulfur-containing			
Kraft (Sulfate) process	NaOH, Na_2S	soft- and hardwoods	*Kraft* lignin
Sulfite pulping	$Ca(HSO_3)_2$ or $Mg(HSO_3)_2$	Spruce, beech, eucalyptus	lignosulfonates
Ionic liquids	alkyl- and arylsulfonates, imidazoles etc.	wood, biomass	lignin
sulfur free			
Soda process	NaOH, anthraquinone	annual plants (non-wood)	*Soda* lignin
Steam explosion	H_2O	wood, biomass	lignin
Solvent pulping	MeOH, EtOH, H_2O, phenol, monoethanolamine, acids etc.	annual plants (non-wood)	*Organosolv* lignin
Annikki process	EtOH or *i*PrOH, H_2O, NaOH	annual plants, preferred wheat straw	*Annikki* lignin

KRAFT PULPING

The *Kraft* (or *Sulfate*) process was developed by C. F. Dahl in 1884 to obtain cellulose from wood.[9] The term *Kraft* refers to the same german word meaning strength and thus expresses the superiority of the obtained *Kraft* pulps in comparison to *Sulfite* pulps. This process, further enhanced in the course of time, using sodium hydroxide and sodium sulfide is still the leading technical pulping process and hence produces the greatest quantities of lignin.[3] Delignification proceeds under strong alkaline conditions at elevated temperatures (150–170 °C) whereas the ether linkages in lignin are cleaved.[3] The main conversion of the *Kraft* process is the transfer of phenols into quinonemethide groups, which are able to add hydrogen sulfide ions in α position, yielding benzylthiolate anions (Scheme 1). The latter abstract the β-phenolate anion in a displacement reaction, generating moieties with free phenolic groups which can again undergo the same reaction path as long as their α-carbon features a hydroxyl or non-cyclic ether group. The sulfur can be partly split off from the episulfide moiety at elevated reaction temperatures (~ 170 °C or higher), enabling the formation of carbon-carbon bonds between lignin units (referred to as 'condensation reaction'). These condensation products are hard to cleave in further process steps. Furthermore, the hydrogen sulfide ions can induce demethylation reactions, yielding methyl mercaptan which causes unpleasant odors.[3]

Scheme 1. Mechanism of *Kraft* pulping.[3]
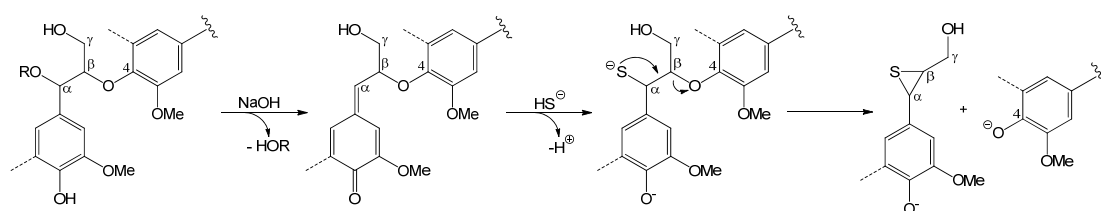
Lignin is usually recovered from the remaining alkaline solution after pulping, the so-called 'black liquor', by precipitation after acidification with sulfuric acid. The obtained hydrophobic *Kraft* lignin features aliphatic thiol groups, responsible for the high sulfur content (1–2 wt%). The latter is the major limitation for high-tech industrial application and hence *Kraft* lignin is mainly utilized for energy generation, such as in the recently developed *Lignoboost*[10] process.[1]

SULFITE PULPING

The second most important pulping process which was developed even before the *Kraft* process in the 1860s, is the *Sulfite* pulping process.[11] The former leading pulping technology includes the reaction of a metal sulfite and sulfur dioxide.[1] Wood is reacted with calcium (pH 1–2) or magnesium sulfite (pH 3–5) at elevated temperatures (125–150 °C) for several hours. During this treatment in acidic media, three main reactions occur simultaneously: sulfonation, hydrolysis and condensation. Both, α- and β-ether linkages are cleaved upon this delignification process, which proceeds probably via the quinone methide intermediate (cp. *Kraft* pulping, Scheme 1), but possibly also via nucleophilic substitution.[1] Lignin becomes

watersoluble due to the introduction of hydrophilic sulfonic acid groups in α position. Benzyl alcohol and ether groups present in lignin are transferred into benzylium ions in the *sulfurous acid* (pH 1–1.6) and in the *acid sulfite* (pH 1.8–3.1) process. These benzylium ions preferably add nucleophilic sulfite ions, but may also undergo condensation reactions (Scheme 2). The generated carbocation reacts with another lignin fragment, whereas a C-C bond is formed with an electron-rich carbon atom of the aromatic ring. The condensation degree decreases with increasing pH wich is the case in the *bisulfite* (pH 4.5) or the *bisulfite-sulfite* (pH 7) process. β-O-4' Alkyl-aryl ethers should be rather stable under acidic conditions. There are also *Sulfite* processes which proceed in neutral or alkaline media, where β-O-4' linkages are probably cleaved.[3,4] The lignosulfonates from the process are necessarily purified in several steps, such as the fermentation of residual carbohydrates to ethanol and the filtration of remaining metal ions. The obtained lignosulfonates are highly crosslinked and feature a sulfur content of approximately 5 wt%. Due to the low pK_a (≤ 2) value of sulfonate groups, lignosulfonates are mostly watersoluble. In general, less cleavage of side chains occurs applying acid catalysis.[3]

Scheme 2. Mechanism of *Sulfite* pulping.[3]
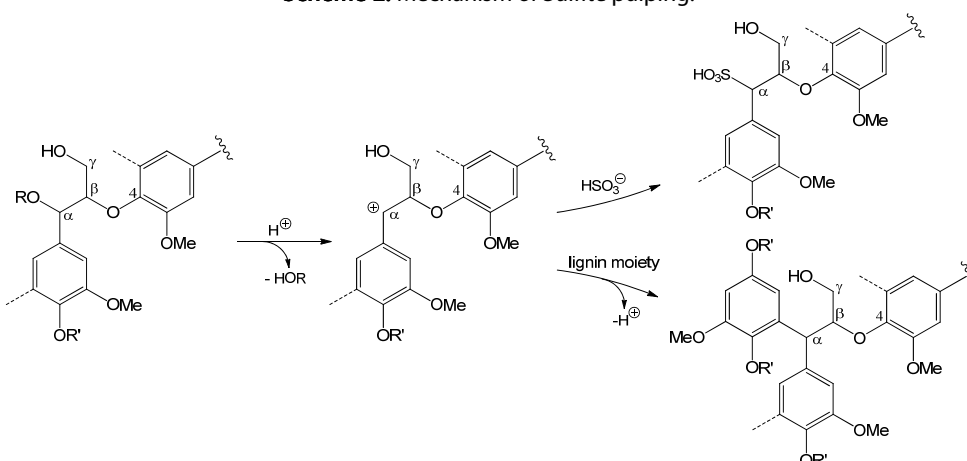
SODA PROCESS

This alkaline hydrolysis of wood was already invented 1845 and is thus the eldest chemical pulping method.[12] In this process, lignin is extracted with sodium hydroxide and the obtained *Soda* lignin is sulfur-free and exhibits a low hemicellulose share. During the last decades, the method was further developed and is nowadays mainly applied to recover lignin from non-wood sources like bagasse or wheat straw for instance. Primarily α-aryl ether linkages in phenolic lignin units are efficiently degraded upon this alkali treatment. To enhance the cleavage of β-O-4 bonds, the redox catalyst system anthrahydroquinone/anthraquinone can be added.[3] A specific procedure for the isolation of lignin from the black liquor (accruing in the production of cellulose from annual plants in small paper factories) is the *Lignin Precipitation System* (LPS®) technology developed by Granit RD SA.[13] The approach provides an electrolytically supported solution to simultaneously recover the corrosive soda and isolate high quality lignin.[14] The sulfur-free lignin is commercially available under the trade name *Protobind*. *Soda* lignin has great potential for an application in high value products as it

contains no sulfur and is comparatively chemically unmodified, apart from a higher amount of carboxylic acids due to oxidation of aliphatic hydroxyl groups.[1,4]

ORGANOSOLV PROCESSES

A variety of sulfur-free pulping methods applying organic solvents was developed during the last decades and was established as *Organosolv* processes. The initial process was developed as milder alternative compared to *Kraft* pulping in the 1960.[15] Aqueous mixtures of methanol or ethanol are widely used (both with and without catalysts), whereas Alcell®[16] and Organocell®[17] are familiar names. There are also processes using formic or acetic acid (e.g. Acetosolv,®[18] Formacell®[19]) as well as other pulping chemicals like phenol or monoethanolamine. However, no organosolv process is hitherto industrially applied, partly due to high corrosion of the plant equipment and low quality pulp. Nevertheless, the obtained hydrophobic lignins exhibit lower ash and carbohydrate contents, lower molecular weights and feature a greater ability to be derivatized.[1,3,4]

STEAM EXPLOSION

This physical pulping method was patented in 1926 by Mason et al. to pretreat wood or biomass.[20] During the steam explosion process, biomass is pressurized with hot water steam (180–290 °C at 10–35 bar) for several minutes. Subsequently, the so-called explosive decompression converts the solid starting material into a fibrous pulp. Cellulose, other carbohydrates and lignin are partly hydrolyzed autocatalytically upon the release of acetic acid from hemicelluloses. Besides this, homolytic cleavage of aryl ether linkages can also occur, as well as the recondensation of lignin moieties. Thus, the lignins obtained from steam explosion feature higher molecular weights than *Kraft*, *Sulfite* or *Organosolv* lignins.[3] Lignin becomes partly water-soluble during this procedure and the rest is extracted with sodium hydroxide solution. With respect to a *green* processing of biomass, this method has a clear advantage as no chemicals except H_2O at elevated temperatures and pressures are used.

IONIC LIQUIDS

One of the more recent developments is the utilization of ionic liquids in biomass fractionation. Ionic liquids generally comprise a large asymmetric organic cation and a smaller anion. They exhibit insignificantly small vapour pressures as well as a wide liquidus temperature range. Cellulose for instance is dissolved with alkylimidazolium upon breakup of the strong intramolecular hydrogen bonds between individual fibers due to coordinaton of small hydrogen acceptors (e.g. Cl^-) to the hydroxyl groups. For the extraction of lignin from sugarcane bagasse, a mixture of 1-ethyl-3-methylimidazolium (cation) and alkylbenzene-sulfonates (anion) at high temperatures (170–190 °C) is utilized. The cleavage of ether bonds in lignin can be facilitated by the addition of xylenesulfonates: sodium ions coordinate to the ether oxygen and thus the carbonium ion character of the ether carbon atom is increased and thus more susceptible to the nucleophilic attack by arylsulfonates of the ionic liquid. Lignins are isolated from the solution upon precipitation whereas the ionic liquid is recycled. The obtained lignins feature molecular weights around 2200 $g \cdot mol^{-1}$, approximately 1.5 wt% sulfur, and a very low amount of hemicelluloses (< 0.1 wt%). A method for the complete

dissolution of wood using *N*-methylimidazole and dimethylsulfoxide followed by precipitation of lignin in a dioxane / water mixture was published by Sixta et al. (2007).[21] The fractionation of biomass using ionic liquids is industrially not established until now. However, many efforts are made within this field and sulfur-free ionic liquids are currently under investigation.[1,4]

ANNIKKI PROCESS

Annikki GmbH developed a low temperature pulping method, whereas deficiencies of established processes are prevented to a great extent. The *Annikki* method can be classified as alkaline *Organosolv* process. Dry lignocellulosic material from annual plants is treated with an aqueous alkaline solution (NaOH, pH 10–14) of an alcohol, preferably isopropanol (30–40 vol%), at comparatively low temperatures (50–70 °C) for several hours. Lignin is dissolved under these conditions, whereas cellulose and hemicellulose can be separated as solids from the pulping solution. The method is characterized by a decoupling of hemicellulose and lignin degradation, which leads to a higher selectivity and economic efficiency of the process. The use of alcohol allows for a lignin degradation of > 80 %, whereas hemicelluloses are simultaneously degraded up to a maximum of 10 %. The yield of lignin, or polysaccharides respectively, can be specifically tuned by variation of the process parameters and composition of the pulping solution.[22]

SUMMARY

Summarizing the described pulping processes, it can be said that the obtained amount of lignin is generally lower in acidic processes due to the coupled degradation of lignin and hemicellulose. High degradation rates of lignin can mainly be achieved using alkaline methods. Usually, sodium hydroxide is applied in high concentrations at elevated temperatures, whereby the degradation of lignin and hemicellulose goes also hand in hand. The obtained lignins are of low quality due to condensation reactions upon the harsh pulping conditions. This may also be the case for most *Organosolv* pulping processes. Ideally, a biorefinery process should exhibit high lignin and low hemicellulose degradation at the same time, require less chemicals and yield a preferably native lignin.

Table 3. Characteristic values of the main technical lignins obtained from various pulping processes.[1,4,23]

Lignin type	M_n / g·mol^{-1}	PDI	T_g / °C	Sulfur / wt%	Solubility
Kraft (Sulfate)	1000–3000	2–4	124–174	1–2.5	alkali, organic solvents
Sulfite	15000–50000	6–8	~130	1.25–2.5	water
Soda	800–6000	9–10	~140	0	alkali
Organosolv	500–5000	2–3	90–110	0	organic solvents
Annikki[a]	1300–1500	4–6	~114	0	alkali, organic solvents

[a] *Gesamtlignin; 'organic solvents' refers to DMF or DMSO here.*

The global lignin market has grown continuously in the last decade, but most of the accruing lignin is used for the energy production to recover process chemicals. Due to this reason, a very low amount of the produced lignins is materially utilized (< 5 %). Sulfur-containing lignins from *Sulfite* or *Kraft* pulping are commercially exploited in amounts of 1 000 000 or 100 000 tons per year respectively. Sulfur-free lignins are not yet commercially available in quanitities greater than 5 000 tons per year. However, the utilization of lignins which accrue during biomass conversion to ethanol, is a growing sector.[24] Currently there are many efforts to develop biorefinery concepts, where lignin is a separate, valuable product stream of high quality, simultaneously approaching the native structure of the biopolymer.

Technical lignins are either applied in unmodified polymeric form (polymer component, feedstock for chemicals etc.) or in converted form (e.g. carbon fibers).[4] More specific examples for the present utilization of unmodified lignin will be given in the following section (1.3).

1.3 State of the Art

Current research activities are to a great extend focused on the characterization, fractionation and purification of lignin. Although lignin is a comparatively old, and intensively investigated subject of research, its structure and features are not yet completely elucidated. In numerous works, lignins from different feed stocks (various annual plants, hardwood or softwood) and pulping processes (cp. section 1.2.1) are analyzed and compared, as major differences concerning structure and properties arise upon the various isolation methods. A detailed understanding of lignin structure and properties is the key for most higher value added applications and facilitates the handling and further manufacturing of the biopolymer.

Lignins, as they are recovered from the respective pulping process, can be applied, apart from energy generation, as component in thermoplastics and thermosets or as surfactant for instance. The major obstacles to overcome for a reasonable utilization of lignins in polymeric materials are the compatibility and the heat deformability.[24] The surface energy is a crucial parameter for the compatibility of two components. Non-ionic lignins feature a surface energy of approximately 70 mJ·m^{-2} with a dispersive contribution of ~45 mJ·m^{-2}. Thus, the quality of an interface including lignin will strongly depend on the structure of the second component. Non-polar polymers, e.g. polyolefins, will cause a relatively high interfacial energy and hence poor adhesion. Polymers featuring polar functionalities, like polyesters, provide interfaces with much higher compatibility and thus strong adhesion. Modifications of lignin are often necessary to address sufficient compatibility or specific issues, however, the synthesis and utilization of lignin derivatives will be discussed in section 3.1. One major point to be stated here is, that polymers containing renewable materials always compete with existing petroleum based low-price products. Thus, the incorporation of lignin should preferably not be accompanied by inefficient, costly transformations. Ideally, lignins can be introduced as obtained from the delignification process.

This reviewing chapter about applications of non-modified lignins is mainly oriented according to a book chapter written by M. N. Belgacem and A. Gandini.[25] Of course the following section will provide just a superficial, and certainly not complete overview of the manifold research and developments concerning lignin.

The use of lignin as additive, filler or composite material for thermoplasts, duromers and elastomers is widely spread, whereas the mechanical properties are influenced both positively and negatively.[1,26,27,28,29] Lignin, incorporated as additive in polymers is able to appear as stabilizing agent against oxidation, UV-radiation or thermal stress, but opposite it can also facilitate biodegradation.[1,30] Lignin is already utilized in most diverse fields, whereas new applications and possibilities are continuously emerging.

The application of lignin as component in duromers such as formaldehyde resins, polyurethanes and epoxy resins was investigated by numerous research groups.[24,31,32]

Lignin is a natural analog to phenol formaldehyde (PF) resins and thus, the application as phenol substituent is one of the most straightforward utilizations of lignin and has been explored very intensely.[33] PF resins are industrially of great importance, whereas the toxicity of the main components phenol and formaldehyde is the key motivation to replace these substances. As numerous commercial products are related with PF resins, namely particle boards, plywood or fiberboards, an application as renewable adhesive therefor is very promising and lucrative. A major drawback of lignin is the limited reactivity of phenolic OH groups due to steric hindrance caused by higher substitution. This issue can be addressed by methylolation of lignin and adding diisocyanates as co-reagents. Thus, more than 50 wt% of methylolated lignins were introduced into the resins.[34] Sodium lignosulfonate was applied in small amounts (~ 5 wt%) into PF-resol resins and was found to promote condensation reactions.[35] Although many efforts have been done to replace phenol by lignin, a complete substitution is hitherto not possible due to a weakening of the material characteristics with increasing lignin proportion. The use of *Kraft* or *Sulfite* lignins results in disturbing odor development during processing. Hence these lignins are inappropriate for the production of chipboard panels. Additionally, the reactivity of the available lignins with formaldehyde is considerably lower compared to phenol, resulting in prolonged processing times.[36] Due to this reasons only few procedures became marketable although decade-long research.

The incorporation of lignin into urea formaldehyde (UF) resins has also been investigated intensively. Particleboards filled with ~ 10 wt% lignosulfonates were successfully applied in industry. Due to the hydrophobic contribution of lignin, the resins featured an improved water resistance.[34]

Lignins are mostly modified prior to incorporation into polyurethane (PU) products, but nevertheless there are also mixtures with unmodified lignins reported. Feldman and coworkers introduced 5–20 wt% *Kraft* lignin in PU-ureas and showed that lignin was covalently bound into the network.[37] Other approaches tried to enhance the reactivity of lignin by the use of a diol as third monomer, ideally dissolving lignin. Thus, PU foams using *Kraft* lignin (~ 40 wt%), hexamethylene isocyanate and oligocaprolactone were prepared.[38] Later studies showed that *Alcell* lignin exhibited a notedly higher reactivity compared to *Kraft* lignin. The work was also extended to *Organosolv* lignins and it was found that the solvent used for delignification plays a key role for the subsequent reactivity of lignin as it influences the hydroxyl content.[39] Hatakeyama et al. investigated different lignins in formulations of oligoether diols and multi-functional aromatic isocyanates. A broad variety of PUs, such as foams, sheets or gels, is accessible using the hydroxyl groups of lignins as active sites.[40] Straw lignin from a steam explosion process was tested as macromonomer for the synthesis of PUs with diisocyanates and in some cases ethylene glycol as comonomer. Unusual was the much lower amount of polymers obtained with regard to the applied monomers.[41] Recently, a study of PU caotings consisting of a polyisocyanate and unmodified, but extracted *Kraft* lignin in different weight ratios was published. Characterization of the materials revealed higher thermal stability, better film forming ability and increased hydrophobic character compared

to samples without a crosslinked precursor. Furthermore, the coatings exhibited high adhesion on various surfaces such as glass, wood or metal.[42]

Not many reports are published dealing with the use of unmodified lignins associated with epoxy resins. Mainly due to compatibility reasons, lignins are modified prior to their utilization in epoxy resins. A straightforward 'drop in' approach was demonstrated with the production of printed circuit boards.[43] Solubility problems due to high ionic contents arose using *Kraft* and *Soda* lignins, whereas *Organosolv* lignins could be used directly. Life cycle assessment (LCA) of the resins revealed considerable energy savings when lignin was incorporated.[24]

Organosolv lignins are used as partial replacement of phenolic powder resins, which are applied as binders in the fabrication of friction products.[44] Resins prepared with 20 wt% lignin featured comparable, or even better characteristics compared to pure phenolic resins. Thus, the concept was industrially applied in the production of automotive brake pads and moldings. The stability of the friction coefficient upon temperature changes as well as the wear behavior were improved by lignin implementation. Another successful commercial utilization is the substitution of phenolic binders by *Organosolv* lignins in amounts of 5–25 wt% for oriented strand boards.[24,45]

THERMOPLASTICS & ELASTOMERS

Lignin is admixed to polyolefins and rubbers in order to stabilize the polymers against degradation, caused by various external influences such as UV radiation, thermal stress or free radicals. The antioxidant character of lignin due to its phenolic structure is well known, and the stabilizing effect, even added in small percentages, against photo-oxidation processes was established. The latter was shown for polypropylene (PP) and natural rubber.[46,47] Increasing lignin content in PP also provides higher temperature resistance. Inhibited UV degradation was reported for polyethylene (PE) with lignin as additive.[48] *Kraft* lignin was also implemented into light weight polyolefins (e.g. PE, PP) as reinforcing agent. It was found, that the affinity to the polyolefin matrix improves with increasing molecular weight of lignin. However, chemical modifications were suggested to improve the compatibility and enhance the mechanical properties.[49]

Introduced into styrene-butadiene rubber in significant amounts, the phenolic biopolymer acts as reinforcing filler.[50] Lignosulfonates can also be applied as dope additive for polyaniline. The versatile conducting high-tech material is known under the trade name LIGNO-PANI™.[51]

There is a growing demand for plastics from renewable resources. Thus, the development of thermoplastic materials based on starch and lignin was investigated. Admixed lignin should reduce the hydrophilic character of starch without losing thermomechanical properties. Although blends were mostly heterogeneous, the morphology was not affected. The overall compatibility could be enhanced by moisture, and if lignins with lower molecular weights were applied. Lignosulfonates showed the tightest interaction with starch, whereas more hydrophobic lignins were able to improve the water resistance.[52] Other examples for renewable thermoplasts are ARBOFORM®,[53] ARBOFILL® and ARBOBLEND®. The

composite materials developed by Tecnaro GmbH, Germany, are based on cellulose, lignin as well as other biopolymers.[54]

Lignin is known to exhibit strong inter- and intramolecular hydrogen bonds, which are partly responsible for the weak solubility characteristics.[55] However, this property can also be useful, namely in the preparation of homogeneous blends with hydrophilic polymers such as poly(ethylene oxide) (PEO). It was shown, that *Kraft* as well as *Organosolv* lignins dissolve in high molecular weight PEO due to intermolecular hydrogen bond formation between the phenolic OH groups of lignin and the ether oxygen atoms of PEO. The mixtures were found to be homogeneous within the whole composition range, which is remarkable for blends with unmodified lignins.[56,57] Homogeneous thermoplastic materials were obtained using poly(vinyl acetate) and *Kraft* lignin, by only adding plasticizers.[58] Mixtures with poly(vinyl alcohol) were, however, unexpectedly heterogeneous.[25,59] Lignin is compounded as additive with other polar thermoplasts such as polyamides, poly(lactic acid) (PLA), polycaprolactone (PCL) or polyhydroxybutyrate (PHB) to a share of 60 wt%, whereas not only costs are reduced, but also the thermal and mechanical behavior is improved.[4,60]

DISPERSANTS

Lignin in its original form is often applied where polyelectrolytes or surface-active substances are required, namely as dispersant or emulsifier.[4] *Soda* lignins recovered by the already mentioned LPS® method of Granit RD SA, were found to exhibit dispersant properties as well as bacteriostatic and biocidal activity.[24] A formulation to inhibit the growth of microbial populations in industrial water circuits, e.g. like paper machine recirculating waters, was developed by the Austrian company Bioconsult GmbH für Biotechnologie.[61]

Lignosulfonates were shown to improve the wettability of hydrophobic powders.[62] The results revealed that sodium lignosulfonates with higher molecular weights and less sulfone groups exhibited a higher surface activity. Applied to difenoconazole, a fungicidal triazol, a reverse trend was observed and thus it was found that the distribution of lignin molecules at the solid / liquid interface, depending on the molecular structure, was the key factor.

Particles of *Alcell* lignin were incorporated into a series of viscous commercial products and their effect on the rheological properties was studied. Noticable improvements concerning the tack and misting behavior were found upon lignin addition to printing inks, varnishes and paints.[63]

CONSTRUCTION MATERIALS

Lignosulfonates (usually calcium or sodium salts) are used as concrete admixtures, which accounts for the major utilization of these particular lignins, especially in China and Japan.[64] Lignosulfonates as additives for concrete should introduce numerous enhancing effects into one of the most important construction materials. Thus, e.g. the crack resistance[65] can be increased and already amounts of 0.1−0.3 wt% lignosulfonate are able to retard the setting[3] of concrete. The growing interest in this field suggests the rapidly increasing consumption of lignins for this purpose within the next years.

Another similar application is the use of lignin as road binder or asphalt additive, serving various functions. Examples include lignin-based emulsifiers,[66,67] bitumen compositions[68], or

fibers which increase the water stability[69] and similar. A significant market for crude lignosulfonate liquors, is the application as dust controlling agent to stabilize insurfaced roads.[3]

AGRICULTURE

Studies indicate the chemical stabilization of organic nitrogen in soil by residues of phenolic lignin in anaerobic agroecosystems. Thus, lignin is attractive to be applied as fertilizer.[70] Lignin can also be admixed to nutritient media which are utilized in the restoring of vegetation.[71] Another important application is as a binder ($\leq$ 4 wt%) in feed pellets for animals to increase the durability and abrasive resistance.[3] By contrast, water-soluble lignosulfonates were shown to ideally disperse pesticide formulations, depending on the content of sulfonic groups.[72]

FOOD & COSMETICS

Lignin is of high interest in bio-based food packaging because of its antioxidant activity, caused by the presence of sterically hindered phenolic hydroxyl groups. The addition of lignin to poly(lactic acid) resulted in maintained mechanical as well as barrier properties at increased antioxidant activity.[73] The incorporation of lignin in latex- or starch-based coatings displayed a high oxygen consumption rate as well as an enhanced water stability. Hence these materials would be recommended for the packaging of high-moisture foodstuff.[74]

Due to its highly antioxidant character, lignin is attractive to be applied in cosmetic formulations as free radical scavenger. Moreover, lignin was shown to be completely harmless for skin and eyes.[75] Lignin is also able to increase the antibacterial character of cosmetic products.[76] Very lately, it was found that lignin, already when added in small percentages (2 wt%), features outstanding properties as UV absorbant in broad-spectrum sunscreens.[77]

CARBON FIBERS

Carbon fibers were synthesized in several steps from lignin, extracted from black liquor using the *Lignoboost* technology, by stabilization, carbonization and in some cases also graphitization of a carbon containing fiber (Innventia, Sweden).[78] Activated carbon fibers (ACFs) with varying lignin contents (8–20 wt%) were synthesized by melt spinning and pyrolysis of lignin-phenol-formaldehyde (LPF) resins. Lignin was found to be the determining factor regarding to the thermal properties and the pore size of the LPF resin und thus of the ACFs. It was found that ACFs containing 14 wt% lignin exhibit enhanced pore structures and adsorption properties.[79]

ENERGY PRODUCTION

Recently, efforts were focused on the production of 'drop-in' fuels by degradation of lignin to low molecular weight compounds (C6-C12), similar to the cracking of petroleum. Compared to bio-ethanol, lignin derived fuels exhibit a higher energy content. Thus, waste lignin from large-scale biorefineries has the potential to replace a large part of petroleum in transportation.[80]

Lignin is also increasingly involved in energy producing devices and substances apart from the simple combustion. Thus, the fabrication of battery components from lignin is reported. Carbonized lignin exhibits a disordered nano-crystalline microstructure and is utilized as free-standing electrodes in lithium ion batteries.[81,82] Also high energy density supercapacitors were produced from lignin derived activated carbon fibers.[83]

Besides this, lignin is also used as component in mixed polymeric elctrodes. Lignin undergoes redox processes at a given electrochemical potential by the conversion of phenolic units into quinone structures. Thus, it can be applied as redox active material in electrodes, whereby the capacity was increased and the relaxation time shortened.[84]

Char, produced from pyrolysis of biomass, can be pelletized with different binders. Among other renewable resources such as starch for instance, lignin can be used as binder. Pellets compressed together with lignin exhibit a high elastic modulus as well as a good bonding behavior.[85]

The hydrothermal carbonization of lignin waste yielded activated carbons featuring an attractive microporosity.[86] The obtained lignin-derived hydrochars exhibited outstanding rates of CO_2 and hydrogen uptake and are thus a promising material in terms of energy storage.
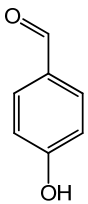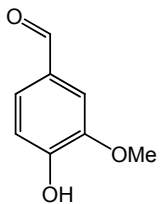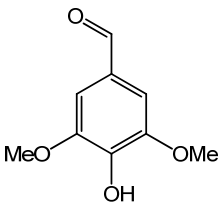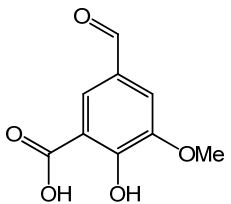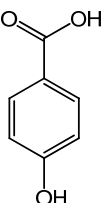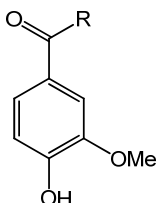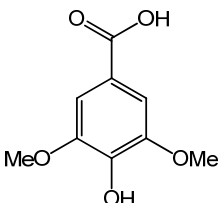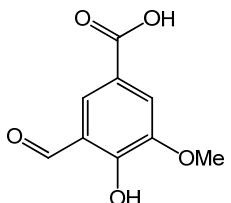
CHEMICALS

Lignin is the unique natural resource containing aromatic units. Thus, the selective depolymerization of the biopolymer and the subsequent production of phenolic monomers or fine chemicals is obvious.[87] But there are many challenges to overcome when converting lignin into value-added aromatic products. As lignin interunit linkages can be considered as very stable, their cleavage requires extraordinary (bio)chemistry. This concern is not easily implemented due to the weak solubility of almost all lignins. Another challenging issue is the heterogeneous structure of the biopolymer, additionally varying upon lignin source and the applied delignification method. Perhaps the major problem in conventional catalyzed depolymerization processes is the competing repolymerization, or recondensation, of lignin fragments.[88]

The oxidation of lignin is one approach to obtain various phenolic molecules (Table 4). The yield of outcoming small-size molecules depends on the oxidant and if a catalyst is applied. Copper(II) or cobalt(II) are able to catalyze the complex conversion and nitrobenzene, metallic oxides, air or oxygen are mostly used as oxidants. The process for the production of vanillin (4-hydroxy-3-methoxybenzaldehyde) from lignosulfonates was already patented in 1945.[89] Vanillin is not only used as flavoring agent, but also as chemical feedstock in pharmaceutical industries and is still the primarily utilized fine chemical derived from lignin.[90] The Norwegian company Borregaard LignoTech has been producing the valuable fine chemical for 50 years now.

Very recently, a reductive fractionation of lignocellulosic materials into and a lignin oil and a carbohydrate pulp was developed. The phenolic mono- and dimers are well-suited precursers for the production of chemicals and the carbohydrate fraction can be converted into sugar polyols in high yields (89 %).[91]

Table 4. Structures of aromatic compounds accessible via lignin oxidation.[23]

p-hydroxy-benzaldehyde	vanillin	syringic aldehyde	5-carboxyvanillin
p-hydroxy-benzoic acid	R = OH: vanillic acid R = Me: acetovanillone	syringic acid	5-formyl vanillic acid

The targeted depolymerization of lignin to fine chemicals is currently investigated using aluminum / platinum catalysts.[92] The amount of β-O-4 alkyl-aryl linkages was found to be the key factor regarding both, the nature and yield of the obtained lignin monomers.

A very promising approach towards the degradation of lignin into valuable aromatic monomers, or fine chemicals respectively, is via enzymes. Naturally, microbial metabolic pathways are responsible for the accumulation of small-sized molecules like vanillin. A detailed review of different enzyme activities concerning lignin digestion is given by Bugg and Rahmanpour.[88]

1.4 OBJECTIVE & MOTIVATION

This contribution is located within a small, but essential part of a whole biorefinery concept, where biomass is transformed into three valuable product streams, namely cellulose, hemicellulose and lignin. Scheme 3 illustrates the production and further manufacturing of lignin from agricultural waste products like wheat straw. Currently, the products are extracted from different feed stocks via pulping processes where mostly cellulose for paper fabrication is the main product. The enormous potential of cellulose was already recognized and thus the polysaccharide is increasingly applied as enhancing nano fibers in various composite materials for instance. Hemicelluloses are either degraded to the corresponding monosaccharides and other fine chemicals, or utilized as film-forming materials and coatings in food packaging.[93]

Aim of the project was the establishment of lignin in higher value added applications and to gain distance from *low profit-* and *low tech*-applications such as combustible, filler or precipitation agent. One approach is the degradation of lignin to fine chemicals, as already established for the production of vanillin.[90] Alternatively, the application possibilities of lignin can be significantly extended after appropriate modification. Thus, lignin should be modified in a sustainable, environmentally friendly and economical procedure. If necessary, an extraction step prior to derivatization could be performed, using furfural derivatives, accruing during the pulping process. The outcoming lignin derivatives should be implemented into various polymer materials. Thus, the value of lignin should be increased through finding a proper processing and application of the natural resource.

An attractive solution to address these requirements is the use of lignin as comonomer. One approach is the modification of the hydroxyl groups present in lignin to increase the solubility in non-polar media on one hand, and to introduce tailored functionalities on the other hand. Hence a covalent anchoring in the polymeric network should be feasible and thus a clear distinction to the use as filling material is given.

Scheme 3. Biorefinery concept for the value-added utilization of straw.
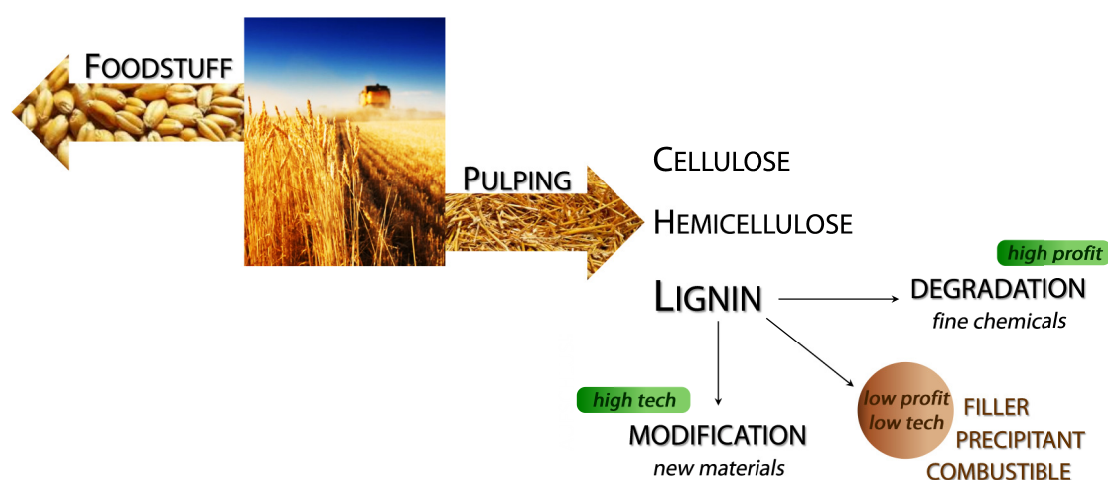
Polydicyclopentadiene (PDCPD) was selected as duroplastic material for the incorporation of modified lignins. PDCPD is a well known and established thermoset with outstanding mechanical properties. Appropriate lignin derivatives may have the capability to enhance the material characteristics of the thermoset besides the *ecological footprint*. Furthermore, the incorporation of lignin or lignin derivatives in PDCPD is a novel and hitherto unexplored approach. Especially copolymers of the petrol chemistry by-product dicyclopentadiene (DCPD) have the potential to replace, for instance, the more expensive epoxy resins in numerous applications. In contrast to epoxy resins PDCPD provides some considerable benefits. As DCPD is a waste product of petrol industry (C_5 fraction), it is available cheap and in large-scale. After distillation of the monomer, the production of the polymer via ring opening metathesis polymerization (ROMP) is feasible in a single reaction step, while the synthesis of epoxy resins requires many reaction steps.[94] Thus the short processing and curing time accelerates and improves the industrial manufacturing significantly. PDCPD gains outstanding mechanical properties with simultaneously lower density and hence less weight. Additionally the thermoset exhibits superior resistance against environmental impacts.[95]

The work was aimed at the synthesis of tailored lignin derivatives by a simple and *green* method. Inspired by numerous published works dealing with lignin modification, the esterification of lignin hydroxyl groups was investigated extensively. On one hand with carboxylic acid chlorides and on the other hand with cyclic esters via ring opening polymerization (ROP). Preferentially lignin should be functionalized with renewable resources, such as fatty acids or lactide for instance.

To address the demands for an utilization as ROMP comonomer, lignin derivatives should exhibit unsaturated substituents to ensure covalent incorporation. Moreover, good solubility in nonpolar media is required. Unsaturated long-chain fatty acids, e.g. oleic acid, should fulfill both prerequisites. Thus, a new material mostly consisting of renewable resources should be developed.

The studies within the framework of the FFG-funded project *Lignin-basierende Polymermaterialen* (no. 838900) were focused on the optimization of already existing methods for the modification of lignin, and of the other part on the development of new, innovative applications. To obtain a *green*, sustainable material out of biomass, the procedure has also to be *green*. Often this core aspect falls into oblivion. Thus, the environmental idea as well as the industrial feasibility were always a crucial parameter within this work.

For this work, Annikki GmbH Graz, provided eight different samples of wheat straw lignin. Thereof five were delivered right after the pulping process without any further purification step, in the following referred to as *Gesamtlignin* (batches GL1-GL5). Low molecular weight lignin (NML) was obtained after an extra fractionionation step of *Gesamtlignin* after pulping. L_HT (GL6) was prepared at higher temperature and additionally fractionated give a tetrahydrofuran-soluble proportion (L_THF (GL6)).The obtained lignin samples were used as received, apart from drying under vacuum.

This chapter will give an overview of the common methods applied for lignin characterization on the basis of a representative sample. The most important values for further modifications (hydroxyl number, molecular weight and dispersity) of all used lignin batches are listed in Table 15.

2.1 NMR SPECTROSCOPY

Lignin and synthesized lignin derivatives were characterized using different NMR methods. For a more accurate picture of the lignin, one- and two-dimensional NMR methods are utilized to determine the functionalities present in the lignin as well as the interunit linkages. In combination with other analysis techniques, NMR experiments provide enough information to characterize lignin and its modifications sufficiently.

2.1.1 ^{31}P NMR SPECTROSCOPY

Phosphorous (^{31}P) NMR spectroscopy for the determination of lignin hydroxyl groups was already established in the 90s by Argyropoulos and coworkers.[96] As there is no phosphorous available in lignin naturally, all hydroxyl groups as well as carboxylic acids and aldehyde groups have to be phosphitylated with 2-chloro-4,4,5,5-tetramethyl-1,3,2-dioxaphospholane (TMDP) (Scheme 4).
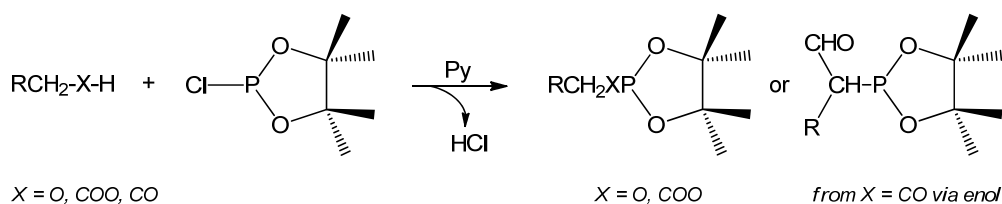
Scheme 4. Derivatization of hydroxyl containing compounds and aldehydes with TMDP.[97]

The samples for quantitative ^{31}P NMR measurements are prepared according to literature.[96] Approximately 30 mg of the lignin sample are dissolved in 100 μL dry DMF / Py (v:v, 1:1) and 100 μL of the internal standard (IS) solution are added. The IS-solution contains of 400 mg cyclohexanol and 50 mg relaxing agent (chromium(III) acetylacetonate) in 10 mL of dry pyridine. 100 μL of the phosphitylating reagent TMDP are mixed with 400 μL CDCl₃ and

added to the dissolved sample. The mixture is stirred for 2 minutes at room temperature und immediately subjected to the NMR spectrometer. ^{31}P NMR measurements were performed on a Varian Unity INOVA 500 MHz (^{1}H 499.894 MHz, ^{31}P 202.32 MHz) FT NMR instrument with a ^{1}H-^{19}F / ^{15}N-^{31}P 5 mm Switchable Probe, using at least 256 scans with inverse gated decoupling and a delay time of 25 s to accumulate spectra. The obtained spectra are referenced to phosphitylated cyclohexanol as internal standard with a ^{31}P chemical shift δ of 145.2 ppm. Spectra can also be referred to the reaction product of TMDP with H_2O which appears at 132.2 ppm. The corresponding resonances of phosphitylated lignin hydroxyl groups appear in the ^{31}P NMR spectrum between 130 and 150 ppm (Figure 3) and can be analyzed quantitatively if a defined quantity of internal standard is added. The content of the different hydroxyl groups can be determined in mmol·g^{-1} applying equations (1) and (2) to the corresponding integral values in the ^{31}P NMR spectrum.[96]

$$[OH] = SF \cdot \frac{A(OH)}{m(sample) \cdot D} \quad (1)$$

$$SF = \frac{V(IS) \cdot [IS] \cdot Purity(IS)}{M(IS)} \cdot 1000 \quad (2)$$

[OH]	hydroxyl content / mmol·g^{-1}
SF	standard factor / mmol
A(OH)	peak area (integral value)
m(sample)	sample weight / g
D	dry content (1 for dry sample)
V(IS)	volume of IS solution / mL
[IS]	concentration of IS in IS solution / g·mL^{-1}
Purity(IS)	0.99 for 99 %
M(IS)	molecular weight of IS / g·mol^{-1}
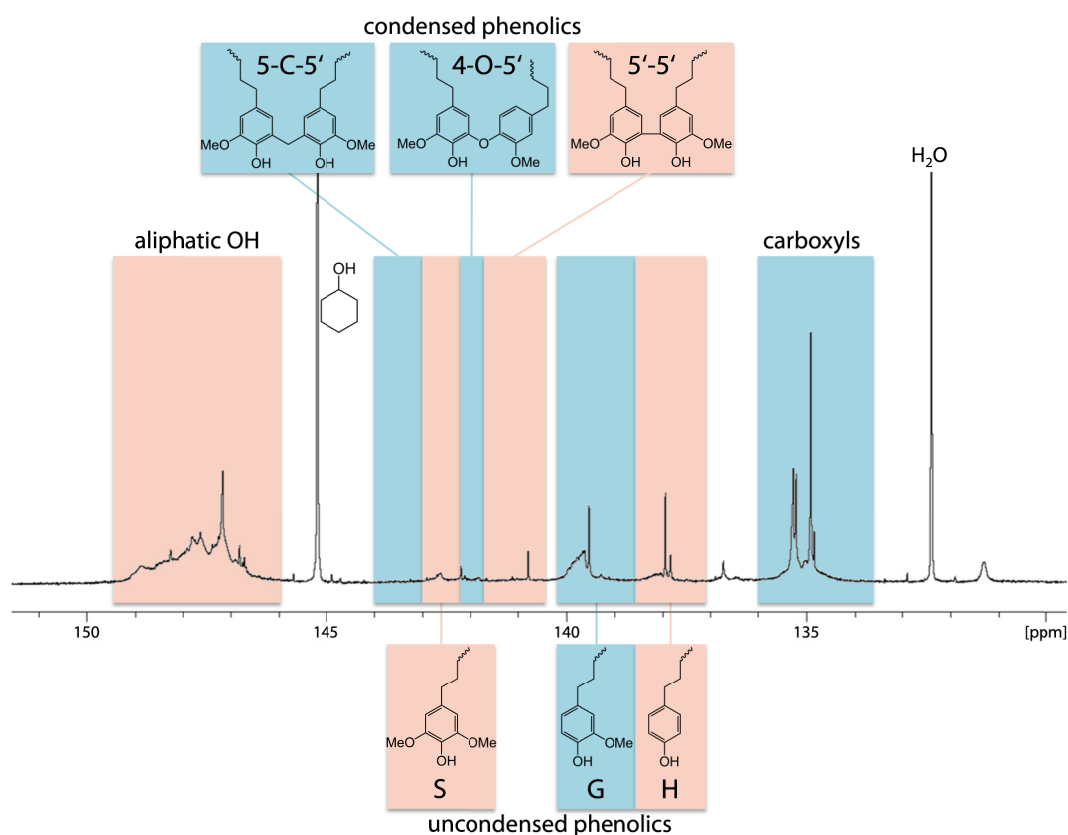
Figure 3. ^{31}P NMR spectrum of phosphitylated Annikki lignin (GL2) (25 °C, 200 MHz, CDCl$_3$).

The results of a quantitative ^{31}P NMR spectroscopy of GL2 are listed in Table 5. The according spectrum is shown in in Figure 3, with assigned integration regions for the different hydroxyl and functional groups.

Table 5. Content of different functionalities in GL2 determined via ^{31}P NMR quantitative analysis.

Functional group	Content in GL2 / mmol·g^{-1}
Total hydroxyls	4.32
Aliphatic OH	3.35
Total phenolics	0.97
Total uncondensed phenolics	0.86
Syringyl-OH	0.05
Guaiacyl-OH	0.56
p-Hydroxy-phenyl-OH	0.24
S / G / H ratio (phenol-terminated)	1.0 / 10.5 / 4.5
Total condensed phenolics	0.11
5-C-5′ diphenyl-methane	0.02
4-O-5′ diaryl ether	0.04
5-5′ diphenyl	0.05
Carboxyls	1.21

2.1.2 2D ^{13}C-^{1}H HSQC NMR Spectroscopy

Heteronuclear single quantum coherence nuclear magnetic resonance (HSQC NMR) was utilized to identify the structural moieties as well as the interunit linkages in lignin. The two-dimensional ^{13}C-^{1}H HSQC NMR measurement provides detailed information about the various monomeric units and can also be evaluated semi-quantitatively. Numerous comprehensive studies have been published in the last years, revealing continually new structural elements present in lignin.[98]

50 mg dry lignin samples dissolved in DMSO-d_6 were added to standard 5 mm glass NMR tubes. Spectra were acquired at 35 °C on a Varian Unity INOVA 500 MHz (^{1}H 499.894 MHz, ^{13}C 125.687 MHz) FT NMR instrument with a ^{1}H {^{15}N-^{31}P} 5 mm PFG Indirect Detection Probe using a standard adiabatic gradient Varian pulse sequence implementation (gHSQCAD). The phase-sensitive HSQC spectra were conducted with an acquisition time of 150 ms with an F2 spectral width of 7998 Hz (16 ppm) in 2400 data points using 128 transients for each of 512 t1 increments of the F1 spectral width of 26393 Hz (210 ppm). Dummy scans (32) were used to establish equilibrium conditions at the start of the experiment. A coupling constant ($^1J_{CH}$) of 146 Hz was used and ^{13}C-decoupling during acquisition was performed by WALTZ40 composite pulse from the high-power output-decoupling channel.

For semi-quantitative analysis the 2D correlation peaks were integrated and compared using MestReNova NMR processing software. The DMSO solvent peak was used as an internal reference for all samples (δ_C 39.51 and δ_H 2.50 ppm). The ^{13}C-^{1}H correlation signals were assigned according to several studies about the structural changes in lignin during hydrothermal,[98,99] autohydrolytic[100] or other degrading and cleaving[101] conditions which have been published recently. Primarily the contributions on wheat straw lignin of Ralph and coworkers have been consulted for the interpretation of 2D spectra.[98,101] Figure 4 displays the complete ^{13}C-^{1}H HSQC NMR spectrum of *Annikki Gesamtlignin* (GL2) with assigned spectral regions of interest. The highlighted areas include the aliphatic lignin sidechain region (δ_C/δ_H 50–90/2.5–6.0), where also non-anomeric polysaccharide correlations are found, the polysaccharide anomeric region (δ_C/δ_H 90–110/4.0–6.0) and the aromatic structures (δ_C/δ_H 90–150/6.0–7.7). Signals in the unlabeled areas of the spectrum derive from aliphatic long chain molecules (fatty acids, both saturated and unsaturated) present in the lignin sample. The correlations found in the aliphatic and aromatic regions will be discussed in detail within this chapter and a color-coded plot is shown in Figure 5. The correlation signals with according assignments are listed in Table 6 and the corresponding structures are depicted in Figure 6.
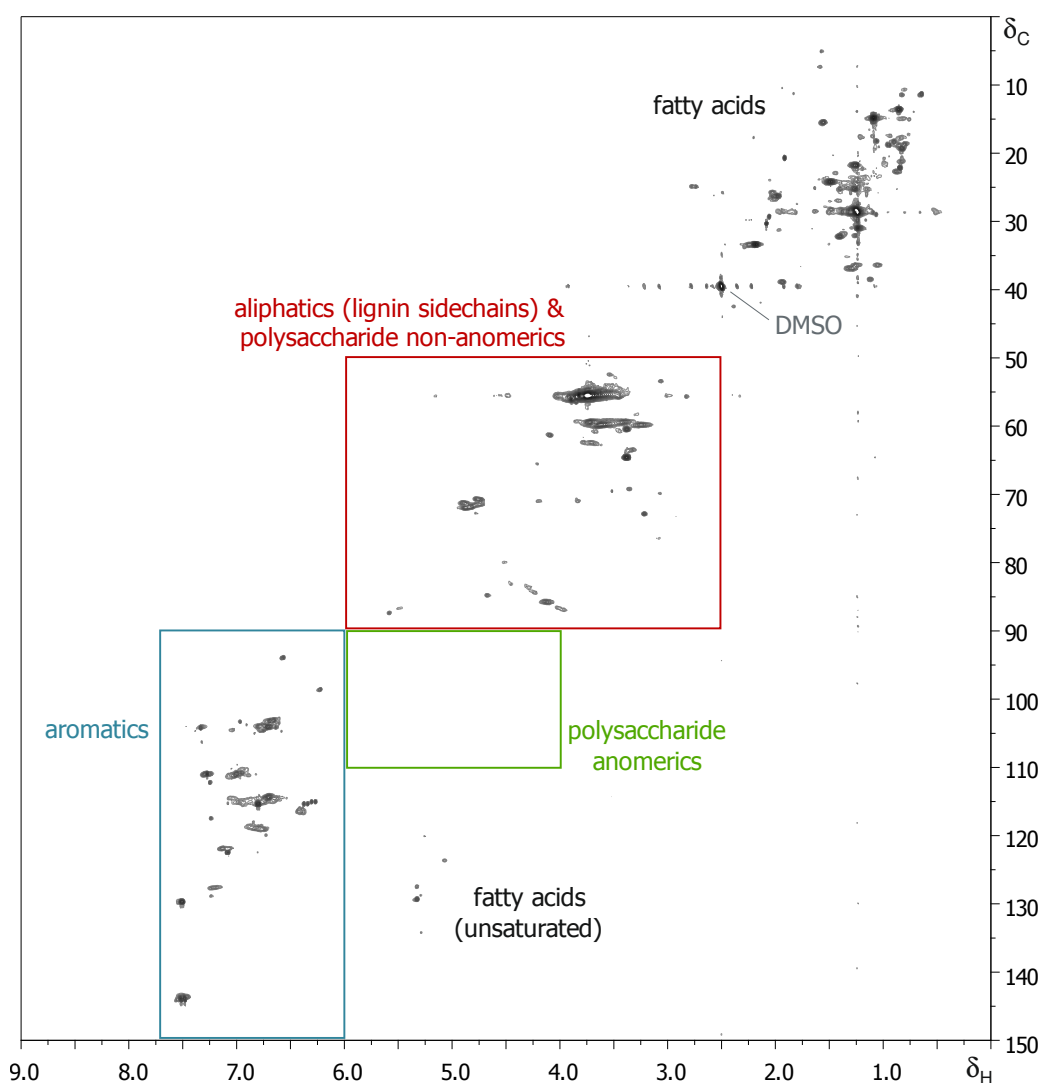
Figure 4. ^{13}C-^{1}H HSQC NMR spectrum of *Annikki Gesamtlignin* (GL2) with assigned spectral regions.

The distribution of the three main lignin monomers (S, G, H) was determined from the ^{13}C-^{1}H correlation signals in the HSQC spectrum. Guaiacyl (G) and syringyl (S) moieties were found to be the main monomeric building blocks of *Annikki Gesamtlignin*. Particular units for grass lignins, namely cinnamyl alcohol (X1), *p*-coumarates (PCA) and ferulates (FA) were also clearly identified. Additionally, strong signals derived from tricin (T), which is known to be widely distributed in grasses and grains, could be found. A low correlation peak may originating from xylanes was found (δ_C/δ_H 72.87/3.21), but further according signals from this particular carbohydrate were not detected. Anyway, this resonance was the only indication of polysaccharides present in the lignin sample as no correlation signals could be found in the polysaccharide anomeric region (δ_C/δ_H 90–110/4.0–6.0) (cp. Figure 4).
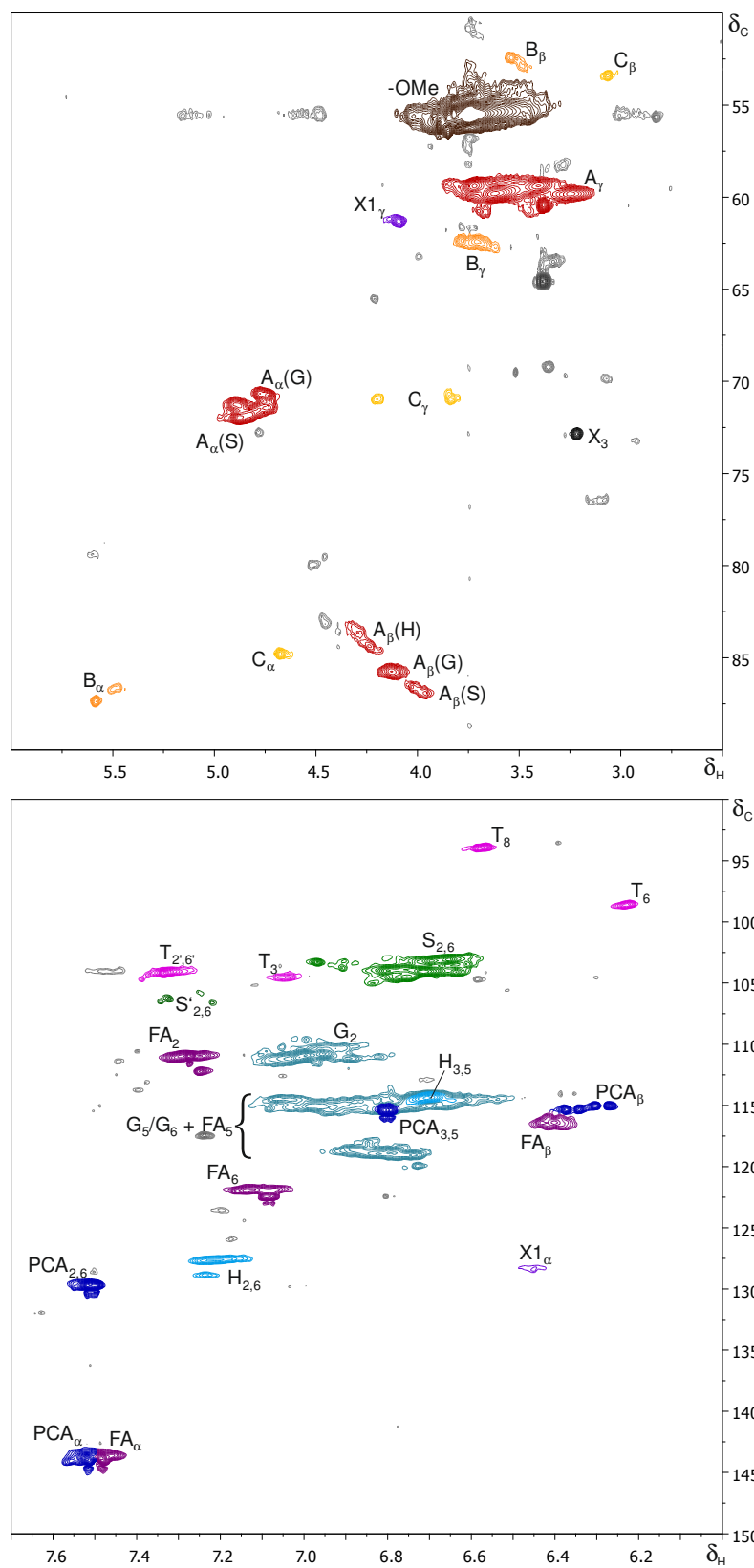
Figure 5. Expanded aliphatic sidechain (δ_C/δ_H 50–90/2.5–6.0) and aromatic (δ_C/δ_H 90–150/6.0–8.0) regions of the ^{13}C-^{1}H HSQC NMR spectrum of *Annikki Gesamtlignin* (GL2). (50 mg, 25 °C, 500 MHz, DMSO-d_6).

Information about the different lignin inter-unit linkages can be deducted from the aliphatic-oxygenated region (δ_C/δ_H 50–90/2.4–6.0) of the HSQC spectrum. The β-O-4 linkage (A) correlation peak was the most prominent inter-unit linkage signal found in the *Annikki Gesamtlignin*. Weaker signals originating from resinol (β-β) structures (C) as well as phenylcoumaran (β-5') moieties (B) could be identified.
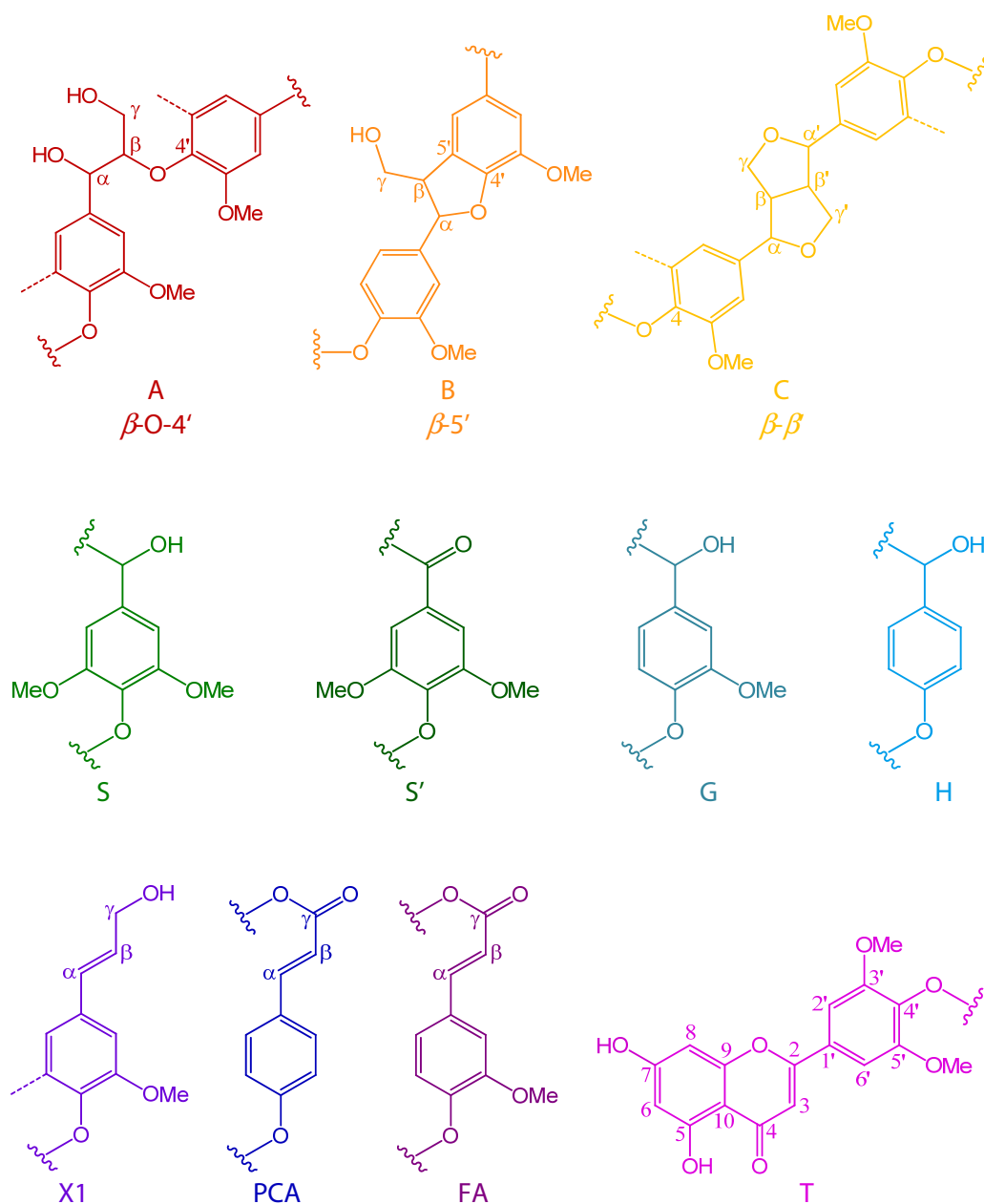
Figure 6. Main structures present in *Annikki Gesamtlignin*: β-O-4' alkyl-aryl ethers (A); phenylcoumarans (B, β-5' linkage); resinols (C, β-β linkage); p-hydroxyphenyl units (H); guaiacyl units (G); syringyl units (S) and their α-oxidized analogues (S'); cinnamyl alcohol end-groups (X1); p-coumarates (PCA); ferulates (FA) and tricin (T, 5,7,4'-trihydroxy-3',5'-dimethoxyflavone).

Table 6. Labeled ^{13}C-^{1}H cross signals in the HSQC NMR spectrum of *Annikki Gesamtlignin* (GL2).

Label	*Annikki Gesamtlignin* (GL2)	
Aliphatics	δ_C/δ_H / ppm	**Assignment**
C_β	53.4 / 3.06	C_β-H_β in β-β resinol substructures (C)*
C_γ	71.0 / 3.83 and 4.19 *(low intensity)*	C_γ-H_γ in β-β resinol substructures (C)
C_α	84.8 / 4.67 *(low intensity)*	C_α-H_α in β-β resinol substructures (C)
OMe	55.6 / 3.75	C-H in methoxyls
A_γ	60.4 / 3.38	C_γ-H_γ in β-O-4' substructures (A)
	59.4 / 3.41 and 3.72	C_γ-H_γ in γ-hydroxylated β-O-4' substructures (A)
	59.8 / 3.24 and 3.62	C_γ-H_γ in β-O-4' substructures (A)
A_α(G)	70.7 / 4.76 and 71.4 / 4.76	C_α-H_α in β-O-4' substructures (A) linked to a G-unit
A_α(S)	71.3 / 4.89 and 71.9 / 4.85	C_α-H_α in β-O-4' substructures (A) linked to a S-unit
A_β(H)	83.6 / 4.28 and 84.4 / 4.23	C_β-H_β in β-O-4' substructures (A) linked to a H-unit
A_β(G)	85.8 / 4.12	C_β-H_β in β-O-4' substructures (A) linked to a G-unit
A_β(S)	86.8 / 3.99	C_β-H_β in β-O-4' substructures (A) linked to a S-unit
B_α	86.7 / 5.48 and 87.4 / 5.58	B_α-B_α in β-5' substructures (B)
B_β	52.4 / 3.54 and 52.9 / 3.48	B_β-B_β in β-5' substructures (B)
B_γ	62.5 / 3.70	B_γ-B_γ in β-5' substructures (B)
$X1_\gamma$	61.3 / 4.09	C_γ-H_γ in cinnamyl alcohol end groups (X1)
Aromatics	δ_C/δ_H / ppm	**Assignment**
$X1_\alpha$	128.2 / 6.46 *(low intensity)*	C_α-H_α in cinnamyl alcohol end groups (X1)
$X1_\beta$	128.2 / 6.23 *(very low intensity)*	C_β-H_β in cinnamyl alcohol end groups (X1)
T_8	93.9 / 6.56	C_8-H_8 in tricin (T)
T_6	98.7 / 6.22	C_6-H_6 in tricin (T)
$T_{2',6'}$	104.1 / 7.33	$C_{2'}$-$H_{2'}$ and $C_{6'}$-$H_{6'}$ in tricin (T) linked to syringyl units at C_2
T_3	104.5 / 7.05	C_3-H_3 in tricin (T)
$S_{2,6}$	103.7 / 6.67	C_2-H_2 and C_6-H_6 in syringyl units (S)
$S'_{2,6}$	106.3 / 7.33 and 106.2 / 7.23	C_2-H_2 and C_6-H_6 in α-ketone syringyl units (S')
G_2	110.7 / 6.95	C_2-H_2 in guaiacyl units (G)
G_5/G_6	115.1 / 6.87 and 118.7 / 6.80	C_5-H_5 and C_6-H_6 in guaiacyl units (G)
FA_2	110.9 / 7.27	C_2-H_2 in ferulate (FA)
FA_6	121.9 / 7.11	C_6-H_6 in ferulate (FA)

(Table 6 continued).

FA_5	*within G_5/G_6 correlation peak*	C_5-H_5 in ferulate (FA)
FA_β	116.4 / 6.40	C_β-H_β in ferulate (FA)
PCA_β	115.2 / 6.32	C_β-H_β in p-coumarate (PCA)
FA_α	143.9 / 7.48	C_α-H_α in ferulate (FA)
PCA_α	144.0 / 7.52	C_α-H_α in p-coumarate (PCA)
$PCA_{3,5}$	115.4 / 6.80	C_3-H_3 and C_5-H_5 in p-coumarate (PCA)
$PCA_{2,6}$	129.7 / 7.51	C_2-H_2 and C_6-H_6 in p-coumarate (PCA)
$H_{3,5}$	114.4 / 6.72	C_3-H_3 and C_5-H_5 in p-hydroxyphenyl units (H)
$H_{2,6}$	127.6 / 7.21 and 128.9 / 7.24	C_2-H_2 and C_6-H_6 in p-hydroxyphenyl units (H)

* assigned as B_β in other works[102]

Both saturated and unsaturated fatty acids were detected in the high field region (δ_C/δ_H 0–50/0–2.4) of the spectrum as well as by resonances at δ_C/δ_H 127.4 and 129.3/5.33 ppm. The amount of fatty acids present in *Annikki Gesamtlignin* was also investigated quantitatively by lignin extracts analyzed by ^{1}H NMR and GC-MS and was found to be approximately 8 wt%. The ratio of fatty acids in GL estimated from the 2D spectrum is situated in the same order of magnitude, whereas less than one sixth of the detected fatty acids is unsaturated.

Other substructures which have already been identified in HSQC spectra of wheat straw lignins, namely dibenzodioxins (D), spirodienones (F) and α,β-diaryl ethers (E) (Figure 7), were not detected in this sample. The investigated lignin sample may contain amounts of these structures below the detection limits. Additionally, the spin-spin coupling of resonances can result in signals with very low intensities disappearing in the noise of the ^{13}C-^{1}H HSQC spectrum.
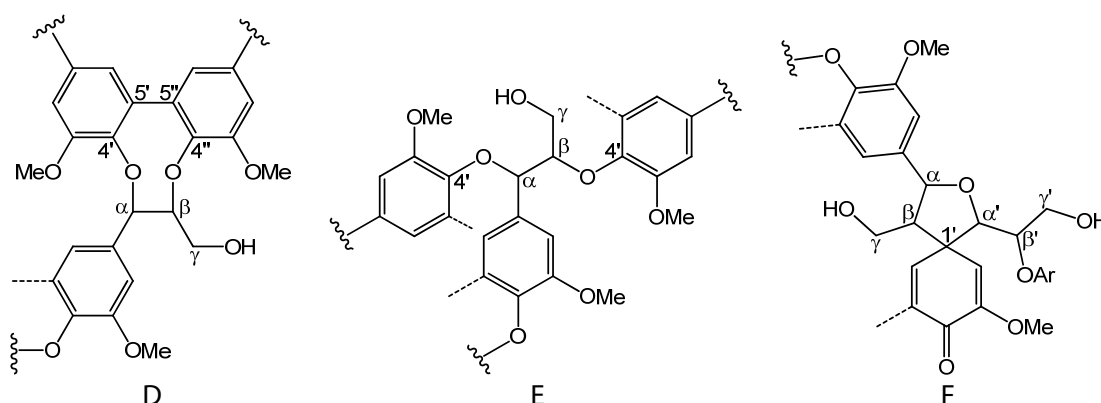
Figure 7. Structurs of dibenzodioxins (D), α,β-diaryl ethers (E) and spirodienones (F).

Based on the integral values of the correlation peaks of S, G and H moieties, the relative monomeric ratio of *Annikki Gesamtlignin* was calculated. According to the common practice in literature, the X1, PCA and FA content as well as the T content are given as a percentage of the sum of regular aromatic lignin monomers (S+G+H).[103] The determined ratios are listed in Table 7 and the integral values used for the calculation are listed in Table 47 (Appendix).

Table 7. Monomeric ratio of main monomeric units as well as *p*-hydroxycinnamic acids (*p*HCA) and tricin (T) present in *Annikki Gesamtlignin*. Additionally, the relative abundance of the different inter-unit linkages is indicated.

Lignin aromatic units	
S / %	38
G / %	56
H / %	6
S / G / H ratio	6 / 9 / 1
Lignin interunit linkages	
β-O-4' aryl ethers (A$_\gamma$) / %	85
β-5' phenylcoumarans (B$_\gamma$) / %	10
β-β resinols (C$_\gamma$) / %	5
A / B / C ratio	17 / 2 / 1
dibenzodioxins (D) / %	n.d.
α,β-diaryl ethers (E) / %	n.d.
spirodienones (F) / %	n.d.
p-Hydroxycinnamates (*p*HCAs)	
p-coumarates (PCA) / %	11
ferulates (FA) / %	17
PCA / FA ratio	0.6
Lignin end groups	
cinnamyl alcohol end groups (X1) / %	3
Tricin	4

n.d. = not detected

Additionally, we determined the ratios of lignin monomeric units in a slightly altered way, which provides, at least to our understanding, a more comprehensive picture of the *Annikki* wheat straw lignin sample. Thus, α-oxidized and *p*HCA structures are included into the term ‚main lignin units‘ and expressed as share of the according aromatic moiety. Structures X1 and T are set as part of the main units as well, but are expressed as separate units due to their different or not clearly assignable substructure. Therefore, the ratios of the monomeric units are determined from the sum of integrals belonging to all detected moieties: (S+S')+(G+FA)+(H+PCA)+X1+T (Table 8). According to this evaluation, a significantly different S / G / H ratio of 2 / 4 / 1 is specified since the integral value of H units (including PCA) is set to 1.

Table 8. Ratio of lignin monomeric units including p-hydroxycinnamic acids (pHCA), end group X1, tricin (T) and different interunit linkages.

Ratio of lignin aromatic units	
S	2.4
6.2 % in α-oxidized form (S')	
G	4.2
24 % as ferulates (FA)	
H	1
64 % as p-coumarates (PCA)	
cinnamyl alcohol end groups (X1)	0.2
tricin	0.3
Ratio of lignin interunit linkages	
β-O-4' aryl ethers (A$_\gamma$)	17
β-5' phenylcoumarans (B$_\gamma$)	2
β-β resinols (C$_\gamma$)	1

Interestingly, the ratio of interunit linkages varies strongly, depending on the CH groups integrated of the respective moiety. Thus, A / B / C is given 17 / 2 / 1 if the γ-protons are integrated, 7 / 1.5 / 1 with α-protons and 11 / 2 / 1 with β-protons (compare Figure 6). This finding strongly indicates that the correlation signals are of A$_\gamma$ are superimposed by other signals and hence the content of β-O-4' alkyl-aryl ethers is slightly overestimated.

Of course we are aware about the remainig questions concerning the lignin structure and that this is only a small attempt to clarify this complex construction of different monomeric units. We must assume that there are numerous monomeric units present in the lignin sample which are on one hand simply not detectable, or on the other hand, overlap with other correlations not allowing for clear assignment. α-Oxidized G and H units for instance or other substructures (Figure 7) are most likely existing in the lignin framework, but below detection limit (refers to amounts smaller than 3 %). It would also be conclusive that the X1 moiety is present in the γ-oxidized form as aldehyde or even as carboxylic acid, but the according correlations were not detected. However, the splitted correlation of the alkene proton in the p-coumarate unit (PCA$_\beta$) (Figure 5) indicates that this moiety is present both in esterified form as well as free carboxylic acid, hence refering to an end group. Such subtle structural differences are hard to detect via ^{13}C-^{1}H chemical shift and would need further evidence from other analytical methods.

2.1.3 LIGNIN MONOMERIC UNIT

In a revolutionary work, Crestini *et al.*[104] proposed lignin, more specifically softwood milled wood lignin, to be a linear, slightly branched oligomer. They specified a theoretical C_9 unit based on various analysis techniques, such as ^{31}P and ^{13}C-^1H HSQC NMR, elemental analysis, the Zeisel method[105] as well as molar mass determinations, coupled with a degradative protocol (DFRC — derivatization followed by reductive cleavage[106]). Additionally, the degree of polymerization (DP) and branching of the lignin subunits was determined. Thus, they concluded that lignin is composed of oligomers, which are tightly packed in supermolecular aggregates. This is in contrast to the prevailing opinion of lignin to be a crosslinked polymer network.

Inspired by this work, a representative lignin monomeric unit as well as the degree of polymerization (DP) will be given. Results of NMR spectroscopy , both ^{31}P and ^{13}C-^1H HSQC, elemental analysis (cp. section 2.3) as well as HPLC-SEC (cp. section 2.4) were taken into account for this simplistic, theoretical assessment of *Annikki* wheat straw lignin.

Based on the elemental composition of *Annikki Gesamtlignin* (GL2), a theoretical C_9 monomeric unit of lignin is given (Figure 8). This repeating unit (RU), featuring a molecular weight of 196.2 g·mol^{-1}, would be representative for the majority of the lignin sample.

Elemental analyis	
Theoretical C_9 unit	*Annikki* GL2
61.2 % C	62.4 % C
6.2 % H	6.5 % H
32.6 % O	29.4 % O
–	1.3 % N
–	0.4 % S
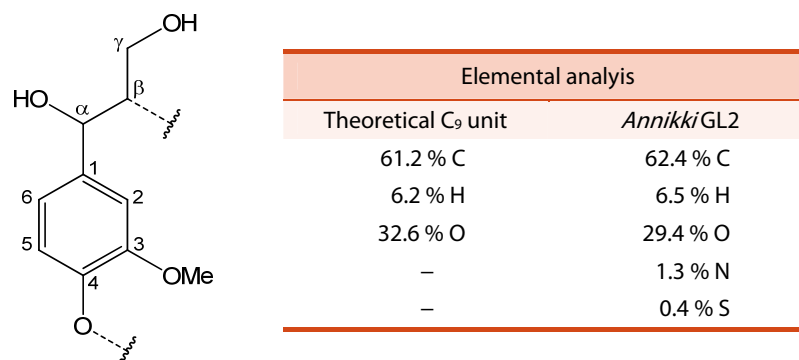
Figure 8. Theoretical C_9 repeating unit of lignin, representative for the majority of *Annikki* lignin.

Evaluation of semiquantitative ^{13}C-^1H HSQC NMR measurements revealed a S / G / H ratio of 2.4 / 4.2 / 1 (31.6 % S, 55.3 % G and 13.1 % H) including S', FA as well as PCA units (Table 8). Cinnamyl alcohol end groups (X1) and tricin units (T) are excluded from this consideration. The majority (85 %) of the monomeric units is connected via β-O-4' aryl ether linkages and further 10 % are linked via β-5' phenylcoumaran units (cp. Figure 6 and Table 8). Resinols (β-β), 1,2-diarylpropanes (β-1) and biphenyl (5-5') linkages were dedected not at all or rather in traces (~ 5% β-β). The total amount of hydroxyl groups in this lignin sample (GL2) is given by quantitative ^{31}P NMR with 4.32 mmol·g^{-1}, whereas 3.35 mmol·g^{-1} refer to aliphatic and 0.97 mmol·g^{-1} to phenolic hydroxyl groups. More precisely, 0.86 mmol·g^{-1} of the latter originate from phenol-terminated S, G and H units and 0.11 mmol·g^{-1} can be assigned to condensed lignin units, namely 5-C-5' diphenylmethane, 4-O-5' diaryl ether and 5-5' diphenyl moieties (cp. Figure 3 and Table 5, section 2.1.1).

According to the disclosure of Crestini *et al.*,[104] the phenolic hydroxyl groups can be regarded as lignin end groups. If lignin were a linear polymer, connected via β-O-4' and β-5' interunit

linkages, each polymer chain would comprise one phenolic end group. In consideration of the different interunit linkages, the end units of lignin chains can be unambiguously determined (cp. equation 3). As there are only data from quanitative ^{31}P NMR available, β-β as well as β-1 interunit linkages must be excluded from the evaluation, which should, however, have negligible consequences. Diphenyl moieties (5-5') feature two phenolic hydroxyl groups, meaning that the half value of the obtained amount has to be considered. Thus, the lignin chains, or end groups respectively, for GL2 can be assessed according to equation 4 and are specified by 0.945 mmol·g⁻¹.

$$\text{lignin chains = end groups = phenolic OH } - [\beta - \beta + \beta - 1 + 5\text{-}5'] \qquad (3)$$

$$\text{lignin chains (GL2) = phenolic OH } - \frac{5 - 5'}{2} = 0.97 - \frac{0.05}{2} = 0.945 \text{ mmol·g}^{-1} \qquad (4)$$

As the amount of phenolics directly reflects the amount of polymer chains in the sample, the amount of aliphatics corresponds to the repeating units (RU) (equation 5). As lignin monomeric units, which are connected via β-O-4' linkages (85 %), feature two aliphatic hydroxyl groups, the half value has to be used for the calculation ($3.35 \times 0.85 \times 0.5 = 1.424$ mmol·g⁻¹). Moieties, connected via β-5' linkages (10 %) exhibit one aliphatic OH and are given as follows: $3.35 \times 0.1 = 0.335$ mmol·g⁻¹. With this correlation, the degree of polymerization (DP) is accessible (equation 6). The obtained DP of 1.8 according to this considerations is much lower than expected, meaning that the lignin sample comprises mainly dimers and also a relevant amount of monomers. DPs in the range of 5–12 were stated for milled wood lignins in contrast.[104]

$$\text{repeating unit = aliphatic OH} \cdot \left(\frac{\%\beta\text{-O-4}'}{2} + \%\beta\text{-5}' \right) \cdot \frac{1}{100} \qquad (5)$$

$$\text{repeating unit (GL2) = } 3.35 \cdot \left(\frac{85}{2} + 10 \right) \cdot \frac{1}{100} = 1.759 \text{ mmol·g}^{-1}$$

$$\text{DP} = \frac{\text{repeating unit}}{\text{lignin chains}} \qquad (6)$$

$$\text{DP (GL2) = } \frac{1.759}{0.954} = 1.8$$

Thus, taking the molecular weight of the theoretical lignin monomeric unit (Figure 8) into account, a molecular weight of 362 g·mol⁻¹ can be stated. This is much lower than the number average molecular weight (M_n) of 1280 g·mol⁻¹ obtain via HPLC-SEC (cp. Table 11, section 2.4). If the DP, determined with our simplified method is in the correct order of magnitude, this is a strong indication of tightly aggregated of lignin moieties.

2.2 ATR-FTIR Spectroscopy

Infrared spectra were recorded on a Bruker ALPHA-P FT-IR spectrometer equipped with a diamond attenuated total reflection (ATR) unit. Fourier transformation (FT), processing and evaluation were done using an OPUS 6.5 software package. IR spektroscopy is a commonly used analysis technique for lignins.[1] Figure 9 shows an ATR-FTIR spectrum of *Annikki Gesamtlignin* (GL2). The absorption bands were assigned according to literature[2,107] and are listed in Table 9. The method is appropriate for estimating the conversion of hydroxyl groups in lignin modification reactions for instance. Thus, a significant decrease of the broad hydroxyl absorption band (~ 3300 cm^{-1}) and simultaneous occurence of an ester absorption band (~ 1740 cm^{-1}) indicates a successful esterification of hydroxyl groups (see chapter 3.2.1).
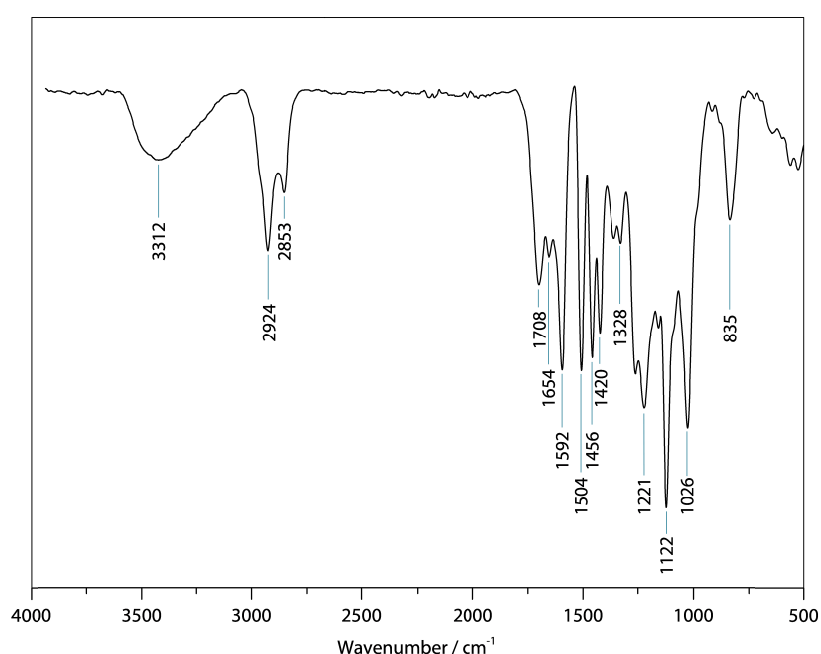
Figure 9. ATR-FTIR spectrum of *Annikki Gesamtlignin* (GL2).

Table 9. Assignment of GL2 absorption bands according to literature.[8]

FT-IR-bands / cm^{-1}	Assignment
3312	O-H
2924	aliphatic C-H
2853	aliphatic C-H
1740	C=O ester
1708	C=O carboxylic acid
1654	aliphatic C=C, amide
1592	aromatic C-C
1504	aromatic C-C
1456	aromatic CH$_3$
1420	aromatic C-C
1328	C-O ether
1221	C-O phenolic
1122	aromatic C-H
1026	C-O
835	aromatic C-H

2.3 ELEMENTAL COMPOSITION

Elemental analyses (CHNS) of the different lignins were performed on a Vario EL III Element Analyzer from Elementar GmbH. Double determination gave a composition of 62.4 % carbon, 6.5 % hydrogen and 1.3 % nitrogen for an *Annikki Gesamtlignin* (GL2) sample. This results in an oxygen content of 29.4 % (Table 10). A minor percentage of nitrogen was found, which directly correlates to the amount of proteins in the lignin. By multiplying the nitrogen content with the factor 6.25, the protein content in lignin samples is given in wt%.[96a] Thus, a protein content of 8.1 wt % would be stated for GL2.

The sulfur content of Kraft lignin is naturally higher compared to *Annikki* lignins which should not encounter any sulfur or sulfur compounds derived from the pulping process. Thus, the traces of sulfur also originate most likely from proteins.

Table 10. Elemental composition of the different lignins used.

Lignin	% N	% C	% S	% H	% O*
NML	1.3	61.2	n.d.	6.3	31.2
GL1	2.2	62.9	n.d.	6.7	28.2
GL2	1.3	62.4	0.4	6.5	29.4
GL2 extracted	1.4	60.9	0.5	6.3	30.9
GL3	1.4	62.1	0.5	6.6	29.4
GL4	1.0	62.2	0.3	6.5	30.0
GL5	1.3	62.1	n.d.	6.5	30.1
L_HT (GL6)	0.8	63.9	n.d.	6.3	29.0
L_THF (GL6)	0.4	64.2	n.d.	7.0	28.4
KL2	0.7	62.4	2.5	5.8	28.6

* calculated value; n.d. = not determined

2.4 MOLAR MASS DISTRIBUTION

The molecular weight of lignin in situ is unknown and that of isolated lignins depends strongly on the isolation conditions.[3] Lignin is mostly reported to be a highly complex, crosslinked natural polymer, but there are numerous factual assumptions that lignin is a sparsely branched, rather linear oligomer.[104] Lignin is known to exhibit a high propensity for self-aggregation due to intermolecular hydrogen bond formation (between carboxylic acid groups and various ether oxygens and hydroxyl groups) and van der Waals attraction of polymer chains. Hydrogen bonds induce strong non-covalent interactions whereby lignin molecules are reported to associate into a loose network structure of supermolecular complexes up to 200-300 nm in diameter and consisting of 10^3-10^4 molecules.[108] Furthermore, the aggregation of lignin due to non-covalent bonding interactions among the aromatic moieties (π-stacking) was already proposed in the early 1980s by Sarkanen and coworkers.[109]

Various methods can be used for the determination of the molar mass distribution of lignins, such as vapor osmometry, cryoscopy, isopiestic methods, ultrafiltration, size excluscion chromatography (SEC), MALDI-ToF mass spectrometry (MS) or light scattering analysis.[104] But every method will give slightly different results: Values obtained from ultrafiltration will be higher than those of MALDI-ToF MS and vapor osmometry, whereas M_n values derived from the latter will be affected by aggregates. Light scattering analyses can be used to determine M_w and to detect supermolecular aggregates. However, light scattering is, as well as SEC, dependent on the concentration, solvent, pH and also the lignin isolation method. Aggregation phenomena will not be detected via SEC with UV absorbance. One of the main problems is the lack of proper standards with a hydrodynamic volume (V_H) comparable to lignin. The results are also dependent on the freshness of the sample as lignin shows a high tendency to from aggregates. The selection of the solvent system and concentration are as well of great importance. Non-hydrogen bonding solvents like dioxane or tetrahydrofuran (THF) may undergo self-aggregation in lignin and thus can interfere the measurement.[104]

Despite decades of research, the structure and degree of polymerization of the biomaterial are hitherto not fully understood. This is largely due to the lack of suitable analytical tools available. Aggravating this situation, the high tendency of lignin to aggregate results in the distortion of SEC results. Thus, the reliable determination of lignin molecular weight distribution would be an insightful disclosure.[104] From this point of view, we have to scrutinize SEC results always critically and cannot assume, that actual size and structure are reflected thoroughly by the measured values. Nevertheless, gel permeation chromatography is reported to produce reliable estimations of lignin molecular weight, both in aqueous and non-aqueous systems.[110]

SEC of lignin samples was performed on an Agilent 1200 Infinity instrument with three TOSOH TSK-GEL Alpha Series colums (TSKgel Alpha-2500, -3000 and -4000) in a row at Annikki GmbH, Graz. The native lignin sample (~ 5 mg) was dissolved in DMF (1 mL) and lithium bromide was added (1 g·L^{-1}) to improve dissolution by the reduction of associative effects.[111] 20 μL of this mixture were injected for analysis and eluted (90 min) with a solution of LiBr (1 g·L^{-1}) in DMF at 50 °C. Lignin or lignin derivatives, respectively, were measured

Table 11. Molecular weights of lignins determined by HPLC-SEC relative to PS standards (50 °C, DMF).

Lignin	M_n / g·mol^{-1}	M_w / g·mol^{-1}	PDI
GL1 (I)	1380	7060	5.1
GL1 (II)	1430	7870	5.5
GL1 (III)	1340	5650	4.2
GL2	1280	5510	4.3
GL4	1250	5080	4.1
GL5 (I)	1200	4480	3.7
GL5 (II)	1280	5230	4.1
L_HT (GL6)	1050	4390	4.2
KL2	1380	12900	9.3

against polystyrene standards and analyzed by dual UV absorption (280 nm) and refractive index detection (Figure 10). In Table 11, the number (M_n) and weight (M_w) average molecular weights as well as the resulting polydispersities (M_w / M_n, PDI) of the lignins used in this contribution are listed. The roman numerals in parantheses refer to double or triple determination of these samples. The obtained molecular weights from the multiple determinations given in Table 11, reveal that the values deviate significantly (cp. GL1 (III)). This finding indicates aggregation of the investigated lignin samples.

In general, the reproducibility of M_n is higher than M_w. Differences observed in M_n can originate from adsorption effects, whereas front tailing, caused by high-molar-mass lignin-carbohydrate complexes (LCCs) or aggregation, distorts M_w using dual UV (280 nm) absorption and RI detection, higher values for M_w are obtained with the UV detector as it features a higher sensivity for lignin.[112]

Considering the elution profile of GL1 (Figure 10), it can be seen that a tailing due to lower molar masses is observed (30–50 min) which may be caused by polysaccharides or proteins. Front tailing on the contrary is not visible in this chromatogram.
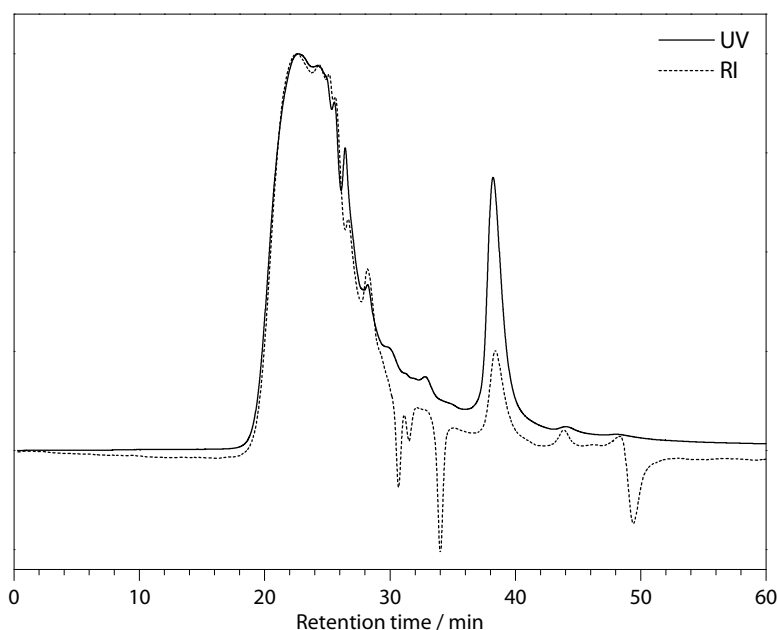
Figure 10. HPLC-SEC elution profile of GL1 analyzed by dual UV (280 nm) and RI detection (50 °C, DMF).

2.5 THERMAL PROPERTIES

The thermal properties of the complex biopolymer are influenced by a number of factors such as origin and isolation of lignin, molecular weight and moisture content.[3] Generally, lignin can be classified as amorphous thermoplastic polymer. Whereas the glass transition temperature (T_g) of native lignins was calculated between 65 and 85 °C for hardwoods and 90–105 °C for softwoods, the T_g of isolated lignins varies over a wide range. It was found, that the T_g shifts to lower values with increasing moisture content and decreasing molecular weight. A similar trend was observed for the decomposition temperature, which is explicitly delayed at higher molecular weights. As expected, the thermal stability increases with growing molar masses. These effects have been demonstrated for a low (620 g·mol^{-1}) and a high (180 000 g·mol^{-1}) molecular weight *Kraft* lignin. Thus, a T_g of 32 °C in contrast to 173 °C and an increasing start of decomposition from 181 to 238 °C were reported.[113]

Simultaneous thermal analyses (STA) were performed on a Netzsch Simultaneous Thermal Analyzer STA 449C (crucibles: aluminium from Netzsch) with a heating rate of 3 °C / min and a helium flow of 50 mL / min in combination with a protective flow of 8 mL / min. The corresponding DSC-curves and the mass losses for original and dried low molecular weight *Annikki* lignin (NML) is shown in Figure 11. The mass loss of 2 % for dry NML compared to NML agrees with the weight loss obtained gravimetrically after drying the received lignin under vacuum. The mass loss is most likely caused by the evaporation of remaining water and ethanol from the pulping process. The decomposition of the investigated lignin samples extends from ~ 150 °C over the whole temperature range investigated (to 550 °C). Mass losses up to 200 °C may be attributed to the vaporization of residual water, which cannot be removed at lower temperatures under vacuum due to interactions with lignin hydroxyl groups.[114] Subsequently, the thermal decomposition of lignin low molecular weight building blocks (extractives) proceeds. The predominated mass loss appears between 320 and 390 °C, suggesting the decomposition of aromatic rings. The determined inflection points of the decomposition maximum rate are 356 °C (GL2), 333 °C (NML) and 339 °C (NML dry), which is slightly lower than a reported value for *Alcell* wheat straw lignin (374 °C).[115] The simultaneously obtained DSC traces of GL2 and NML show a plateau in this range, while the curve of dry NML shows a continuous growth. All DSC traces exhibit a peak in the range of 420–425 °C, which is more pronounced for GL2 and dry NML. The NML trace shows another plateau in this temperature range, whereas the energy consumption increases starting from ~ 445 °C. Contrary to NML, the DSC curve of GL2 decreases, whereas NML (dry) appears rather flat. Thus, the decomposition in this temperature range must be accompanied by different processes, e.g. condensation reactions, which are dominating in each sample investigated. The different molecular weights ($M_{n(NML)}$ ~ 900 g·mol^{-1} vs. $M_{n(GL2)}$ ~ 1400 g·mol^{-1}) may also come into account at this point.

The mass curves appear very similar and the amount of volatiles (~ 60 % at 550 °C) is in good accordance to literature values for wheat straw lignins,[115] albeit higher than for softwood *Kraft* lignin (~ 40 %).[116] In general, it can be said that wheat straw lignins contain more volatiles at lower temperatures compared to wood-derived *Kraft* lignins. Thus, for a softwood *Kraft* lignin the highest mass losses are found between 350 and 450 °C. The remaining mass of the investigated *Annikki* lignins can be assumed to further decrease up to temperatures of 1000 °C. For *Alcell* wheat straw lignin, 36.6 % char have been indicated at 1000 °C,[115] which is in the same range as softwood *Kraft* lignins (30–40 % char at 1000 °C).[116] Thus, the mass loss will slightly increase up to 1000 °C, as approximately 60 % mass loss were already obtained at 550 °C (Figure 11). In general, lignins which are closer to the native form of the biopolymer (e.g. ball milled wood lignin) exhibit the maximum thermal degradation at lower temperatures than technical lignins. This is due to a higher content of β-O-4 bonds, which are easier degradable than other interunit linkages. It is known, that condensation processes involving lignin hydroxyl groups take place upon thermal treatment, mainly in the range of 150–270 °C. Condensation processes are increasingly taking place if high amounts of hydroxyl groups are available.[115] The decomposition of the biopolymer is counteracted by condensation reactions of lignin moieties and as a result, the amount of residual char is rather high.
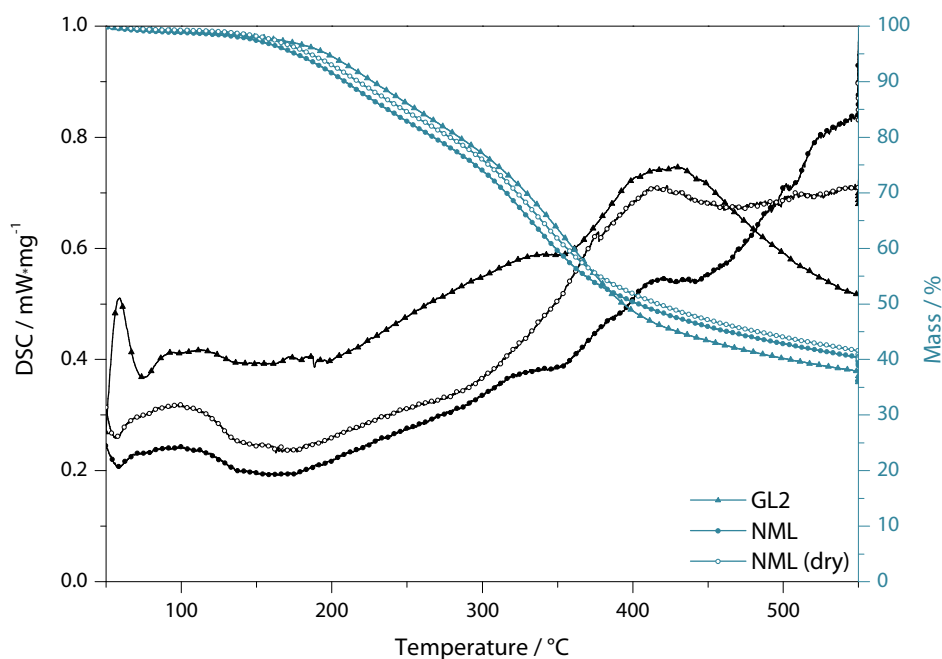
Figure 11. DSC and mass loss of GL2, NML and dried NML, determined by STA.

The glass transition temperatures (T_g) of GL2 and KL2 were determined by differential scanning calorimetry (DSC). The analyses were measured on a DSC 8500 instrument (Perkin Elmer) in a temperature range from −20 to 180°C with a heating rate of 20 °C / min for both runs, whereas the T_g values were retrieved from the second heating run. The T_g of KL2 was determined with 147.6 °C, which is in good accordance to literature.[116] Deviations may occur due to numerous factors such as moisture content, molecular weight, crosslinking degree, hydrogen bonding or contaminations, as already mentioned above. The T_g of GL2 was found to be 113.8 °C, which is within the reported values for wheat straw lignins.[115]

Both investigated lignin samples exhibited no melting point (T_m) within the measured temperature range. Only very few lignin types have been reported to have a T_m, e.g. a hardwood *Kraft* lignin after organic solvent extraction. [117] However, disperse and heterogeneous lignin samples melt in a broad temperature range, which is not unequivocal detectable.
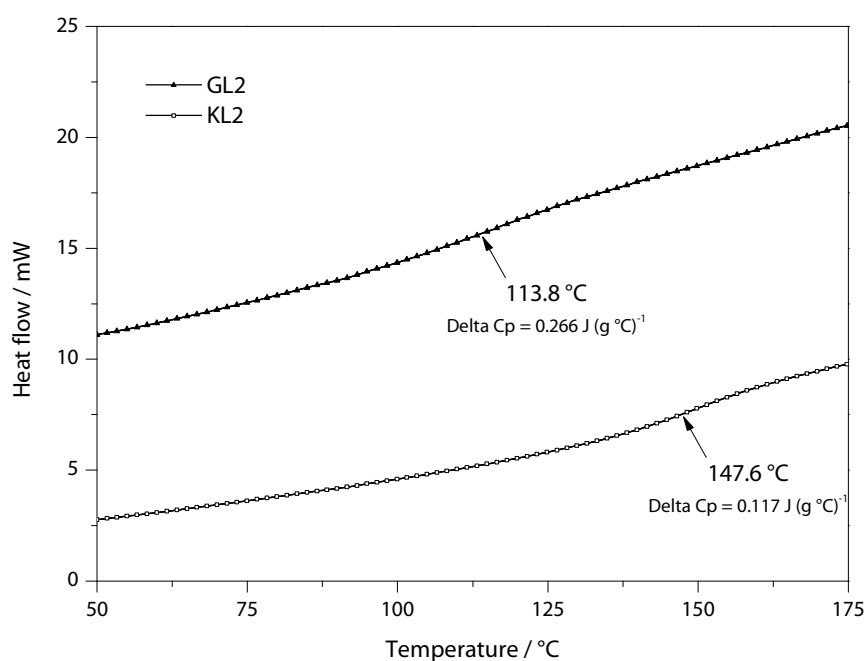
Figure 12. DSC curves of GL2 and KL2 with assigned T_g values (half Cp extrapolated).

2.6 Solubility

In order to facilitate the design of experiments, the solubility of *Annikki* lignin in different solvents and reagents was investigated. As expected, the solubility of lignin in most conventional organic solvents is very low. In a detailed study by Horvath[118] comprising the solubility of wood and its components including lignin, numerous solvents were investigated for their ability to dissolve lignin. It was found that low molecular volume ketones, esters and ethers are not able to dissolve lignin. The solubility and swelling of lignin is increased in hydroxylated solvents like methanol, ethanol, phenol or water. A maximum solubility of isolated wood lignins was observed in dioxane, acetone, tetrahydrofuran (THF), DMF and DMSO. In general, the ability of solvents to dissolve lignin increases with their hydrogen-bonding capacity.

As can be seen from Table 12, the solubility of *Annikki* wheat straw lignin is rather limited. Well solubility in dioxane, acetone or THF was not observed in contrast to wood lignins. Thus it is indispensable to use toxic and high-boiling solvents like *N,N*-dimethyl formamide (DMF) or dimethyl solfoxide (DMSO) for conversions of lignin. The doping of different solvents with pyridine to improve lignin dissolution showed also no impact.

Table 12. Solubility of *Annikki* lignin in varying solvents

Rather soluble	aqueous NaOH (1 mol·L^{-1})
	pyridine
	DMSO
	DMF
	acetyl chloride
	acetic anhydride
	divinyl sulfone
Insoluble (to a great extent)	H_2O
	MeOH, EtOH
	acetone
	acetonitrile
	CH_2Cl_2, $CHCl_3$
	1,4-dioxane
	dimethoxyethane
	n-pentane, cyclohexane
	THF
	toluene, benzene

2.7 LIGNIN EXTRACTIVES

Low molecular weight *Annikki* lignin (NML) was extracted with dichloromethane to identify and to quantify soluble parts of the biopolymer. By extraction of NML with CH_2Cl_2 (3 × at 40 °C) 25 wt% low molecular substances were removed. During the first extraction run 20.2 wt% were dissolved and further 2.4 wt% during the second and third run. The extractives are mainly low molecular weight fractions of lignin, which are dissolving in dichloromethane under these conditions. A significant proportion accounts for fatty acids present in *Annikki* lignin. The ^{13}C-^1H HSQC spectrum (Figure 13) of the first extract appears substantially like a typical HSQC spectrum of lignin, albeit with less correlations in the aliphatic side chain (δ_C/δ_H 50–90/2.5–6.0) and aromatic (δ_C/δ_H 90–150/6.0–7.7) regions (discussed in section 2.4.1).
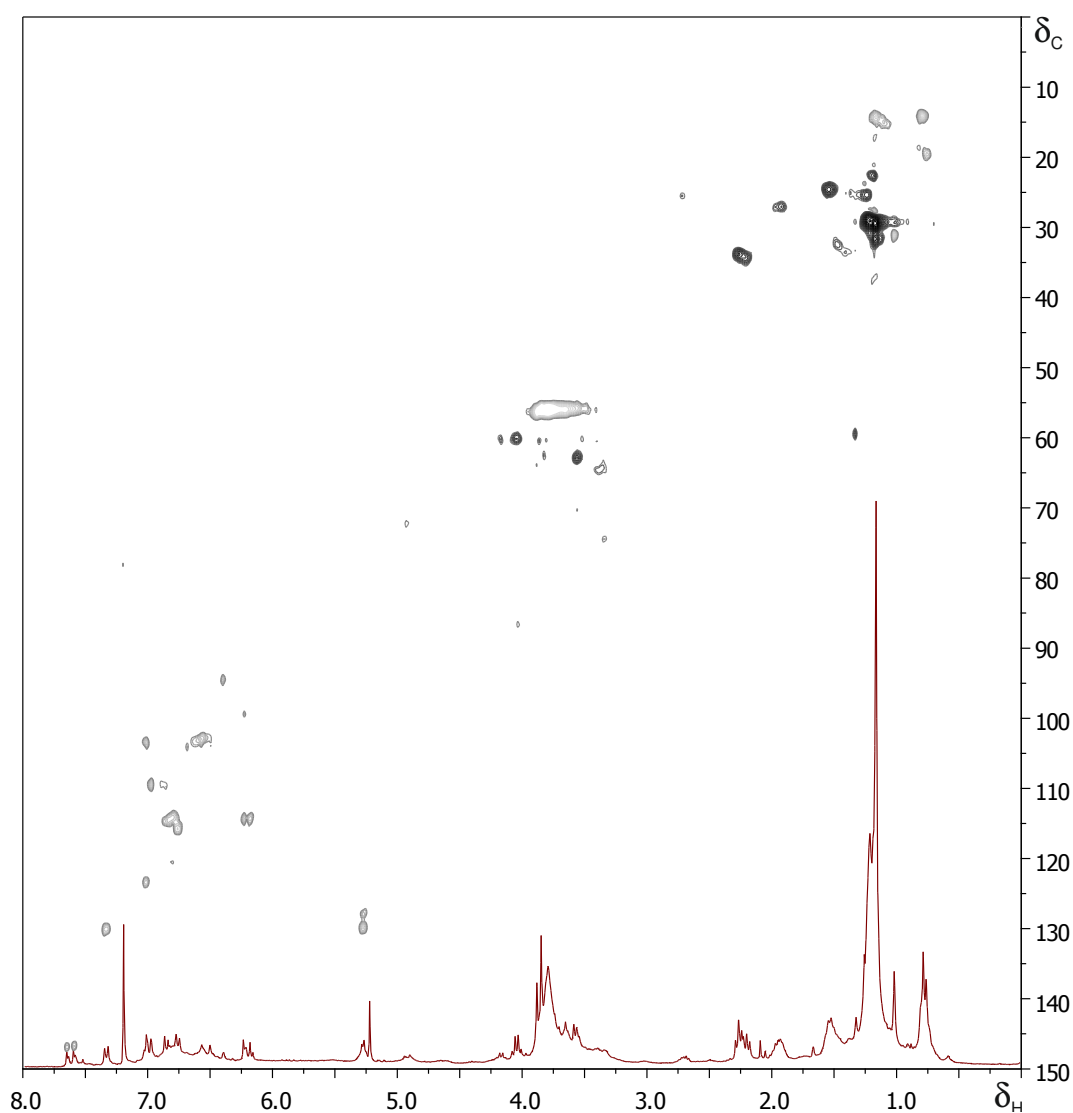
Figure 13. ^{13}C-^1H HSQC spectrum (*^1H spectrum inserted*) of the 1st NML extract (25 °C, 300 MHz, CDCl$_3$).

Table 13. Results of the elemental analysis (CHN) of the CH_2Cl_2 extract and extraction residue of NML.

Sample	% C	% H	% N	% O*
Annikki NML	61.2	6.3	1.6	30.9
extraktion residue	59.5	5.6	2.2	32.7
1st extract	58.7	7.0	0.1	34.2

* calculated value

The increased oxygen content of the extract indicates the removal of carbohydrates although any correlations were found in the polysaccharide anomeric region of the ^{13}C-^1H HSQC spectrum of the first NML extract (Figure 13). The carbohydrate content was not quantified exactly, but it might be possible that the amount is below the HSQC detection limit and drops into noise signals. The decreased carbon and hydrogen content in the solid extraction residue also suggests the removal of fatty acids. On the contrary, proteins were obviously not removed as the nitrogen content is slightly enriched in the extraction residue (Table 13).

The findings from 2D NMR and elemental analysis are in good agreement with the results of the simultaneous thermal analyses (Figure 9). The 1st extract exhibits the highest mass loss of the measured samples with 79.5 wt%, indicating the presence of low molecular, temperature labile compounds. The sample starts to decompose at approximately 100 °C whereas the solid extraction residue exhibits a slightly increased temperature resistance compared to dry *Annikki* NML due to the removal of these labile compounds.
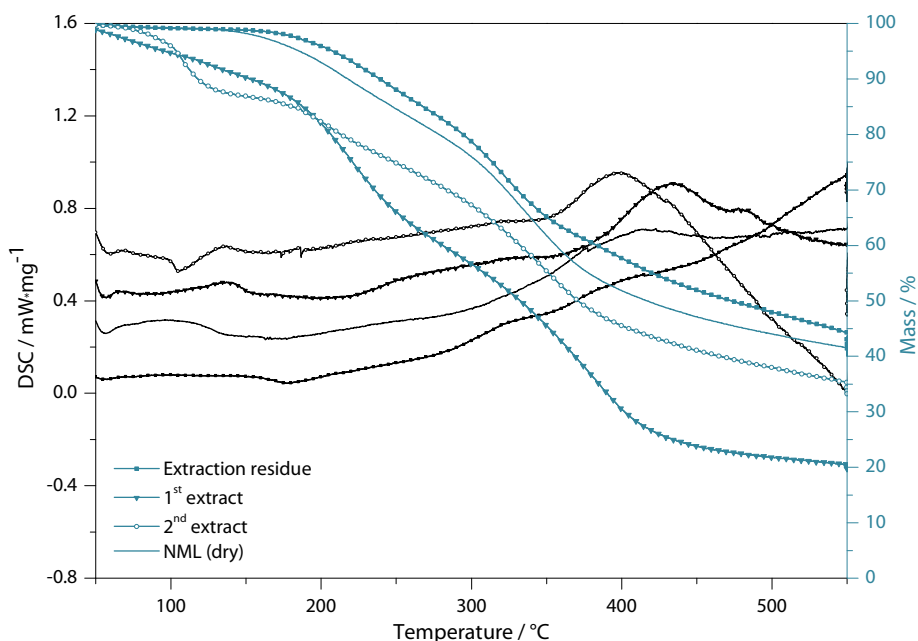
Figure 14. Mass loss (black) und DSC curves (turquoise) of extraction residue and extracts of NML.

Phosphitylation and subsequent ^{31}P NMR measurement showed, that the extraction residue clearly exhibits less sharp signals (Figure 15). This observation is again consistent with the previous analyses and the decrease of sharp signals is most likely due to the loss of low

molecular lignin subunits as well as fatty acids (134.94 ppm). In Table 14 the contents of different functionalities present in original and extracted low molecular weight *Annikki* lignin (NML) are compared. The values were determined by quantitative evaluation of ^{31}P NMR measurements according to point 2.4.1. The amount of phenolics in extracted NML is reduced by 11 % in contrast to original NML, whereas guaiayl (G) subunits account for the largest part amongst the uncondensed phenolics. The condensed phenolics, 4-O-5' and 5-5', are reduced by one third and by half. The amount of aliphatic hydroxyl groups is, on the contrary, slightly increased by four percent. The reduction of carboxylic groups by 5 % can be reduced to the extraction of fatty acids, which, however, is lower than expected.

Table 14. Functionalities present in original and extracted low molecular weight *Annikki* lignin (NML).

Functionalities	NML / $mmol \cdot g^{-1}$	Extracted NML / $mmol \cdot g^{-1}$	^{31}P Chemical shift[*] / δ ppm
aliphatic OH	2.97	3.09 (+4 %)	148.24 147.17 146.82
total phenolics	1.05	0.93 (−11 %)	
condensed phenolics	0.14	0.09 (−36 %)	
Diphenyl-methane	0.00	0.00	
4-O-5'	0.12	0.08 (−33 %)	142.22 142.13
5-5'	0.02	0.01 (−50.0 %)	140.81
uncondensed phenolics	0.91	0.84 (−8 %)	
S	0.09	0.10 (+11 %)	142.92
G	0.53	0.47 (−11 %)	139.57 139.32
H	0.29	0.28 (−3 %)	137.85 137.38
carboxyls	1.09	1.04 (−5 %)	135.31 135.24 134.92 (fatty acids)

Sharp signals which disappeared or significantly decreased upon extraction with CH_2Cl_2; n.a. = not assigned.
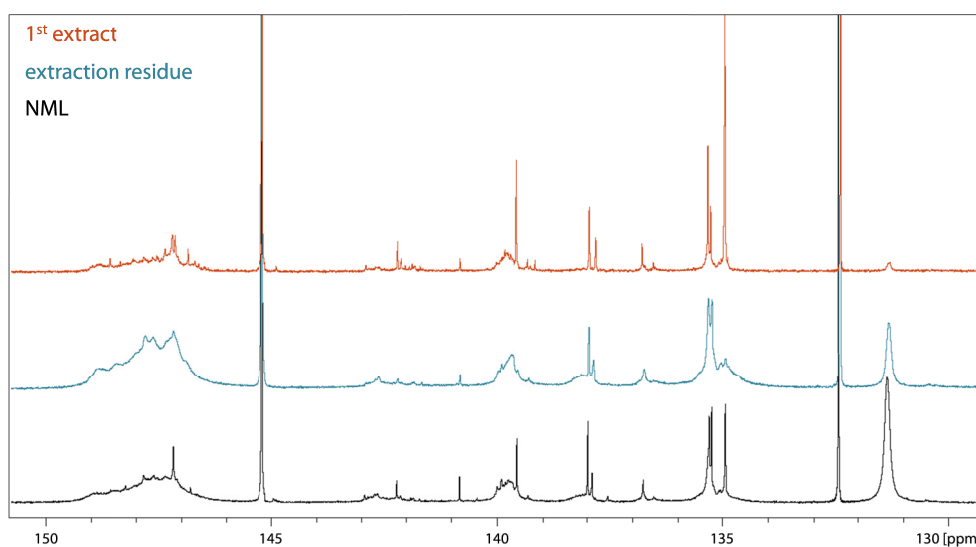
Figure 15. ^{31}P NMR spectra of original and extracted NML as well as 1st DCM extract (, 25 °C, 200 MHz, $CDCl_3$).

2.8 LIGNIN BATCHES

The wheat straw lignins provided by Annikki GmbH Graz were used as received, apart from drying under vacuum. The obtained samples differ either in the batch or in the fractionation after the pulping process. Lignins, delivered right after the pulping process without any further purification step are referred to as *Gesamtlignin* (batches GL1-GL5). GL6 was produced at higher temperature and is hereafter called L_HT. NML (low molecular weight lignin) and L_THF (in tetrahydrofuran soluble fraction of GL6) were obtained after an additional fractionation step after pulping.

Hydroxyl number, molecular weight and polydispersity of all used lignin samples are listed in Table 15. The amount of hydroxyl groups in *Annikki* lignins was found to be approximately 4 mmol·g^{-1}, which is slightly lower compared to the commercially available *Kraft* lignin 2 (KL2). The hydroxyl number of KL1 could not be determined as the sample was to a great extend insoluble in the DMF / pyridine ^{31}P NMR solution. Thus, any characterization of the sample was not feasible and mainly KL2 was used as comparative sample to *Annikki* lignins. The calculations of molar ratios for the modification reactions of lignin are based on this hydroxyl number (specified as 1 equivalent).

Lignin batches GL2-GL5 were produced in the same way and thus feature very similar molecular weight distributions. The molecular weight distribution was determined via HPLC-SEC by Annikki GmbH (cp. section 2.4). As not every delivered sample was investigated, a representative value is given. This is also the case for the methoxy number. The elemental composition for all lignin batches is given in Table 10 (section 2.3).

Table 15. Amount of total hydroxyls, number average molecular weight (M_n), polydispersity (PDI) and methoxy number of the different lignins.

Lignin	Batch	Total hydroxyls / mmol·g^{-1}	M_n / g·mol^{-1}	PDI	OMe / %
NML	*unknown*	4.0	~900	–	–
GL1	*unknown*	3.9	~1380	~4.9	–
GL2	GL_L23	4.3			
GL2 extracted	GL_L23	4.3			
GL3	GL_L27	4.4	~1250	~4.0	12.3
GL4	GL_L49	4.8			
GL5	GL_L57_3,4,5	4.3			
L_HT (GL6)	GL_L66	4.1	~1050	~4.2	13.1
L_THF (GL6)	GL_L66	4.0			
KL1	KL (471003-100G)	*n.d.*[a]	*nd*[a]	*nd*[a]	–
KL2	KL (370959-100G)	5.2	1380	9.3	–

[a] nd = not determined due to insolubility; specified by a M_w of ~10000 by Aldrich

Summary — wheat straw lignin provided by Annikki GmbH

- *3.9–4.8 mmol OH / g (mainly aliphatic) (^{31}P NMR after phosphitylation)*
- *Consists mainly of S and G units connected via β-O-4' linkages (^{13}C-^{1}H HSQC NMR)*
- *M_n ~ 1250 g·mol^{-1} (polydispersity ~ 4) (HPLC-SEC)*
- *T_g = 113.8 °C (DSC)*
- *~ 60 % mass loss at 550 °C (STA)*
- *~ 8 wt% fatty acids (gravimetrically determined after DCM extraction)*

3.1 STATE OF THE ART

Many efforts have been made, and are still made, to transmute the highly complex biopolymer lignin into a homogeneous, organosoluble feedstock suitable for further industrial applications. The central focus is to gain distance from low value applications such as combustion or bulking agent. However, chemical modifications of lignin are often necessary to achieve sufficient compatibility with conventional polymers, when applied as filler or integral part in composite materials. Up to now, the highly complex structure of the biopolymer prevented its applications in high-end uses. This issue should be overcome by the introduction of specific functionalities to attain tailored properties. A successful, efficient and sustainable modification of lignin is the key prerequisite for higher value adding of the natural resource.

Lignin bears various functional groups and thus potential sites for modifications. Besides the modification of hydroxyl groups, novel chemical active sites can be introduced by reactions like halogenation, sulfonation, amination, hydroxyalkylation, alkylation, dealkylation or nitration. However, these reactions were less intensively investigated than reactions involving hydroxyl groups, such as esterification, etherification, oxidation, reduction, phenolation, silylation or urethanization (Table 16).[23]

Main reason for the modification of lignin is to achieve improved solubility, or compatibility respectively, in non-polar media.[119] Functionalization of the natural resource is often done by esterification or etherification of the free hydroxyl groups, both aliphatic and aromatic, present in lignin. Mostly, carboxylic acid anhydrides or chlorides, also derived from fatty acids, are applied in alkaline media of triethylamine for instance.[2,120,121] Esterification of the hydroxyl group is probably still one of the easiest modification methods regarding reaction compounds as well as conditions. It is also reported, to selectively esterify the phenolic hydroxyl groups by using NEt$_3$ as base.[23] Acetylated lignin is often synthesized in this manner to facilitate characterization by achieving solubility in organic media as not completely dissolved samples constitute a serious source of error.[112]

In 1988 Dournel *et al.* described the anchoring of polymerizable groups onto lignin through etherification of the hydroxyl groups via phase transfer catalysis.[122] However, this method was not further pursued and nowadays, besides the use of alkyl sulfonates or halogenides, the etherification with alkylene oxides is mainly applied.

The highly complex biopolymer can also be liquefied to meet tailored viscosity or compatibility requirements. A widely used method therefore is the alkoxylation with ethylene or propylene oxide, catalyzed by sodium or potassium hydroxide at elevated temperatures (160–290 °C). Besides lowering the viscosity and increasing the solubility, the numerous functional groups are unified and a polyol featuring exclusively aliphatic hydroxyl groups is obtained. Thus, the reactivity of the biomaterial is significantly enhanced, especially for applications in polyurethanes, epoxy or phenol formaldehyde resins.[24,123,124]

Table 16. Summary of the main types of lignin modification reactions.[23]

Type	Lignin site	Reagents	Introduced moiety
esterification	-OH	carboxylic acid anhydrides or chlorides (O=C(Cl)R), base (e.g. NEt₃)	-C(O)R
urethanization (reaction with isocyanates)	-OH	isocyanate (RNC=O),	-C(O)NHR
etherification	-OH (mainly phenolic)	alkylene oxides, base (KOH, NaOH)	-oligoethers
oxidation	-OH	nitric acid, permanganate, chlorine, chlorine dioxide, hypochlorite	-COOH elimination of OMe and phenolic OH
phenolation (phenolysis)	-OH	phenol, sulfuric acid	-(2-hydroxyphenyl)
silylation	-OH	silanes (R3SiCl, R2SiCl2)	-SiR3, -SiR2
sulfomethylation-sulfonation	-OH, -CO, -COOH	CH₂O, NaOH, Na₂S₂O₅	-CH₂SO₃Na
amination	*ortho* position of a phenolic OH	diethylamine, formaldehyde	-CH₂N(CH₃)₂
hydroxyalkylation	C₅ of G units; α to C=O and β of α-β unsaturated units in side chains	aldehydes (O=CH-R), NaOH	-CH(OH)R
alkylation	-OH	alkyl sulfate, base (NaOH) alkyl iodide, base (K₂CO₃)	-alkyl
dealkylation	-OMe	sulfur (liquid), NaOH	elimination of OMe groups
nitration	aromatic ring, -OH	nitric acid, acetic anhydride (also acetic or sulfuric acid)	-NO₂
halogenation	aromatic ring	chlorine, bromine or iodine gas	-Br, -Cl, -I

Chemically modified lignins are either applied as physical components or as (macro-) co-monomers for polymeric materials. In the first case, modifications are mostly necessary to obtain sufficient compatibility between the components. By the targeted 'masking' of functional groups, increasing the solubility and transforming lignin into a more homogeneous material, the interfacial energy between lignin and the matrix can be reduced and thus their compatibility enhanced. In the second case, the introduction of specific reaction sites, suitable to be covalently bound into the respective polymeric network, is required.[25]

Unfortunately, the use of lignin as main raw material often seems to be negatively counterbalanced by the transformations carried out. The laborious modifications are often to the detriment of sustainability, efficiency and price of the renewable resource. It should be taken into account, that costly transformations prior to utilization are only justified in the case of particular improvements or lack of alternatives. Sustainability, efficiency and

industrial feasibility should be main concerns when developing new modification protocols. This consideration seems to be consistent, but nevertheless this aspect is often disregarded.[25]

In this contribution, special attention was paid on the development of a modification method which meets the criteria of a *green* and sustainable synthesis. Thus, the use of metal catalysis, petroleum-derived chemicals and of most solvents should be avoided as far as possible. In terms of industrial feasibility, a one pot synthesis which requires no additional purification step is desirable.

This chapter is mainly based on the reviews of A. Gandini *et al.*,[25] S. Laurichesse *et al.*[23] and E. Ten *et al.*,[80] which are all primarily about modifications of lignin and the use of lignin derivatives in polymers. As there is a large variety of transformations (cp.Table 16) and utilizations of lignin, the most important will be described briefly to impart a comprehensive overview of this extremely broad field.

THERMOSETS

Lignin is widely used as polyol precursor in the synthesis of polyurethanes as well as epoxy resins. The principal purpose of modifying lignins is to have as many reactive and easily accessible hydroxyl groups available as possible. Additional requirements to address are a uniform molar mass and less hyperbranching, which is often realized by modifications with alkyleneoxides.

Already in the 1980s, Glasser *et al.*[125] synthesized propoxylated lignin and applied the macropolyols for the production of PUs and epoxy resins. The etherification of lignins with alkylene oxides yields, in contrast to the starting material, well soluble polyols. In the presence of a basic catalyst (usually NaOH or KOH) lignin oxianions are formed, which then react with oxiranes. Mostly propylene oxide (PO) is used, whereas the phenolic hydroxyl groups are selectively etherified by this 'grafting from' approach (Scheme 5).[123a, 126] Homopolymerization as well as isomerization of PO occur as side reactions and lead inevitably to product mixtures. It was found, that the homopolymer content decreases with higher lignin / PO ratio, independently from the catalyst content.[123b]

Scheme 5. Propoxylation of lignin.

(R = OMe or H)
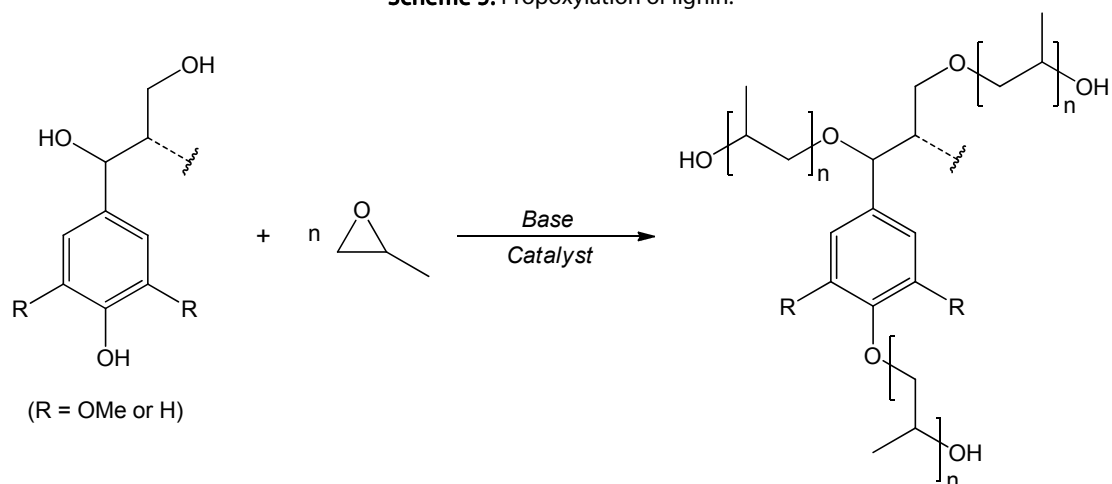
Although the homopolymer content influences reactivity and mechanical properties of the final products, rigid PU foams with these modified lignins exhibit good thermal properties and dimensional stability, even after aging. The formulations were prepared without any other polyol or chain extender.[124,127] Poly(ethylene glycol) (PEG) can be mixed with lignin as additional polyol to facilitate the reaction with isocyanate for instance.[128] Propoxylated lignins are well suited as composite material for polyurethane foams, as they also affect properties like moisture stability and flame restistance positively.[24,129]

Another strategy to provide as many hydroxyl groups as possible for the condensation with diisocyanates, is to partially 'block' hydroxyl groups by ethylation with diethyl sulphate prior to propoxylation. Thus, a chain extension of the remaining hydroxyl groups, terminated by primary or secondary hydroxyl groups, is achieved. The lignin derivatives can be used as macromonomers in the synthesis of numerous PUs using aliphatic or aromatic diisocyanates. In some cases, poly(ethylene glycol) is added as macrodiol comonomer. Rigid as well as elastomeric PUs were obtained and their physical and technological properties were specified. The crosslinking degree was determined via dynamic mechanical thermal analysis (DMTA) and possible applications were examined.[130]

Aminated lignin, featuring an aminoethyl group adjacent to phenolic OH groups, were synthesized by the reaction with diethanolamine. The lignin polyol reacts with diphenylmethane diisocyanates and glycol to form PU foams using H_2O as blowing agent.[131]

Nitrolignin was synthesized by reacting lignin with nitric acid in nonaqueous solvents (e.g. acetic anhydride, acetic acid or fuming sulfuric acid) and used for the preparation of graft interpenetrating polymer networks from PU.[132]

D'Alelio patented already in 1975 lignin derivatives containing copolymerizable oxirane groups.[133] Later, Glasser and coworkers reacted partially oxypropylated lignins with epichlorhydrin and obtained macromonomers bearing multiple oxirane groups.[134] The crosslinking of these polyoxiranes according to standard procedures with aromatic diamines was studied by DMTA. The high content of aromatic compounds led to premature vitrification resulting in a slow-down of the late curing stages.

Sodium lignosulfates were treated with epichlorhydrin and then reacted with maleic anhydride to form novel epoxy resins, whereas primarily the network formation was investigated in this contribution.[135] Wool *et al.* added butyrated lignin to unsaturated epoxy resins, synthesized via radical polymerization of acrylated epoxidized soybean oil and styrene.[136] Furthermore the esterification of lignin with acrylates and subsequent preparation of resins via atom transfer radical polymerization (ATRP) is known.[137]

Lignins bearing alkenyl units were investigated as macromonomers for chain polymerizations. However, it is not feasible to reach uniformity of the lignin macromonomers and thus, the chain growth cannot be controlled. Lignins featuring acrylic moieties were obtained upon reaction with acryloyl chloride or methacrylic anhydride. However, a high degree of substitution was accompanied by free radical polymerizations or copolymerizations with ill-defined products.[2,138] The reaction of lignin with chloroethyl vinyl ether and following cationic polymerization of the derivatives yielded insoluble crosslinked materials.[122]

ADHESIVES

One of the most prominent fields of lignin application is the substitution of non-renewable phenol in wood adhesives, namely in phenol formaldehyde (PF) resins. Besides the utilization of unmodified lignin (see section 1.3), lignin is also applied after demethylation, phenolation or methyloleation. The latter is the introduction of methylol groups in C_5 position of G units and also to a small extend at side chains. Using this derivative, the substitution of 40 wt% phenol was possible while the glue maintained satisfactory bonding strength.[139] Phenolation (or phenolysis) is the treatment of lignin with phenol in acidic medium, whereas phenol condenses with aromatic units as well as side chains. Phenolysis is primariliy applied for lignosulfonates to increase the content of phenolic hydroxyl groups. Thus, a higher reactivity as phenol substitute can be reached due to the presence of phenolics featuring free ortho and para positions. These derivatives can also function as crosslinking agent.[140]

Demethylated lignin, prepared upon treatment with molten sulfur and sodium hydroxide, and polyethylenimine were used for a new, formaldehyde-free water resistant wood adhesive.[141] Dimethylsulfide, accruing during demethylation of lignin, can be oxidized to produce DMSO (Gaylord Chemical Company, US).[23]

A composite material of PVC / wood-flour fabrics containing aminated lignin (2 wt%) with enhanced mechanical performance was reported.[142] The improved interfacial bonding of the polymer matrix led to higher tensile and impact strength as well as decreased water absorption.

THERMOPLASTICS & ELASTOMERS

In thermoplastics and elastomers, modified lignins often appear as reinforcing agent in order to increase the thermal, mechanical or UV stability.[80]

Methylated or ethylated *Kraft* lignins were prepared using diethyl sulphate and diazomethane and blended with aliphatic polyesters, whereas in some cases also poly(ethylene glycol) (PEG) was added.[143] As expected, the obtained materials featured viscoelastic behavior in the region of the T_g, but are not competitive due to costly lignin fractionation and functionalization.

Reaction products of lignins and lignosulfonates with epichlorhydrin were tested in blends as well as reactive compositions with PE / PP,[144] hydroxypropyl cellulose[145] and polyalkanoates.[146]

Kraft lignin was modified with maleimide featuring an aromatic carboxylic acid, and homogeneous blends with poly(vinyl alcohol) (PVA) were produced.[147] The thermal as well as the photochemical stability were increased upon the addition of 5–15 wt% modified *Kraft* lignin. Improvements may be induced by hydrogen bond formation between the two components.

Esterification of lignin using bifunctional reactants results in polyester networks, whereas often co-macromonomers such as PEG, which is simultaneously a co-solvent, are added.[148]

More and more frequently, lignin is utilized as copolymer in biocomposites. Glasser and coworkers [149] reported blends of various *Organosolv* ligninesters with biodegradable thermoplastics, such as cellulose esters, polyhydroxybutyrate (PHB) or starch-caprolactone copolymers. The introduction of ligninesters was necessary as blends with unmodified lignins didn't meet the requirements.

Poly(lactic acid) (PLA) exhibits only low impact strength, small elongation at break, weak thermal properties and poor UV-light barrier properties.[150] Composites with lignin are proposed to improve the thermal as well as the mechanical characteristics of the polyester. A more recent approach is the modification of lignin via ring opening polymerization (ROP) of lactones and lactide.[151] Waymouth *et al.*[152] published a solvent-free, organocatalyzed method to prepare lignin / PLA copolymers (Scheme 6). The smart synthesis of these lignin-grafts is catalyzed by *N*-centered nucleophiles and can be performed in bulk at elevated temperatures (100–150 °C). They reported a high grafting capacity of lignin, whereas preferably aliphatic hydroxyl groups are involved. The graft length is controllable by the blend ratio of lignin and lactide as well as via previous acetylation.

Scheme 6. Synthesis of a renewable lignin-PLA copolymer.[152]
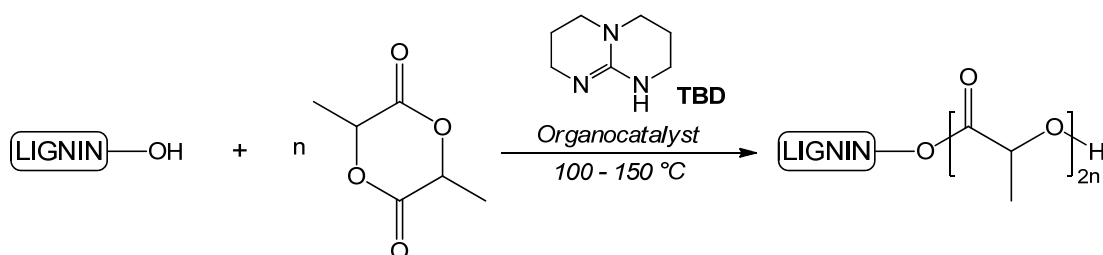
Lignin-layered double hydroxide (lignin-LDH) complexes were melt compounded to prepare styrol-butadiene rubber (SBR) / LDH composites. The obtained rubber composites featured improved mechanical properties such as modulus, tensile strength, elongation at break as well as hardness. Elastic deformation led to better stress transfer at the interface due to the high aspect ratio of the lignin-LDH reinforcement. The LDH particles were found to be well dispersed in the rubber matrix in the presence of lignin.[153]

Hexamethylenetetramine modified lignin was also used to reinforce rubber. In contrast to carbon black filled rubber, lignin containing rubbers did not achieve the requirements due to a reduced tensile strength. The weak performance may be reduced to the approximately one order of magnitude larger particle sizes of lignin. Additionally, the interfacial adhesion between polar lignin and hydrophobic matrix is rather poor.[154]

CONSTRUCTION MATERIALS

Kraft lignin was oxidized prior to sulfomethylation to increase the reactivity between lignin and the methylene sulfonic group (due to less steric hindrance as methoxyl and phenolic hydroxyl groups are eliminated during oxidation). The transformation showed hardly any effect on the molecular weight, but the dispersity was notedly decreased. The lignin derivative was tested as dispersing agent for cement mixtures. The adsorption of sulfonated lignin on the surface of cement particles was higher than that of other lignin derivatives due to increased charge density. Thus, the fluidity of the cement paste could effectively be improved by the addition of 0.5 wt% sulfonated lignin.[155]

CARBON FIBERS

Carbon fibers exhibit outstanding mechanical and thermal properties at low weight, which makes them extremely valuable in various industries. Amongst many different applications, carbon fibers are often embedded into polymeric materials as reinforcing agent. Currently, there is an increasing demand for high performance light-weight materials and lignin constitutes a well-suited bio-based precursor for this growing sector. Kessler *et al.* patented carbon fibers produced from a composition consisting of esterified lignin and PLA.[156] Lignin was esterified with butyric anhydride and the derivative was mixed with PLA. Fibers were spun from this blend and subsequently heated to give carbon fibers.

Lignin was modified using dicarboxylic acid anhydrides and melt-processed by fiber extrusion.[157] Subsequent oxidative stabilization and carbonization yielded microstructured carbons. It was found, that the modification contributes decisively to the later structure of the carbon fibers. Thus, phthalic anhydride modified lignin exhibited a higher micro-scale porosity than carbon fibers from unmodified lignin.[80]

BIOMEDICAL APPLICATIONS

Hydrogels are three-dimensional networks of crosslinked hydrophilic homopolymers, copolymers or macromonomers. The insoluble polymer matrices can absorb a multiple of liquid compared to their dry weight. This feature makes the materials highly attractive for biomedical applications, apart from their biocompatibility. They could be utilized for the transport of drugs, metabolites or nutrients in and out of cells.[80] The microbially produced polysaccharide xantham gum can be used for the synthesis of biodegradable hydrogels, but the properties are rather poor. Copolymers of xantham gum and lignin are expected to feature better thermo-chemical properties and higher reactivity, while providing thermo-oxidative and antimicrobial activity.[158]

Vermerris *et al.* published the synthesis of lignin nanotubes and -wires.[159] A lignin base layer was crosslinked onto an aluminium membrane, ensued by the peroxidase-catalyzed addition of dehydrogenation polymer and dissolution of the membrane in dilute phosphoric acid. The obtained materials bear a potential as efficient, cost-effective and biocompatible carrier for DNA or therapeutic agents. The cytotoxicity of the lignin nanotubes is reported to be notedly lower compared to carbon nanotubes. The materials may be able to target specific cells, tissues as well as organs and can thus be suitable to transport anticancer drugs.

3.2 ESTERIFICATION OF LIGNIN

Lignin was successfully esterified using carboxylic acid anhydrides[1] or chlorides and *N*-centered bases / nucleophiles (pyridine, 4-dimethylamino pyridine or triethyl amine). All performed esterification reactions are listed in Table 23 according to the standard operating procedure (SOP) described in section 3.2.2. Acid catalyzed conversions proceeded generally worse and thus the research activites were focused on esterifications in alkaline medium. The synthesized ligninesters are categorized according to their introduced functionalities (Table 17) and compared hereafter (section 3.2.1). Lignins received from Annikki GmbH were used without any further fractionation or purification except drying in vacuum. Thus, the straight-forward use directly from the pulping process could be demonstrated.

The synthesized ligninesters were characterized by ATR-FTIR spectroscopy, ^{31}P NMR spectroscopy, HPLC-SEC, CHN elemental analysis and simultaneous thermal analysis (STA) as described in chapter 2 and the results are discussed in detail in the following section.

Table 17. Moieties introduced by esterification of lignin.

Esterifications of lignin were conducted to increase the solubility of the biopolymer in non-polar media. Firstly, lignin was acetylated according to literature protocols[2] and subsequently the chain length of the esterification reagents was increased. Thus, the solubility of the synthesized ligninesters could be enhanced by moving from acetyl groups up to C_{18} units. The quantities of esterification reagents were calculated based on the total number of hydroxyl groups of the according starting lignin, determined via ^{31}P NMR spectroscopy (see section 2.1.1).

The majority of the modifications was performed applying carboxylic acid chlorides due to their easier accessibility compared to the corresponding anhydrides. Besides this, carboxylic acid chlorides are the more reactive species compared to anhydrides and the esterification proceeds in better stoichiometry accumulating less side products as not one equivalent of free carboxylic acid is generated with every newly formed ester bond.

The idea of developing higher value added materials from renewable resources directed us towards the use of naturally available fatty acids for lignin modification. Thus the straight-forward use of long chain fatty acids was also explored (entries 30, 31, 51 and 81, Table 23), as well as the transesterification of fatty acid methyl esters (entries 52, 53 and 77 Table 23). Unfortunately numerous trials to achieve ligninesters via the direct use of fatty acids to economize the process failed.

Thus, lignin esterification was pursued using long chain and cyclic carboxylic acid chlorides. By the use of 10-undecenoyl chloride, a terminal alkene is introduced into the lignin network while the solubility is simultaneously enhanced by the C_{11}-chain. The terminal double bond is not only an appropriate moiety for poymerizations, but also an eminently suited site for further modifications. Using palmitoyl and oleoyl chloride, the solubility of the ligninesters was further enhanced, thus even solubility in non-polar solvents like cyclohexane could be achieved. With oleoyl chloride, an internal double bond is introduced additionally. Attempts were also made to introduce norbornene units by esterification of lignin with norbornenoyl chloride (entries 19–24, Table 23), to achieve lignin derivatives for ring opening metathesis polymerization (ROMP). The introduction of the cyclic, strained norbornene unit was successful, but due to weak solubility in nonpolar media this modification was not further pursued. Even the double functionalization of lignin, first, with norbornenoyl chloride and second with palmitoyl chloride could not overcome this issue.

Another critical point was the amount of remaining free fatty acids (FFAs) in the product, which are formed upon hydrolyzation of the esterification reagent. Suitable methods for the determination of the FFA content as well as their removal from the ligninester will be discussed in section 3.2.1.

In the following, the characteristics of the obtained ligninesters will be described and results of successful modifications will be illustrated in detail.

3.2.1 RESULTS - LIGNINESTERS

ATR-FTIR spectroscopy is a well suited tool for the rapid characterization of esterified lignins. Figure 16 shows the ATR-FTIR spectra of the synthesized short chain ligninesters (entries 2, 3, 12, 16, Table 23) in comparison to original *Annikki* lignin (NML) (top) as well as the long chain esters (entries 29, 35, 80, Table 23) in comparison to GL1 (below). The distinctive resonance of the ester C=O vibration (1750–1730 cm^{-1})[160] allows for a quick evaluation of a successful esterification reaction. A detailed interpretation of a lignin ATR-FTIR spectrum is given in chapter 2.2 (Figure 9).
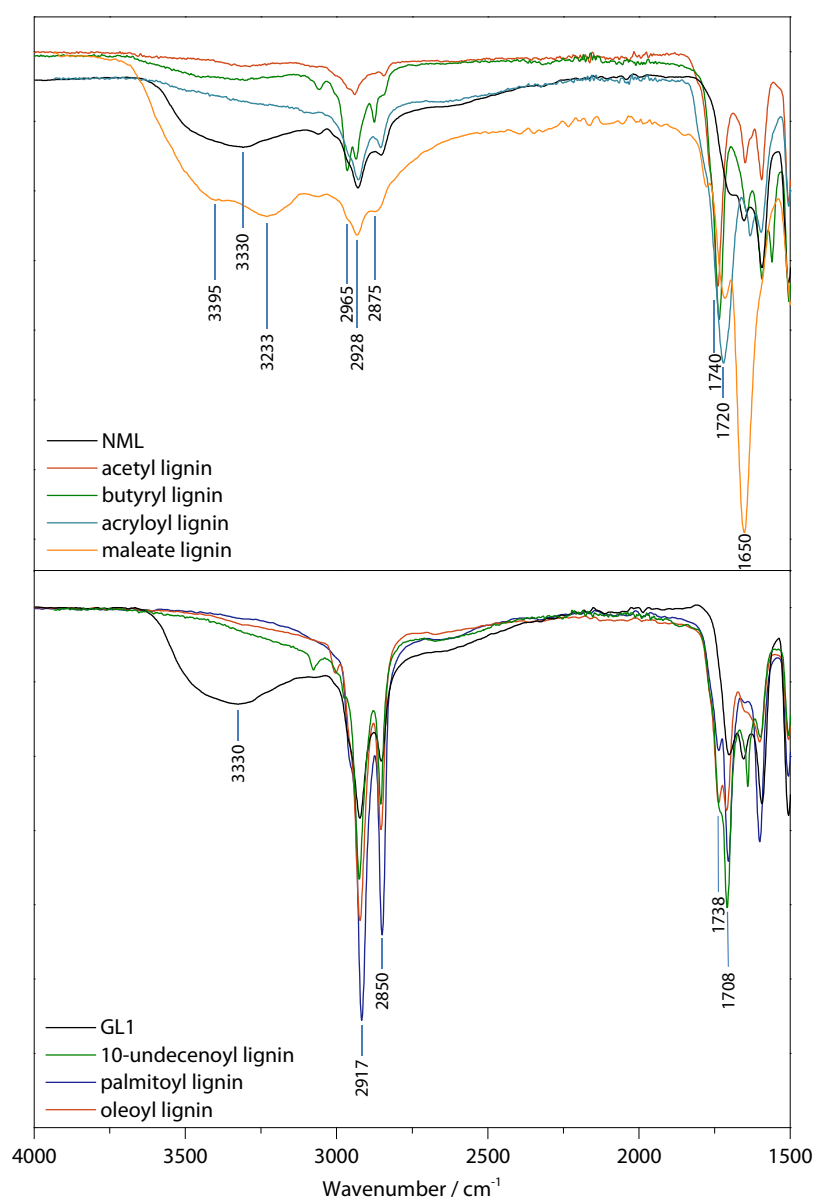
Figure 16. ATR-FTIR spectra of selected short chain ligninesters (samples 2, 3, 12 and 16) in comparison to original *Annikki* lignin (NML) (top) and long chain ligninesters (samples 29, 35 and 80) in comparison to GL1 (below).

The hydroxyl resonance (3330 cm^{-1}) disappears in the spectra of acetyl, butyryl as well as acryloyl lignin samples and the carboxyl resonance of the formed ester linkages arises at 1740 cm^{-1}. The less pronounced resonance visible in this region (1720 cm^{-1}) of the NML spectrum may originates from ester moieties or carboxylic acids present in lignin. Acryloyl and maleoyl lignin also show a resonance at this wavenumber, which is most likely the result of remaining hydrolyzed esterification reagent in the product. Maleoyl lignin additionally shows a very pronounced resonance at 1650 cm^{-1}, most likely originating from the introduced carboxylic acid groups which also contribute to the hydroxyl resonances at 3395 and 3233 cm^{-1}. In case of long chain ligninesters (Figure 16, below), the hydroxyl resonance (3330 cm^{-1}) completely disappeared, indicating a successful esterification. The according ester C=O vibrations are detected at 1738 cm^{-1}. As is the case for short chain ligninesters, resonances of hydrolyzed carboxylic acid chlorides appear at 1708 cm^{-1}. Very pronounced vibrations of the introduced CH$_2$ groups appear from 2970–2850 cm^{-1} in the spectra of long chain ligninesters. In the case of short chain ligninesters, they are partly overlayed by resonances of aliphatic lignin side chains (2928 and 2850 cm^{-1}).

^{31}P NMR spectroscopy of the ligninesters after phosphitylation allows for a more accurate determination of the amount of esterified hydroxyl groups, the so-called degree of substitution (DS). In Table 18, the amount of the different hydroxyl groups of acetyl lignin is compared with the according original *Annikki Gesamtlignin* (GL1). Acetyl lignin provides the most detailed comparison of esterified hydroxyl groups as excess acetyl chloride or the corresponding hydrolyzation product can be easily removed. In the ^{31}P NMR spectrum of acetyl lignin compared to *Annikki Gesamtlignin* (GL1) (Figure 17), the decrease of the hydroxyl signals is also clearly recognizable. The aliphatic hydroxyl groups (δ 150–146 ppm) exhibit the sharpest dropping (97 %), but also the phenolic hydroxyl groups (δ 144–137 ppm) decrease distinctly by 79 %. Due to the three times higher amount of aliphatic hydroxyl groups in contrast to phenolic hydroxyl groups, their less complete esterification is only of little consequence. From the results of ^{31}P NMR spectroscopy, a distinction of the accessibility of lignin hydroxyl groups was deduced. As the ratio of phenol-terminated S, G and H units is altered in lignin derivatives, there must be a reactivity difference between these three units. The phenol-terminated G and H units are obviously preferably esterified with acetyl chloride compared to S units. A possible explanation would be the steric hindrance caused by adjacent methoxyl groups, shielding the intermediate hydroxyl group of the S moiety. The content of condensed phenolics is only slightly decreasing, but these moieties account anyway for the least contribution of the total hydroxyl number. The drastic decrease of carboxyls is most probably due to the removal of the fatty acids present in lignin during work-up.

As the ^{31}P NMR results are determined in dependence of the sample weight, the values were corrected according to the 'real' lignin content in the sample. This correction was introduced for all long chain ligninesters due to their significant contribution to the sample weight. Thus, for a lignin derivative where 1 g of lignin was reacted with 1 g of fatty acid chloride, the experimentally obtained values have to be compared with halved values from the starting lignin due to the 'real' lignin content of 50 wt% in the sample. This approach should avoid the underestimation of the amount of residual, not esterified hydroxyl groups. If NML is used as

starting lignin, the total hydroxyls of palmitoyl lignins have to be compared with 1.92 mmol OH / g ($\cong$ 48 wt%) and those of oleoyl lignins with 1.83 mmol OH / g ($\cong$ 45 wt%) if 1 equivalent (with respect to the lignin hydroxyl groups) of fatty acid chloride was applied. The collected values for all used starting lignins regarding to palmitoyl and oleoyl lignins are listed in Table 50 (Appendix).

Table 18. Amount of different functionalities present in GL1 and acetylated GL1 (sample 10, Table 23), determined by quantitative ^{31}P NMR spectroscopy.

Functional group	GL1 / mmol·g^{-1}	Acetyl lignin / mmol·g^{-1}
total hydroxyls	3.86	0.17 *(–96 %)*
aliphatic OH	3.28	0.09 *(–97 %)*
total phenolics	0.58	0.08 *(–87 %)*
total uncondensed phenolics	0.47	0.07
syringyl-OH	0.09	0.01
guaiacyl-OH	0.14	0.03
p-hydroxy-phenyl-OH	0.24	0.03
S / G / H ratio (phenol-terminated)	1.0 / 1.0 / 2.6	1.0 / 3.6 / 3.6
total condensed phenolics	0.10	0.01
diphenyl-methane	0.02	0.00
4-O-5´	0.04	0.01
5-5´	0.04	0.00
carboxyls	1.21	0.7
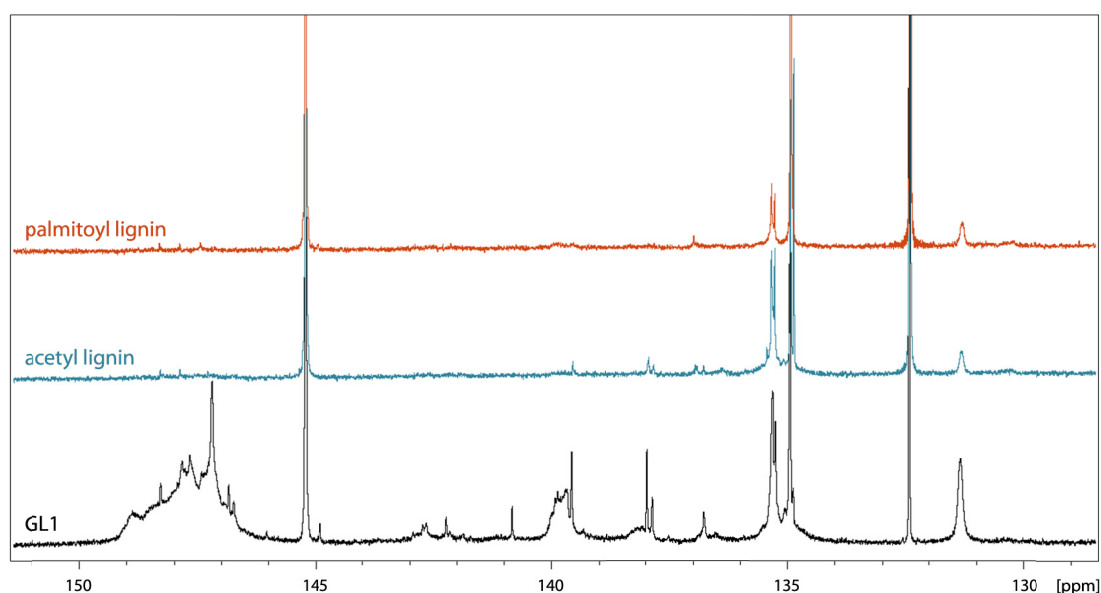
Figure 17. ^{31}P NMR spectra of starting lignin (GL1), acetyl and palmitoyl lignin (samples 10 and 35, Table 23), (25 °C, 200 MHz, CDCl$_3$).

The degree of substitution (DS) obtained with long chain fatty acid chlorides was far from the DS being achieved with acetyl chloride (96 %) (Table 51, Appendix). Evaluation of ^{31}P NMR data revealed that 34–93 % of the hydroxyl groups could be esterified using palmitoyl chloride and 27–77 % using oleoyl chloride, but also one sample featuring a DS of 93 % was observed (Table 52 and Table 53, Appendix). The obtained DS values are distributed over a wide range, whereas mostly a DS between 50 and 60 % was reached using long chain fatty acid chlorides. This leads to the assumption, that the size or bulkiness of the esterification reagent has an impact on the DS attained. A reaction series of NML and different amounts of oleoyl chloride (0.4, 0.6 and 0.8 equivalents with respect to the lignin hydroxyl groups) was performed in DMF at 23 or 65 °C respectively (Table 19). Less than 1 eqivalent of oleoyl chloride was used to avoid high amounts of FFAs in the resulting ligninester. Satisfying yields (62–84 %) were obtained and the DS was in the range of 27–62 %. It can be seen that the DS is notedly lower for ligninesters synthesized at RT (samples 62, 63 and 68). The highest DS (62 %) is observed upon reacting 0.8 equivalents oleoyl chloride at 65 °C with NML. By lowering the amount of oleoyl chloride to 0.6 or 0.4 equivalents at 65 °C, the DS decreases to 42 or 29 % respectively. Thus, a reasonable degree of substitution and satisfying yield can be reached by applying 0.8 equivalents of fatty acid chloride at moderate reaction temperature (65 °C). The FFA content (19–26 wt%) seems to be largely unaffected by the varying amount of applied oleoyl chloride as well as by the reaction temperature.

Table 19. Yields and DS observed by reacting NML with different amounts of oleoyl chloride in dry DMF in the presence of Et$_3$N (1 eq) at 23 or 65 °C.

Lignin sample	Oleoyl chloride / eq	Reaction temperature / °C	Yield / %	DS / %	FFA / wt%
60	0.6	65	65	42	22
61	0.4	65	62	29	20
62	0.6	23	79	27	26
63	0.4	23	84	28	19
67	0.8	65	76	62	22
68	0.8	23	73	47	21

Elemental analyses (CHN) of original and selected modified *Annikki* lignins show the increased carbon and hydrogen contents of lignins, esterified with long chain substituents. The nitrogen content originates naturally from proteins present in the starting lignin. Possibly enhanced nitrogen values of modified lignins are caused by residual triethylamine hydrochloride or dimethylformamide. The collected values are listed in Table 59, Appendix.

The molecular weight distribution of the synthesized ligninesters is slightly altered in contrast to the original lignin (Table 20). As expected, the number average molar mass (M_n) of acetyl lignin (entry 10, Table 23) is only somewhat higher than the M_n of original GL1 as only an acetyl group was introduced. However, the M_n of palmitoyl lignin (entry 35, Table 23) and oleoyl lignin (entry 80, Table 23) is notedly increased in contrast to original GL1, indicating the esterification with long chain substituents (C_{16} or C_{18}) in several positions per lignin moiety. Collected values from the HPLC-SEC measurement are summarized in Table 56

(Appendix). The values listed in Table 20 do not indicate the breaking of aggreagates during the esterification reaction. All obtained values are higher compared to that of GL1.

Table 20. Molecular weight values retrieved from HPLC-SEC analysis in DMF against PS standards (50 °C, DMF).

Ligninester (sample #)	M_n / g·mol^{-1}	M_w / g·mol^{-1}	PDI
acetyl lignin (10)	1670	8320	4.97
norbornenoyl lignin (19)	2150	29600	13.8
10-undecenoyl lignin (30)	1860	24210	13.0
palmitoyl ligin (35)	2150	12300	4.88
oleoyl lignin (80)	2860	13400	4.68
Gesamtlignin (GL1)	1340	5650	4.23

Simultaneous thermal analyses of selected ligninesters were recorded in order to receive information about any transition or decomposition points. Figure 18 shows the mass loss of acetyl, butyryl, palmitoyl and oleoyl lignin in comparison to original low molecular weight *Annikki* lignin (NML). The mass loss curves of NML and acetyl lignin appear equal, indicating that the introduction of acetyl units does not alter lignin to a greater extent. The minimal mass loss in the temperature range from 20–100 °C is most likely reducible to humidity or solvent residuals in the samples. The stated temperatures at 5 % mass loss indicate a slightly increased temperature resistance of the modified lignins, whereas a considerable difference between short and long chain ligninesters is noticeable. The short chain ligninesters show a lower mass loss, also indicating a higher degree of substitution compared to the long chain ligninesters. The higher thermal stability of esterified lignin could be explained by the prevented elimination of hydroxyl groups which would result in the release of H_2O and double bond formation.[161] Remaining free fatty acids also contribute to the obtained high mass loss of palmitoyl and oleoyl lignin. The associated DSC curves are shown in Figure 63 (Appendix).
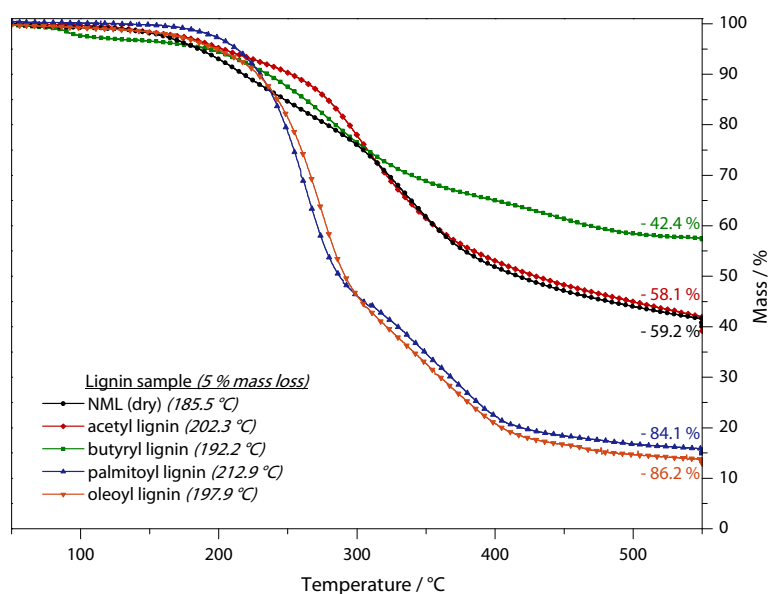

Figure 18. Mass loss of the synthesized ligninesters (samples 2, 3, 34 and 59) determined by STA.

The solubility of long chain ligninesters in non-polar media, namely in dicyclopentadiene (DCPD), was investigated with selected samples of palmitoyl (entries 36 and 37, Table 23) and oleoyl lignin (entries 78, 79, 82 and 83, Table 23). The ligninesters (5 or 20 wt%) were stirred in dicyclopentadiene (DCPD) (80 or 95 wt%) for 24 h at room temperature. Then, the mixtures were centrifuged three times (10 min at 5300 rpm) and the supernatant solution was decanted. The solid residue was collected in cyclohexane, filtered, dried in vacuum and quantified gravimetrically (Table 21).

The palmitoyl and oleoyl lignins investigated were synthesized with different starting lignins under the same reaction conditions. The results of the solubility determination listed in Table 21 indicate that esterified *Annikki* lignins are more inhomogeneous compared to ligninesters of the commercially available *Kraft* lignin (KL2). The solubility of batches 37 and 82 are in good agreement, suggesting that solubility differences are not caused by the applied fatty acid chloride. Furthermore, the quantity of the undissolved residue is obviously not dependent on the applied concentration in DCPD. The degree of substitution (DS) of the investigated ligninesters is in the rather narrow range of 52–61 %. Thus the observed solubility gaps between batches 78, 79, 36 and 83 must have other causes.

Elemental analyses of the DCPD-insoluble residue revealed a notedly increased nitrogen content. On one hand the nitrogen content may originate from residual DMF or, on the other hand from $Et_3N \cdot HCl$, formed during the esterification reaction. Depending on the size of the precipitate formed upon pouring the reaction mixture in deionized H_2O and the duration of the washing process, the salt may not be thoroughly washed out. Thus, $Et_3N \cdot HCl$ is concentrated in the DCPD-insoluble residue. Calculating the theoretical amount of the formed $Et_3N \cdot HCl$ proportion would largely agree with the remaining portion of undissolved solid. Ultrasonic treatment of the DCPD-insoluble residue of samples 78 and 79 in D_2O and subsequent ^1H NMR measurements revealed $Et_3N \cdot HCl$ as well as traces of DMF. Hence, the obtained values could be explained best by the work-up, or rather the morphology of the formed precipitate. Additionally, the presence of lignin aggregates, which were not broken up during the esterification reaction, cannot be completely excluded.
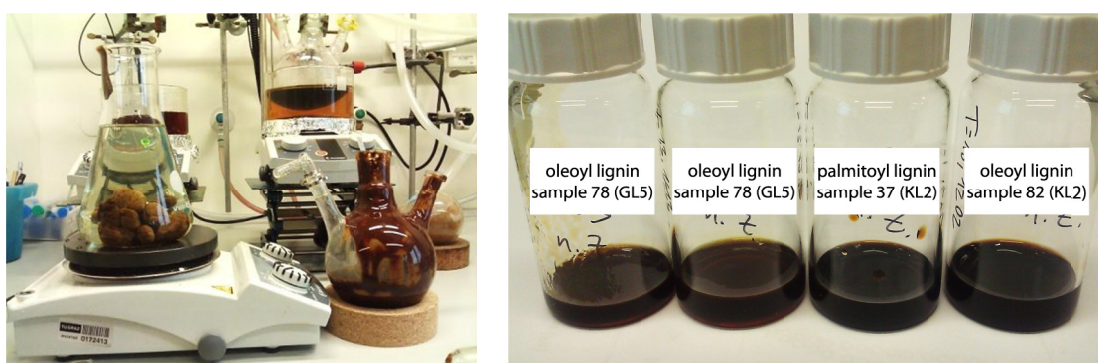
Figure 19. Precipitation of oleoyl lignin in deion. H_2O *(left)* and DCPD-ligninester solutions after centrifugation *(right)*.

Table 21. Solubility determination of palmitoyl and oleoyl lignin in dicyclopentadiene.

Sample no.	DS / %	Ligninester / mg	DCPD / g	Insoluble residue / wt% (mg)	Soluble proportion / wt%
palmitoyl lignin		*5 wt%*	*95 wt%*		
37 (KL2)	56	100.58	1.9002	15.2 (15.2)	84.8
oleoyl lignin		*5 wt%*	*95 wt%*		
78 (GL5)	61	100.39	1.9002	55.0 (55.3)	45.0
79 (GL5)	61	101.02	1.9002	40.4 (40.8)	59.6
82 (KL2)	58	100.97	1.9002	9.6 (9.68)	90.4
palmitoyl lignin		*20 wt%*	*80 wt%*		
36 (L_THF)	54	100.34	0.400	44.2 (44.3)	55.8
37 (KL2)	56	406.4	1.6256	11.9 (48.7)	88.1
oleoyl lignin		*20 wt%*	*80 wt%*		
78 (GL5)	61	451.4	1.6616	32.7 (135.7)	67.3
79 (GL5)	61	403.4	1.6136	14.9 (60.1)	85.1
82 (KL2)	58	407.8	1.6312	8.7 (35.6)	91.3
83 (L_THF)	52	102.32	0.400	4.5 (4.56)	95.5

Table 22. Nitrogen content of the DCPD-insoluble residue in comparison to the ligninester as well as to the starting lignin, determined by elemental analysis (CHN).

Lignin sample	% N Starting lignin	% N Ligninester	% N Undissolved residue	Enrichment of N in the undissolved residue
78	1.3 (GL5)	2.1	3.3	+ 57 %
79	1.3 (GL5)	1.9	8.3	+ 337 %
37	0.7 (KL2)	1.4	3.0	+ 114 %
82	0.7 (Kl2)	1.5	5.7	+ 280 %

Full characterization of the ligninesters requires knowledge of the amount of free fatty acids (FFAs) present. The FFA content can be determined via HPLC-SEC after appropriate calibration with fatty acids (see Table 57, Appendix). Thus, the FFA content in palmitoyl lignin is given in the range of 8–43 wt% and 11–30 wt% for oleoyl lignin.

The FFA content is also ascertainable via quantitative ^{31}P NMR spectroscopy by investigating the amount of carboxylic acids in the sample. The number of carboxyls present in the ligninesters is increased due to hydrolyzed fatty acid chlorides compared to the starting lignin. The difference can be specified as the amount of FFAs (mmol·g^{-1}) present in the sample. Thus, the amounts of FFAs present in selected large scale batches was found to be 6–15 wt% in palmitoyl lignins and 4–14 wt% in oleoyl lignins (Table 52 and Table 53, Appendix). However, a comparison of the FFA content with the according values obtained from HPLC-SEC indicates an underestimation by quantitative ^{31}P NMR spectroscopy.

Investigating the synthesized ligninesters, it was found that the variation of reaction conditions has hardly any impact on the amount of remaining free fatty acids (cp. Table 19). Possible applications of the ligninesters are interfered by the presence of FFAs. Thus, many efforts have been made to completely remove free fatty acids, such as extraction, precipitation or salting out. The extraction failed as well as other mentioned methods due to the high solubility of the ligninesters in non-polar solvents. The full removal of FFAs succeeded solely by flash chromatography. A portion of palmitoyl lignin (sample 36, 120.5 mg) was applied onto a plug of silica gel and washed with cyclohexane / ethyl acetate (20:1 (v:v)) until no palmitic acid could be detected via TLC (CH / EA 3:1 (v:v), R_f = 0.28). The remaining lignin ester was then eluted with dichloromethane / methanol (10:1 (v:v)) and finally with pure methanol until the eluent was colorless. Thus 32 wt% (39 mg) palmitic acid were removed and 75 mg (62 wt%) pure palmitoyl lignin were obtained. The severed proportion of free palmitic acid is in good accordance with the amount determined by HPLC-SEC. Column chromatography is certainly the method of choice in small scales, but is inappropriate especially with regard to industrial feasibility.

Summary — esterification of lignin with fatty acid chlorides
- *Esterification of Annikki lignin with carboxylic acid chlorides in DMF at 65 °C*
- *Et₃N as base*
- *DS of long chain ligninesters mainly in the range between 50 and 60 %*
- *Lower DS at lower reaction temperature (23 °C)*
- *Presence of FFAs distorts yield and DS*
- *High solubility in non-polar dicyclopentadiene (45–95 wt%)*
- *8–43 wt% free fatty acids (FFAs) (determined by HPLC-SEC)*
- *Removal of FFAs via flash chromatography*

3.2.2 EXPERIMENTAL DETAILS

STANDARD OPERATING PROCEDURE (SOP) FOR THE ESTERIFICATION OF LIGNIN

Lignin was dissolved in dry DMF, or any other solvent, under inert atmosphere of N_2 and heated to 65 °C. The promoting agent, in most cases triethylamine, was added to the solution in an amount of 1 equivalent based on the number of free hydroxyl groups present in the lignin. The according esterification reagent (carboxylic acid anhydride or chloride) was added in an amount of 1–2 equivalents and the reaction mixture was stirred under inert atmosphere of N_2 at 65 °C for at least 20 h, maximum 72 h. For work-up, *deion.* H_2O was added to precipitate the formed product.* After filtration and washing with *deion.* H_2O the product was dried under vacuum.

* If the formed product was not precipitating, dichloromethane was added to the mixture and the solution was extracted twice with *deion.* H_2O. The combined organic phases were concentrated under reduced pressure and dried under vacuum. As described above, the obtained products were characterized via ATR-FTIR spectroscopy, ^{31}P NMR spectroscopy, HPLC-SEC, elemental analysis and simultaneous thermal analysis (STA).

Batches 37, 42–46, 71–76, 78, 79 as well as 82 were performed in larger scale of 18–30 g starting lignin according to the described standard operating procedure. The fatty acid chlorides were injected directly into the lignin solution with a syringe. The work-up was restricted to precipitation in iced *deion.* H_2O, collecting the precipitate in toluene, concentrating under reduced pressure and intense drying under vacuum.

The determined yields (wt%) in Table 23 are stated without any purification, therefore the remaining free fatty acids also contribute to this value, which has significant consequences for palmitoyl and oleoyl lignin. If no yield is specified (labeled with *nd* = not determined), the partial loss during work-up (extraction or filtration experiments) was very high (> 50 wt%) or otherwise, the yield was found to be > 100 %, indicating a high content of residual FFAs or DMF. If a minus sign is written instead of a yield, the desired conversion was not successful and the reaction mixture was discarded.

Table 23. Esterification reactions of *Annikki* lignin (applied quantities, reaction conditions and yields; reaction time was at least 16 h, maximum 3 d).

Sample	Starting lignin		Esterification reagent		Promoting agent		Solvent	T	Yield	DS
	name	mmol OH (g)	name	mmol (mL)	name	mmol	name (mL)	°C		%
			short chain							
1	NML	0.048 (0.012)	acetic anhydride	1.81 (0.200)	DMAP	nk	–	23	nd	nd
2	NML	0.8 (0.200)	acetic anhydride	2.50 (0.236)	DMAP	nk	DCM (0.5)	50	158 mg (54 %) brown solid	nd
3	NML	0.8 (0.200)	butyric anhydride	2.50 (0.409)	DMAP	nk	DCM (0.5)	50	180 mg (51 %) brown solid	nd
4	NML	0.068 (0.017)	acetyl chloride	2.32 (0.200)	acetic acid	31.7	acetic acid (2.0)	23	–	–
5	NML	0.16 (0.040)	acetyl chloride	2.32 (0.200)	DMAP	1.16	EtOH (2.0)	23	–	–
6	NML	0.8 (0.204)	acetyl chloride	14.0 (1.00)	py DMAP	1.14 nk	–	40	227 mg (75 %) brown solid	nd
7	NML	2.0 (0.500)	acetyl chloride	1.83 (0.261)	Et₃N	1.83	DMF (10)	65	nd	nd
8	NML	4.0 (1.00)	acetyl chloride	11.0 (0.781)	Et₃N	3.65	DMF (15)	65	nd	nd
9	NML	4.0 (1.00)	acetyl chloride	8.4 (0.600)	Et₃N	4.20	DMF dry (10)	65	940 mg (75 %) brown solid	nd
10	GL1	1.95 (0.500)	acetyl chloride	4.20 (0.300)	Et₃N	2.20	DMF abs. (5)	65	nd	nd
11	NML	1.2 (0.300)	acryloyl chloride	12.3 (1.00)	Et₃N	3.35	DCM (4.0)	23	–	–
12	NML	1.2 (0.300)	acryloyl chloride	12.3 (1.00)	Et₃N	3.35	DMF dry (15)	40	239 mg (50 %) brown solid	nd
13	NML	8.04 (2.00)	acryloyl chloride	82.6 (6.73)	Et₃N	22.3	DCM dry (40)	40	–	–
14	NML	2.0 (0.500)	methacryloyl chloride	2.1 (0.205)	Et₃N	2.1	DMF abs. (8)	65	0.267 g (41 %) brown solid	nd
15	NML	0.4 (0.100)	ethyl acetate	20.4 (2.00)	DBU	0.033	EA (2)	80	–	–
16	GL1	3.9 (1.00)	maleic anhydride	7.39 (725 mg)	1-MIM	0.63	DMF abs. (5)	65	nd	nd
			cyclic							
17	NML	4.0 (1.00)	*cis-endo*-bicyclo[2.2.1] hept-5-ene-2,3-dicarboxylic anhydride	4.38 (719 mg)	Et₃N	3.65	DMF dry (10)	60	-	–
18	NML	4.0 (1.00)	*cis-endo*-bicyclo[2.2.1] hept-5-ene-2,3-dicarboxylic anhydride	3.65 (600 mg)	*p*TSA	0.36	DMF dry (10)	60	–	–

vac = under vacuum; nk = not known; nd = not determined

Table 23 continued.

Sample	Starting lignin		Esterification reagent			Promoting agent		Solvent	T	Yield	DS
	name	mmol OH (g)	name		mmol (mL)	name	mmol	name (mL)	°C		%
19	GL1	3.9 (1.00)	bicyclo[2.2.1]hept-5-ene-2-carbonyl chloride		5.65 (0.704)	Et₃N	3.72	DMF abs. (6)	65	331 mg (18 %) brown solid	nd
20	KB/S2	0.37 (0.101)	bicyclo[2.2.1]hept-5-ene-2-carbonyl chloride		0.37 (0.046)	Et₃N	0.37	THF (1.5)	55	104 mg (71 %) brown solid	nd
21	KB/S5	3.7 (1.00)	bicyclo[2.2.1]hept-5-ene-2-carbonyl chloride		3.70 (0.461)	Et₃N	3.70	DCM abs. (10)	50	874 mg (60 %) soft brown solid	nd
22	KB/S3	3.7 (1.00)	bicyclo[2.2.1]hept-5-ene-2-carbonyl chloride		3.70 (0.461)	Et₃N	3.70	DCM abs. (10)	50	1.278 g (88 %) sticky brown solid	nd
23	GL1	1.95 (0.500)	bicyclo[2.2.1]hept-5-ene-2-carbonyl chloride		2.40 (0.300)	Et₃N	2.20	DMF abs. (5)	65	*product could not be isolated*	nd
24	GL1	0.39 (0.100)	bicyclo[2.2.1]hept-5-ene-2-yl(ethyl)-chlorodimethylsilane		0.77 (0.167)	py	0.38	–	70	222 mg (83 %) brown solid	nd
			long chain								
25	NML	1.2 (0.300)	10-undecenoyl chloride		3.35 (0.720)	Et₃N	3.35	DMF dry (15)	40	nd	nd
26	NML	2.4 (0.600)	10-undecenoyl chloride		6.70 (1.44)	Et₃N	6.70	DMF dry (20)	65	nd	nd
27	NML	4.0 (1.00)	10-undecenoyl chloride		3.65 (0.784)	Et₃N	3.65	DMF (15)	65	230 mg (14 %) brown solid	nd
28	NML	4.0 (1.00)	10-undecenoyl chloride		3.65 (0.784)	Et₃N	3.65	DMF dry (10)	65	1.34 g (82 %) brown solid	nd
29	NML	4.0 (1.00)	10-undecenoyl chloride		3.65 (0.784)	Et₃N	3.65	DMF (15)	65	1.3395 g (83 %) brown solid	37
30	GL1	0.39 (0.100)	undec-10-enoic acid		0.40 (0.081)	TA	0.04	–	120	–	–
31[162]	GL1	1.98 (0.508)	undec-10-enoic acid		9.94 (2.01)	TA	0.13	–	125	452 mg (55 %) brown solid	79
32	NML	4.0 (1.00)	palmitoyl chloride / palmitoyl anhydride		1811 mg (undefined mixture)	Et₃N	3.65	DMF (15)	65	nd	nd
33	NML	4.0 (1.00)	palmitoyl chloride		3.65 (1.275)	Et₃N	3.65	DMF (15)	65	nd	49
34	NML	8.0 (2.00)	palmitoyl chloride		12.6 (3.823)	Et₃N	8.40	DMF abs. (15)	65	nd	nd
35	GL1	1.95 (0.500)	palmitoyl chloride		3.20 (0.950)	Et₃N	2.20	DMF abs. (5)	65	nd	93
36	L_THF	4.01 (1.00)	palmitoyl chloride		3.41 (1.03)	Et₃N	4.01	DMF abs.(6)	65	1.746 g (96 %) brown solid	64

vac = under vacuum; nk = not known; nd = not determined

Table 23 continued.

Sample	Starting lignin		Esterification reagent		Promoting agent		Solvent	T	Yield	DS
	name	mmol OH (g)	name	mmol (mL)	name	mmol	name (mL)	°C		%
38	KL1	nk	palmitoyl chloride	1.75 (0.531)	Et₃N	1.75	DMF abs. (5)	65	758 mg (82 %) brown solid	nd
39	KL2	2.66 (0.508)	palmitoyl chloride	2.03 (0.616)	Et₃N	2.00	DMF abs. (5)	65	731 mg (74 %) brown solid	56
40	L_HT	4.13 (1.00)	palmitoyl chloride	3.54 (1.08)	Et₃N	3.52	DMF abs. (10)	60	1458 mg (79 %) brown solid	48
41	L_THF	4.00 (0.997)	palmitoyl chloride	3.99 (1.21)	Et₃N	3.99	THF abs. (10)	55	1054 mg (54 %) brown solid	65
42	GL2	108.0 (25.01)	palmitoyl chloride	100 (30.3)	Et₃N	(13.9)	DMF abs. (50)	60	nd	78
43	GL3	109.5 (25.01)	palmitoyl chloride	100 (30.5)	Et₃N	(13.9)	DMF abs. (50)	60	nd	82
44	GL3	80.29 (18.33)	palmitoyl chloride	73.3 (22.2)	Et₃N	(10.2)	DMF abs. (40)	60	nd	69
45	GL2 extr.	90.31 (21.10)	palmitoyl chloride	105 (31.8)	Et₃N	(11.7)	DMF abs. (50)	60	nd	86
46	GL2 extr.	91.38 (21.35)	palmitoyl chloride	106 (32.2)	Et₃N	(11.8)	DMF abs. (50)	60	nd	93
47	NML	4.0 (1.00)	palmitoyl chloride bicyclo[2.2.1]hept-5-ene-2-carbonyl chloride	2.1 (0.637) 2.1 (0.262)	Et₃N	4.20	DMF (15)	65	1480 mg (82 %) brown solid	41
48	NML	4.0 (1.00)	palmitoyl chloride bicyclo[2.2.1]hept-5-ene-2-carbonyl chloride	3.15 (0.956) 1.05 (0.131)	Et₃N	4.20	DMF (15)	65	1700 mg (88 %) brown solid	nd
49	NML	4.0 (1.00)	palmitoyl chloride bicyclo[2.2.1]hept-5-ene-2-carbonyl chloride	3.15 (0.956) 1.05 (0.131)	Et₃N	4.20	DMF (15)	65	1700 mg (88 %) brown solid	52
50	NML	4.02 (1.00)	palmitoyl chloride bicyclo[2.2.1]hept-5-ene-2-carbonyl chloride	3.00 (0.910) 1.00 (0.125)	Et₃N	4.00	DMF abs. (10)	60	1226 (65 %) brown solid	55
51	NML	1.2 (0.300)	oleic acid	5.02 (1.59)	H₂SO₄ conc	3 drops	–	100 (vac)	–	–
52	NML	1.2 (0.300)	methyl oleate	5.02 (1.70)	pTSA	0.052	–	150 (vac)	–	–
53	NML	1.2 (0.300)	methyl oleate	5.02 (1.70)	pTSA	0.052	–	180 (vac)	–	–

vac = under vacuum; nk = not known; nd = not determined

Table 23 continued.

Sample	Starting lignin		Esterification reagent		Promoting agent		Solvent	T	Yield	DS
	name	mmol OH (g)	name	mmol (mL)	name	mmol	name (mL)	°C		%
54	NML	4.0 (1.00)	oleoyl chloride	4.20 (1.326)	Et₃N	4.20	DMF (15)	65	1780 mg (79 %) brown solid	nd
55	NML	1.2 (0.300)	oleoyl chloride	6.70 (2.20)	Et₃N	3.35	DMF dry (10)	40	990 mg (84 %) brown oil	nd
56	NML	1.2 (0.300)	oleoyl chloride	3.35 (1.10)	Et₃N	3.35	DMF dry (15)	40	nd	nd
57	NML	4.0 (1.00)	oleoyl chloride	4.20 (1.326)	Et₃N	4.20	DMF (15)	65	1.8725 g (79 %) brown solid	27
58	NML	8.0 (2.00)	oleoyl chloride	12.6 (4.166)	Et₃N	8.40	DMF abs. (15)	65	nd	nd
59	KL2	2.62 (0.501)	oleoyl chloride	2.00 (0.661)	Et₃N	2.00	DMF abs. (5)	65	686 mg (67 %) sticky brown solid	60
60	NML	2.01 (0.503)	oleoyl chloride	1.25 (0.413)	Et₃N	1.06	DMF abs. (5)	65	544 mg (65 %) sticky brown solid	42
61	NML	2.02 (0.504)	oleoyl chloride	0.835 (0.276)	Et₃N	1.06	DMF abs. (5)	65	447 mg (62 %) sticky brown solid	29
62	NML	2.02 (0.506)	oleoyl chloride	1.26 (0.417)	Et₃N	1.16	DMF abs. (5)	23	665 mg (79 %) sticky brown solid	27
63	NML	2.01 (0.502)	oleoyl chloride	0.832 (0.275)	Et₃N	1.06	DMF abs. (5)	23	607 mg (84 %) sticky brown solid	28
64	NML	2.02 (0.504)	oleoyl chloride	2.02 (0.668)	Et₃N	2.02	THF (5)	60	814 mg (78 %) sticky brown solid	58
65	NML	2.01 (0.503)	oleoyl chloride	2.01 (0.665)	Et₃N	2.01	dioxane (5)	60	944 mg (91 %) sticky brown solid	62
66	NML	2.03 (0.507)	oleoyl chloride	2.03 (0.671)	Et₃N	2.02	THF abs. (5)	60	561 mg (54 %) sticky brown solid	40
67	NML	2.03 (0.507)	oleoyl chloride	1.62 (0.536)	Et₃N	2.03	DMF abs. (5)	65	713 mg (76 %) sticky brown solid	62
68	NML	2.00 (0.501)	oleoyl chloride	1.60 (0.530)	Et₃N	2.00	DMF abs. (5)	23	673 mg (73 %) sticky brown solid	47
69	L_HT	4.12 (1.00)	oleoyl chloride	3.51 (1.16)	Et₃N	3.51	DMF abs. (10)	60	1214 mg (63 %) brown solid	45
70	L-THF	4.04 (1.01)	oleoyl chloride	4.03 (1.33)	Et₃N	4.03	THF abs. (10)	55	–	nd
71	GL4	120.0 (25.01)	oleoyl chloride	100 (33.1)	Et₃N	(13.8)	DMF abs. (50)	60	nd	74

vac = under vacuum; nk = not known; nd = not determined

Table 23 continued.

Sample	Starting lignin		Esterification reagent		Promoting agent		Solvent	T	Yield	DS
	name	mmol OH (g)	name	mmol (mL)	name	mmol	name (mL)	°C		%
72	GL4	120.0 (25.01)	oleoyl chloride	100 (33.1)	Et₃N	(13.8)	DMF abs. (50)	60	nd	72
73	GL4	120.0 (25.01)	oleoyl chloride	100 (33.1)	Et₃N	(13.8)	DMF abs. (50)	60	nd	73
74	GL4	92.78 (19.33)	oleoyl chloride	77.3 (25.6)	Et₃N	(10.7)	DMF abs. (40)	60	nd	76
75	GL4	88.42 (18.42)	oleoyl chloride	73.7 (24.4)	Et₃N	(10.2)	DMF abs. (40)	60	nd	78
76	KL1	nk	oleoyl chloride	1.75 (0.579)	Et₃N	1.75	DMF abs. (5)	65	–	–
77	NML	0.8 (0.200)	methyl oleate	0.88 (0.299)	TBD	0.0076	DMF abs. (5)	60	–	–
78	GL5	77.96 (18.30)	oleoyl chloride	73.2 (24.2)	Et₃N	(10.1)	DMF abs. (50)	60	nd	63
79	GL5	77.96 (18.30)	oleoyl chloride	73.2 (24.2)	Et₃N	(10.1)	DMF abs. (50)	60	nd	62
80	GL1	1.95 (0.500)	oleoyl chloride	3.50 (1.15)	Et₃N	2.20	DMF abs. (5)	65	nd	93
81[162]	GL1	1.98 (0.506)	oleic acid	8.51 (2.70)	TA	0.13	–	125	469 mg (47 %) brown solid	33
82	KL2	157.5 (30.06)	oleoyl chloride	120 (39.8)	Et₃N	(19.5)	DMF abs. (70)	60	nd	59
83	L_THF	4.01 (1.00)	oleoyl chloride	3.41 (1.13)	Et₃N	4.01	DMF abs. (6)	65	1860 mg (98 %) brown solid	58

vac = under vacuum; nk = not known; nd = not determined

3.3 ESTERIFICATION / GRAFTING OF LIGNIN

The ring opening polymerization (ROP) of lactide and lactones gained a lot of attention and was studied with high intensity during the last decade.[163] The interest of substituting conventional polymers by biodegradable materials derived from renewable resources is enormous, but the rather poor mechanical properties have prevented a complete replacement hitherto. Many efforts have been made to address the required qualifications, for instance by the preparation of various composite materials with poly(lactic acid) (PLA)[164] or polylactones.[151] It was found that intermolecular interactions like hydrogen bonding play a key role in composites comprising of polymers featuring hydroxyl and carbonyl groups.[164]

Usually, stannous octoate is applied as catalyst for the ROP of lactide and lactones, but meanwhile organocatalytic protocols are well established. The metal-free catalysis of ROP of cyclic esters using the guanidine base 1,5,7-triazabicyclo[4.4.0]dec-5-ene (TBD) was developed by Waymouth and Hedrick in 2006.[165] Alcohols, aliphatic as well as phenolic,[166] act as initiators, whereas the chain length is controllable via the monomer to initiator ratio.

As the ROP of lactide and lactones can be initiated by hydroxyl groups, it is reasonable that natural hydroxyl containing polymers are utilized as macroinitiators. This so called 'grafting from' approach was already published by Hafrén and Córdova in 2005, where the surface-initiated ROP of lactide onto native cellulose was reported.[162] In the contrary approach, the so-called 'grafting to' method, preformed polymer chains are coupled to a (solid) substrate featuring suitable reactive sites.[167] Due to solubility reasons, cellulose acetate (degree of acetylation < 3) was used as a starting material for the grafting with polyhydroxyalkanoates.[168] The surface grafting of micorfibrillated cellulose with poly(ε-caprolactone) (PCL) was also reported.[169]

Although it is obvious to utilize also lignin as multifunctional initiator in the 'grafting to' approach of lactide and lactones, a covalently bound lignin-poly(lactic acid) was reported only recently by Waymouth and coworkers.[151a] They prepared lignin-PLA copolymers in the melt using organocatalysts, whereas the graft length was controlled by using varying ratios of lignin to lactide monomer. Lignin was used directly without any prior fractionation or modification. Performing control experiments of TBD-catalyzed lactide polymerization, it was found that phenols also act as initiators, although with lower efficiency than aliphatic alcohols. Copolymers with chemically pretreated lignin (hydroxypropylated or acetylated in varying degrees) were prepared by graft polymerization of ε-caprolactone.[170] The synthesis of lignin-PCL copolymers using native lignin was reported more recently.[151b]

In the previous section, the esterification of lignin was already shown to improve the solubility behavior of lignin. The grafting ring opening polymerization using lactide and lactones is an attractive approach to covalently modify lignin and allows for the green and solvent-free synthesis of novel materials with tailored properties. The obtained graft copolymers are promising materials for a variety of applications as well as further modifications.

A series of esterification / grafting reactions of *Annikki* lignin with D,L-lactide (LA) and *ε*-caprolactone (CL) was performed successfully in a ≥ 5 g scale and organosoluble, homogeneous lignin derivatives were obtained. The ratios of lignin to monomer were varied (1:1, 1:2, 1:3, 1:5 and 1:10 (m:m)) to attain varying graft lengths. These different ratios were selected to ensure a lignin content as high as possible in the final product. One variation of process parameters was the type of stirrer employed. Bulk reactions of *Annikki Gesamtlignin* and LA were performed either applying an overhead stirrer, or without any stirrer. In the latter case, all components were mixed with a spatula before heating up. Due to the high viscosity of the reaction mixture, magnetic stirring was not feasible. The largest part of esterification / grafting reactions was catalyzed by the CO_2-sensitive 1,5,7-triazabicyclo[4.4.0]-dec-5-ene (TBD) with a few exeptions, where 1,8-diazabicyclo[5.4.0]-undec-7-en (DBU) or 1,4-diazabicyclo[2.2.2]-octane (DABCO) were used (entries 1, 2 and 4–6, Table 31). The obtained lignin grafts were investigated with ATR-FTIR spectroscopy, ^{31}P NMR spectroscopy, HPLC-SEC, elemental analysis and simultaneous thermal analysis (STA) as per description in section 2 and the results are discussed in detail in the following section.

Table 24. Organocatalysts, monomers and according graft polymers introduced by esterification / grafting reactions of lignin via organocatalyzed ROP.

| 1,5,7-triazabicyclo[4.4.0]-dec-5-ene (TBD) | 1,8-diazabicyclo[5.4.0]-undec-7-en (DBU) | 1,4-diazabicyclo[2.2.2]-octane (DABCO) |

| *β*-butyrolactone (BBL) | D,L-lactide (LA) | *ε*-caprolactone (CL) |

| *poly*(*β*-hydroxybutyrate) (PHB) | *poly*(lactic acid) (PLA) | *poly*(*ε*-caprolactone) (PCL) |

3.3.1 Results - lignin grafts

The ROP monomers (Table 24) were reacted with *Annikki* lignin in bulk at elevated temperatures in the presence of *N*-centered organocatalysts. Simultaneously, control experiments using low molecular hydroxyl derivatives as initiators were performed as proof of concept (entries 48–50, Table 31).

Scheme 7. Esterification / grafting reactions of ROP monomers onto *endo,exo*-bicyclo[2.2.1]hept-5-ene-2-methanol.
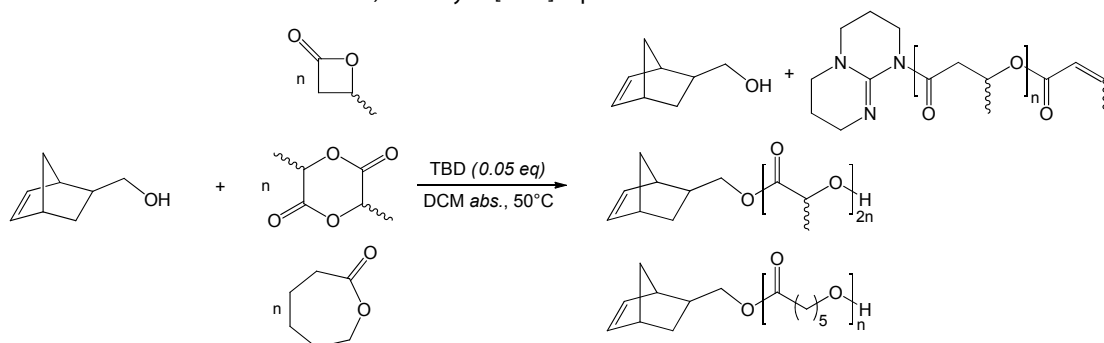
Thus it was found, that the 'grafting to' approach is not accessible with β-butyrolactone (BBL) which is also in accordance with literature.[171] Although BBL is polymerized, the PHB chain is not linked to the norbornene moiety as PHBs were found to be end capped by the used guanidine base. The other chain end features crotonate groups (δ 6.90 and 5.74 ppm) due to the dehydration of the propagation species resulting in termination. Performing grafting reactions with D,L-lactide (LA) or ε-caprolactone (CL), a distinct low-field shift of the norbornene CH$_2$ group adjacent to the hydroxyl groups was detected upon esterification (from δ 3.68 to 4.13 ppm).

Therefore the covalent bonding between PLA or PCL and lignin can be assumed in contrast to the PHB / lignin system, which merely seems to be an excellent blend. However, from ATR-FTIR and ^{31}P NMR measurements after phosphitylation it was actually not apparent, that PHB groups were not covalently grafted onto lignin. The reason for this incorrect interpretation is the formation of strong hydrogen bonds between the lignin hydroxyl groups and the PHB carbonyl groups, which could lead to their disappearance in both the FTIR and ^{31}P NMR spectrum. This phenomenon of pronounced intermolecular interaction was already described for stable blends of lignin and PLA for instance.[164] Even upon column chromatography, the blend was not separable, clearly representing its stability. 215.0 mg were placed on a plug of silica gel and eluted with dichloromethane / methanol 10:1 (v:v) and finally pure methanol until the eluent was colorless. 203.5 mg (95 wt%) were recovered, indicating a successfully grafted lignin sample. Thus it turned out during the investigation of lignin-PHB derivatives, that results observed by various measurements do not reflect the factual circumstances.

The lignin / PHB mixtures were also investigated by ATR-FTIR spectroscopy (Figure 20) and found to be in good accordance with reported spectra of similar mixtures.[172] It is evident in the spectrum of the binary lignin / PHB 1:3 (m:m) blend, that the intensity of the broad band at 3330 cm^{-1}, corresponding to lignin O-H stretching, significantly decreased and the C=O stretching band (1730 cm^{-1}) is very pronounced. The bands centered around 2900 cm^{-1} arise from C-H stretching of aliphatic CH and methoxy groups of both lignin and PHB. Apart from the remaining hydroxyl band at (3510 cm^{-1}), the ATR-FTIR spectrum of the lignin / PHB blend is virtually equal to the spectrum of pure PHB. Differently than expected, a shift of the carbonyl stretching band (1730 cm^{-1}) due to intermolecular hydrogen bond formation of PHB carboxyl groups with lignin hydroxyl groups was not observed. A induced shift of 5 cm^{-1} to lower wave numers was reported investigating lignin / PLLA blends by FTIR spectroscopy.[164]
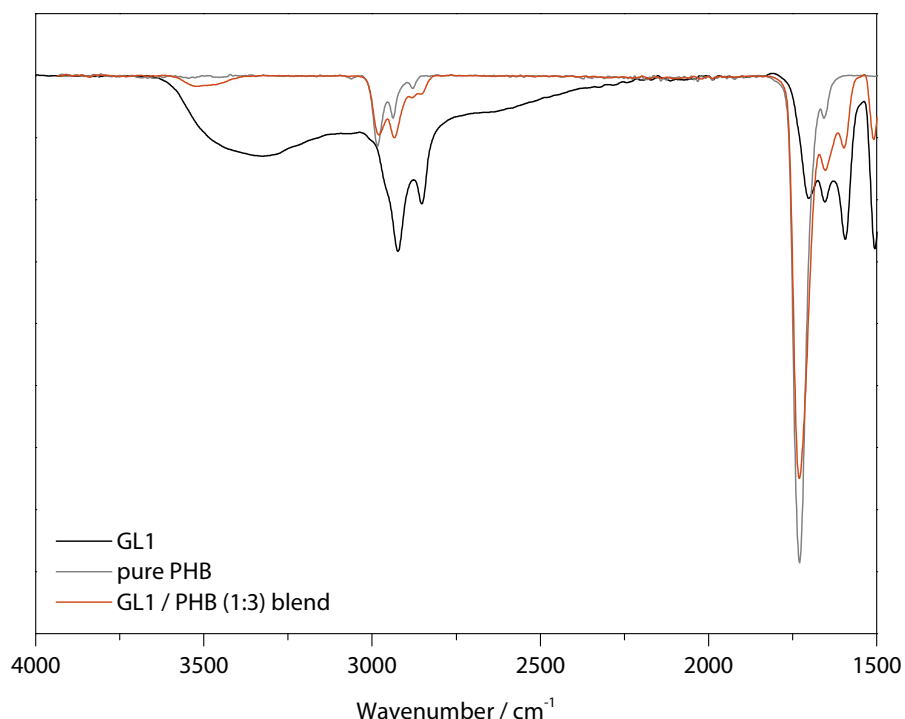
Figure 20. ATR-FTIR spectrum of a lignin / PHB (1:3) (m:m) blend (sample 3) in comparison to original lignin (GL1) and pure PHB.

The obtained ATR-FTIR spectra of lignin-PLA and -PCL grafts (Figure 21) appear very similar compared to the lignin / PHB blend. The O-H stretching resonance of lignin hydroxyl groups completely vanished, whereby a complete esterification of lignin cannot be considered with certainty as strong hydrogen bonding would appear almost identical. The C=O band of the formed lignin-graft-polyesters (1:3) (m:m) is present with high intensity at similar wave numbers (1746 cm^{-1} in case of lignin-PLA and 1723 cm^{-1} for lignin-PCL). Resonances between 2850 and 3000 cm^{-1} originate from aliphatic CH and methoxy groups of both lignin and polyesters.
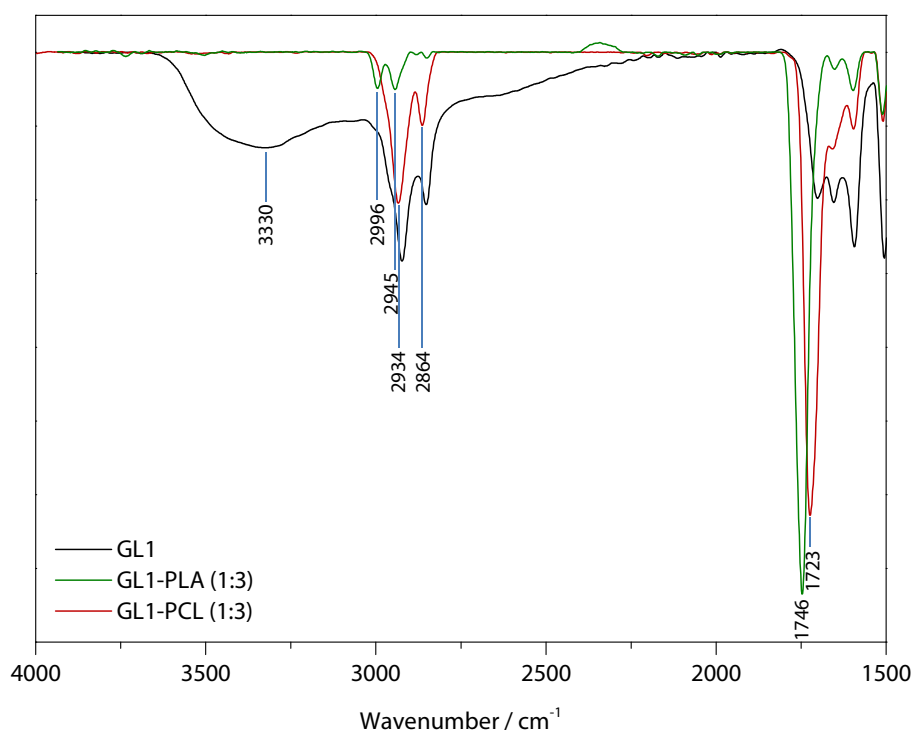
Figure 21. ATR-FTIR spectra of lignin-PLA and -PCL (1:3) (m:m) (samples 17 and 34) grafts in comparison to original lignin (GL1).

The mixtures and grafts were also investigated via HPLC-SEC in DMF (50 °C, relative to PS-standards), whereas another characteristic of lignin particularly emerges. Lignin is known to exhibit a high propensity for self-aggregation due to intermolecular hydrogen bond formation, van der Waals attraction and π-stacking of aromatic groups (see also section 2.4). Significant changes in molecular weight of lignin subunits were detected upon the introduction of graft chains (Table 25). Additionally, the HPLC-SEC traces appear clearly more homogeneous compared to original lignin. It can be reasonably assumed, that the strong aggregrates of lignin subunits are broken up during the grafting reactions at elevated temperatures in the melt.
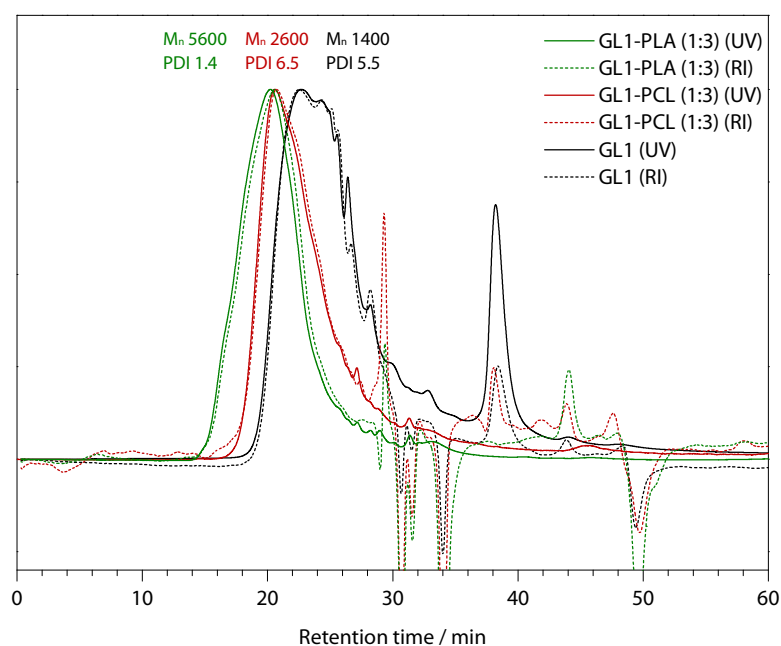
Comparing the HPLC-SEC traces of the lignin / PHB (1:3) (m:m) blend with the original lignin (GL1), the peak with the shortest retention time (22.7 min) is missing in the chromatogram of the blend, where the shortest retention time is 24.5 min (Figure 22). This finding is on one hand a strong indication for the breaking apart of lignin aggregates upon the applied reaction conditions, and as well of exceptional blending on the other hand.
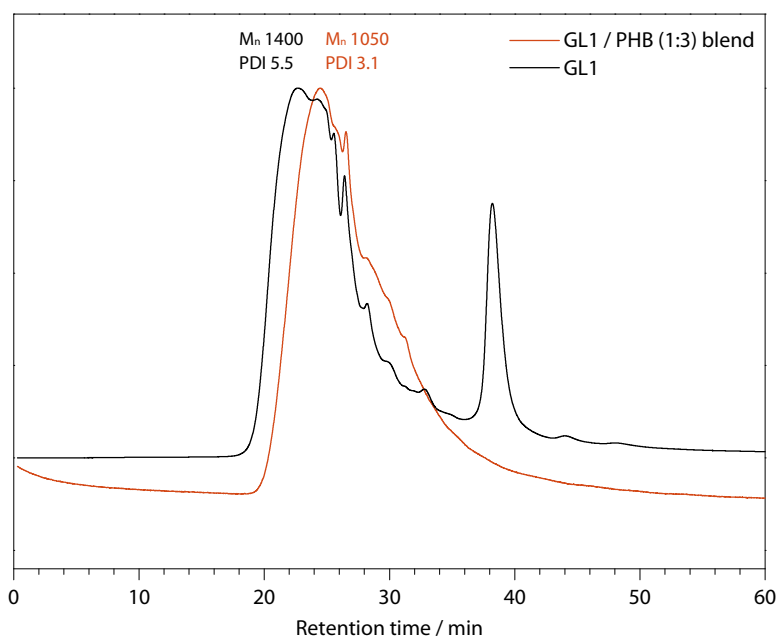
Figure 22. HPLC-SEC traces (UV) of the GL1 / PHB (1:3) (m:m) blend (sample 3) and original GL1 (DMF, 50°C).

HPLC-SEC traces of lignin samples, successfully grafted with PLA and PCL are shown in Figure 23. LA and CL were mixed in a three fold mass proportion with lignin (entries 19 and 39, Table 31), which refers to a molar excess of 5.4 equivalents with regard to lignin hydroxyl groups for LA and 7.4 equivalents in the case of CL. Thus a theoretical graft length of 10.8 D,L-lactide (n = 5.4) or 7.4 ε-caprolactone (n = 7.4) monomeric units should be obtained, resulting in slightly higher molecular weights for lignin / PCL grafts. As expected, the peaks of the lignin grafts are clearly shifted to shorter retention times, hence to higher molecular weights. Beside this, the chromatograms (UV trace) appear much more homogeneous in contrast to the sample of original lignin (GL1), as already observed for the lignin / PHB blends (Figure 22). The small peaks visible from a retention time of 26 minutes may refer to little amounts of unreacted lignin remaining in the sample. Differently than expected, the lignin / PCL grafts did not exhibit higher number average molecular weights (M_n) than lignin / PLA grafts in the same blend ratio, except one batch synthesized in toluene (sample 16, Table 25). This observation indicates, that the esterification / grafting with LA proceeds better than with CL.

Investigating the successful grafting reactions with LA and CL, the homopolymer formation (PLA / PCL chains not linked to a lignin moiety or cyclic polyesters) must not be neglected. Moisture present in the reaction mixture can lead to increased homopolymerization of LA or CL respectively. The presence of LA- or CL cycles due to backbiting during the graft ROP also has to be considered. Homopolymers are detectable via HPLC-SEC if exploited with both UV (280 nm) and refractive index (RI) detector. Theoretically all species featuring lignin moieties should be visible via UV-detection and PLA-/PCL-homopolymers or cycles should appear (as well as the lignin species) in the RI traces (dashed lines, Figure 23). However, if the molecular weights of the different species are very similar, a differentiation is not possible anymore.

Figure 23. HPLC-SEC traces (UV and RI) of the GL1-PLA and -PCL (1:3) (m:m) grafts (samples 19 and 39) in comparison to original lignin (GL1) (DMF, 50°C).

Considering the values listed in Table 25, it can be seen that the obtained values of the individual batches synthesized under the same reaction conditions are not very consistent. The polydispersity indeces of lignin / PLA grafts (samples 17 and 19) differ greatly (20 vs. 1.4) for instance. Such inhomogeneities can be found throughout all synthesized lignin / polyester grafts. As the latter cannot be explained by varying reaction conditions, they must originate from the lignin itself. Consequently, the desired reproducibility is not given.

Considering the values for esterification / grafting reactions with CL, the yields (Table 31) are notedly lower compared to lignin-PLA grafts and the obtained number average molecular weights (M_n) are lower than expected in most cases. This may be the result of the CO_2 sensitivity of TBD. It is known, that the formed TBD-CO_2 complex dissociates at approximately 135 °C, again liberating active TBD.[173] Therefore it is possible that the organocatalyst remained inactive under the applied reaction conditions (110 °C, inert atmosphere of nitrogen).

Another essential role is assigned to the work-up. Those reaction mixtures which were precipitated in diethyl ether after solubilization in DCM exhibit lower yields, most likely due to the removal of unconverted ROP monomers LA or CL. As a consequence, the yields may be overestimated if the reaction mixture was not precipitated in diethyl ether. The formed homopolymers additionally contribute to the distortion of the yields, regardless of precipitation. Reactions of lignin and LA dispersed in toluene at 110 °C (samples 11, 12, 15, 16, 18, 30 and 31, Table 31) also give notedly lower yields than comparable reactions at 150 °C in the melt.

Table 25. Collected results of HPLC-SEC analysis of lignin / polyester blends and grafts (50 °C, DMF).

Lignin / ROP monomer (m:m)	Sample	M_n / g·mol^{-1}	M_w / g·mol^{-1}	PDI
–	GL1	1400	7900	5.5
lignin / PHB 1:3	3	1000	3300	3.1
	4	1200	1300	11
	5	1500	7500	5.0
lignin / PHB 1:10	1	1500	4500	3.1
lignin-LA 1:1	11	8200	238500	29
	22	2400	61700	25
	23	2100	48700	2.4
lignin-LA 1:2	20	2600	103400	40
	21	2900	34300	1.2
	13	3400	62200	18
lignin-LA 1:3	16	2900	24900	8.5
	18	3700	53000	1.4
	17	4600	90300	20
	19	5600	78800	1.4
lignin-LA 1:6	6	1800	14400	8.0
	7	5300	65000	12
lignin-CL 1:1	40	3500	225500	64
	41	2000	86300	4.3
lignin-CL 1:2	38	2800	20700	7.5
	33	3000	23500	8.0
	33[a]	3500	58300	1.7
lignin-CL 1:3	39	2600	16900	6.5
	34	3000	21100	7.1

[a] double determination

The synthesized lignin grafts were also investigated via ^{31}P NMR spectroscopy after phosphitylation. Again, as already described in the previous chapter (section 3.2.1), the obtained values have to be referred to the corrected amount of total hydroxyls in the starting lignin (according to the 'real' lignin content in the sample) (see also Table 50, Appendix). Figure 24 shows ^{31}P NMR spectra of the lignin / PHB blend as well as those of lignin-PLA and -PCL grafts, in all cases in a ratio of 1:3 (m:m). The corresponding values are listed in Table 26. The decrease of OH peaks and the signal arising from the according polyester hydroxyl end groups after phsophitylation are clearly visible. Interestingly, samples of lignin-PLA grafts were partial insoluble in the NMR solution, although they were completely soluble in dichloromethane right after the grafting reaction via ROP of LA. As already mentioned previously, it is not obvious from the shown spectra that PHB is not covalently grafted onto lignin. The spectrum of the blend appears optically, as well as those of lignin grafts, with notedly less signals of lignin hydroxyl groups.
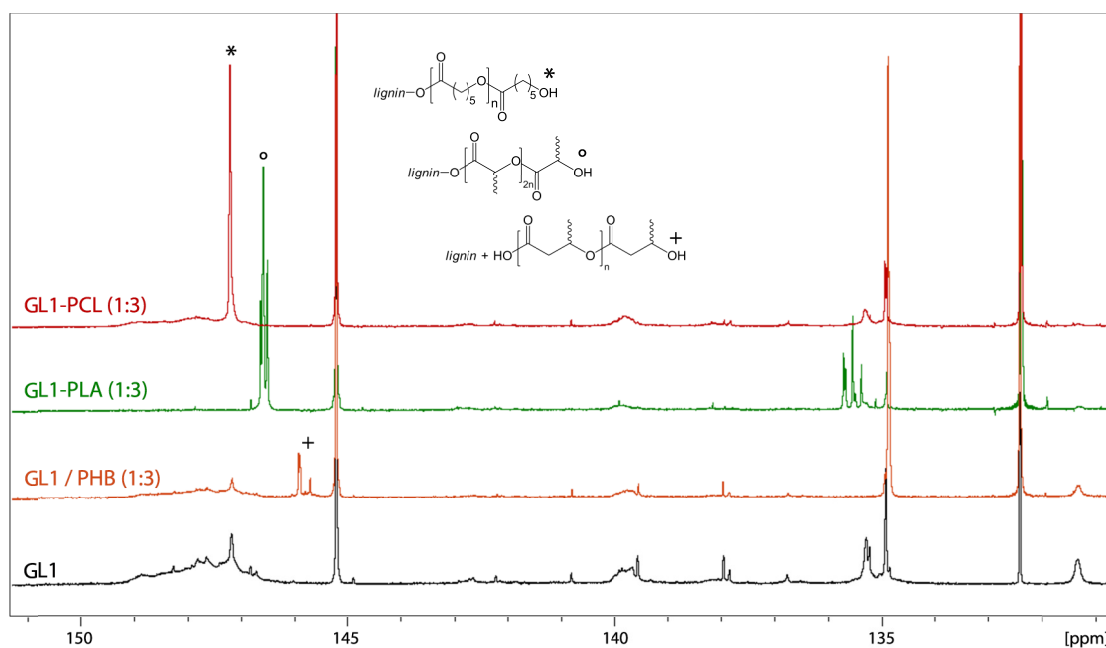
Figure 24. ^{31}P NMR spectra of lignin / PHB blend, lignin-PLA and -PCL grafts (samples 3, 19 and 39) (25 °C, 200 MHz, CDCl₃).

Obviously, guaiacyl (G) units (δ 140.2–138.6 ppm) are less preferred in this conversion as the according signal remains present in the ^{31}P NMR spectra of the blends, or the grafts respectively. Investigating the values listed in Table 26, it can be seen that the obtained results are very diverse, especially for graftings with D,L-lactide and ε-caprolactone. The binary blends of lignin with PHB (1:3) (m:m) exhibit a lignin hydroxyl number corresponding rather exactly to the corrected amount of the starting lignin (GL1) respective to the applied blend ratio. For both blend samples, it can be observed that the amount of phenolic hydroxyl groups slightly increased at the expense of aliphatic hydroxyl groups. This finding could indicate structural changes of lignin under the applied reaction conditions, like the cleavage of β-O-4 linkages for instance. Interestingly, the amount of carboxyl groups is extremely increased in both lignin / PHB samples. The additional carboxyl groups may originate from PHB chains, where the initial guanidine base is substituted by TMDP upon phosphitylation prior to the ^{31}P NMR measurement. The amount of carboxyls is also slightly enriched in PLA- and PCL samples, which could be an evidence of PLA or PCL homopolymer formation due to moisture in the samples. If the ROP of LA or CL is initiated by water, a carboxylic acid would appear at the beginning of the chain.

Lignin-PLA grafts exhibit notedly less remaining OH groups than unmodified lignin in this mass share on one hand, and than lignin-PCL grafts on the other hand. The only exception is sample 18, again showing that the reaction in dispersion (in toluene) proceeds obviously not very well. Far better results were expected for the lignin-PCL grafts. One possible explanation is the reaction temperature of 110 °C, which is too low to reactivate the organocatalyst TBD in case of a dorming state due to CO₂ complexation.

Table 26. Selected values from ^{31}P NMR spectroscopy of GL1 / PHB blends as well as GL1-PLA and GL1-PCL grafts (1:3 (m:m)).

| Lignin / ROP monomer (m:m) | Sample | Content of functionalities / mmol·g^{-1} | | | | | | DS % |
		Total lignin hydroxyls	Aliphatic OH	Total phenolics	S/G/H ratio (phenol-terminated)	Carboxyls	Polyester end group	
1:0	GL1	3.86	3.28	0.58	1 / 1.6 / 2.6	1.21	–	–
reference values for 1:3 mixtures	GL1	0.97	0.82	0.15	1 / 1.6 / 2.6	0.30	–	–
lignin / PHB 1:3	3	1.12	0.81	0.31	1 / 4.5 / 1.7	1.14	0.22	–
	4	0.96	0.71	0.26	1 / 7.9 / 2.3	2.13	0.22	–
lignin-LA 1:3	16^{a*}	0.45	0.19	0.26	1 / 6.4 / 2.5	0.44	0.88	54
	18^{a*}	1.04	0.67	0.37	1 / 11 / 4.4	1.52	2.05	–
	17*	0.27	0.06	0.21	1 / 2.9 / 1.0	0.54	0.96	72
	19*	0.33	0.08	0.25	1 / 3.2 / 0.9	0.55	1.12	66
lignin-CL 1:3	39	1.77	0.91	0.86	1 / 0.6 / 0.2	0.50	1.01	–
	34	0.76	0.48	0.28	1 / 9.3 / 4.4	0.50	0.65	44

PLA endgroup = 146.6 ppm; PCL endgroup = 147.2 ppm
[*] not completely dissolved, [a] performed in toluene at 100 °C

The degree of substitution (DS) was determined from the results of quantitative ^{31}P NMR measurements. The amount of total hydroxyls (excluding the polyester end group) in the sample is considered in relation to the amount of total hydroxyls of the starting lignin in the corresponding weight proportion (see Table 50, Table 54 and Table 55, Appendix). In the best case, a degree of substitution (DS) (decrease of hydroxyl groups) of 83 % (samples 24 and 27, Table 31) could be reached with equimolar mixtures (corresponds to a weight ratio of 1:0.7) of lignin (KL2) and D,L-lactide. The obtained values for lignin-PLA grafts (19–83 %) are considerably higher compared to the DS values obtained for the ligninesters (cp. Table 23, section 3.2.2). The observed DS values for lignin-PCL grafts is in the range of 14–54 %, which is notedly lower compared to lignin-PLA grafts. This is in good accordance with the already mentioned partial inactivity of TBD under the applied reaction conditions. However, the investigation of the lignin grafts via ^{31}P NMR spectroscopy wouldn't reveal the homopolymer content, as particularly cyclic species won't be detected due to the lack of hydroxyl or carboxylic acid groups.

Figure 25 shows the results of simultaneous thermal analysis (STA) of selected lignin-PLA and -PCL grafts (1:3 (m:m)). The mass loss (dashed lines) and DSC traces (solid lines) are depicted in comparison to the starting lignin (GL1). The lignin-PLA sample (green) starts to decompose at approximately 212 °C (onset) and exhibits a pronounced decomposition peak (maximum 267 °C). Contrary to our expectations, a slight shift to lower decomposition temperatures is observed if the lignin ratio is increased in the PLA grafts (Figure 64, Appendix). Lignin-PCL grafts lack such a distinct decomposition peak and the mass loss of the sample is also significantly lower. The slight bend in the DSC traces at 294 °C could be interpreted as decomposition. Again, the same shift of this bend to lower temperatures can be seen with increased lignin content in the samples (Figure 65, Appendix).
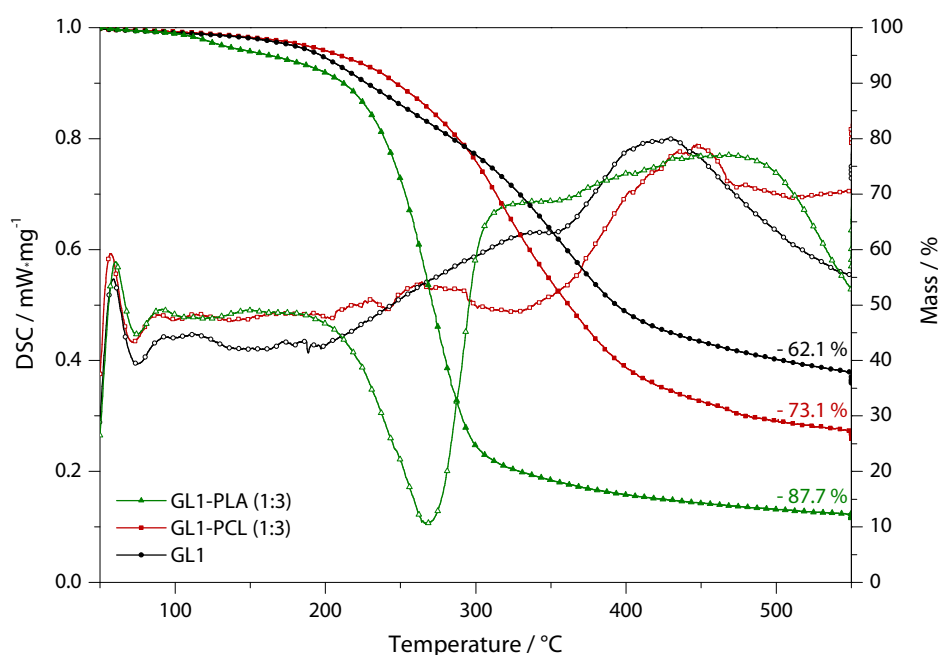
Figure 25. DSC (solid) and mass loss (dashed) traces of lignin-PLA and -PCL (samples 17 and 39) grafts.

The results obtained from different analyses correspond very well in most cases. One interesting finding is, that some of the derivatives become partly insoluble after drying and storage, although they were completely soluble in dichloromethane right after synthesis. Maybe this can be related to the already considered 'aggregates' which are probably formed due to exceptional strong hydrogen bonding between the carbonyl groups of the introduced polyester and remaining lignin hydroxyl groups.

An end group functionalization via esterification with bicyclo[2.2.1]hept-5-ene-2-carbonyl chloride of lignin-PLA derivatives (samples 16, 17 and 39) also proceeded successfully (see Table 23, entries 20–22).

Several of the synthesized lignin grafts were investigated by column chromatography (silica gel) using dichloromethane and methanol as eluents (DCM / MeOH 20:1 (v:v), gradient to pure MeOH) and fractions were collected until the eluent was colorless (Table 27).

Table 27. Recovery of lignin derivatives after column chromatography.

	(m:m)	Sample	Amount applied to the column / mg	Recovery / mg
	1:2	20	303.6	259.9 (85.6 %)
GL1-PLA		18[b,c]	301.2	171.1 (56.8 %)
	1:3	19[a,b]	304.1	285.0 (93.7 %)
GL1-PCL	1:3	39[b]	504.2	396.5 (78.6 %)

[a] overhead stirrer; [b] precipitation in Et$_2$O; [c] reaction in toluene (110 °C)

If lignin features no graft chains, it is insoluble in dichloromethane / methanol and won't be eluted. In case of sample 20, the product applied to the column was not completely dissolved and therefore not fully recovered. The purified samples were also investigated by quantitative ^{31}P NMR spectroscopy (selected values are listed in Table 28). Considering the values of functionalities before and after purification, the differences for sample 20 are in the range of tolerance, whereas sample 39 shows larger deviations. Possible explanations for that could be the incomplete conversion of CL during the reaction due to inactivity of the organocatalyst TBD. This would also agree with the incomplete recovery of the sample after column chromatography.

To summarize, the collected data and recovery rates of the lignin-polyester grafts after column chromatography suggest that conversions performed in the melt were successful. As already the low yields and the recovering of unreacted CL showed for reactions in toluene, the recovery of sample 18 was very low. As expected, this finding is in good agreement with results of other analyses and simultaneously the proof of this experiment.

Table 28. Selected values from ^{31}P NMR of samples 20 and 39 before and after purification.

Sample	Content of functionalities / mmol·g^{-1}					
	Total hydroxyls *(without end group)*	Aliphatic OH	Total phenolics	S/G/H ratio (phenol-terminated)	Carboxyls	Polyester end group
reference values for 1:2 mixtures (GL1)	1.29	1.09	0.20	1 / 1.6 / 2.6	0.40	–
20	1.05	0.60	0.45	1 / 4.4 / 1.6	1.04	1.36
20_pure	0.96	0.41	0.45	1 / 4.5 / 1.6	0.99	1.31
reference values for 1:3 mixtures (GL1)	0.97	0.82	0.15	1 / 1.6 / 2.6	0.30	–
39	1.77	0.91	0.86	1 / 0.6 / 0.2	0.50	1.01
39_pure	1.42	0.95	0.47	1 / 7.0 / 2.1	0.98	1.47

STRUCTURAL CHANGES OF LIGNIN UNDER THE APPLIED REACTION CONDITIONS

Serious changes in the lignin structure and interunit linkages may be caused due to elevated reaction temperatures and the applied organocatalysts. The harsh reaction conditions during esterification / grafting reactions (150 °C, transesterification catalyst) may lead to β-O-4' bond cleavage, resulting in an increased content of phenolic hydroxyl groups or the elimination of H_2O, generating double bonds. In order to detect structural changes in lignin caused by the applied reaction conditions, lignin (GL2) was dissolved in dry DMF and treated with the organocatalyst TBD at 150 °C (sample 47, Table 31). The sample was investigated via two-dimensional ^{13}C-^{1}H HSQC NMR spectroscopy under adiabatic conditions as described in section 2.1.2 to determine any structural changes. The lignin moieties mentioned in the following are depicted in Figure 6 (section 2.1.2). The obtained spectrum was analyzed semiquantitatively and the obtained values were compared with those of starting lignin GL2. Considering the values in Table 29, it can be seen that the S / G / H ratio as well as the amount of unsaturated moieties (FA, PCA) is clearly altered in the lignin sample treated with TBD at 150 °C. The amount of S and G units is notedly increased with respect to H units. α-Oxidized syringyl units (S') are decreased as well as the proportions of FA and PCA moieties with regard to G and H units. The increased amount of S and G units indicates the preferred cleavage of β-O-4' linkages concerning these moieties. The amount of cinnamyl alcohol end groups (X1) is also notedly increased, whereas the number of tricin units (T) can be considered as unaltered. As already found in the ^{13}C-^{1}H HSQC NMR analysis of GL2 (section 2.1.2), the determination of the interunit linkage ratio strongly differs, depending on the correlation signals integrated (α-, β- or γ-protons): A / B / C: 10.5 / 0.96 / 1.0 (α-protons); 9.4 / 1.4 / 1.0 (β-protons) and 15 / 1.5 / 1.0 (γ-protons). The most reasonable values, at least to our understanding, would be the ones determined by integration of β-protons as they are adjacent to the linkage concerned. Considering these values (Table 29), it can be seen that the amount of β-O-4' linkages (A) as well as that of phenylcoumarans (β-5') (B) is decreased with regard to resinols (β-β) (C) which is in accordance with the findings from ^{31}P NMR analysis.

Table 29. Ratio of lignin monomeric units in sample 47 and starting lignin GL2, including *p*-hydroxycinnamic acids (*p*HCA), end group X1, tricin (T) and different interunit linkages.

Ratio of lignin aromatic units	Sample 47	GL2
S	9.3	2.4
in α-oxidized form (S') / %	*6.0*	*6.2*
G	9.1	4.2
as ferulates (FA) / %	–	*24*
H	1.0	1.0
as p-coumarates (PCA) / %	–	*64*
cinnamyl alcohol end groups (X1) / %	–	0.2
tricin (T) / %	0.5	0.3
Ratio of lignin interunit linkages		
β-O-4' aryl ethers (A$_\beta$)	9.4	11
β-5' phenylcoumarans (B$_\beta$)	1.4	2.1
β-β resinols (C$_\beta$)	1.0	1.0
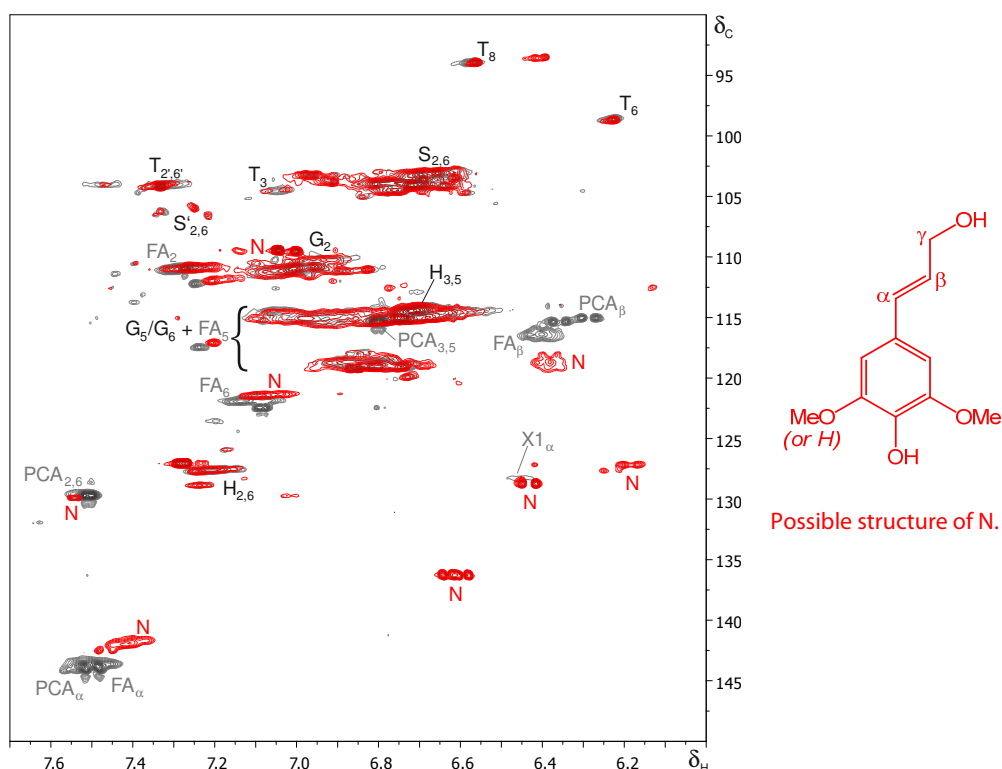
Figure 26. Expanded aromatic region of the ^{13}C-^{1}H HSQC NMR spectrum of sample 47 (red) in comparison to original *Annikki Gesamtlignin* (GL2, grey), (50 mg, 25 °C, 500 MHz, DMSO-d_6).

Moreover, new correlation signals were found in the aromatic region (δ_C/δ_H 90–150/6.0–7.7) (see also Table 48, Appendix), which are most likely signals of the unsaturated product of cleaved β-O-4' units. In Figure 26, the newly appeared correlations are signed with *N* (red) and the absent peaks in the spectrum of sample 47 are signed in grey. Obviously the unsaturated *p*-coumarate (PCA) and ferulate (FA) moieties are converted under the applied reaction conditions. As TBD is a highly active organocatalyst, it can promote various conversions,[174] and thus it is possible that the electron deficient double bonds of PCA and FA units react with hydroxyl groups for instance, to form new interunit linkages. Simultaneously, the new structures, most likely formed upon β-O-4' cleavage and subsequent H_2O elimination, would appear similar to cinnamyl alcohol end-groups (X1), possibly also in their γ-oxidized form featuring an aldehyde end group (compare Figure 6, section 2.1.2). Alterations in the correlations of aromatic rings are more difficult to detect and to quantify as many signals are overlayed and thus the differentiation must be made via the side chain correlations. In the aliphatic side chain region (δ_C/δ_H 50–90/2.5–6.0), one new correlation signal could be unequivocally located (59.8/3.98 ppm) which belongs most probably to the γ-CH_2 group of the newly formed species.

The sample was also investigated by ^{31}P NMR spectroscopy after phosphitylation as per the method described in section 2.1.2. Quantitative evaluation revealed significant differences in the detected amount of hydroxyl and carboxyl groups (Table 30). The number of total hydroxyls is reduced by 14 %, whereas the aliphatic hydroxyls are most affected. The amount of total phenolics can be considered as unaltered in total. Regarding the individual values which contribute to the total phenolics, a slight shift is noticeable: syringyl-OH units appear decreased whereas the number of condensed phenolics is increased. The amount of carboxyls is drastically reduced by 46 %. These findings indicate on one hand the cleavage of β-O-4' linkages, preferred concerning syringyl units, and condensation reactions of lignin moieties on the other hand, which is in good accordance with the results of ^{13}C-^{1}H HSQC NMR spectroscopy as well as literature studies.[175]

Table 30. Content of functionalities in sample 47 compared to original lignin (GL2), determined by ^{31}P NMR spectroscopy.

Functional group	Content in GL2 / mmol·g^{-1}	Content in sample 47 / mmol·g^{-1}
Total hydroxyls	4.32	3.71 *(–14.1 %)*
Aliphatic OH	3.35	2.62
Total phenolics	0.97	1.09
Total uncondensed phenolics	0.86	0.92
Syringyl-OH	0.05	0.15
Guaiacyl-OH	0.56	0.58
p-Hydroxy-phenyl-OH	0.24	0.19
S / G / H ratio (phenol-terminated)	1.0 / 10.5 / 4.5	1 / 3.7 / 1.2
Total condensed phenolics	0.11	0.17
Carboxyls	1.24	0.67 *(–46.0 %)*

Summary — esterification / grafting of lignin via ROP
- *Successful grafting of lignin via ROP of D,L-lactide and ε-caprolactone using 1,5,7-triazabicyclo[4.4.0]-dec-5-ene (TBD) as organocatalyst*
- *Solvent-free synthesis at elevated temperatures (110–150 °C)*
- *Green, sustainable route towards renewable, organosoluble lignin derivatives*
- *No covalent grafting with β-butyrolactone — only lignin / PHB blends observed*
- *Structural changes of lignin under the applied reaction conditions (cleavage of β-O-4' bonds, H$_2$O elimination as well as condensation reactions)*
- *Lignin-PLA grafts feature degrees of substitution (DS) in the range of 19–83 %*
- *Lignin-PCL grafts feature lower DS values (14–54 %) than lignin-PLA grafts*
- *Homopolymer formation leads to a distortion of yield and DS*

3.3.2 Experimental details

Standard operating procedure (SOP) for esterification / grafting reactions

Lignin was placed in a Schlenk flask and stirred under vacuum for 30 minutes before grafting monomer and *N*-centered organoinitiator were added. (If not stated otherwise, the syntheses were performed in bulk without any solvent.) The mixture was stirred at elevated temperatures (110 °C with CL and 150 °C with LA) under inert atmosphere of N_2 for at least 3 h, maximum 24 h. The remaining highly viscous liquid was dissolved in DCM or methanol and the product was precipitated in *n*-pentane or diethyl ether. (In case of BBL, the excess of grafting monomer was removed under vacuum before.) The product was dried under vacuum after decantation of *n*-pentane or diethyl ether to yield mainly brown solids or highly viscous brown liquids, whereas only DCM-soluble parts were considered as functionalized lignin and insoluble parts were discarded.

Note: TBD is known to be CO_2 sensitive and exposure to CO_2 would result in entire inactivity. A reactivation of the guanidine base is possible via heating to ~135 °C under inert atmosphere.[176] Thus, the fixed CO_2 is released and the TBD is recovered. We can assume that TBD was reactivated in situ in all bulk reactions of lignin and D,L-lactide due to temperatures of ~150 °C. Unfortunately, this was not the case for reactions in toluene as well as for reactions with ε-caprolactone due to lower reaction temperatures (~110°C). This explains the low yields obtained for these samples.

Table 31. Esterification / grafting reaction of lignin by the ring opening polymerization of lactide and lactones.

Sample	Starting lignin		Grafting monomer	Initiator		Temperature	Yield	DS
	name	mmol OH (g)		name	mmol	°C		%
			β-butyrolactone (BBL) / mmol (mL)					
1	GL1	0.39 (0.100)	12.3 (1.00)	DBU	0.033	80	1118 mg (97 %) highly viscous brown liquid	–
2	GL1	1.93 (0.500)	61.3 (5.00)	DBU	0.17	80	5576 mg (96 %) highly viscous brown liquid	–
3	GL1	1.94 (0.503)	18.1 (1.48)	TBD	0.10	80	1011 mg (50 %) brown solid	–
4	GL1	1.94 (0.503)	19.0 (1.55)	DABCO	0.11	80	888 mg (42 %) brown solid	–
5	KL1	nk (0.506)	18.6 (1.52)	DBU	0.17	80	1592 mg (75 %) brown solid	–
			D,L-lactide (LA) / mmol (g)					
6	GL1	1.96 (0.508)	20.9 (3.02)	DABCO	0.25	120 (vacuum)	373 mg (11 %) brown solid	–
7	GL1	1.95 (0.505)	18.9 (2.73)	TBD	0.10	125	2648 mg (82 %) highly viscous brown liquid	80
8	GL1	1.96 (0.508)	9.4 (1.35)	TBD	0.10	125	856 mg (46 %) brown solid	74
9	KL1	nk (0.508)	18.8 (2.70)	TBD	0.11	125	3076 mg (96 %) highly viscous brown liquid	nd
10	KL1	nk (0.516)	19.1 (2.77)	–	–	125	nd	nd
11	GL1	4.47 (1.16)	7.98 (1.15)	TBD	0.20	100 (in 5 mL toluene abs.)	1089 mg (47 %) brown solid	50
12	GL1	7.84 (2.03)	8.15 (1.18)	TBD	0.40	100 (in 3 mL toluene abs.)	2591 mg (81 %) brown solid	nd
13	GL1	19.34 (5.01)	69.6 (10.03)	TBD	0.93	150	10.1 g (67 %) brown solid	47
14	GL1	19.38 (5.02)	69.5 (10.01)	TBD	0.93	150	13.9 g (92 %) brown solid	66
15	GL1	19.3 (5.00)	34.7 (5.00)	–	–	110 (in 50 mL toluene)	–	–
16[b]	GL1	19.3 (5.00)	104.1 (15.0)	TBD	0.93	110 (in 50 mL toluene)	10.9 g (54 %) brown solid	54
17[b]	GL1	19.3 (5.00)	104.2 (15.0)	TBD	0.93	150	18.7 g (94 %) brown solid	72

[a] without stirring; [b] precipitated in diethyl ether; nk = not known, nd = not determined

Table 31 continued.

Sample	Starting lignin		Grafting monomer	Initiator		Temperature	Yield	DS
	name	mmol OH (g)		name	mmol	°C		%
18[b]	GL1	19.3 (5.00)	104.1 (15.0)	TBD	0.93	110 (in 250 mL toluene)	6.66 g (33 %) brown solid	–
19[b]	GL1	19.3 (5.00)	104.1 (15.0)	TBD	0.93	150	9.54 g (48 %) brown solid	66
20[a]	GL1	19.3 (5.00)	69.4 (10.0)	TBD	0.94	150[a]	14.8 g (99 %) brown solid	19
21[a]	GL1	19.3 (5.00)	69.4 810.0)	TBD	0.94	150[a]	14.3 g (95 %) sticky brown solid	78
22[a]	GL1	19.3 (5.00)	34.7 (5.00)	TBD	0.94	150[a]	9.99 g (99 %) sticky brown solid	58
23[a]	GL1	19.3 (5.00)	34.7 (5.00)	TBD	0.94	150[a]	9.47 g (95 %) sticky brown solid	64
24	KL2	15.7 (3.00)	15.3 (2.17)	TBD	0.10	125[a]	5.15 g (99 %) brown solid	83
25	KL2	15.8 (3.01)	30.0 (4.33)	TBD	0.10	125[a]	2.76 g (38 %) brown solid	57
26	KL2	15.7 (3.00)	45.0 (6.49)	TBD	0.11	125[a]	7.23 g (76 %) brown solid	73
27	KL2	15.7 (3.00)	15.1 (2.18)	TBD	0.10	125[a]	5.02 g (97 %) brown solid	83
28	KL2	15.7 (3.00)	29.9 (4.32)	TBD	0.10	125[a]	1.90 g (26 %) brown solid	62
29	KL2	15.7 (3.00)	45.0 (6.49)	TBD	0.10	125[a]	1.24 g (13 %) brown solid	24
			ε-caprolactone (CL) / mmol (mL)					
30	GL1	1.95 (0.506)	1.87 (0.199)	TBD	0.40	50 (in 3 mL toluene abs.)	358 mg (50 %) brown solid	nd
31	GL1	1.93 (0.501)	3.73 (0.396)	TBD	0.10	50 (in 3 mL toluene abs.)	824 mg (89 %) brown solid	nd
32	GL1	1.95 (0.504)	9.31 (0.988)	TBD	0.10	50	158 mg (10 %) brown solid	nd
33[b]	GL1	19.3 (5.00)	90.2 (10.00)	TBD	0.93	110	8.78 g (57 %) highly viscous brown liquid	14
34[b]	GL1	19.3 (5.00)	135.4 (14.31)	TBD	0.93	110	13.0 g (64 %) highly viscous brown liquid	22
35[b]	KL1	26.2 (5.00)	135.4 (14.31)	TBD	0.93	110	–	nd

[a] without stirring; [b] precipitated in diethyl ether; nk = not known, nd = not determined

Table 31 continued.

Sample	Starting lignin		Grafting monomer	Initiator		Temperature	Yield	DS
	name	mmol OH (g)		name	mmol	°C		%
36[b]	GL1	13.1 (3.39)	148.6 (15.71)	TBD	0.63	110	11.8 g (58 %) brown liquid	–
37[b]	GL1	4.83 (1.25)	109.5 (11.57)	TBD	0.23	110	2027 mg (15 %) brown liquid	–
38[a,b]	GL1	19.3 (5.00)	94.6 (10.00)	TBD	0.93	110	6.70 g (42 %) brown solid	–
39[a,b]	GL1	19.3 (5.00)	141.9 (15.00)	TBD	0.93	110	5.96 g (28 %) highly viscous brown liquid	–
40[a]	GL1	19.3 (5.00)	47.3 (5.00)	TBD	0.96	150[a]	10.2 g (98 %) sticky brown solid	44
41[a]	GL1	19.3 (5.00)	47.3 (5.00)	TBD	0.96	150[a]	8.94 g (86 %) sticky brown solid	nd
42	KL2	15.7 (3.00)	15.0 (1.585)	TBD	0.11	110[a]	2.07 g (44 %) sticky brown solid	54
43	KL2	15.7 (3.00)	30.1 (3.180)	TBD	0.10	110[a]	4.05 g (63 %) sticky brown solid	50
44	KL2	15.7 (3.00)	54.0 (4.760)	TBD	0.10	110[a]	6.81 g (84 %) sticky brown solid	31
45	GL2	21.6 (5.00)	219 (23.15)	TBD	0.219	150	11.5 g (37 %) highly viscous brown liquid	nd
46	GL2	8.64 (2.00)	175 (18.52)	TBD	0.175	150	3.50 g (15 %) highly viscous brown liquid	nd
47	GL2	2.00 (0.50)	–	TBD	0.215	150 (5 mL dry DMF)	–	–

	endo,exo-Bicyclo[2.2.1] hept-5-ene-2-methanol	ROP monomer	Initiator		Reaction conditions	¹H NMR analysis of reaction solution	
			name	mmol	°C (solvent)	25 °C, 300 MHz, CDCl₃	
48	0.81 mmol (97.4 µL)	BBL 4.03 (329 µL)	TBD	0.04	50 (2 mL DCM abs.)	PHB	–
49	1.38 mmol (167.8 µL)	LA 6.94 (1.00 g)	TBD	0.07	rt (2 mL DCM abs.)	PLA-grafted endo,exo-bicyclo[2.2.1]hept-5-ene-2-methanol	–
50	0.81 mmol (97.4 µL)	CL 4.03 (427 µL)	TBD	0.04	50 (2 mL DCM abs.)	PCL-grafted endo,exo-bicyclo[2.2.1]hept-5-ene-2-methanol	–

[a] without stirring; [b] precipitated in diethyl ether; nk = not known, nd = not determined

4 APPLICATION OF LIGNIN DERIVATIVES

This chapter is about reasonable applications of the synthesized lignin derivatives described in the previous section. First, the incorporation of lignin and lignin derivatives in polydicyclopentadiene is demonstrated (section 4.1). Second, the fabrication of bicomponent thin films with cellulose is presented (section 4.2).

4.1 LIGNIN-PDCPD THERMOSETS

The incorporation of lignin or lignin derivatives into polydicyclopentadiene (PDCPD) networks is a completely novel approach. Based on preliminary studies in the framework of the *FFG*-funded project (*Biomimetischer Lignocellulose-Aufschluss,* 830107/14233SCK/SAI) thermosets based on unsaturated lignin derivatives and dicyclopentadiene were synthesized via ring opening metathesis polymerization (ROMP).[177]

PDCPD is a cheap, petroleum based thermoset featuring outstanding material characteristics such as high impact strength, low weight and superior resistance against chemicals as well as environmental impacts. The incorporation of the renewable resource lignin would constitute a higher value added application for the biopolymer and simultaneously make PDCPD *greener*. Appropriate lignin derivatives may not only have the capability to enhance the material characteristics, but also the ecological footprint of the thermoset.

Table 32. Monomers and initiator used for the synthesis of PDCPD / lignin resins.

| dicyclopentadiene (DCPD) | palmitoyl lignin | oleoyl lignin | Umicore M2 |
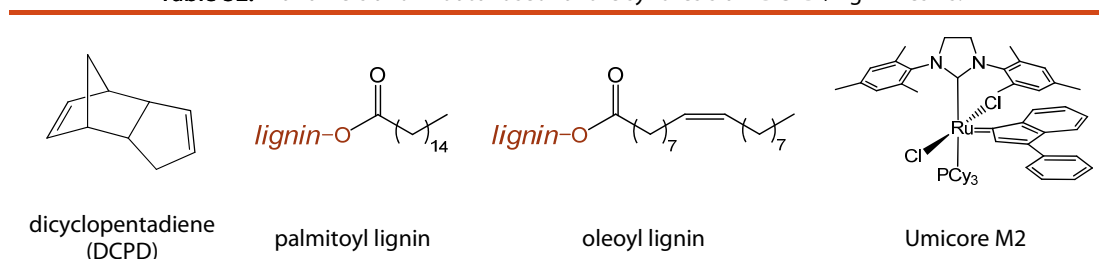
The ring opening metathesis polymerization (ROMP) of DCPD was performed in bulk at elevated temperatures (80 °C) using the commercially available 2nd generation initiator *Umicore* M2 (Table 32, Scheme 8 and Figure 27, A). Unmodified lignin was admixed as insoluble filling agent in varying amounts (5–30 wt%) and the dispersions were cured in preheated steel molds (Figure 28). The synthesized ligninesters (section 3.2) were used as soluble / reactive fillers at comparatively high loadings (20 wt%). Palmitoyl lignin can be considered as soluble filling agent (Figure 27, B). Oleoyl lignin, in contrast, can be assumed as reactive soluble filler for DCPD as it features a double bond and hence the ability to be covalently bound into the network by a cross metathesis reaction (Figure 27, C). The most ideal network will be obtained with *rompable* lignin, e.g. featuring a norbornene moiety, as co-monomer for DCPD (Figure 27, D).

Scheme 8. Ring opening metathesis polymerization of DCPD and resulting PDCPD network.

curing (M2, 80 °C)

(A) PDCPD | *(B) PDCPD with lignin as filler* | *(C) PDCPD with lignin as reactive filler* | *(D) PDCPD-lignin copolymer*
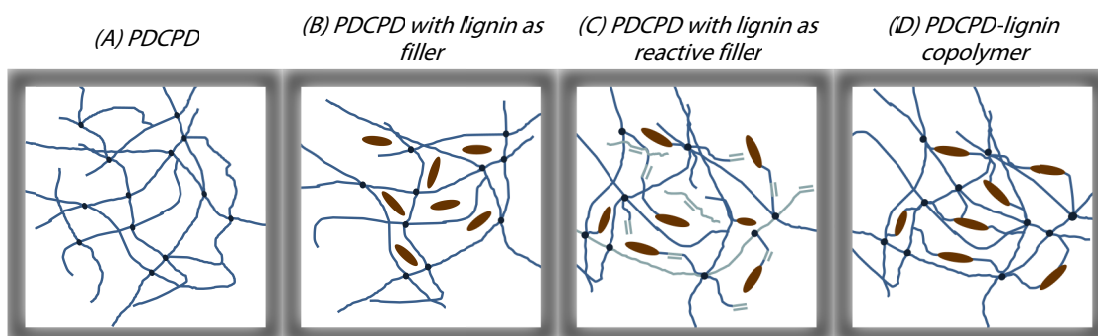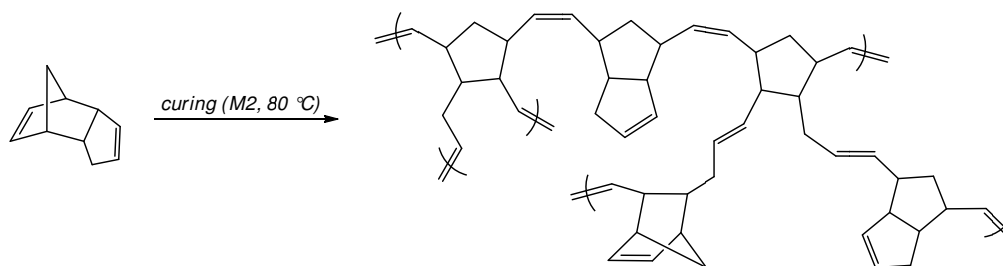
Figure 27. Schematic illustration of lignin incorporation in the PDCPD network.

The mechanical properties of the obtained shouldered test bars (Figure 28) were investigated via tensile strength tests, Shore D hardness measurements as well as scanning electron microscopy images. The following section is splitted in two parts: first, unmodified lignin as insoluble filler for PDCPD and second, soluble / reactive lignin derivatives as filler for PDCPD.

Figure 28. PDCPD shouldered test bars filled with insoluble lignin.

4.1.1 LIGNIN AS INSOLUBLE FILLER

A series of PDCPD shouldered test bars was prepared applying different lignins as filler, namely *Kraft* lignin (KL1), low molecular weight *Annikki* lignin (NML), *Annikki Gesamtlignin* (GL2) and extracted GL2. Mixtures of lignin (5–30 wt%) and dicyclopentadiene (DCPD, 95–70 wt%) were cured via ring opening metathesis polymerization (ROMP), initiated by the commercially available ruthenium carbene complex M2 (75 ppm with respect to DCPD). Reference specimens were prepared without admixed lignin.

For the preparation of one specimen, 1.5 mL monomer solution are required. The appropriate amount of lignin (980 mg, 20 wt%) was placed in a glass vial and DCPD (3920 mg, 4.0 mL, 29.65 mmol, 80 wt%) as well as toluene (200 µL) were added. In order to disperse the lignin powder, the mixture was stirred vigorously at RT. A stock solution of the initiator M2 (10 mg / mL toluene) was prepared. The initiator (63.3 µL, 75 ppm with respect to DCPD) was added to the monomer solution (1.5 mL). The mixture was immediately poured into a preheated steel mold (80 °C). For curing the mixtures were placed in an oven at 80 °C for 1–20 h (Figure 29). The mold used for producing shouldered test bars was a standardized hardened steel mold with the below stated dimensions (Figure 30).

Figure 29. Steel mold for shouldered test bars (left) and prepared specimens (right), (neat DCPD (10), DCPD + 20 % wt NML (21) and DCPD + 30 % wt NML (22)).

l_3	90 mm
l_2	54 mm
l_1	30 mm
r	30 mm
b_2	10 mm
b_1	5 mm
h	2 mm
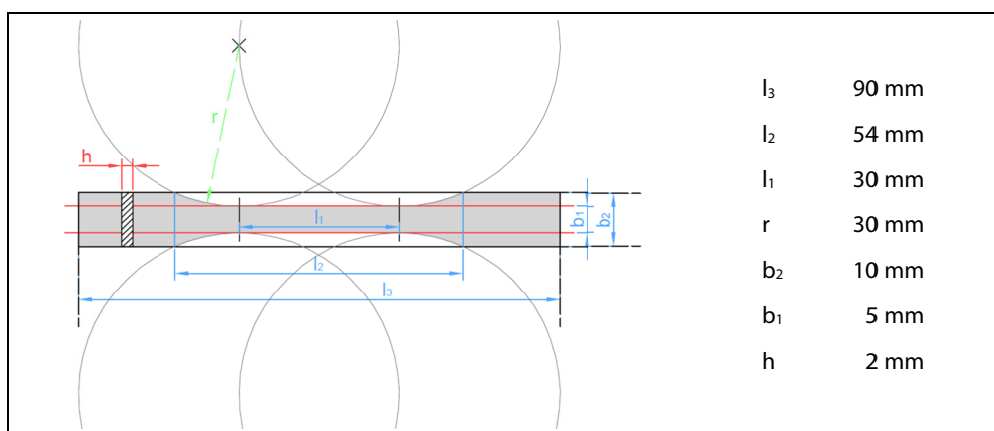
Figure 30. Mold for shouldered test bars, according to DIN EN ISO 3167 and 527 respectively (left), and dimensions of test specimen type 1BA (right).

This series was prepared to investigate the effect of lignin as filler on the mechanical properties of PDCPD and to compare different lignin samples. Thus, two Annikki lignins (NML and GL2) featuring different molecular weights were used. Additionally, GL2 was extracted prior to its admixture to remove fatty acids present in lignin. Fatty acids would negatively influence the ROMP of DCPD,[178] hence the samples with extracted GL2 are expected to feature better mechanical properties. Another series using a commercially available *Kraft* lignin (KL1) as filler was prepared additionally. The mechanical properties of the specimens were investigated via tensile strength tests at constant speed rate (1 mm / min). Measurements were performed on a Shimadzu Autograph AGS-X machine, with a force measuring range from 0.01–10 kN. The clamping length of the samples was 53 mm and an initial tension of 10.0 N was applied. The according values of tensile strength and elastic modulus are listed in Table 33. Figure 31 shows the progress of ultimate tensile strength (R_m) and elastic modulus (E) with increasing content of lignin filler (average value of two specimens, except for samples containing 5, 10 and 15 wt% NML). The according stress-strain diagrams of the lignin-filled PDCPD thermosets are shown in Figure 32 (NML), Figure 33 (GL2), Figure 34 (extracted GL2) and Figure 35 (KL1).

The ultimate tensile strength (R_m) of lignin containing specimens is far below that of the PDCPD reference sample. Already 5 wt% lignin result in a drastical drop of the R_m values, independently of the lignin type admixed. In general, the progress is not very constant, whereas the *smoothest* progress for both, E and R_m, is observed with extracted GL2. This finding indicates that extracted GL2 is more homogeneous compared to the other lignin samples. Due to the vigorous stirring during extraction with cyclohexane, a better dispersion of lignin in DCPD is probably achieved. Additionally, the removal of fatty acids (~ 8 wt%) has a positive impact on the ROMP of DCPD, as those are believed to interfere the curing process of DCPD. This assumption is supported by the deviating R_m and E values of PDCPD filled with GL2 in contrast to that of specimens containing extracted GL2.

Table 33. Tensile strength (R_m) and elastic modulus (E) of specimens.

Filler / wt%	Tensile strength R_m / MPa				Elastic modulus E / MPa			
	NML	GL2	GL2 extracted	KL	NML	GL2	GL2 extracted	KL
0	46.0				1320			
5	31.7	41.9	33.6	37.9	1290	1840	1530	1280
	–	41.9	32.1	36.6	–	1860	1500	1010
10	22.5	38.5	31.0	32.7	1570	1700	1630	1630
	–	34.5	28.6	31.0	–	1600	1390	1650
15	26.9	35.7	30.6	31.9	1760	1330	590	1690
	–	34.8	28.3	29.2	–	1370	1500	1550
20	23.6	26.0	27.0	32.3	1710	1630	1650	1770
	26.1	24.6	25.6	31.3	1730	1070	1650	1760
25	22.0	27.5	24.7	29.2	1840	1410	1580	1730
	20.1	23.6	23.6	28.5	1800	1300	1860	1890
30	16.2	25.7	23.8	20.2	1780	1630	1680	1000
	18.9	23.0	21.3	19.9	2060	1690	1760	1380
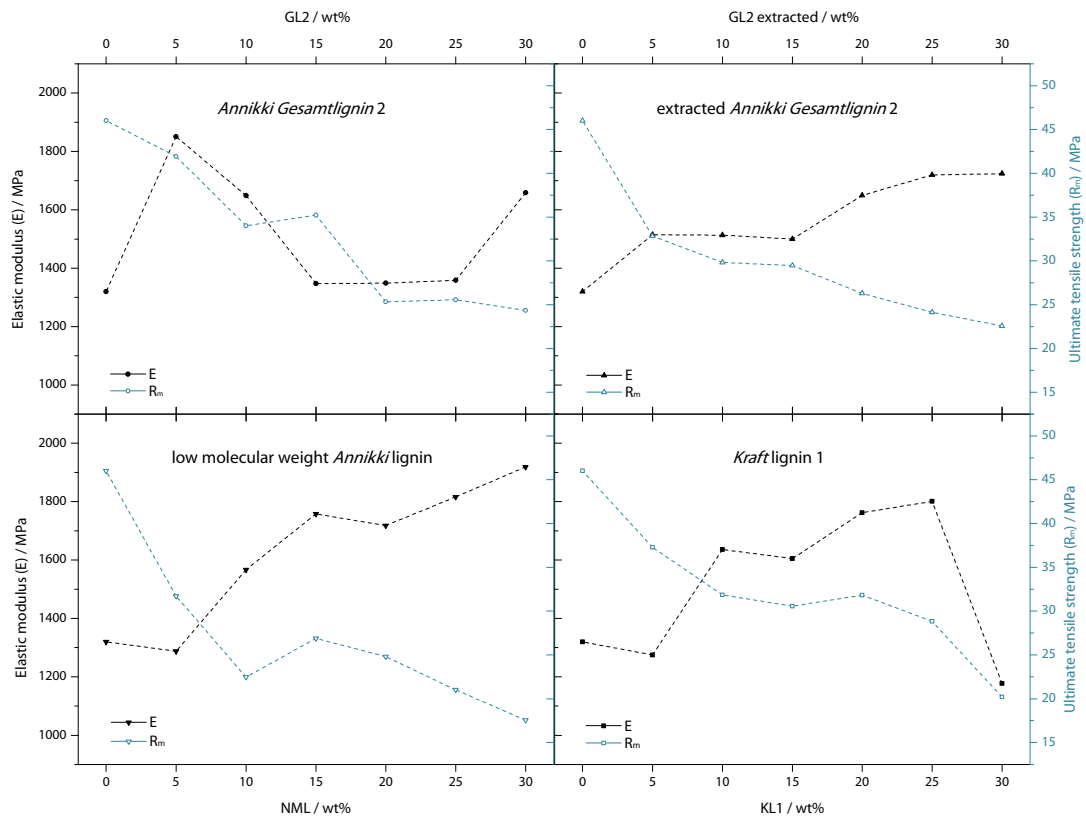
Figure 31. Comparison of R_m (blue, open symbols) and E (black, filled symbols) with increasing lignin contents.

Notedly increased shrinkage, not in length but in height, was observed for specimens containing lignin in amounts ≥ 20 wt%. A significant meniscus was formed at the surface of these test bars. This can be explained by augmented evaporation of DCPD monomer at 80 °C due to decelerated curing behavior (≥ 1 h) caused by admixed lignin. As a result, lignin was found to concentrate at the bottom of the mold.

Considering the tensile strength (R_m, blue in Figure 31), the decreasing progress is consistent with increasing content of lignin filler in all cases. Interestingly, the largest drop of R_m at low admixed amounts of lignin (5 and 10 wt%) is observed with NML. Obviously, the molecular weight of the filler applied exhibits a remarkable influence on the mechanical properties.

In contrast, the elastic modulus (E, black in Figure 31) slightly increases with the amount of admixed lignins. Specimens with extracted GL2 show the most uniform trend as E is continuously increasing with the applied lignin content. The value with 30 wt% KL can be considered as outlier. Specimens with GL2 do not show any clear trend as the values of samples with 0 and 15–25 wt% GL2 are very similar. Deviations of individual values are referred to processing inaccuracies and to intrinsic inhomogeneities of lignin.

Considering the stress-strain diagrams for the four different lignin-filled PDCPD series below (Figure 32 - Figure 35), it can be seen that tensile strength as well as elongation are far below that of neat PDCPD. This already comes into account when admixing 5 wt% of lignin. The highest tensile strength (R_m) with 5 wt% lignin filler was obtained with GL2 (> 40 MPa) and the worst with NML (< 30 MPa). R_m values > 25 MPa were obtained with specimens containing 30 wt% GL2. In general, the tensile strength decreases continuously with

increasing amount of admixed lignin particles, albeit with some deviations as can be seen in Figure 31. The best mechanical properties were obtained with GL2 and not with extracted GL2, as expected.

The elongation is also notedly reduced for lignin containing samples. Especially if amounts ≥ 20 wt% lignin are admixed, the strain hardly exceeds 5 %. The maximal stress is reached between 1 and 3 % strain. Proper cured PDCPD shoulder bars reach the maximal stress at approximately 5 % strain, break up from 10 % strain and can even stretch until 90 % or more. Thus, it can be concluded that lignin-filled PDCPD thermosets exhibit an increased brittleness.

The elastic modulus of lignin containing samples is higher than that of neat PDCPD (Table 33). This is also obvious in the stress-strain diagrams at the higher gradients in the linear initial range of the curves.

The hardness of the specimens was determined using a digital PCE-DD-D Shore D durometer (0–100 Shore D) from PCE Instruments UK Limited. Samples comprising lignin feature a similar hardness as pure PDCPD (70–80 Shore D). Specimens, filled with NML and GL feature rather decreased values (65–72 Shore D), whereas samples containing KL1 are slightly harder (74–78 Shore D).
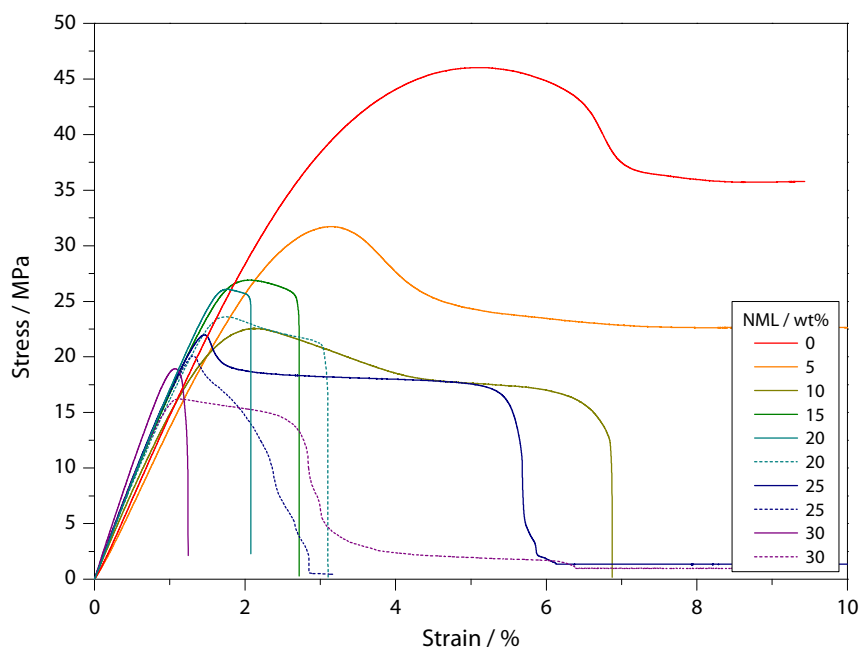
Figure 32. Stress-strain diagrams of PDCPD shouldered test bars filled with NML.
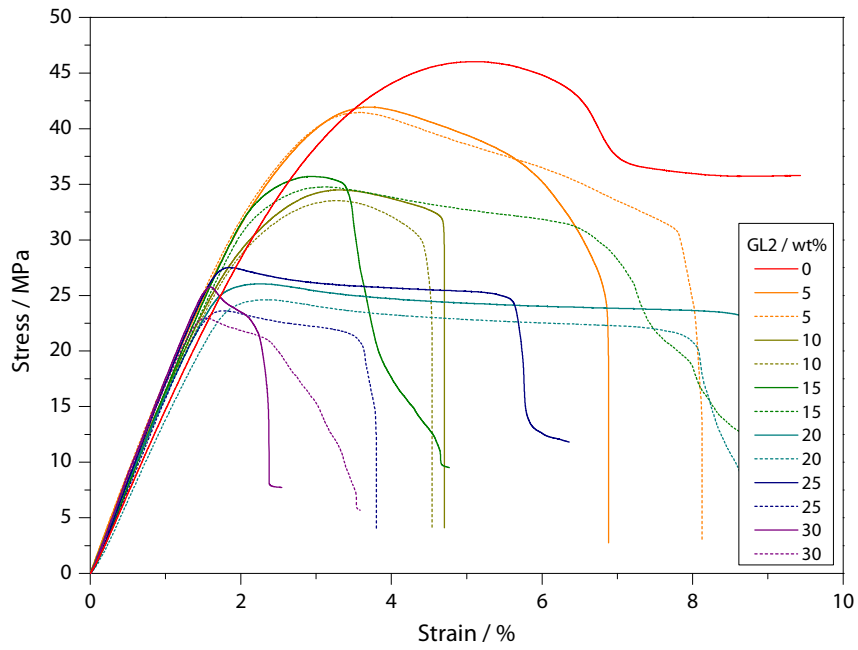
Figure 33. Stress-strain diagrams of PDCPD shouldered test bars filled with GL2.
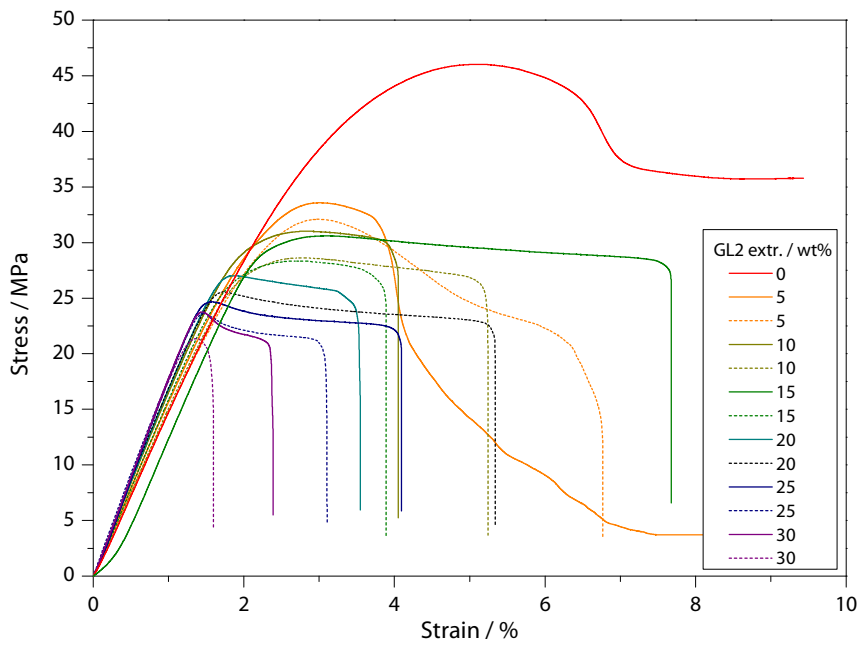
Figure 34. Stress-strain diagrams of PDCPD shouldered test bars filled with extracted GL2.
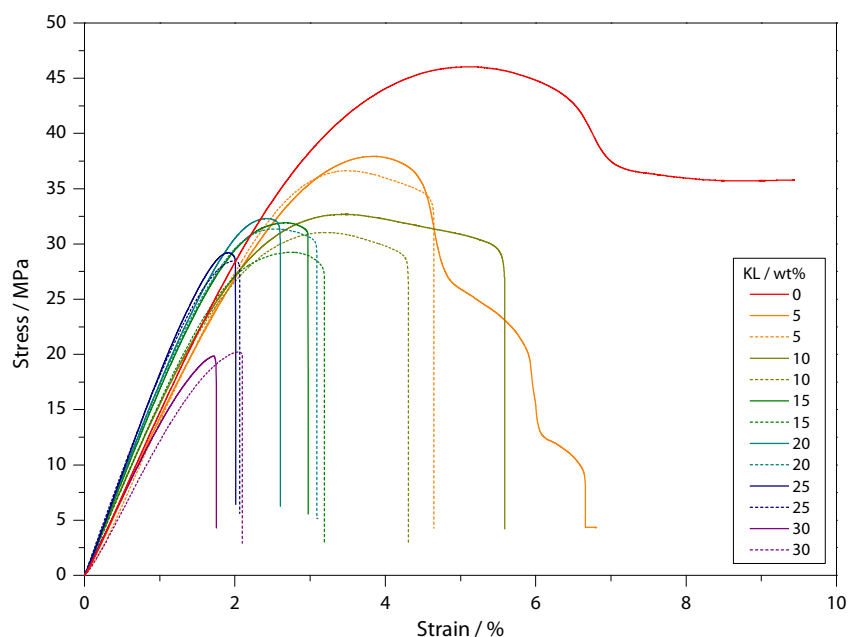
Figure 35. Stress-strain diagrams of PDCPD shouldered test bars filled with KL.

Several test bars were investigated by scanning electron microscopy (SEM). Images were obtained from a VEGA3 SB easy probe microscope from TESCAN Orsay Holding. The site of fracture after the tensile strength test served as appropriate cross section surface (Figure 36). The perceptible difference between the neat PDCPD and the lignin composite is obvious. The surface of the breaking point of lignin containing samples appears like a porous structure. Wheras the fracture of neat PDCPD (Figure 36, upper left corner) is rather smooth, that of lignin-filled samples features an inhomogeneous and fringed texture. It is very likely that lignin exists in the form of spherical particles in the polymer matrix, as it is insoluble in DCPD (cp. Figure 36). Unfortunately, the particle size of the lignin samples could not be determined. However, the lignin particles are clearly visible in the PDCPD matrix (cp. Figure 36, loadings ≥ 20 wt%) and thus the particle size is estimated from SEM images to be in the order of 1–10 μm. It can be assumed that the particle size as well as the dispersion of the filler significantly influence the mechanichal properties of the thermoset.

There is only very few literature about PDCPD composites containing particles. Thus, enhanced hardness and bending strength of the PDCPD matrix was reported upon incorporation of grafted silica nanoparticles in low amounts (0.25–2.0 wt%).[179] Another approach is the reinforcement of PDCPD by admixing carbon fibers and nanotubes as well as graphene oxide. Mechanical tests of the composites showed that the incorporation of the different fillers in low amounts (0.4 wt%) significantly enhanced material characteristics like tensile strength, elongation at break or thermal stability.[180] However, these findings are not comparable with lignin as filler, first, due to the tremendous difference in size of the particles and second, in terms of the quantities applied (≤ 2 wt% in contrast to 30 wt%).
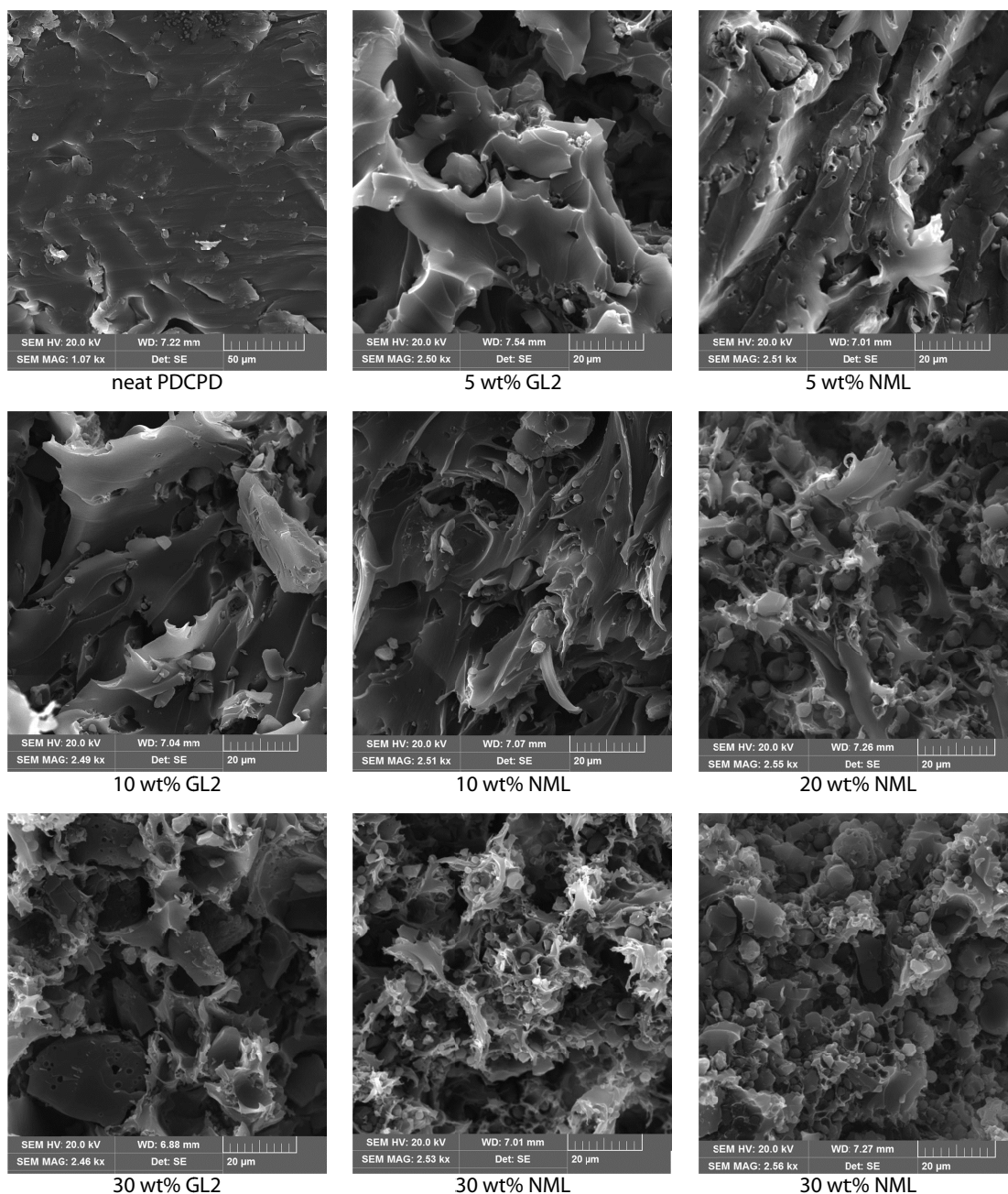
Figure 36. Morphology of PDCPD with 0, 5, 10, 20 and 30 wt% NML or GL2 after tensile strength test at breaking point.

A sample of PDCPD filled with 20 wt% low molecular weight lignin (NML) was extracted with dichloromethane (RT, 72 h). The specimen showed no externally visible changes or swelling upon the treatment with dichloromethane. Gravimetric analysis of the DCM-soluble residuals revealed 1.4 wt% extractives. Therefore, it can be reasonably assumed that the lignin particles are well embedded into the PDCPD network. Nevertheless, the key characteristics of the material are lost when applying unmodified lignin as filler in the investigated composition. The weak mechanical properties can be attributed to a low compatibility of lignin with the non-polar polymer matrix as well as an uneven distribution of the particles.

The enhancement of elastic modulus and the simultaneous reduction of tensile strength and elongation were also observed when blending lignin with other polymers, more precisely thermoplastics.[181]

4.1.2 LIGNIN AS SOLUBLE / REACTIVE FILLER

The synthesized palmitoyl and oleoyl lignins are to a great extent soluble in DCPD (Figure 37). The amount of dissolved ligninester is in the range of 45–95 wt% (Table 21, section 3.2.1). The other two long chain ligninesters which were synthesized as comonomer for the ROMP of DCPC, namely 10-undecenoyl and palmitoyl / norbornenoyl lignin (Table 17, section 3.2.1), were for the most part insoluble in DCPD. Thus, no copolymers were obtained from these ligninesters. The lignin-poly(lactide) and -poly(ε-caprolactone) grafts are, as expected, completely insoluble in the non-polar DCPD.

Mixtures for shouldered test bars were prepared in the same manner as described in the previous section. Palmitoyl- and oleoyl-lignin (980 mg, 20 wt%) were dissolved in DCPD monomer (3920 mg, 80 wt%) (Figure 37) and cured with M2 initiator (63.3 µL from a 10 mg / mL stock solution in toluene, 75 ppm with regard to DCPD) at 80 °C for at least 5 h.
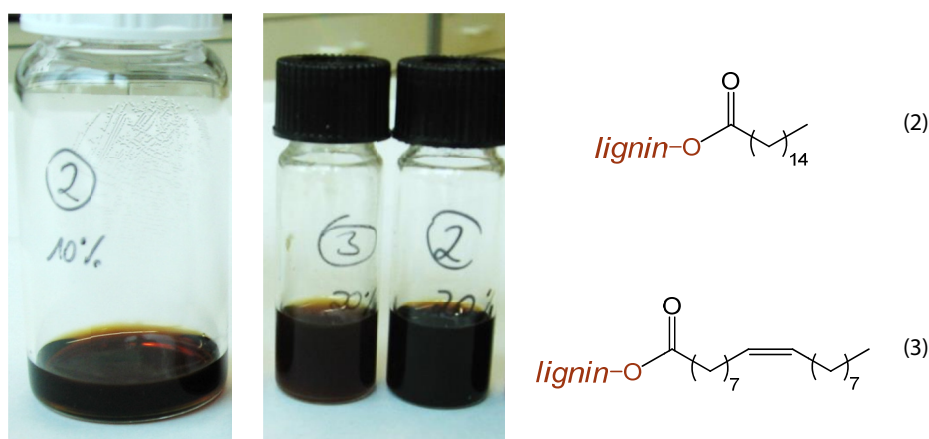
Figure 37. 10 wt% (left) and 20 wt% (right) palmitoyl lignin (2) and oleoyl lignin (3) dissolved in DCPD.

The applied ligninesters exert great influence on the mechanical characteristics of the cured PDCPD thermosets. Apart from the insufficient solubility of the derivatives in neat DCPD, the impact of the ligninesters on the ROMP of DCPD is highly disadvantageous. By applying palmitoyl lignin as soluble filler for DCPD, often very brittle materials, which could not be removed from the steel mold or be fixed in the tensile testing clamps without damage, were obtained. The curing of mixtures containing oleoyl lignin yielded mainly viscous liquids instead of hardened thermosets. Thus, most of the DCPD / oleoyl lignin copolymers could not be investigated via tensile strength tests. The mechanical characteristics of the obtained shouldered test bars, if possible, were again characterized via tensile strength tests, the according values are listed in Table 34 and the stress-strain diagrams are shown in Figure 38. The mechanical performance of PDCPD containing soluble / reactive ligninesters is even lagging far behind that of unmodified lignin applied in the same amount (20 wt%).

Table 34. Tensile strength (R_m) and elastic modulus (E) of specimens.

Tensile strength R_m / MPa	Elastic modulus E / MPa	Elongation at break / %
46.0	1320	9.4
20 wt% palmitoyl lignin		
12.7 (45)	1160	1.3
10.4 (44)	1163	1.0
8.2 (75)	1182	0.7
5.6 (76)	962	0.7
20 wt% oleoyl lignin		
2.5 (53)	490	0.6
20 wt% NML		
26.1 (8)	1731	2.1
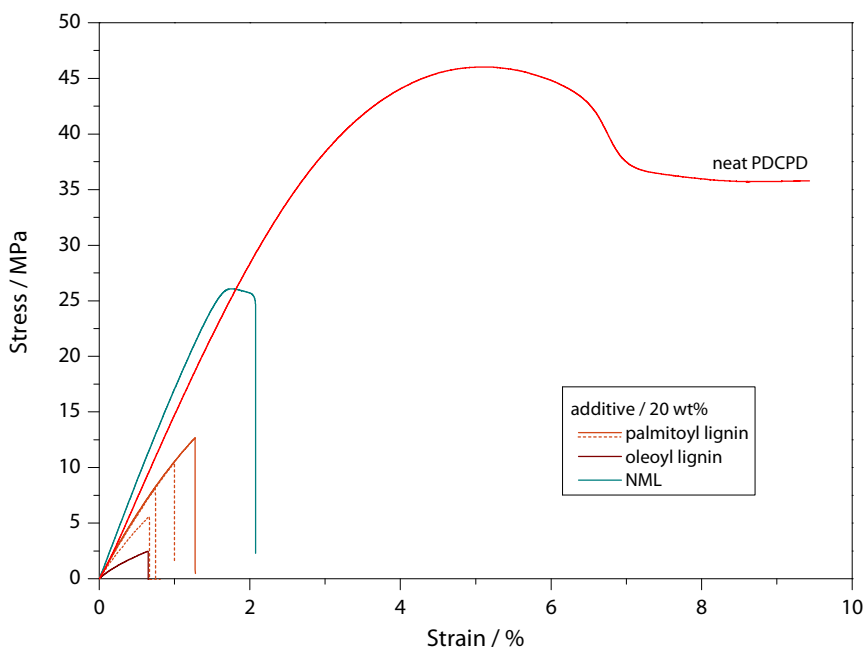
Figure 38. Stress-strain diagram of PDCPD shouldered test bars with varying additives (20 wt% palmitoyl lignin, oleoyl lignin or NML).

The poor mechanical performance of the specimens containing palmitoyl or oleoyl lignin respectively, may also be explained by the presence of free fatty acids in the lignin derivative (≤ 30 wt%, which would account for ≤ 6 wt% in the thermosetting mixture). What has not affected the mechanical properties in small amounts (GL2 contains ~ 8 wt% fatty acids, which would account for ≤ 1.6 wt% in the thermosetting mixture), obviously becomes noticeable in higher amounts. However, the dramatical loss of the material properties when adding these long chain ligninesters cannot solely be attributed to the free fatty acids.

Larock *et al.* published a study about composite materials comprising DCPD and Dilulin (linseed oil featuring one norbornene moiety per triglyceride) in varying ratios.[178] The thermosets prepared via ROMP were found to become more soft and weak with increasing content of Dilulin (30–60 wt%). Extractions of the materials with dichloromethane revealed a leachable fraction of 10–17 wt%, depending on the composition. Dilulin as well as DCPD oligomers and unreacted triglycerides were identified in these extracts. They explain the soluble parts to act as plasticizing agent, which softens the resin. Additionally, the fatty ester side chains of Dilulin internally plasticize the thermoset and are thus responsible for the higher flexibility of the material with increasing content of the triglyceride. For example the ultimate tensile strength dropped from 29 to 0.5 MPa and crosslink density decreased from 382 to 99 mol·m^{-3} upon increasing the amount of Dilulin from 30 to 60 wt%.[178]

It can be assumed, that these findings also apply to the PDCPD / ligninester thermosets. The obtained material characteristics indicate the applied ligninesters to act as plasticizing agents. The unsaturated fatty chain of oleoyl lignin was meant to provide a covalent linkage to the PDCPD matrix and hence to maintain, or even enhance the material characteristics. However, oleoyl lignin additionally can undergo cross metathesis (CM) reactions both with DPCD and itself when applying a metathesis initiator (Scheme 9). Thus, numerous side products can be formed, such as I and II upon ring insertion cross metathesis (RICM) with DCPD or the self metathesis products III and IV. Even a larger variety of products will be obtained, if the second double bond of DPCD is also involved. These reactions will result in the chain termination of DCPD polymerization and hence to a less crosslinked polymer backbone. The formed oligomers will additionally account to the plasticizing effect of the fatty esters, or acids respectively.

Scheme 9. Cross metathesis (CM) of dicyclopentadiene (DCPD) and oleic acid.
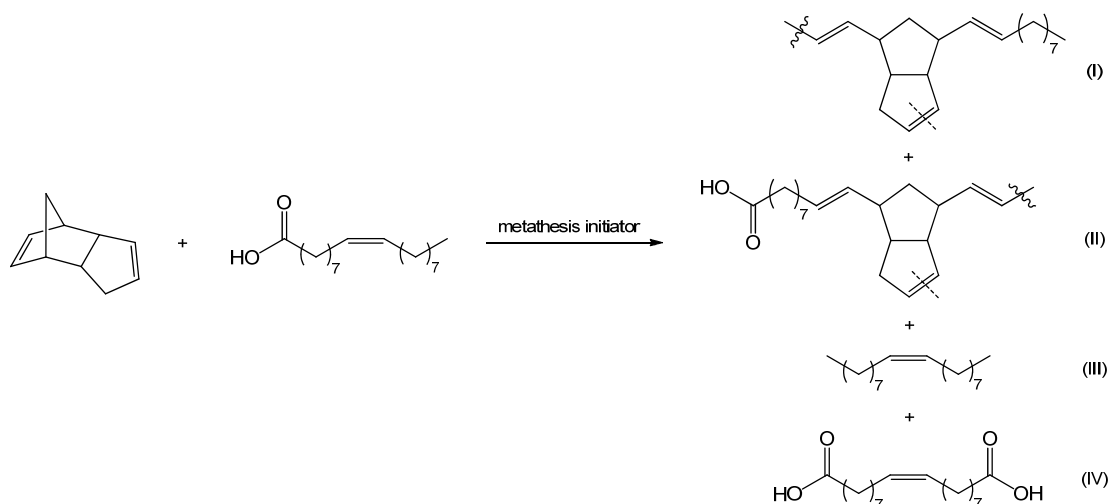
An extraction of a PDCPD / oleoyl lignin copolymer was conducted with dichloromethane at RT for 72 h. The copolymer swelled strongly upon the treatment with dichloromethane. Gravimetric analysis of the DCM-soluble residuals revealed 39 wt% extractives. This great leachable part demonstrates the decreased crosslinking of DCPD containing the unsaturated ligninester. Cross metathesis products I and III (Scheme 9) could be identified via ^{1}H NMR measurement of the extract (Figure 39). Structures II and IV could be excluded due to the missing resonance of the CH_2 group adjacent to the carbonyl moiety (assigned with X in Figure 39), giving additionally evidence of the lack of free oleic acid. Thus, the carboxylic acid or ligninester moiety must be incorporated into the polymeric backbone.
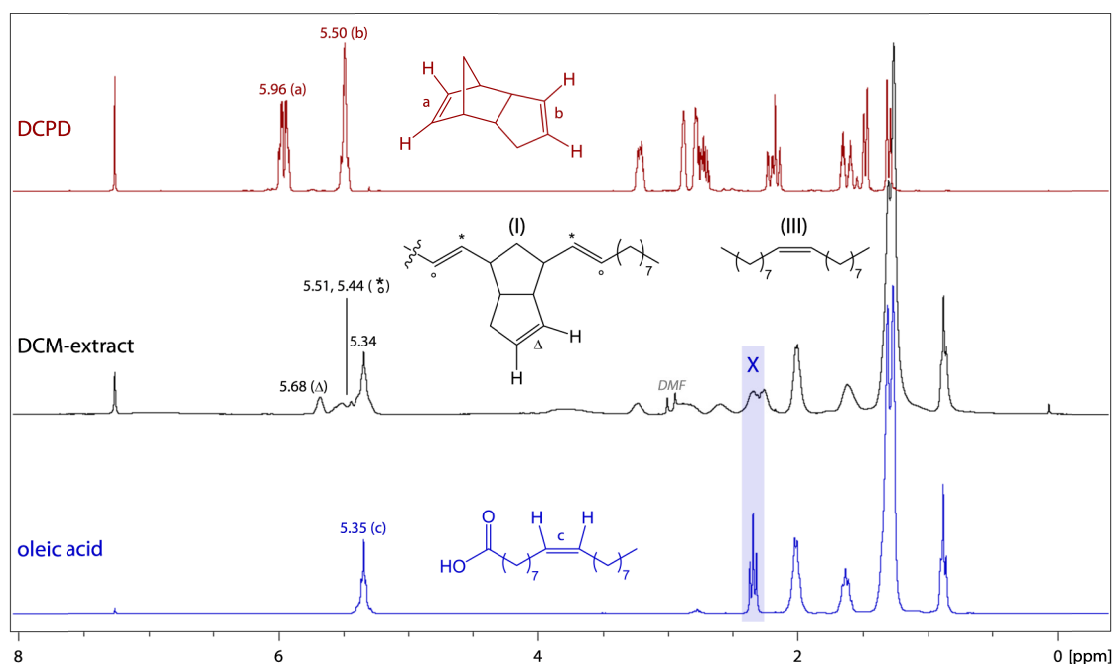
Figure 39. ^{1}H NMR spectrum of the DCM-extract of a DCPD / oleoyl lignin copolymer (R = lignin or H) in comparison to DPCD monomer and oleic acid (25 °C, 300 MHz, CDCl$_3$).

The complete interpretation of the ^{1}H NMR spectrum of the DCM-extract (Figure 39, black) is as follows: ^{1}H NMR (300 MHz; CDCl$_3$, 25 °C): δ 5.68 (m, 1.18H, CH^{Δ}), 5.51, 5.44, (m, 1.81H, $CH^{*\circ}$), 5.34 (m, 4.24H, CH^{III}), 3.23 (m, 1.07H, $CH^{\ddagger}$), 2.89 (m, 2.70H, $CH^{\ddagger}$), 2.60 (m, 1.46H, $CH^{\ddagger}$), 2.33, 2.26 (m, 4.60H, CH_2^{I}), 2.00 (m, 5.49H, $CH_2^{I,III}$), 1.62 (m, 3.95H, CH_2^{I}), 1.30, 1.26 (m, 34.66 H, $CH_2^{I, III}$), 0.88 (m, 6.00H, $CH_3^{I, III}$) ppm.

Samples of PDCPD containing 20 wt% palmitoyl lignin were also investigated by scanning electron microscopy (SEM) (Figure 40). The fracture site of PDCPD filled with the DCPD-soluble palmitoyl lignin appears significantly different compared to that of neat PDCPD (Figure 36) as well as PDCPD containing 20 wt% unmodified lignin. Platelet- or rather needle-like structures are apparent on the surface of samples with palmitoyl lignin in contrast to the spherical particles observed with unmodified lignin. The observed pattern may be attributed to free palmitic acid present in the lignin derivative.

20 wt% palmitoyl lignin (NML)

20 wt% NML

20 wt% palmitoyl lignin (GL2)
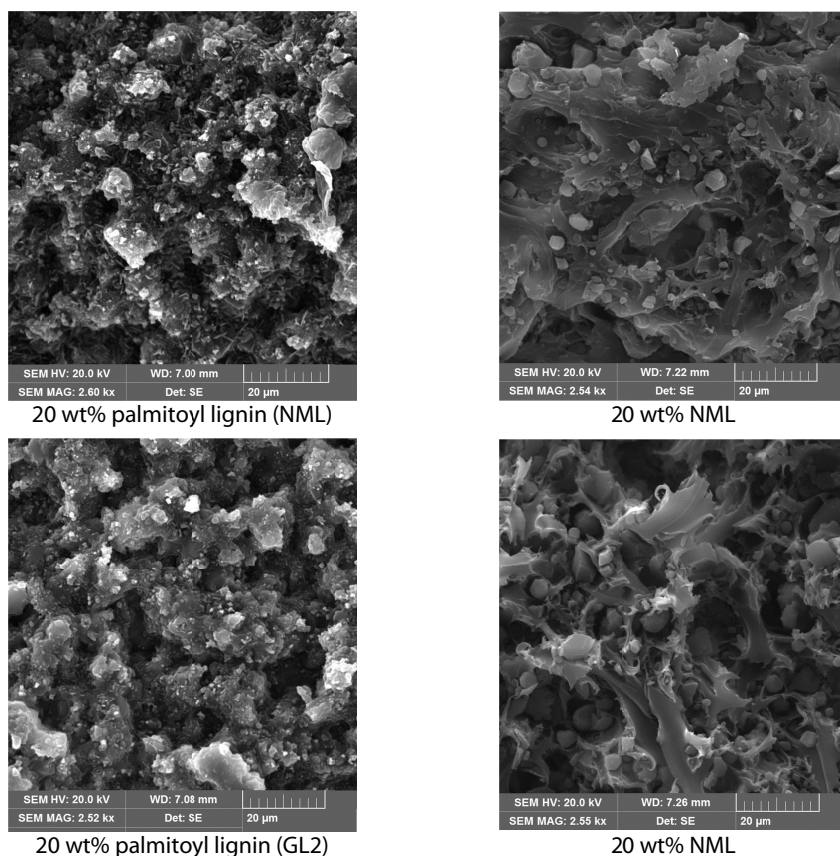
20 wt% NML

Figure 40. Morphology of PDCPD with 20 wt% palmitoyl lignin (left) in contrast to PDCPD with 20 wt% NML (right) after tensile strength test at breaking point.

Further characteristics like oxidation stability or resistance against chemicals were not investigated, as the mechanical properties of the specimens did not meet the expectations. To successfully apply lignin as copolymer for PDCPD, the plasticizing effect of the ligninesters has to be reduced. The substitution of the rigid crosslinker DCPD by a softening agent in higher amounts will inevitably result in the loss of duroplastic material characteristics.

We tried to meet this requirement by the additional introduction of *rompable* moieties in lignin while preserving the solubility in DCPD (norbornenoyl / palmitoyl lignin, cp. Table 17, section 3.2). Unfortunately, the double-functionalization approach did not yield the desired effect, as the solubility in DCPD was not sufficient.

Summary — lignin as filler / reactive component for polydicyclopentadiene
- *Unmodified lignin as insoluble filler for PDCPD slightly enhances the elastic modulus at the expense of maximal loading capacity and strain.*
- *Ligninesters act as plasticizing agents: palmitoyl lignin (soluble filler) / PDCPD specimens exhibit worse mechanical properties than PDCPD filled with the same amounts of unmodified lignin.*
- *Oleoyl lignin (soluble, reactive filler) led to a drastic loss of the material properties due to cross metathesis side reactions.*

4.2 BICOMPONENT THIN FILMS

In order to imitate real conditions in plant cell walls, bicomponent films of lignin and cellulose are frequently reported in the last period.[182] The physicochemical properties such as wettability and microphase separation were explored in particular, in order to closer understand how the components interact with proteins. Bovine serum albumin serves usually as marker for unspecific protein adsorption.

Bicomponent thin films were prepared using the obtained organosoluble lignin derivatives (see chapter 3.2 and 3.3) and trimethylsilyl cellulose (TMSC) by spin coating on silica supports. TMSC was regenerated in acidic atmosphere of HCl to obtain ligninester / cellulose films (Scheme 10). Morphology and wettability of the bicomponent thin films were determined by atomic force microscopy and water contact angle measurements. Furthermore, the interaction of proteins with the bicomponent surface was investigated by adsorption of bovine serum albumin (BSA) using a quartz crystal microbalance with dissipation (QCM-D) device.

Table 35. Ligninesters and trimethylsilyl cellulose used for the fabrication of bicomponent thin films, and BSA applied for protein adsorption experiments.

palmitoyl lignin	oleoyl lignin
lignin-PLA	lignin-PCL
trimethylsilyl cellulose (TMSC)	bovine serum albumin (BSA)
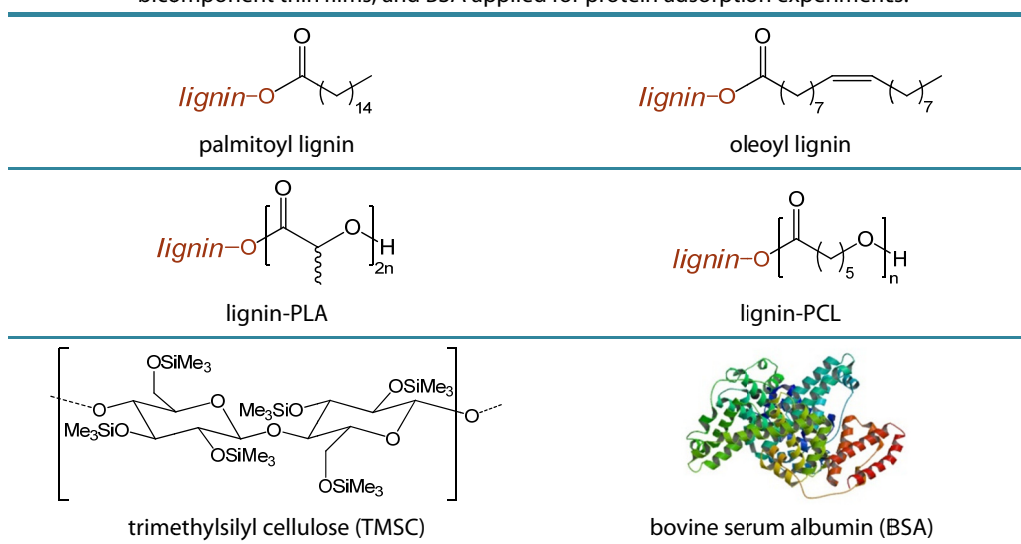
Solutions of ligninester and TMSC were prepared in chloroform (10 mg / mL) and combined to give different ratios of the two components (3:1, 1:1 and 1:3 (v:v)). Thin films were fabricated by static spin coating of the mixed solutions (100 µL) onto silica wafers (1.5 × 1.5 cm²). A Polos MCD wafer spinner (APT corporation, Germany) was operated at 4000 rpm for 60 s (acceleration 2500 rpm·s⁻¹). The coated films were exposed to HCl vapors (3 M, 12 wt%, 12 min) to obtain fully regenerated ligninester / cellulose thin films.

Scheme 10. Regeneration of trimethylsilyl cellulose (TMSC) to cellulose with HCl gas.
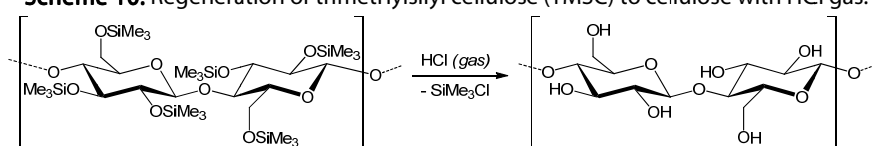
Palmitoyl lignin was the only ligninester of the four investigated derivatives which yielded homogeneous, smooth blend films. Thus, the following results and discussion refer exclusively to palmitoyl lignin / cellulose bicomponent thin films. Sample 36 (cp. Table 23) was purified by flash chromatography (see section 3.3.2) to remove the free fatty acids (32 wt%) prior to the use as component in the blend thin films.

The thickness of the blend films was determined profilometrically with a DEKTAK 150 Stylus Profiler from Veeco (Plainview, NY, USA). A set scan length of 1000 µm (for 3 s) was applied using a diamond stylus with a radius of 12.5 µm at 3 mg force with a resolution of 0.333 µm / sample and a measurement range of 6.5 µm. The profile was set to 'hills and valleys'. The surface of the coatings was scratched prior to the surface scanning in order to determine the thickness using a step-height profile at three independent positions. The films were measured before and after regeneration and the obtained values are listed in Table 36. It is known that TMSC significantly shrinks upon conversion to cellulose in the acidic atmosphere of HCl vapors.[183] It is expected that the lignin domains remain unaffected upon regeneration (Scheme 11). With increasing content of palmitoyl lignin, the difference in height before and after regeneration becomes smaller, wheras a pure TMSC film shrinks by 59 % from 94 to 39 nm. The cellulose fraction densifies during the regeneration procedure due to hydrogen bond formation. There are also recent indications of other rearrangements proceeding, caused by the partial depolymerization of cellulose and leading to tighter packing.[184]

Table 36. Thickness of palmitoyl lignin / TMSC thin films before and after regeneration upon HCl gas.

Film thickness / nm	1:0	3:1	1:1	1:3	0:1
not regenerated	palmitoyl lignin / TMSC				
	58.1 ± 0.4	47.9 ± 1.6	53.2 ± 3.6	75.1 ± 1.5	93.8 ± 6.3
regenerated	palmitoyl lignin / cellulose				
	51.9 ± 0.5	40.6 ± 2.1	47.5 ± 1.1	42.4 ± 0.7	38.7 ± 1.2

Scheme 11. Regeneration of ligninester (LE) / TMSC films to ligninester / cellulose films.
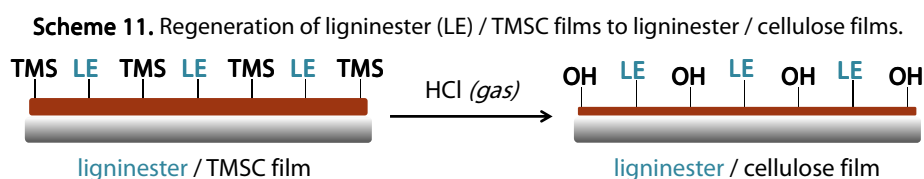
The wettability of the blend films was investigated using the contact angle measurement system OCA15+ (Dataphysics, Germany), applying the sessile drop method (drop volume of 3 µL, RT). The static contact angles (SCA) were determined by analyzing the drop shape using the software provided by the manufacturer (SCA 20). The average value of at least three drops per surface was given as SCA (Table 37). It is well known that the hydrophilicity of neat TMSC films distinctly increases upon exposure to HCl vapors, whereas the wettability is adjustable by the regeneration time (Scheme 12).[185]

Scheme 12. Increase of hydrophilicity upon regeneration of TMSC to cellulose with HCl gas.[185]

regeneration time / hydrophilicity
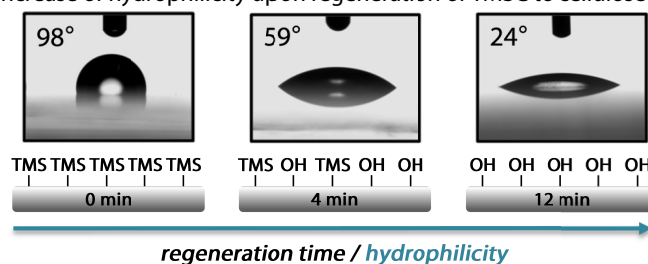
All palmitoyl lignin / TMSC bicomponent films exhibit static water contact angles close to 100°, which is more or less identical to the SCA of neat TMSC films. After regeneration, the SCA for palmitoyl lignin containing films is in the range between 38° and 43°, which is notedly higher than neat cellulose films (30°). Contrary to our expectations, the ligninester share does not significantly alter the SCA after regeneration.

Table 37. Static water contact angles of palmitoyl lignin / TMSC blend films before and after regeneration.

Static water contact angle (SCA) / °	3:1	1:1	1:3	0:1
not regenerated	palmitoyl lignin / TMSC			
	95 ± 1	98 ± 1	98 ± 2	97 ± 1
regenerated	palmitoyl lignin / cellulose			
	38 ± 1	42 ± 1	43 ± 1	30 ± 2

The surface morphology of the bicomponent thin films was characterized by atomic force microscopy (AFM). An 5500 AFM multimode scanning probe microscope (Agilent, Santa Barbara, CA) was used in tapping mode at room temperature in air and the images were acquired after drying the samples in a nitrogen gas stream. Silicon cantilevers (ATEC-NC-20, Nanosensors, Germany) were used to scan the surfaces with a resonance frequency of 320 kHz and a force constant of 42 N·m^{-1}. The obtained images were processed using a Gwyddion software package.

AFM height images of the different blend films, as well as neat palmitoyl lignin and TMSC films, before and after regeneration are shown in Figure 41 (2 × 2 µm) and Figure 42 (10 × 10 µm). The z-scales for each image are indicated above the bar (left) and the roughness (Rq) is stated below each image. The morphology of the bicomponent blend films significantly changes with different compositions. The neat TMSC films show a rather low roughness, even after regeneration to cellulose. However, in the blend films different morphologies are obtained depending on the proportion of ligninester. The formation of bicontinuous phases on the surface before regeneration is more pronounced for samples with increasing content of palmitoyl lignin, partially featuring holes in the µm scale. These holes can unambiguously be assigned to the palmitoyl lignin regions since a subsequent regeneration step leads to an inversion of the structures, meaning that the holes are converted into pillars. Shrinking regions are mainly composed of previously TMSC domains.
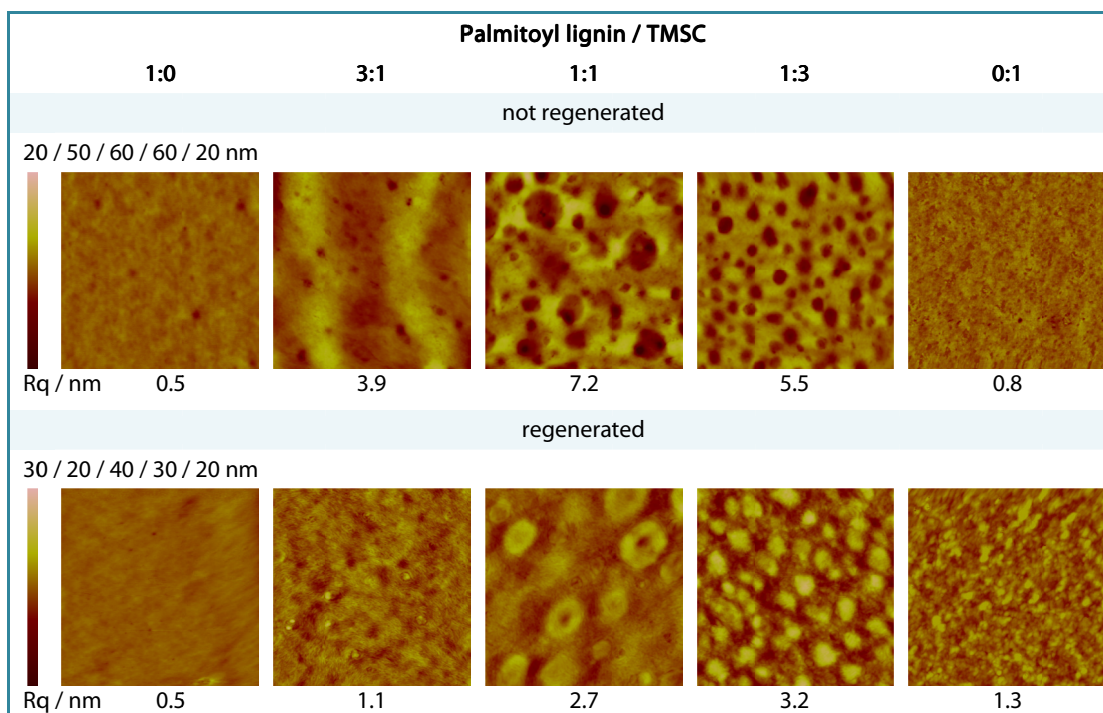
Figure 41. AFM height images (2 × 2 μm) of thin films with purified palmitoyl lignin and TMSC in varying ratios before (up) and after (below) regeneration.
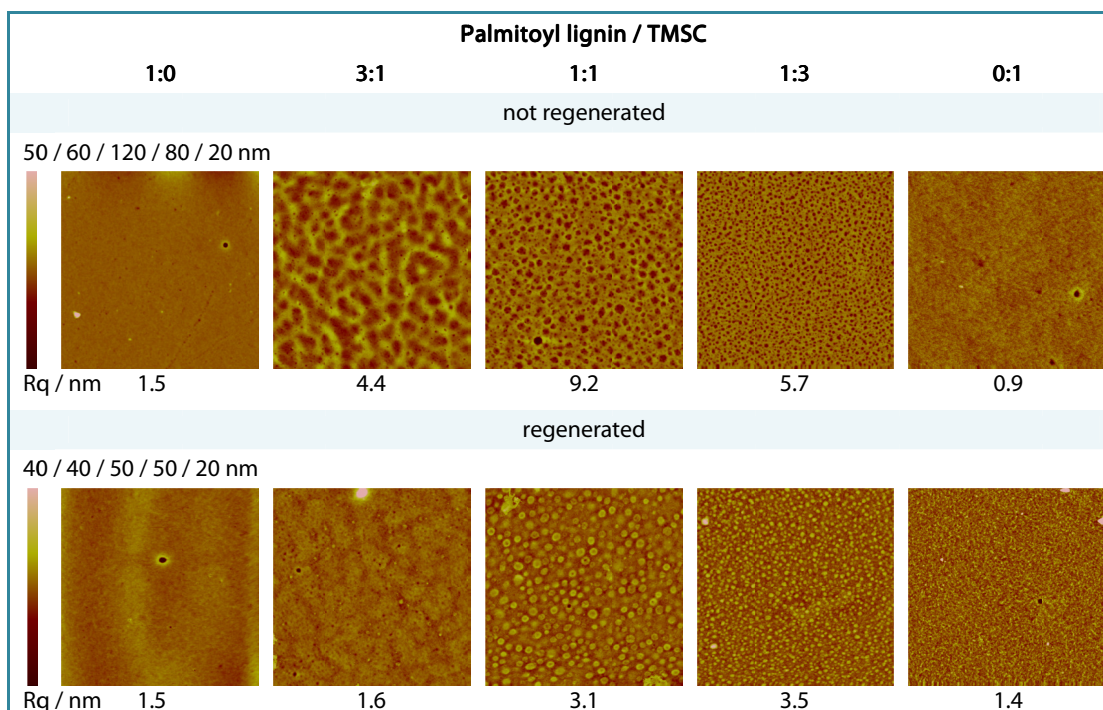
Figure 42. AFM height images (10 × 10 μm) of thin films with purified palmitoyl lignin and TMSC in varying ratios before (up) and after (below) regeneration.
.

It cannot be excluded that the ligninester is hydrolyzed upon HCl treatment, resulting in original lignin and palmitic acid chloride. The SCA of the pure palmitoyl lignin surface after exposure to HCl vapors remained on the same level, but this may also be the result of cleaved off fatty acid chains. A simple and elegant way to prove the existence of palmitoyl lignin in the regenerated (blend) films, is the performance of a simple rinsing step with chloroform. If palmitoyl lignin is not degraded by HCl, it should be well soluble in chloroform and washed away. Thus, the insoluble cellulose areas should remain unaltered on the substrates. In the case of a decomposed ligninester, the resulting lignin parts are insoluble in chloroform as well and will also be preserved on the substrate. Hence, the morphology of the obtained surfaces should appear equally as already shown (Figure 42 and Figure 43).

After careful rinsing the blend films with chloroform, it is obvious that the structures assigned to palmitoyl lignin disappeared. Instead, nanostructured cellulose thin films featuring a honeycomb-like pattern are obtained.
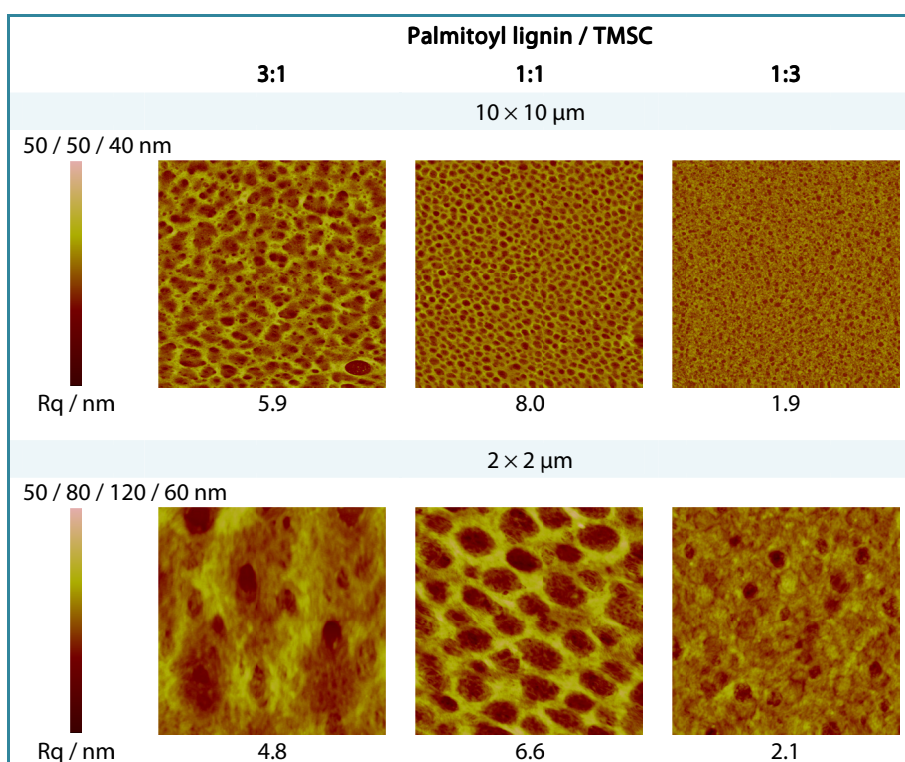
Figure 43. AFM images of the regenerated thin films after washing with CHCl$_3$, yielding cellulose structres.

The behavior of the bicomponent blend film towards unspecific protein adsorption was investigated by QCM-D experiments (cp. Figure 44) using bovine serum albumin (BSA). The characteristics of BSA adsorption on pure cellulose and lignin films are reported in several studies. Especially cellulose is known to be a weak protein carrier.[186] The adsorption of BSA is mainly controlled by hydrophobic interactions between protein and surface. Thus, films containing hydrophobic palmitoyl lignin should be more receptive to protein adsorption than films consisting mainly of cellulose. This affinity would allow for the efficient immobilization of proteins on such bicomponent surfaces, which could be interesting for future sensor applications.

A Quartz crystal microbalance with dissipation (QCM-D) (model E4, Q-Sense, Gothenburg, Sweden) was used for protein adsorption experiments. The instrument simultaneously detects resonance frequency (Δf) and energy dissipation (ΔD) alterations via mass changes of an oscillating piezoelectric crystal upon added or deduced mass on the crystal surface. The dissipation is related to frictional losses which result in attenuated oscillation, according to the viscoelastic properties of the material. The resonance frequency Δf_n is given by the Sauerbrey equation[187] (3) for an adsorbed, rigid layer which is completely coupled to the oscillation of the crystal. In case of soft (viscoelastic) films, the mass is not completely coupled to the oscillation and hence, equation 3 is no longer valid due to energy dissipation in the film during oscillation.

$$\Delta m = C \; \frac{\Delta f_n}{n} \qquad (3)$$

Δf_n .... observed frequency shift

C .... Sauerbrey constant (-0.177 mg·Hz^{-1}·m^{-2} for a 5 MHz crystal)

n .... overtone number (1, 3, 5 etc.)

Δm ... mass change of the crystal due to an adsorbed layer

$$D = \frac{E_{diss}}{2\pi \; E_{stor}} \qquad (4)$$

D .... dissipation (or damping)

E_{diss} ... energy dissipated during one oscillation cycle

E_{stor} ... energy stored in the oscillator during one cycle
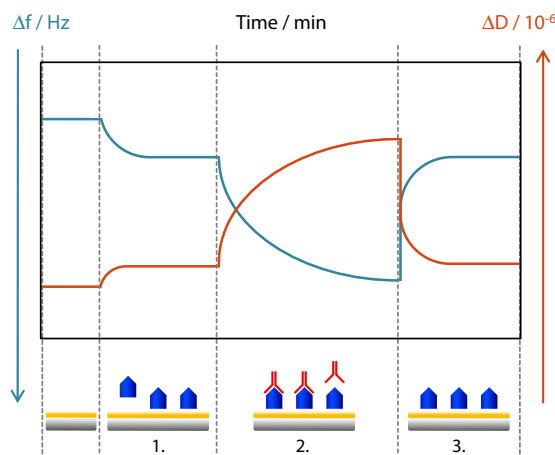
Figure 44. Principle of a QCM-D experiment: equilibration of the film in buffer solution (1), protein adsorption (2) and rinsing with buffer solution (3).

The different blend films as well as pure palmitoyl lignin and TMSC films were prepared on gold coated QCM-D sensor crystals. Prior to spin coating, the substrates were immersed in a mixture of H_2O / H_2O_2 (30 wt%) / NH_4OH 5:1:1 (v:v:v) for 10 minutes at 70 °C and then soaked in a solution of H_2O_2 (30 wt%) / H_2SO_4 (98 wt%) 1:3 (v:v) for 1 minute. Finally, the crystals were rinsed with Milli-Q water and dried in a stream of nitrogen gas. The palmitoyl lignin / TMSC solution (CHCl₃, 70 μL) was dropped onto the static QCM-D crystal, which was subsequently rotated at 4000 rpm for 1 minute (acceleration of 2500 rpm·s⁻¹). The coated sensors were regenerated by exposing them to HCl vapors in a covered polystyrene Petri dish (diameter 5 cm) containing HCl (3 mL, 3 M) for 1 minute. After regeneration, the surfaces were steadily flushed (flow rate = 0.1 mL·min⁻¹) with BSA solution (1 mg·mL⁻¹ in phosphate buffered saline (PBS)) in a QCM-D chamber. After 90 minutes, the films were rinsed with phosphate buffered saline (PBS, pH 7.4) (Figure 45).

As already mentioned, the protein adsorption of BSA on pure cellulose films is rather low and a Δf_3 of ~ −15 Hz is observed after rinsing the surfaces with PBS solution. The protein deposition correlates with the amount of palmitoyl lignin in the bicomponent blend films, albeit opposite than expected. It is obvious that higher amounts of palmitoyl lignin result in lower deposition of BSA on the surfaces. Although the films are very stable in the PBS solution at pH 7.4, ligninester containing films exhibit a positive change in frequency. This finding indicates, that the pillar like structures obtained after regeneration (cp. Figure 41 and Figure 42) are most likely peeled off by the BSA. In this case BSA acts as a tenside. However, complete removal of palmitoyl lignin was not observed and even for neat ligninester films, a Δf_3 of +60 Hz was monitored, which indicates a rather slow complexation process with BSA. The desorption of loosely attached BSA molecules by better interaction partners, such as other BSA molecules, could be a possible explanation for this behaviour. Upon desorption, palmitoyl lignin is peeled off the surface due to complexation. This implies that the ligninester serves as sacrificial component in the films, preventing protein adsorption.
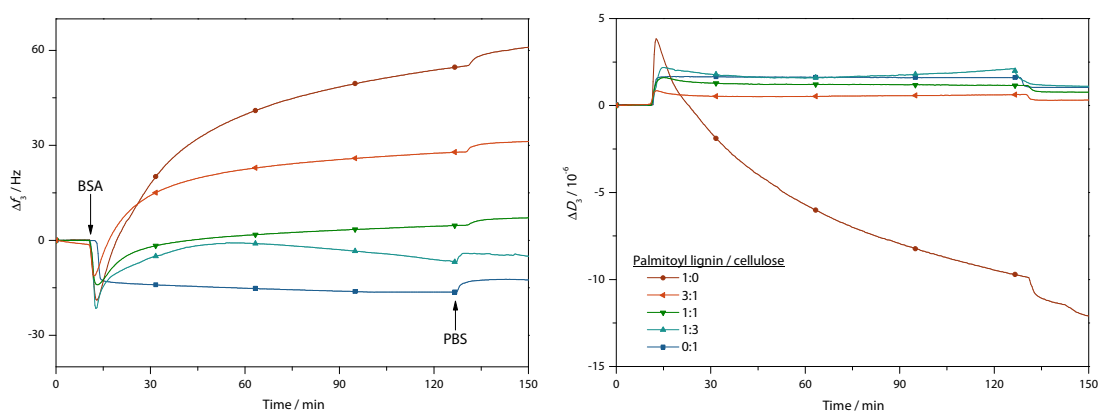
Figure 45. Adsorption of BSA on different bicomponent thin films as well as on pure palmitoyl lignin and cellulose films monitored by QCM-D in the frequency (Δf_3) and dissipation channels (ΔD_3). The shown curves are averaged from three parallels.

Another factor contributing to this finding could be an amphiphilic character of the ligninester. As the lignin hydroxyl groups are not completely esterified, the presence of rather flexible hydroxyl groups besides the hydrophobic fatty acid chains cannot be excluded. Thus, the emulsification process with BSA would be facilitated.

It is not yet clarified what contributes most to the observed effects, but it can be concluded that BSA does not accumulate on the investigated bicomponent surfaces. The blend films are very resistant to unspecific protein adsorption.

Summary — bicomponent thin films
- *Palmitoyl lignin was suitable for the preparation of blend films with trimethylsilyl cellulose in varying ratios*
- *Spin coating on silica supports and on gold coated QCM-D sensors*
- *Regeneration to palmitoyl lignin / cellulose films upon exposure to HCl vapors*
- *Palmitoyl lignin is not affected by the regeneration step*
- *Determination of wettability by static water contact angle measurements before (95–98°) and after (38–43°) regeneration*
- *Profilometric determination of the film thickness before (48–45 nm) and after (41–48 nm) regeneration*
- *Films shrink and hydrophilicity increases upon regeneration*
- *Formation of bicontinuous phases was revealed by AFM (honeycomb-like pattern of cellulose)*
- *Blend films are resistant to unspecific protein adsorption as obtained from QCM-D experiments with BSA*

5 Prospecting for Novel Lignin Modifications

5.1 Model reactions - *ROMPable* lignin

In order to obtain novel lignin derivatives featuring tailored properties for the ring opening metathesis polymerization (ROMP) (cp. section 4.1), several model reactions towards *rompable* lignin were performed. The investigated conversions are briefly presented in the following. Unfortunately, the reactions proceeded less successfully and hence were not further implemented to lignin modifications.

5-Norbornene-3-octyl-2-octanoic acid methyl ester

With the aim of employing lignin as comonomer for ROMP, it was tried to synthesize methyl oleate featuring a norbornene moiety. Therefore, methyl oleate was converted with freshly cracked cyclopentadiene in ethyl acetate at RT as well as 80 °C (Scheme 13). After 3 days, traces of the desired compound were detected via ^{1}H NMR. As expected, the double bond of methyl oleate is electronically hardly accessible for a Diels-Alder reaction.

A similar, commercially available substance is Dilulin™, a linseed oil featuring approximately one norbornene unit per triglyceride.[188] The modified oil is synthesized in industrial-scale by a high temperature, high pressure Diels-Alder reaction between linseed oil and dicyclopentadiene, which cracks under the applied conditions to form 2 equivalents cyclopentadiene. Unfortunately, Dilulin™ exhibits no suitable site to be grafted onto lignin.

Scheme 13. Supposed Diels-Alder reaction of methyl oleate and cyclopentadiene.
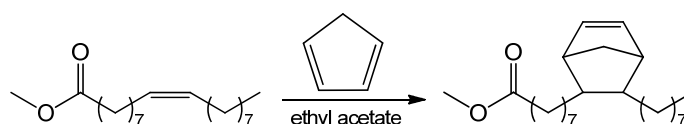
12-((((5-Norbornen-2-yl)ethyl)dimethylsilyl)oxy)-octadec-9-enol

Another approach towards *rompable* lignin - or rather to a suitable precursor therefor - was the modification of methyl ricinoleate with a norbornene moiety (Scheme 14). The hydroxyl group is utilized as linker between norbornene moiety and solubilizing fatty acid chain.

Scheme 14. Conversion of methyl ricinoleate and 5-norbornen-2-yl-(ethyl)chlorodimethylsilane (I) to give methyl-12-((((5-norbornen-2-yl)ethyl)dimethylsilyl)oxy)-octadec-9-enoate (II).
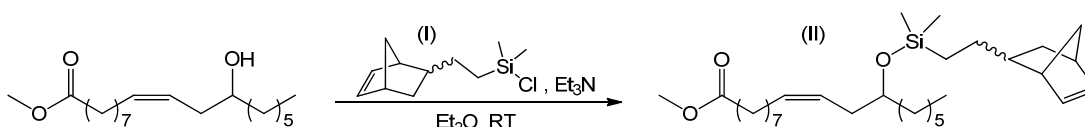
As transesterifications of methyl oleate and lignin failed with various catalysts, the carbonyl group has to be activated prior to a conversion with lignin. Thus the derivative (II) was saponified with aqueous sodium hydroxide to obtain the corresponding fatty acid (III). ^{29}Si-NMR analysis of norbornene-2-yl-(ethyl)chlorodimethylsilane, modified methyl ricinoleate as well as of the substance subsequent to treatment with aqueous NaOH revealed that the Si-O bond was cleaved upon saponification, yielding solely hydrolyzed educt (I) (7.17 or 7.18 ppm, Figure 46).
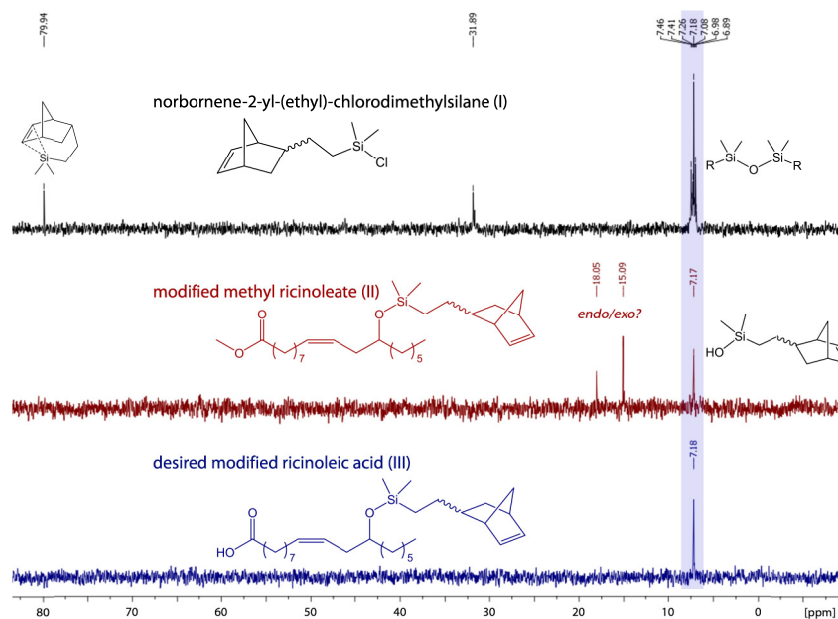
Figure 46. ^{29}Si NMR spectra of educt (I), modified methyl ricinoleate (II) and desired modified fatty acid (III) (25 °C, 59.6 MHz, CDCl$_3$).

3-(OCTADEC-9-ENOATE)-BICYCLO[2.2.1]HEPT-5-ENE-2-CARBOXYLIC ACID

(E)-Octadec-9-enol was reacted with *cis-endo*-bicyclo[2.2.1]hept-5-ene-2,3-dicarboxylic anhydride under basic conditions to yield 3-(octadec-9-enoate)-bicyclo[2.2.1]hept-5-ene-2-carboxylic acid in good yields (94 %) (Scheme 15).[189] Starting compound *(E)*-octadec-9-enol[190] was synthesized by reducing methyl oleate with lithium aluminium hydride.

The carboxylic acid moiety is intended as linking site to lignin and the C$_{18}$ chain should provide sufficient solublity in non-polar media. Unfortunately, the esterification of lignin with 3-(octadec-9-enoate)-bicyclo[2.2.1]hept-5-ene-2-carboxylic acid after activation with 1,1'-carbonyl-diimidazole was not successful.

Scheme 15. Reaction of *E*-octadec-9-enol with norbornene anhydride to obtain 3-(octadec-9-enoate)-bicyclo[2.2.1]hept-5-ene-2-carboxylic acid.
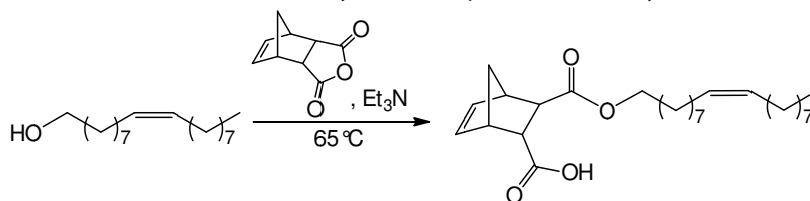
5.2 oxa-Michael addition

The oxa-Michael addition is considered to be a particularly promising reaction for the modification of lignin. Firstly, this reaction type was published in 1960s in connection with the modification of cellulosic hydroxyl groups. Hence, the application of related protocols to lignin is a very obvious idea. Initially, as a proof of concept, various simple alcohols served as model substances and were reacted with an electron deficient olefin. Suitable reaction partners and catalysts as well as proper reaction conditions have been investigated extensively. The following chapter will provide a comprehensive excursus in the oxa-Michael addition of alcohols to divinyl sulfone, including general introduction (section 5.2.1), a detailed results section (5.2.2) as well as an experimental part (5.2.3). Moreover, the use of multifunctional reaction partners allows for the preparation of addition polymers which is described in section 5.3.

5.2.1 Introduction and general aspects

The Michael reaction,[191] the addition of a nucleophile (Michael donor) to an electron deficient olefin (Michael acceptor), is one of the most versatile and powerful tools in organic synthesis. A Michael type addition results in the formation of covalent adducts at a soft electro(nucleo)philic center without expulsion of a leaving group.[192] A wide range of synthetically useful products is accessible due to the facile combination of various Michael donors and acceptors. Not only the introduction of carbon-carbon, but also of carbon-heteroatom bonds is feasible under mild reaction conditions while simultaneously meeting the precepts of atom economy[193] and click chemistry.[194] α,β-Unsaturated compounds meet the structural requirements for Michael acceptor electrophiles. The higher the olefinic π-bond is polarized by an adjacent electron withdrawing substituent, the better are the Michael acceptor characteristics.[192] Thus, activated olefins like α,β-unsaturated esters[195] and ketones,[193] (meth)acrylates,[196] maleimides,[193] acrylonitriles,[193] cinnamates,[193] crotonates,[197,220] nitroalkenes,[198] ethene-tricarboxylates,[199] conjugated imines and iminium salts,[200] vinyl sulfones and phosphonates,[201,202] nitriles[203] as well as acrylamides[204,205] are appropriate electrophiles for Michael type addition reactions.

The suitable counterpart for (hetero) Michael additions are nucleophilic donor molecules such as thiols,[216,206] nitrogen nucleophiles[207] and hydroxyls.[208,209]

Amongst all Michael reactions, the oxa-Michael reaction has received comparably less attention, although it grants efficient access to oxygen-containing heterocylces for instance. However, this situation is changing recently and addition reactions of oxygen nucleophiles to various conjugated electron-deficient systems appear increasingly in synthetic as well as macromolecular applications. Drawbacks of the oxa-Michael reactions are the relatively poor nucleophilicity of alcohols and the reversibility of the alcohol addition step. A collection of common oxa-Michael reaction pathways and new synthetic protocols can be found in the review of C. F. Nising and S. Bräse.[208]

Already in the early 1960s, this reaction gained special interest with regard to cellulose modification in alkaline media. Studies concerning the reaction of cellulose with reactive dyes, namely a vinyl sulfone compound of the remazole type, were reported[210] and soon

afterwards the first kinetic studies of the base-catalyzed addition of alcohols to activated vinyl compounds were published. They stated an increasing addition rate with electron withdrawing groups in the order:

amides < esters < sulfonamides < nitriles < sulfones < enones ≤ phosphines

Substitution on either vinyl carbon lowers the rate, whereas α-substitution exerts a greater effect than β-monosubstitution. They also observed the addition to the first vinyl group to proceed notedly faster than the subsequent addition to the second vinyl group.[211]

Imai *et al.*, on the contrary, investigated the reactivity of hydroxyl groups in different tactic sequences on poly(vinyl alcohol) by adding vinyl sulfones amongst others, catalyzed by sodium hydroxide.[209] The degree of substitution mainly depends on the accessibility of the OH-groups.

Conventionally, metals or strong bases are mainly used to catalyze (oxa-) Michael addition reactions. Thus, potassium *tert*-butoxide is applied either in stoichiometric amounts (1.1 eq)[197] or in catalytic quantities (0.2 eq)[212] regarding to the alcohol. Amongst metal catalysts, copper(II) chloride (0.1 eq) is reported to efficiently support the Michael addition of primary alcohols and acrylic derivatives in the presence of base (Cs_2CO_3, K_2CO_3, K_3PO_4 or KO^tBu). Interestingly, the yield decreases when reducing the amount of base. Without base, only product traces have been observed. The best yields were obtained using Cs_2CO_3 and excess alcohol in dichloromethane.[204] Furthermore, a sodium hydride catalyzed oxa-Michael addition is reported by Menche and coworkers.[213] They achieved the best results in the synthesis of tetrahydropyrans with nitro-substituted Michael acceptors. Already in the early 1970s, a study dealing with the anionic polymerization of methyl vinyl sulfone initiated by alkali metals was published.[214] They showed that the acid-base exchange between the formed carbanions and the monomer methyl vinyl sulfone competes with the polymerization under various conditions. Thus, only little polymer with low molecular weight, lacking a correlation to the initiator concentration, was obtained.

The oxa-Michael addition is also feasible in alkaline aqueous media, providing a particularly attractive method in terms of *green* and natural substances chemistry, namely polysaccharides and lignin. Chau *et al.* applied this protocol to hyaluronic acid and other water-soluble polymers.[195] Divinyl sulfone is also an appropriate cross linking agent for hydroxyl-functional polymers, enhancing the network stability and related characteristics.[215]

Organocatalysis has rapidly evolved over the last decade and is enjoying increasing popularity in all fields of synthesis, also holding true for Michael addition reactions. Hence, the traditional procedures become obsolete and highly efficient, harmless organocatalysts are successfully utilized under mild reaction conditions. Thus, nitrogen-[216] and phosphorous-centered[217] nucleophiles as well as *N*-heterocyclic carbenes (so called NHCs)[218,219] are increasingly applied for various (hetero) Michael addition reactions. Bowman *et al.* catalyzed the rapid, efficient thiol-Michael addition of divinyl sulfone and various thiols with triethylenediamine, 4-dimethylaminopyridine and 1-methyl imidazole for instance.[220] They also reported a chemical clock protocol which allows temporal control over the thiol-Michael addition reaction by formulating a base generating system from an activated vinyl and a

nucleophile, e.g. a phosphine.[221] The hence formed zwitterionic species catalyzes the following addition reaction after a certain induction period which depends on the relative concentrations of the different components in the system.[222] Within this study, vinyl sulfone was also demonstrated to exhibit a relatively higher reactivity towards Michael type additions than acrylates due to its greater electron deficiency. Most of the organocatalyzed conversions mentioned are supported by phosphines, such as the Michael additions of oximes[205] and alcohols[217,223] onto activated olefins.

Bowman *et al.* showed that the thiol-ene reaction is also a powerful tool in macromolecular applications by employing a visible-light induced thiol-Michael addition photo-polymerization system.[224] The set-up is able to provide stoichiometric, spatial and temporal control over this reaction while simultaneously inhibiting radical side reactions. Another step towards polymerizations of thiol-vinyl sulfone formulations is the development of glassy step-growth networks with improved glass transition temperatures compared to thiol-acrylates.[225] Bowman and coworkers obtained polymeric films from monomeric compositions containing triphenylphosphine and methane sulfonic acid as initiating component at ambient conditions. These hitherto sparsely characterized polymers are a promising new class of highly reactive resins which may be applied as dental materials, optical devices or protective coatings for example. Another application of vinyl sulfone reactive monomers is the preparation of polyamide-sulfones with diamines.[226] The organosoluble and thermal stable polymers may be utilized as permselective membranes for CO_2 separation.

The following section reports the application of the well-known organocatalyzed thiol-ene click chemistry[216] to alcohols. The organocatalyzed oxa-Michael addition represents a powerful tool for the formation of carbon-oxygen bonds under mild reaction conditions. Divinyl sulfone was utilized as double-sided electron-deficient counterpart to the alcoholic nucleophilic Michael donors. Addressing the initial objective of divinyl sulfone, namely as reactive dye for cellulose, this set-up should enable a tailor-made modification of nature derived hydroxyl-containing polymers like lignin, cellulose and other polysaccharides. Taking the advantage of introducing non-hydrolyzable ether bonds, divinyl sulfone also implies the possibility of further modifications via Diels-Alder reaction, cross metathesis or a second Michael addition, just to mention some. In general, the necessity of multifunctional polymeric structures is given, particularly of nature derived materials. Divinyl sulfone is also able to function as linking agent between the biopolymer and a second polymeric matrix for instance.

The investigated conversions should additionally serve as model reactions for the modification of the above-mentioned hydroxyl-functional polymers. But most importantly, the performed reaction series should advance the understanding of the reaction behavior and the knowing of proper reaction conditions. As most reports are principally concerned with the addition of primary alcohols to activated olefins, the major challenge is to accomplish the addition of secondary, tertiary as well as sterically demanding hydroxyls of this type. Furthermore, selective catalysts and exact stoichiometric ratios are required to achieve only single-sided addition to divinyl sulfone.

5.2.2 RESULTS AND DISCUSSION

Divinyl sulfone (DVS) was chosen as electron-accepting part of the reaction set-up for two reasons: Firstly, vinyl sulfones, albeit less frequently considered, are excellent Michael acceptors as the sulfone moiety has a higher electron withdrawing capability compared to a carbonyl group for instance.[222] Secondly, utilizing DVS, macromolecular networks become easily accessible.[225] Most efforts in the field of hetero Michael type addition reactions have been directed to the so-called thiol-ene 'Click-chemistry', where thiol-Michael addition photopolymerization protocols were established.[220,224] Regarding to Michael type carbon-oxygen bond formation, the addition of alcohols to acrylic compounds[217] as well as the oxa-Michael addition polymerization of hydroxyl bearing acrylates is known.[218] Another useful purpose is the post-polymerization functionalization of hydroxyl-containing polymers with vinyl sulfone groups, which is also possible in aqueous media as Chau *et al.* showed 2012.[195]

Following the example of the popular thiol-ene click reaction, a straightforward method for the addition of alcohols to electron-deficient olefins was developed.[227] The use of less acidic[228] and less nucleophilic alcohols instead of thiols would be desireable as much more alcohols are readily commercially available. Furthermore, some inherent drawbacks of thiols, such as their tendency to oxidative disulfide formation, their (often) bad odour and toxicity can be circumvented by applying alcohols instead of thiols. Triphenylphosphine and 4-dimethylaminopyridine were found to promote the oxa-Michael addition of alcohols to divinyl sulfone. Under solvent-free conditions, the reactions is exceedingly fast and allows for the preparation of polymers.[227]

Initially, the oxa-Michael addition of benzyl alcohol (3 eq) to divinyl sulfone (1 eq) was chosen as a model system to test a series of potential nucleophiles for this conversion (cp. Scheme 16 and Table 38). The nucleophiles were applied in an amount of 0.1 eq regarding to divinyl sulfone if not stated otherwise. Reactions were carried out in dry dichloromethane at 40 °C in Schlenk tubes with a DVS concentration of 0.55 mol·L^{-1}. The reactions were monitored via ^{1}H NMR spectroscopy and the amounts of mono- and diadduct present in the reaction solution after 2 and 24 h are given in Table 39. The ratio of mono- and disubstituted sulfone as well as unreacted divinyl sulfone (not specified in Table 39) was determined from the CH$_2$ and CH groups adjacent to the sulfone moiety (referred to one proton and one moiety being responsible for the resonance).

Scheme 16. Nucleophile-mediated addition of benzyl alcohol to divinyl sulfone, yielding mono- and diaddition products.
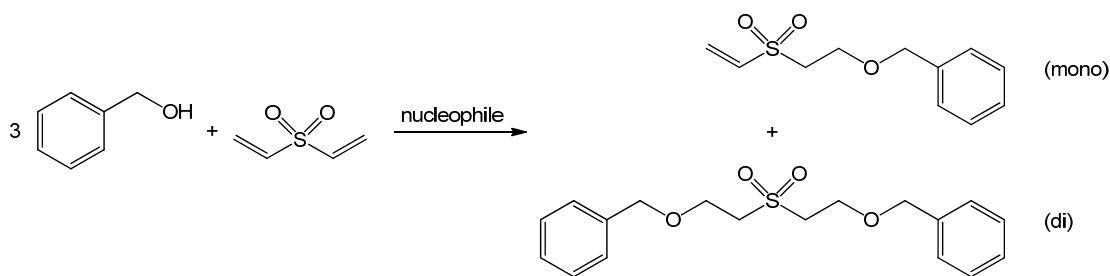
| 1-MIM | DABCO | NEt₃ | DMAP | PPh₃ |
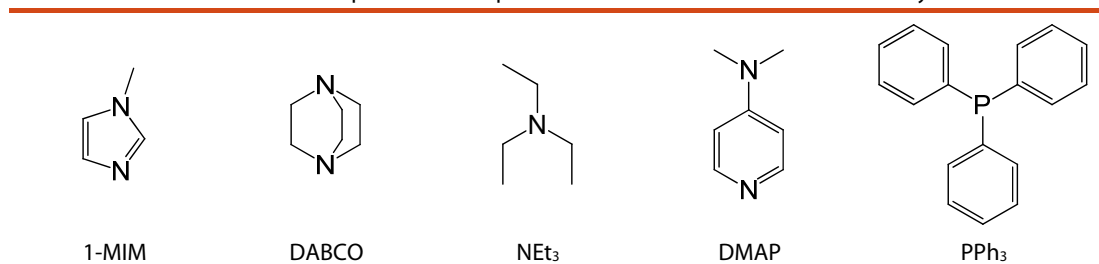
1-Methylimidazole (1-MIM), 1,4-diazabicyclo[2.2.2]octane (DABCO) and triethylamine (NEt$_3$) gave hardly any conversion towards the desired oxa-Michael diaddition product (entries 1–3, Table 39). 4-Dimethylaminopyridine (DMAP) performed better yielding a 1:1 mixture of mono- and diadduct after 24 h (cp. entry 4, Table 39). Triphenylphosphine (PPh$_3$) gave satisfactory results as 83 % of diadduct were observed after 2 h. Complete conversion of DVS to the desired disubstituted product was found after 24 h (entry 5, Table 39). A reduction of the PPh$_3$ loading to 0.025 eq under these reaction conditions did not affect the conversion too much as 91 % disubstituted product were monitored after 24 h (entry 4, Table 42). Additionally, a base-mediated reaction using Cs$_2$CO$_3$ (3 eq with regard to DVS) was carried out under the same reaction conditions (entry 6, Table 39), whereas almost complete conversion was reached after 24 h.

The observed reactivity of the nucleophiles could be correlated with their methyl cation affinities[229] (MCA) (Table 39). MCA values of amines and phosphanes featuring equal substituents differ significantly due to electronic effects. This results in a greater affinity of phosphanes toward carbon electrophiles compared to amine bases with similar proton basicity.[229] In case of the oxa-Michael addition, the observed findings were also in good accordance with the descriptions of organocatalytic activity by Zipse *et al.* The higher the MCA, the better they performed in the double-sided addition of benzyl alcohol to divinyl sulfone. Based on these findings, PPh$_3$ was selected as nucleophilic mediator for the following studies. In contrast to electron-richer alkylphosphines, featuring higher MCA values,[229] PPh$_3$ is air-stable and thus substantially facilitates the reaction set-up.

Table 39. Oxa-Michael addition of DVS (1 eq, [DVS] = 0.55 mol·L⁻¹) and benzyl alcohol (3 eq) in dry DCM at 40 °C in the presence of a nucleophile (0.1 eq with respect to DVS).

			Mono / diadduct / %	
Entry	Nucleophile	MCA / kJ·mol⁻¹	2 h	24 h
1	1-MIM	550	3 / 0	14 / 0
2	DABCO	562	<1 / 0	3 / <1
3	NEt₃	562	0 / 0	1 / 0
4	DMAP	581	42 / 9	53 / 47
5	PPh₃	618	17 / 83	<1 / >99
6	Cs₂CO₃	–	38 / 57	1 / 99

As a next step, the substrate scope of the reaction was investigated. A series of primary, secondary and tertiary alcohols, aliphatic as well as aromatic, were screened in terms of their reactivity towards divinyl sulfone (Table 40). Satisfactory conversions are obtained with simple primary alcohols, namely methanol and ethanol (entries 1 and 2, Table 40). However, with increasing chain length (butyl and dodecyl alcohol, entries 3 and 4, Table 40) complete conversion towards the desired disubstituted product is not reached within 24 h. The obvious slowdown of the addition reaction with these substrates may be the consequence of the growing steric hindrance and bulkiness as the electronic properties stay basically unaltered.

2-Propanol, the simplest secondary alcohol (entry 5, Table 40) is a significantly less favorable Michael donor compared to primary alcohols. Only 13 % of disubstituted product were observed after 24h under the applied reaction conditions. A large proportion of DVS was converted to the corresponding monoadduct, whereas the second addition reaction proceeds only sluggishly. With cyclohexanol as substrate, the conversion towards the diadduct approaches zero (entry 6, Table 40).

Applying an aliphatic tertiary alcohol as Michael donor (entry 7, Table 40), no reaction takes place at all. The benchmark substrate benzyl alcohol is a better substrate than allyl alcohols (entries 9 and 11). Propargyl alcohol was found to be a particularly good substrate (entry 13). Alkyl substituents in positions 3 or 1 resulted in lower conversions compared to the unsubstituted parent substrate. The secondary alcohol derivative featuring a phenyl group in position 1 gave similar results (entry 17), whereas a second phenyl group at this position is adverse to high conversions under the applied reaction conditions. However, the reactions shown in entries 16 and 18 (Table 40) illustrate that also tertiary alcohols featuring lower pK_a values than ^{t}BuOH undergo the oxa-Michael addition reaction. Phenol was shown to be a poor substrate under these reaction conditions.[223]
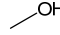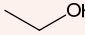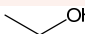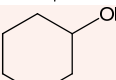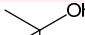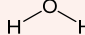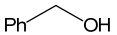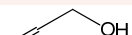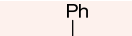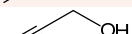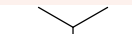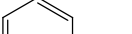
Water classifies between 2° and 3° alcohols in terms of reactivity as Michael donor, yielding considerably more mono- and diadduct than phenol for instance. Thus, the formation of water addition products comes especially into account when applying less preferred substrates.

The findings about the reactivity of the various alcohols towards divinyl sulfone reveal important information in terms of applying this reaction to lignin. Especially the behavior of secondary aliphatic alcohols as well as phenol is of immediate relevance.

Toluene and tetrahydrofuran have been tested as solvents for the oxa-Michael addition of benzyl alcohol and DVS (Table 42). Conversions in toluene were similar to those in dichloromethane, but tetrahydrofuran is detrimental to this reaction. Furthermore, 10 °C was found to be the optimum reaction temperature for this conversion (Table 43, entry 3). However, the difference in conversion towards the disubstituted product at room temperature after 24 h is negligibly small.

Table 40. Substrate scope of the oxa-Michael addition of DVS (1 eq, [DVS] = 0.55 mol·L⁻¹) and alcohols (3 eq) in dry DCM at 40 °C in the presence PPh₃ (0.1 eq with respect to DVS).

Entry	Alcohol				Mono / diadduct[c] / %	
	Structure	Name	pK_a[a]	pK_a[b]	2 h	24 h
1		methyl alcohol	15.20	15.17	1 / 99	<1 / >99
2		ethyl alcohol	15.50	15.24	23 / 77	4 / 96
3		n-butyl alcohol	15.92	15.24	54 / 46	22 / 78
4		dodecyl alcohol		15.20	73 / 7	66 / 34
5		isopropyl alcohol	15.70	15.31	64 / 10	76 / 13
6		cyclohexanol	16.57	15.31	9 / 0	36 / 0
7		$tert$-butyl alcohol	16.84	15.38	0 / 0	0 / 0
8		water	15.7		31 / 9	34 / 13[d]
9		benzyl alcohol	15.44	14.36	17 / 83	<1 / >99
10		α-methyl benzyl alcohol		14.43	77 / 4	86 / 10
11		allyl alcohol	15.52	14.43	19 / 81	11 / 89
12		1-phenyl allyl alcohol		13.61	73 / 27	46 / 54
13		propargyl alcohol	13.60	13.21	<1 / >99	<1 / >99
14		3-methyl propargyl alcohol	14.16	13.14	36 / 64	23 / 77
15		1-isopropyl propargyl alcohol		13.14	48 / 52	23 / 77
16		1,1-dimethyl propargyl alcohol		13.34	65 / 14	67 / 33
17		1-phenyl propargyl alcohol		12.40	<1 / >99	<1 / >99
18		1,1-diphenyl propargyl alcohol		11.58	84 / 16	63 / 37
19		phenol	9.97	9.86	4 / 0	21 / 2

[a] According to reference 228. [b] Calculated using Advanced Chemistry Development Software V11.02 (ACD/Labs), retrieved from Scifinder. [c] Conversion of DVS towards mono- and diadduct was determined by ¹H NMR spectroscopy after 2 and 24 h reaction time. [d] 1,4-Oxathiane-4,4-dioxide was additionally formed to about 17 %.

KINETIC STUDIES

The oxa-Michael addition reaction of divinyl sulfone (DVS, 1 eq) and various alcohols (3 eq) (Scheme 17) was monitored via kinetic ^{1}H NMR experiments. Kinetic measurements were performed with selected alcohols in CDCl$_3$ at room temperature and catalyzed by triphenylphosphine (0.1 eq). Spectra were accumulated every minute for the first quarter hour, then every two minutes until one hour and subsequently with increasing intervals.

Scheme 17. General reaction scheme for kinetic studies performed with DVS and various alcohols in CDCl$_3$ at RT, promoted by PPh$_3$.
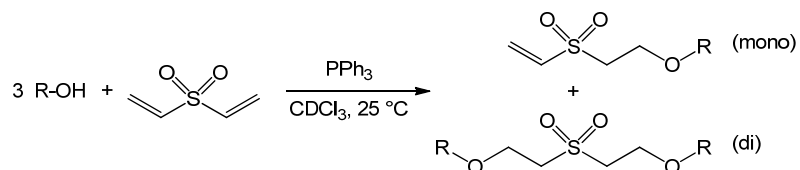
The concentration of DVS in the NMR tube (0.15 mol·L^{-1}) is substantially lower compared to Schlenk reaction conditions (0.55 mol·L^{-1}). The low concentration considerably decelerates the addition progress: In contrast to the observed complete conversion of DVS and propargyl alcohol towards the disubstituted product in the according Schlenk reaction (Table 40, entry 13), the double-sided addition is significantly retarded in the NMR experiment, where only 70 % diadduct were formed after 2 h (Figure 47). The concentration dependent conversion of DVS was investigated independently and is presented in Figure 51.
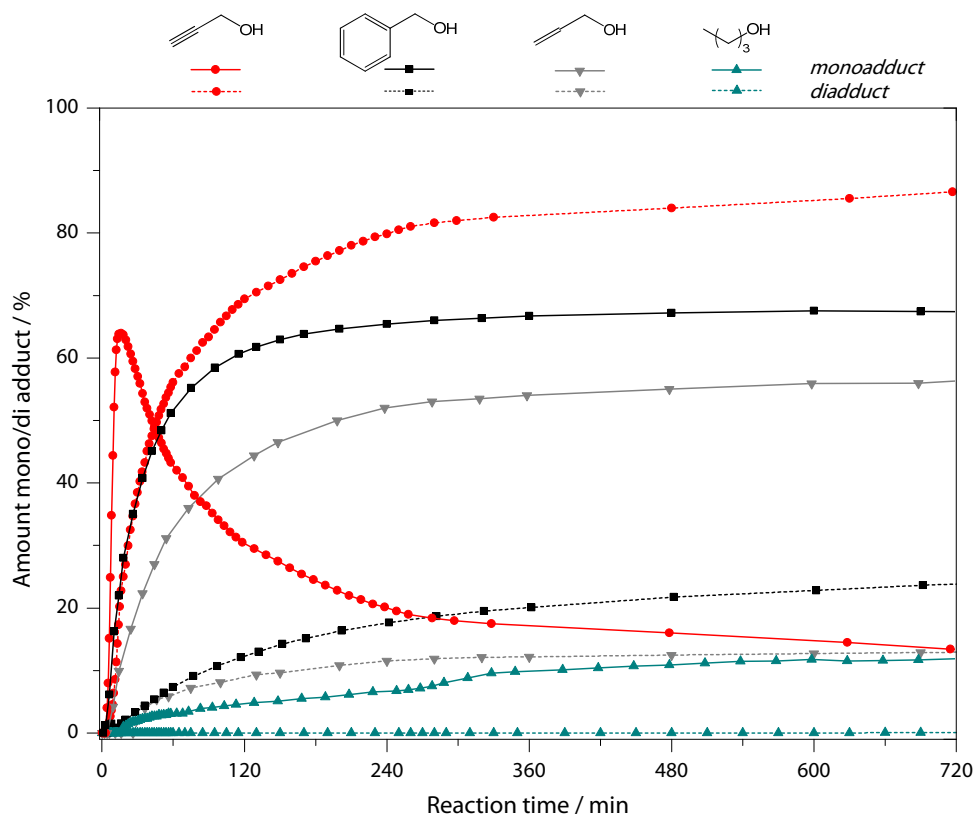
Figure 47. ^{1}H NMR kinetic measurements with DVS (1 eq) and various 1° alcohols (3 eq) (propargyl, benzyl, allyl and *n*-butyl alcohol), catalyzed by PPh$_3$ (0.1 eq), (25 °C, 500 MHz, CDCl$_3$).

The most rapid and most complete conversion of DVS can be observed with propargyl alcohol (Figure 47). The formation of monoadduct is very fast and reaches a maximum after 22 minutes, as the second addition takes place almost simultaneously. Benzyl alcohol and allyl alcohol exhibit reasonable conversions, but are notely slower added to DVS than propargyl alcohol. The major difference is that the second addition of alcohol to the available monoadduct proceeds notely slower. *n*-Butyl alcohol shows hardly any conversion under these reaction conditions.

The outstanding reactivity of propargyl alcohol within the first kinetic series was further investigated with different 1- and 3-substituted propargylic alcohols. The fastest conversions were obtained with propargyl and 1-phenyl propargyl alcohol (Table 40, entries 13 and 17). Although 1-phenyl propargyl alcohol is a secondary alcohol, it is added to DVS as fast as the primary, unsubstituted parent substance. All substituents except of a phenyl group in position 1 have a decelerating effect on the oxa-Michael addition, even the methyl group in position 3. 1-Phenyl propargyl alcohol is the only derivative showing the same reaction progress as propargyl alcohol. The formation of monoadduct proceeds in the same order of reaction rate, even reaching a higher maximum due to the slower diadduct formation. The phenyl substituent obviously exerts an accelerating effect on the first addition step. The primary 3-methyl propargyl alcohol visualizes the influence of the methyl substituent in γ-position to the hydroxyl group.
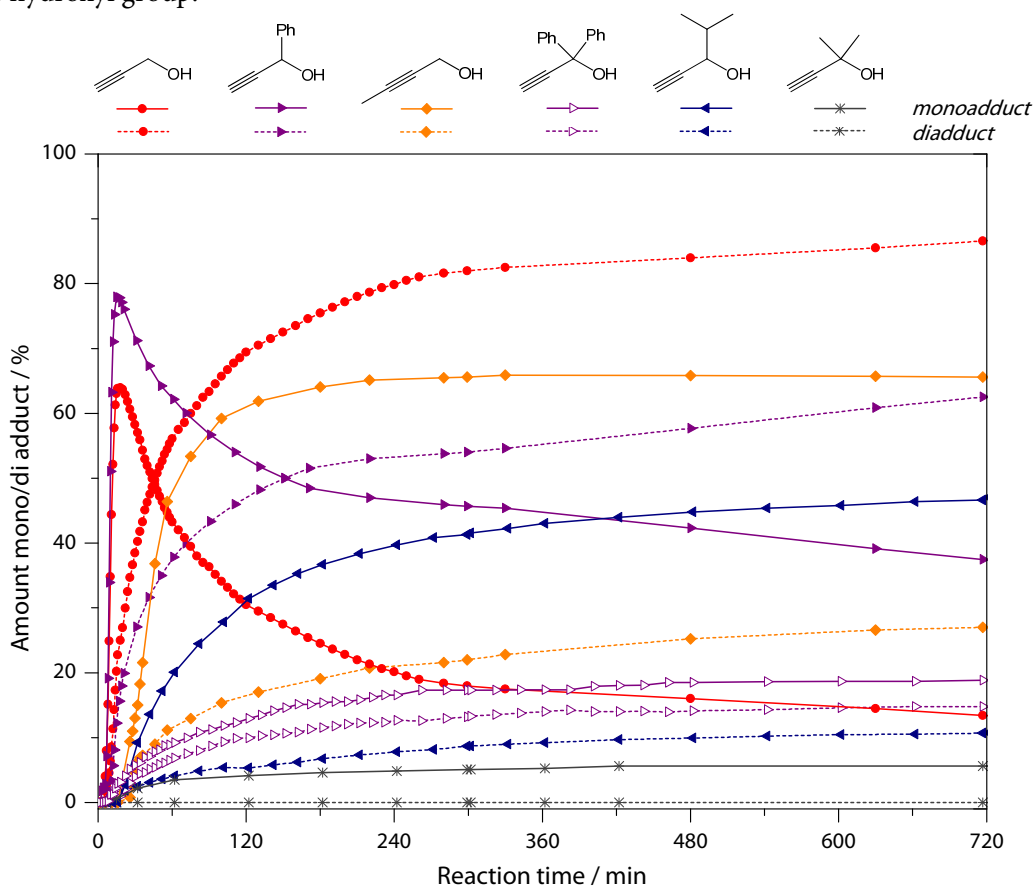

Figure 48. ^{1}H NMR kinetic measurements of DVS (1 eq) and various propargyl alcohols (3 eq) catalyzed by PPh$_3$ (0.1 eq) (25 °C, 500 MHz, CDCl$_3$).

The secondary 1-*iso*-propyl propargyl alcohol with the substituent in α-position to the hydroxyl group shows a distinctly retarded progress, especially when compared with phenyl propargyl alcohol. Supposing the bulkiness of the phenyl and ^{i}Pr substituent comparable, the different electronic effects those two groups exert must play the key role. The major difference between the two substrates is the presence of additional π-electrons in case of the phenyl substituent whereby the electron density of the oxygen is enriched and hence the Michael donor qualities are improved. Thus, the electronic characteristics of the alcoholic species are the decisive part in this conversion. The same effect is observed when comparing the tertiary 1,1-diphenyl and 1,1-dimethyl propargyl alcohols.

Besides the different alcoholic substrates, the consequences of varying the triphenylphsophine loading, the solvent or the concentration of reactants on the oxa-Michael addition have been investigated via kinetic experiments. In order to economize the synthesis, the loading of PPh$_3$ was reduced stepwise and the reaction progress was monitored via ^{1}H NMR kinetic measurements (Figure 49). Whereas a reduction of the originally applied 0.1 eq of PPh$_3$ by half leads to a markedly decelerated formation of disubstituted product, the reduction to one tenth PPh$_3$ (0.01 eq) results in no adduct formation at all.

The reaction progress in CD$_2$Cl$_2$ and CDCl$_3$ shows an approximately identical curve shape. The diadduct formation is slightly retarded in toluene-*d$_8$*, but is even the highest within the time frame of 12 h. The weakest reaction progress is observed in THF-*d$_8$*, which may be a consequence of the lesser ability to stabilize anionic intermediates (Figure 50).
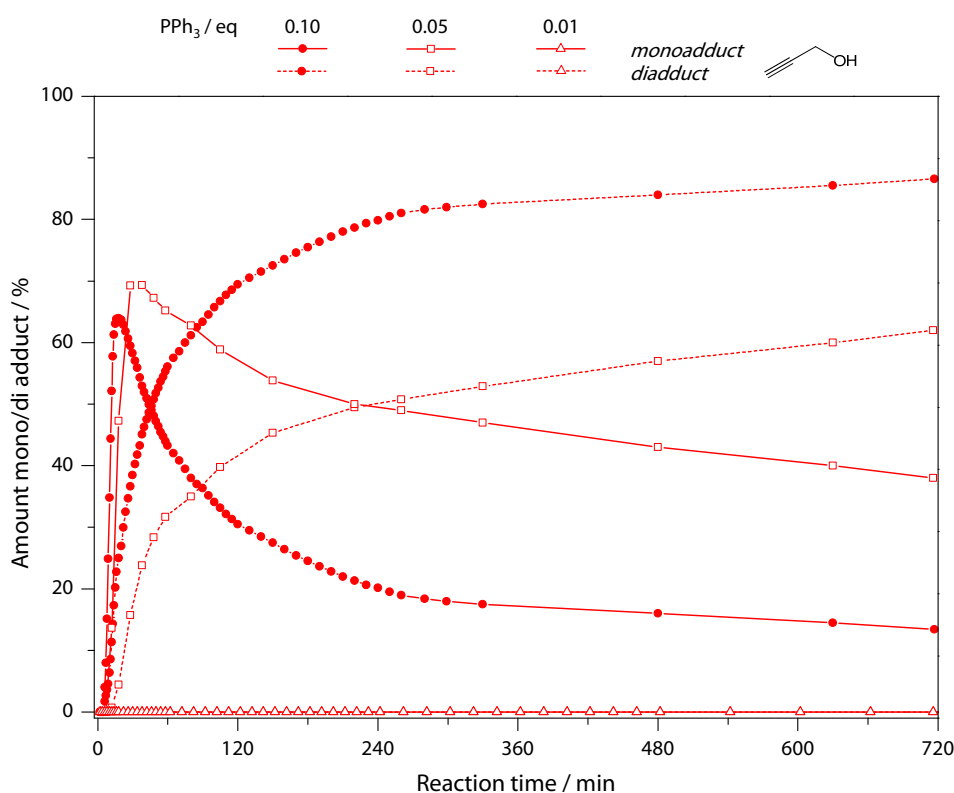
Figure 49. Reaction progress of DVS (1 eq) and propargyl alcohol (3 eq) with reduced PPh$_3$ loadings (25 °C, 500 MHz, CDCl$_3$).
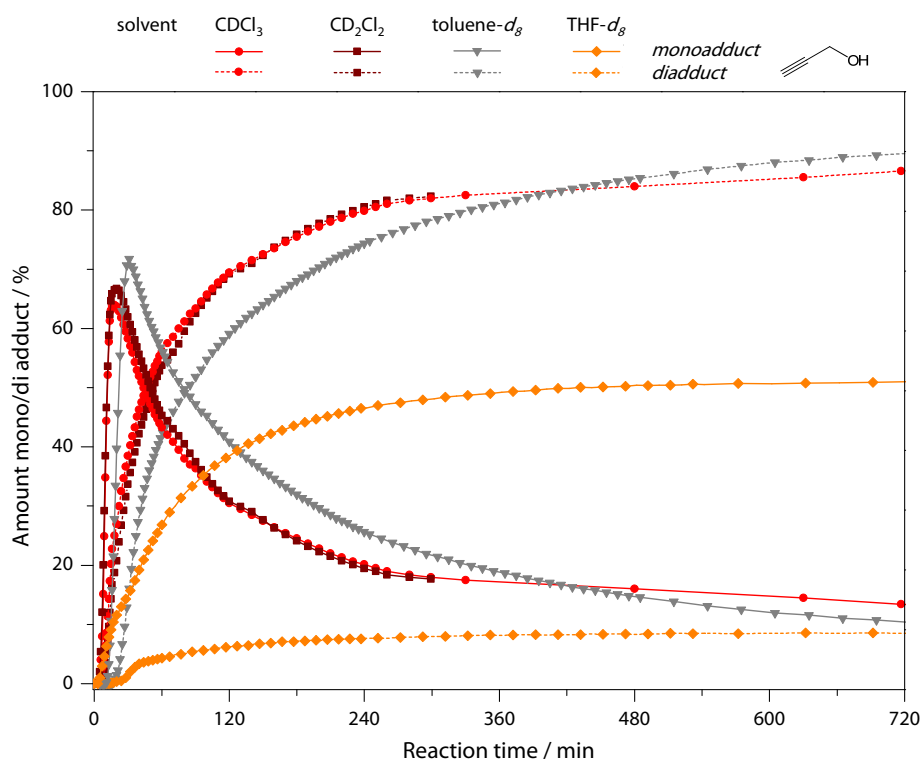
Figure 50. Reaction progress of DVS (1 eq) and propargyl alcohol (3 eq) in different deuterated solvents, supported by PPh₃ (0.1 eq) (25 °C, 500 MHz).
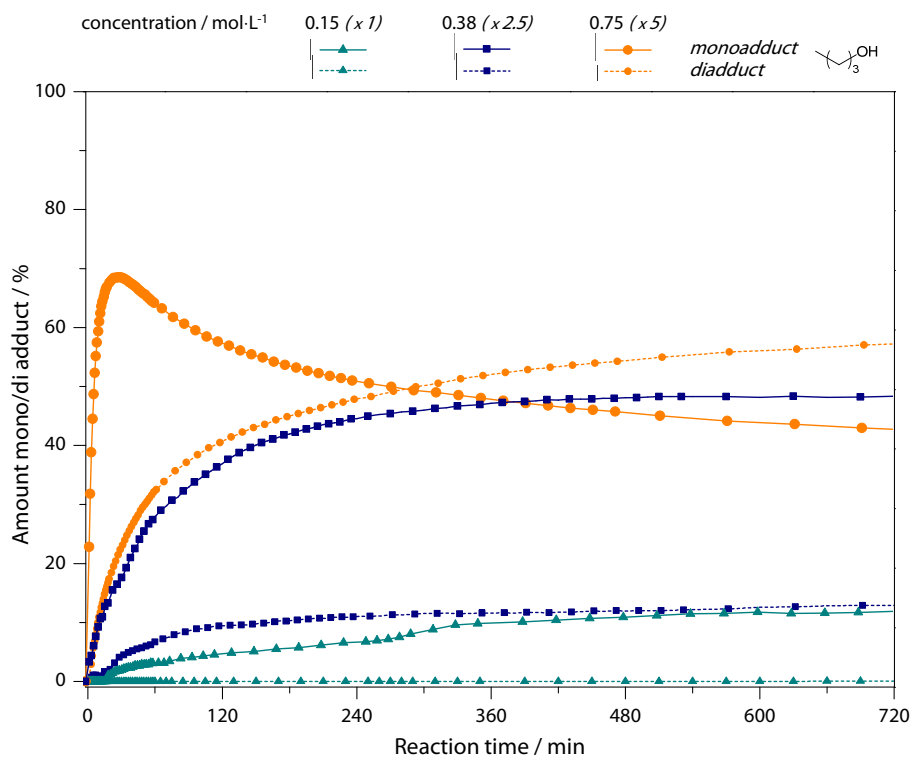
Figure 51. Reaction progress with increasing concentration of DVS (1 eq) and *n*-butanol (3 eq), supported by PPh₃ (0.1 eq), (25 °C, 500 MHz, CDCl₃).

Table 41. Concentration dependent conversion of DVS (1 eq) and *n*-butanol (CDCl₃, 25 °C).

Concentration of DVS / mol·L⁻¹	*n*-BuOH / eq	Mono / diadduct (24 h)/ %
0.15 *(x 1)*	3	13 / < 1
0.38 *(x 2.5)*	3	48 / 14
0.75 *(x 5)*	3	40 / 60
0.91 (bulk)	12	< 1 / > 99

The kinetic ¹H NMR study impressively demonstrates the concentration dependence of the oxa-Michael addition (Figure 51). Thus, it was shown that complete conversion towards the disubstituted sulfone is also feasible within a reasonable time frame using the less preferred *n*-butyl alcohol (Table 41). These findings imply to perform the oxa-Michael addition reaction under solvent-free conditions, provided that PPh₃ is soluble in the applied alcohol. Besides this, the reaction temperature should not exceed room temperature or fall below 10 °C (cp. Table 43, section 5.2.3). The reaction of DVS and 2-propanol is another good exemplary model. Under reaction conditions as specified in Table 40, only 13 % of disubstituted product were formed after 24 h (entry 5). Optimized reaction conditions (applying 26 eq of 2-propanol and 0.1 eq PPh₃ at 23 °C, cp. isolated substance 5, section 5.2.3) gave the diadduct in 75 % isolated yield after purification by column chromatography.

A mechanistic illustration of the oxa-Michael addition reaction is shown in Scheme 18. By initial conjugate addition[230] of PPh₃ to DVS a zwitterion (A) is formed, which is detracted from the chemical equilibrium upon protonation by the alcohol, forming the corresponding phosphonium alkoxide (B). The conjugate addition of the generated alkoxide to DVS forms ion pair C. Protonation of the carbanion by another alcohol results in the formation of the *β*-alkoxy sulfone derivative (D) and phosphonium alkoxide (B) to complete the catalytic cycle. The proton transfer from the alcohol to carbanion A is believed to be the rate-determining step of the reaction, as already stated for related thiol-Michael reactions.[222,216,231] As the entropy values of activation were found to be very negative in a related system, a precise arrangement of PPh₃, the electron-deficient olefin and the proton donor seems to be necessary for the reaction to occur.[232]

Scheme 18. Mechanistic illustration of the oxa-Michael addition.[227]
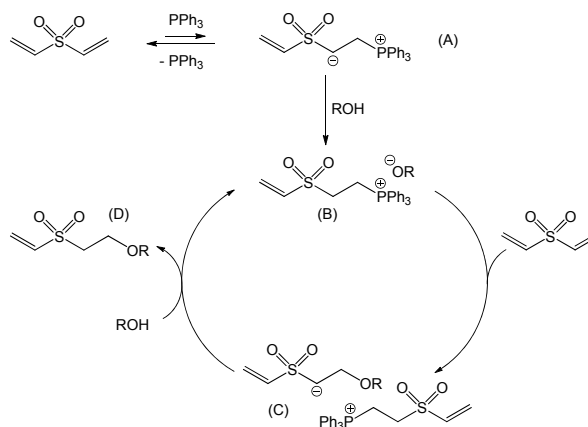
The following results support the briefly outlined mechanistic picture: Deuterium incorporation was found in α-position to the sulfone group upon performing the reaction in CDCl$_3$ or with methanol-d_4 (cp. products I and II, section 5.2.3), indicating the generation of a strong base during the reaction.

The incorporation of deuterium to an extent of approximately 30 % was evidenced via ^{13}C-^{2}D couplings observed in the ^{13}C {^{1}H} NMR spectrum of the deuterated propargyl alcohol diadduct (cp. isolated compound I, section 5.2.3). $^1J_{CD}$ couplings were observed for C^3 as well as C^{s2,s3} and also a $^2J_{CD}$ coupling was detected for C^2 (triplett, 78.3 ppm) (Figure 52).
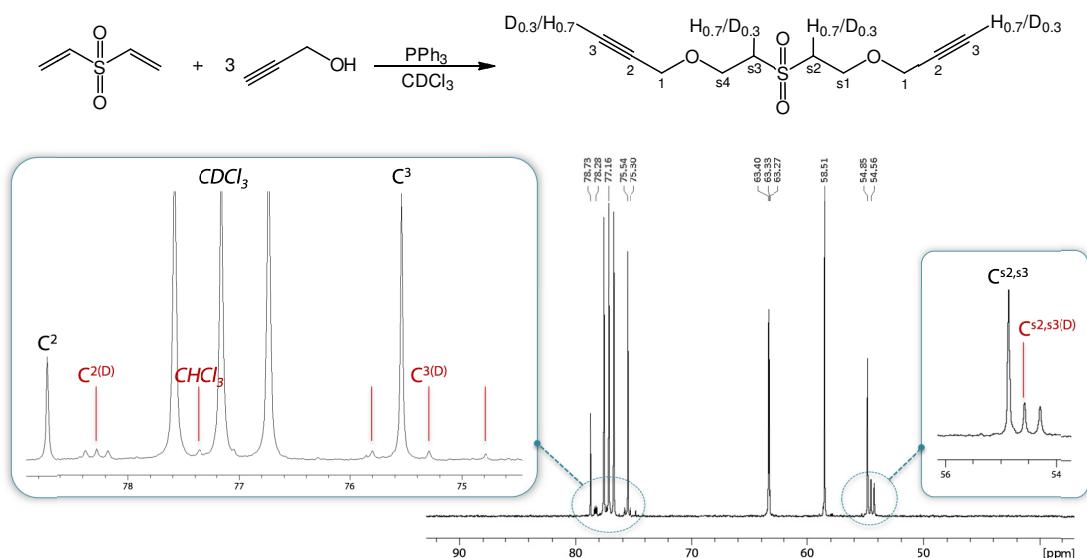
Figure 52. ^{13}C {^{1}H} NMR evidence of deuterium incorporation upon reacting DVS (1 eq) and propargyl alcohol (3 eq) in the presence of PPh$_3$ (0.1 eq) in CDCl$_3$ (25 °C, 75 MHz, CDCl$_3$).

^{31}P {^{1}H} NMR monitoring of the reaction disclosed that no phosphorus signal for the initially formed zwitterion (A) is observable. Not until the addition of alcohol, signals at 24.5 and 24.4 ppm (relative to 85 % H$_3$PO$_4$) appeared which are tentatively assigned to phosphonium-containing ion pairs (B and C) (Figure 53).[233] The sample preparation for ^{31}P {^{1}H} NMR measurements was as follows, whereas the components where mixed in the same order as listed: DVS (20 μL, 0.199 mmol, 1.0 eq, c = 0.31 mol·L^{-1}) and PPh$_3$ (52.3 mg, 0.199 mmol, 1.0 eq) were dissolved in CDCl$_3$ (650 μL) and subjected to ^{31}P NMR measurements (**1**). Then, PA (20 μL, 0.347 mmol, 1.7 eq) was added and the mixture was measured again (**2**). The spectra were compared with the ^{31}P NMR spectrum of the following reaction solution after complete conversion (**3**): PA (1.817 mL, 29.89 mmol, 3.0 eq), DVS (1.00 mL, 9.96 mmol, 1.0 eq, c = 1.99 mol·L^{-1}) and PPh$_3$ (261.3 mg, 0.996 mmol, 0.1 eq) in CDCl$_3$ (5.00 mL).

^{31}P {^{1}H} NMR (200 MHz; CDCl$_3$, 25°C): δ (**1**) 28.47 (O=PPh$_3$), –6.00 (PPh$_3$). (**2**) 28.98 (O=PPh$_3$), 24.49, 24.42 (β-phosphonium salts). (**3**) 30.74 (O=PPh$_3$), 24.30, 24.22, 24.14 (β-phosphonium salts).
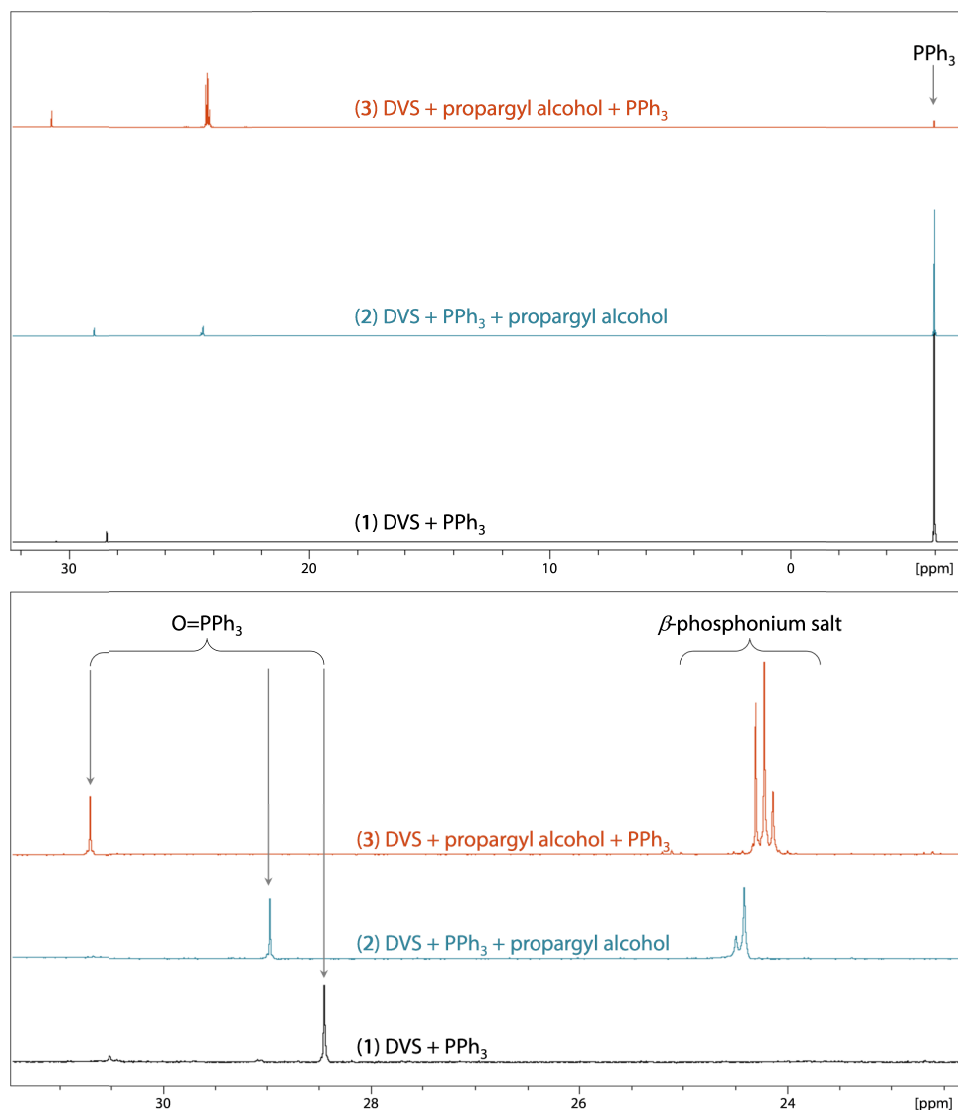
Figure 53. Comparison of ^{31}P $\{^1H\}$ NMR spectra of mixtures containing divinyl sulfone, triphenylphosphine and propargyl alcohol (δ-7 to 32 ppm (top) and 23–31 ppm (below)), (25 °C, 200 MHz, CDCl$_3$).

Summary:
- *PPh$_3$ and DMAP promote the oxa-Michael addition of DVS and varying alcohols*
- *the reactivity of the alcohols decreases in the following order:*
  primary > secondary > phenol > tertiary
- *the simplest 3° alcohol (^{t}BuOH) gave no reaction*
- *allylic, benzylic and propargylic alcohols exhibit a notedly higher reactivity compared to their saturated equivalents*
- *propargyl alcohol is a particularly good substrate*
- *3° propargylic alcohols gave conversions to disubstituted products*
- *particularly fast and efficient reaction under solvent-free conditions and if more acidic alcohols, forming alkoxides with adequate nucleophilicity, are used*

5.2.3 EXPERIMENTAL DETAILS

SCREENING REACTIONS

Table 42. Various PPh$_3$ loadings and solvents for the oxa-Michael addition of DVS (1 eq) and benzyl alcohol (3 eq) at 40 °C; [DVS] = 0.55 mol·L^{-1}.

Entry	Solvent *(dry)*	PPh$_3$ loading / mol%	Reaction time / h	Distribution / %		
				DVS	mono	di
1	DCM	10	2	0	13	87
			24	0	0	>99
2	DCM	7.5	2	0	12	88
			24	0	6	94
3	DCM	5	2	0	30	70
			24	0	8	92
4	DCM	2.5	2	0	34	66
			24	0	9	91
5	DCM	1	2	9	76	15
			24	5	74	21
6	DCM	0.5	2	81	19	0
			24	30	63	7
7	DCM	0.1	2	100	0	0
			24	100	0	0
8	toluene	10	2	0	6	94
			24	0	0	>99
9	toluene	7.5	2	0	22	78
			24	0	6	94
10	toluene	5	2	0	50	50
			24	0	22	78
11	toluene	2.5	2	0	55	45
			24	0	33	67
12	toluene	1	2	13	73	14
			24	9	74	17
13	toluene[a]	1	2	86	14	0
			24	82	18	0
14	toluene[a]	0.5	2	96	4	0
			24	95	5	0
15	toluene[a]	0.1	2	100	0	0
			24	100	0	0
16	THF	10	2	29	64	7
			24	1	69	30
17	THF	7.5	2	42	54	4
			24	1	74	25
18	THF	5	2	76	21	3
			24	21	70	9

[a] *Reaction temperature: 100°C.*

Table 43. Oxa-Michael addition of DVS (1 eq, 0.55 mol·L^{-1}) and benzyl alcohol (3 eq) with PPh$_3$ (0.05 eq) in dry DCM at varying temperatures.

Entry	Reaction temperature / °C	Reaction time / h	Distribution / %		
			DVS	mono	di
1	40	2	0	30	70
		24	0	8	92
2	25	2	0	22	78
		24	0	4	96
3	10	2	0	16	84
		24	0	3	97
4	0	2	0	34	66
		24	0	4	96

PREPARATIVE REACTIONS AND ISOLATED COMPOUNDS

The oxy-Michael addition with the alcohols studied as substrates under the reaction conditions specified in Table 40, were synthesized under optimized reaction conditions (at room temperature and solvent-free if possible). The stated yields were obtained after purification via column chromatography. The according NMR spectra are shown in the electronic supplementary information (ESI) of reference 227.

1	1,1-sulfonylbis[2-methoxy-ethane]	
	$C_6H_{14}O_4S$ [182.24]	
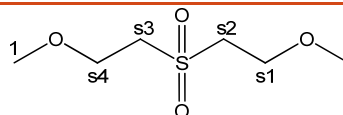
PPh$_3$ (13.1 mg, 0.0498 mmol, 0.1 eq) was dissolved in MeOH (505.0 μL, 12.45 mmol, 25 eq) and DVS (50 μL, 0.498 mmol, 1 eq) was added. The mixture was stirred at 23 °C until complete conversion was monitored via ^{1}H NMR (2h). Excess methanol was removed under N_2 stream and the product was isolated via column chromatography (silica gel, CH/EA 20:1 (v:v)) by sampling the spot with R_f = 0.07 (CH/EA 3:1 (v:v). Yield: 76.8 mg (0.464 mmol, 84.6 %) colorless oil. ^{1}H-NMR (300 MHz, CDCl$_3$, 25 °C): δ 3.83 (t, 4H, $^3J_{HH}$ = 5.51, $CH_2^{s1,s4}$), 3.89 (s, 6H, CH_3^1), 3.33 (t, 4H, $^3J_{HH}$ = 5.51, $CH_2^{s2,s3}$) ppm. ^{13}C {^{1}H} NMR (75 MHz, CDCl$_3$, 25 °C): δ 66.18 (2C, C^{s1,s4}), 59.09 (2C, C^1), 55.00 (2C, C^{s2,s3}) ppm.

2	1,1-sulfonylbis[2-ethoxy-ethane]	
	$C_8H_{18}O_4S$ [210.29]	

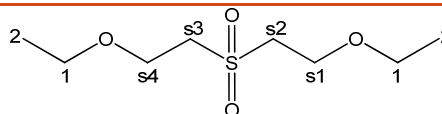Synthesized in the same manner as the methanol diadduct: PPh$_3$ (13.1 mg, 0.0498 mmol, 0.1 eq), EtOH (726.2 μL, 12.45 mmol, 25 eq) and DVS (50 μL, 0.498 mmol, 1 eq) were stirred at 23 °C. Column chromatography (CH/EA 20:1 (v:v)) yielded 86.7 mg (0.412 mmol, 82.8 %) colorless oil by sampling the spot with R_f = 0.12 (CH/EA 3:1 (v:v)). ^{1}H-NMR (300 MHz, CDCl$_3$, 25 °C): δ 3.87 (t, 4H, $^3J_{HH}$ = 5.71, $CH_2^{s1,s4}$), 3.54 (q, 4H, $^3J_{HH}$ = 6.80, CH_2^1), 3.33 (t, 4H, $^3J_{HH}$ = 5.71, $CH_2^{s2,s3}$), 1.21 (t, 6H, $^3J_{HH}$ = 7.02, CH_3^2) ppm. ^{13}C APT NMR (75 MHz, CDCl$_3$, 25 °C): δ 66.81 (2C, C^1), 64.04 (2C, C^{s1,s4}), 55.04 (2C, C^{s2,s3}), 15.04 (2C, C^2) ppm.

3	1,1-sulfonylbis[2-butoxy-ethane]	
	$C_{12}H_{26}O_4S$ [266.40]	
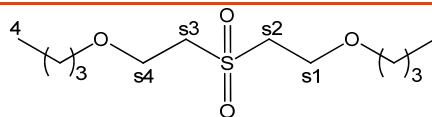
Synthesized in the same manner as the methanol diadduct: PPh$_3$ (13.1 mg, 0.498 mmol, 0.1 eq), BuOH (1139.5 μL, 12.45 mmol, 25 eq) and DVS (50 μL, 0.498 mmol, 1 eq) were stirred 24 h at 23 °C. Column chromatography (CH/EA 20:1 (v:v)) yielded 110.3 mg (0.414 mmol, 83.1 %) colorless oil by sampling the spot with R_f = 0.46 (CH/EA 3:1 (v:v)). ^{1}H-NMR (300 MHz, CDCl$_3$, 25 °C): δ 3.83 (t, 4H, $^3J_{HH}$ = 5.67, $CH_2^{s1,s4}$), 3.45 (t, 4H, $^3J_{HH}$ = 6.57, CH_2^1), 3.31 (t, 4H, $^3J_{HH}$ = 5.71, $CH_2^{s2,s3}$), 1.55 (quintet, 4H, $^3J_{HH}$ = 7.05, CH_2^2), 1.35 (sextet, 4H, $^3J_{HH}$ = 7.39, CH_2^3), 0.91 (t, 6H, $^3J_{HH}$ = 7.26, CH_3^4) ppm. ^{13}C {^{1}H} NMR (75 MHz, CDCl$_3$, 25°C): δ 71.3 (2C, C^1), 64.3 (2C, C^{s1,s4}), 55.0 (2C, C^{s2,s3}), 31.7 (2C, C^2), 19.4 (2C, C^3), 14.0 (2C, C^4) ppm.

4	1-(2-((2-(dodecyloxy)ethyl)sulfonyl) ethoxy)dodecane) $C_{12}H_{58}O_4S$ [490.82]	

PPh$_3$ (522.6 mg, 1.99 mmol, 0.1 eq) and dodecyl alcohol (11.138 g, 59.8 mmol, 3.0 eq) were dissolved in dry DCM (40 mL) and DVS (2.0 mL, 19.92 mmol, 1 eq) was added. The mixture was stirred 24 h at 23 °C, whereas 65% di- and 35% monoadduct were formed. The solution was concentrated under reduced pressure and subjected to column chromatography (silica gel, CH/EA 20:1 (v:v), TLC: R$_f$ = 0.75 (CH/EA 1:1 (v:v)). Yield: 4.762 g (9.70 mmol, 48.7 %) white crystals. ^{1}H-NMR (300 MHz, CDCl$_3$, 25 °C): δ 3.84 (t, 4H, $^3J_{HH}$ = 5.62, CH_2^{s1,s4}), 3.45 (t, 4H, $^3J_{HH}$ = 6.48, CH_2^{1}), 3.32 (t, 4H, $^3J_{HH}$ = 5.62, CH_2^{s2,s3}), 1.65-1.50 (m, 4H, CH_2^{2}), 1.26 (bs, 36H, C$H_2$$^{3-11}$), 0.88 (t, 6H, $^3J_{HH}$ = 6.70 Hz, CH_3^{12}) ppm. ^{13}C {^{1}H} NMR (75 MHz, CDCl$_3$, 25 °C): δ 71.68 (2C, C^1), 64.37 (2C, C^{s1,s4}), 55.05 (2C, C^{s2,s3}), 32.06, 29.82, 29.79, 29.77, 29.75, 29.64, 29.59, 29.50, 26.25, 22.83 (20C, C$^{2-11}$), 14.25 (2C, C^{12}) ppm.

5	2,2'-[sulfonylbis(2,1-ethanediyloxy)] bispropane $C_{10}H_{22}O_4S$ [238.34]	

Was synthesized in the same manner as the methanol diadduct: PPh$_3$ (13.1 mg, 0.0498 mmol, 0.1 eq), i-PrOH (1.0 mL, 12.98 mmol, 26.1 eq) and DVS (50 μL, 0.498 mmol, 1 eq) were stirred at 23 °C. Column chromatography (TLC: R$_f$ = 0.58 (CH/EA 1:1 (v:v)) yielded 89.3 mg (0.375 mmol, 75.2 %) colorless oil. ^{1}H-NMR (300 MHz, CDCl$_3$, 25 °C): δ 3.83 (t, 4H, $^3J_{HH}$ = 5.76, CH_2^{s1,s4}), 3.61 (sep, 2H, $^3J_{HH}$ = 6.15, CH^2), 3.29 (t, 4H, $^3J_{HH}$ = 5.76, CH_2^{s2,s3}), 1.15 (d, 12H, $^3J_{HH}$ = 6.04, CH_3^{1,3}) ppm. ^{13}C APT NMR (75 MHz, CDCl$_3$, 25 °C): δ 72.37 (2C, C^2), 61.66 (2C, C^{s1,s4}), 55.36 (2C, C^{s2,s3}), 21.96 (4C, C^{1,3}) ppm.

6	((sulfonylbis(ethane-2,1-diyl))bis(oxy))dicyclohexane $C_{16}H_{30}O_4S$ [318.47]	

DVS (588.5 mg, 4.981 mmol, 1.0 eq) was added to a solution of cyclohexanol (1.0976 g, 10.96 mmol, 2.2 eq) and PPh$_3$ (130.7 mg, 0.498 mmol, 0.1 eq) in DCM (500 μL) and stirred at 23 °C. After complete conversion of DVS was detected via ^{1}H NMR (> 96 % diadduct after 168 h), the mixture was purified by flash chromatography (silica gel, C/EA 20:1 (v:v)). Sampling the spot with R$_f$ = 0.45 (CH/EA 3:1 (v/v)) yielded 769.3 mg (2.416 mmol, 48.5 %) yellowish oil. ^{1}H-NMR (300 MHz, CDCl$_3$, 25 °C): δ 3.88 (t, 4H, $^3J_{HH}$ = 5.72, CH_2^{s1,s4}), 3.33 (t, 4H, $^3J_{HH}$ = 5.63, CH_2^{s2,s3}), 3.36–3.25 (m, 2H, CH^1), 1.95−1.80 (m, 4H, CH_2^{2,6}), 1.77−1.64 (m, 4H, CH_2^{3,5}), 1.58−1.45 (m, 2H, CH_2^{4}), 1.39−1.14 (m, 10H, CH_2^{2,3,4,5,6}) ppm. ^{13}C {^{1}H} NMR (75 MHz, CDCl$_3$, 25 °C): δ 78.08 (2C, C^1), 61.53 (2C, C^{s1,s4}), 55.47 (2C, C^{s2,s3}), 31.98 (4C, C^{2,6}), 25.85 (2C, C^4), 23.91 (4C, C^{3,5}) ppm.

| 7 | 2-(2-((2-(tert-butoxy)ethyl)sulfonyl) ethoxy)-2-methylpropane

$C_{12}H_{26}O_4S$ [266.40] | |

The reaction mixture was prepared according to the methanol diadduct. A solution of PPh$_3$ (261.3 mg, 0.996 mmol, 0.1 eq), t-BuOH (1.624 g, 21.9 mmol, 2.2 eq) and DVS (1.0 mL, 9.96 mmol, 1 eq) in DCM (0.5 mL) was stirred 5 days at 23 °C. No conversion was detected via ^{1}H NMR.

8	bis(2-hydroxyethyl)sulfone $C_4H_{10}O_4S$ [154.18]	(di)
	2-hydroxyethyl vinyl sulfone $C_4H_8O_3S$ [136.17]	(mono)
	1,4-oxathiane-4,4-dioxide[234] $C_4H_8O_3S$ [136.17]	

A Schlenk tube was equipped with DVS (100 µL, 0.996 mmol, 1 eq), H$_2$O $deion.$ (53.8 µL, 2.99 mmol, 3 eq), DCM (2 mL) and PPh$_3$ (26.13 mg, 0.0996 mmol, 0.1 eq) and stirred at 23 °C. Mono- and diadduct of H$_2$O as well as 1,4-oxathiane-4,4-dioxide were found in the reaction mixture already after 2 h. The different reaction products of DVS with H$_2$O were not isolated separately, but the detected peaks were in good accordance with known data.[235] ^{1}H-NMR (300 MHz, CDCl$_3$, 25 °C): (di) δ 3.99−3.87 (m, 4H, C$H_2^{s1,s4}$), 3.38 (m, 4H, C$H_2^{s2,s3}$) ppm; (mono) δ 6.77 (dd, 1H, $^3J_{HH(Z)}$ = 9.9, $^3J_{HH(E)}$ = 16.9, CH^3), 6.44 (d, 1H, $^3J_{HH(E)}$ = 16.8, C$H^{s4(Z)}$), 6.14 (d, 1H, $^3J_{HH(E)}$ = 9.8, C$H^{s4(E)}$), 3.99–3.87 (m, 4H, C$H_2^{s1,s4}$), 3.27 (m, 4H, C$H_2^{s2,s3}$) ppm; (1,4–oxathiane-4,4-dioxide) δ 4.14 (t, 4H, $^3J_{HH}$ = 5.0, C$H_2^{s1,s4}$), 3.12 (m, 4H, $^3J_{HH}$ = 5.1, C$H_2^{s2,s3}$) ppm.

| 9 | bis(2-benzyloxyethanyl)sulfone

$C_{18}H_{22}O_4S$ [334.43] | |

To a solution of benzyl alcohol (6.22 mL, 59.8 mmol, 3.0 eq) and DVS (2.00 mL, 19.9 mmol, 1 eq) in dry DCM (40 mL), PPh$_3$ (522.6 mg, 1.99 mmol, 10 mol%) was added and the mixture was stirred at 23 °C for 24 h (full consumption of DVS detected via ^{1}H NMR). The solution was concentrated under reduced pressure and the remaining yellowish oil was purified via column chromatography (CH/EE, 10:1, (v:v)). Sampling the spot with R$_f$ = 0.65 (CH/EE, 1:1, (v:v)) yielded 5.437 g (16.26 mmol, 81.6 %) colorless oil. ^{1}H-NMR (300 MHz, CDCl$_3$, 25 °C): δ 7.38–7.25 (m, 10H, CH^{2-6}), 4.51 (s, 4H, CH_2^7), 3.89 (t, 4H, $^3J_{HH}$ = 5.6, C$H_2^{s1,s4}$), 3.36 (t, 4H, $^3J_{HH}$ = 5.6, C$H_2^{s2,s3}$) ppm. ^{13}C APT NMR (75 MHz, CDCl$_3$, 25 °C): δ 137.2 (2C, C^1), 128.4 (4C, C^{3,5}), 127.8 (2C, C^4), 127.7 (4C, C^{2,6}), 73.2 (2C, C^7), 63.7 (2C, C^{s1,s4}), 54.9 (2C, C^{s2,s3}) ppm.

| 10 | (((sulfonylbis(ethane-2,1-diyl)) bis(oxy))bis(ethane-1,1-diyl))dibenzene C$_{20}$H$_{26}$O$_4$S [362.48] | |
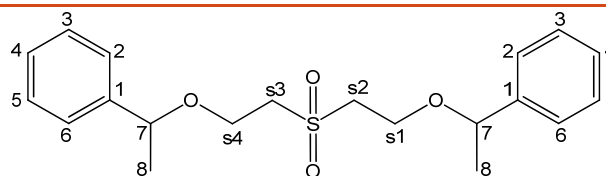
To a solution of α-methyl benzyl alcohol (1.3387 g, 10.96 mmol, 2.2 eq) and PPh$_3$ (130.7 mg, 0.498 mmol, 0.1 eq) in DCM (500 µL) DVS (588.5 mg, 4.981 mmol, 1.0 eq) was added and stirred at 23 °C. After complete conversion of DVS (^{1}H NMR: 99% diadduct after 48 h), the mixture was purified by flash chromatography (silica gel, C/EA 20:1 (v:v)). Sampling the spot with R$_f$ = 0.42 yielded 1.123 g (3.097 mmol, 62.2 %) colorless oil (stereoisomers). ^{1}H-NMR (300 MHz, CDCl$_3$, 25 °C): δ 7.41–7.26 (m, 10H, CH^{2-6}), 4.43–4.51 (m, 2H, CH^7), 3.83–3.65 (m, 4H, C$H_2^{s4,s1}$), 3.51–3.17 (m, 4H, C$H_2^{s2,s3}$), 1.47 (dd, 6H, $^3J_{HH}$ = 6.48, $^3J_{HH}$ = 1.03, CH_3^8) ppm. ^{13}C {^{1}H} NMR (75 MHz, CDCl$_3$, 25 °C): δ 142.87, 142.82 (2C, C$^{1(R,S)}$), 128.76 (4C, C^{3,5}), 127.97 (2C, C^4), 126.28 (4C, C^{2,6}), 78.93 (2C, C^7), 62.40, 62.35 (4C, C$^{s1,s4(R,S)}$), 55.31, 55.23 (4C, C$^{s2,s3(R,S)}$), 23.94 (2C, C^8) ppm.

| 11 | 3-(2-((2-(allyloxy)ethyl)sulfonyl) ethoxy)prop-1-ene C$_{10}$H$_{18}$O$_4$S [234.31] | |
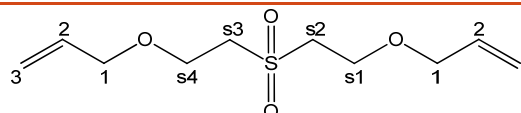
PPh$_3$ (261.3 mg, 0.996 mmol, 0.1 eq), allyl alcohol (1.736 g, 29.9 mmol, 3 eq) and DVS (1.0 mL, 9.96 mmol, 1 eq) were stirred 3 days at 23 °C. Column chromatography (CH/EA 10:1 (v:v)) of the reaction mixture yielded 1.804 g (7.70 mmol, 77.3 %) yellowish oil by sampling the spot with R$_f$ = 0.28 (C/EA 3:1 (v:v)). ^{1}H-NMR (300 MHz, CDCl$_3$, 25 °C): δ 5.98–5.79 (m, 2H, CH^2), 5.29 (dd, 4H, $^3J_{HH}$ = 17.2, $^2J_{HH}$ = 1.5, C$H_2^{3(E)}$), 5.21 (dd, 4H, $^3J_{HH}$ = 10.4, $^2J_{HH}$ = 1.3, C$H_2^{3(Z)}$), 4.03 (dt, 4H, $^4J_{HH}$ = 1.3, $^3J_{HH}$ = 5.7, CH_2^1), 3.88 (t, 4H, $^3J_{HH}$ = 5.6, C$H_2^{s1,s4}$), 3.35 (t, 4H, $^3J_{HH}$ = 5.7, C$H_2^{s2,s3}$) ppm. ^{13}C {^{1}H} NMR (75 MHz, CDCl$_3$, 25 °C): δ 134.0 (2C, C^2), 117.8 (2C, C^3), 72.3 (2C, C^1), 63.8 (2C, C^{s1,s4}), 55.1 (2C, C^{s2,s3}) ppm.

| 12 | (((sulfonylbis(ethane-2,1-diyl))bis(oxy)) bis(prop-2-ene-1,1-diyl))dibenzene C$_{22}$H$_{26}$O$_4$S [386.50] | |
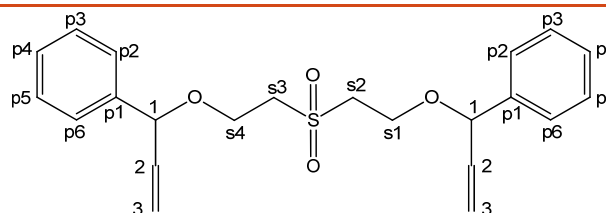
To a solution of α-phenyl allyl alcohol (294.1 mg, 2.192 mmol, 2.2 eq) and PPh$_3$ (26.13 mg, 0.0996 mmol, 0.1 eq) in DCM (200 µL) DVS (117.7 mg, 0.996 mmol, 1.0 eq) was added and stirred at 23 °C. After 168 h, 55.6 % (214.1 mg, 0.554 mmol) diadduct were detected by ^{1}H NMR, which was isolated by flash chromatography (silica gel, C/EA 20:1 (v:v)). Sampling the spot with R$_f$ = 0.44 yielded 172.7 mg (0.447 mmol, 44.9 %) colorless oil. ^{1}H-NMR (300 MHz, CDCl$_3$, 25 °C): δ 7.43–7.26 (m, 10H, CH^{p2-p6}), 5.99–5.83 (m, 2H, CH^2), 5.36–5.18 (m, 4H, CH_2^3), 4.78 (d, 2H, $^3J_{HH}$ = 6.67, CH^1), 3.98–3.73 (m, 4H, C$H_2^{s1,s4}$), 3.50–3.27 (m, 4H, C$H_2^{s2,s3}$) ppm. ^{13}C {^{1}H} NMR (75 MHz, CDCl$_3$, 25 °C): δ 140.19 (2C, C^{p1}), 138.19 (2C, C^2), 128.74, 126.96 (8C, C^{p2,p3,p5,p6}), 128.12 (2C, C^{p4}), 117.09 (2C, C^3), 83.80 (2C, C^1), 62.45 (2C, C^{s1,s4}), 55.20 (2C, C^{s2,s3}) ppm.

| 13 | 3-(2-((2-(prop-2-yn-1-yloxy)ethyl)sulfonyl)ethoxy)prop-1-yne C$_{10}$H$_{14}$O$_4$S [230.28] | |
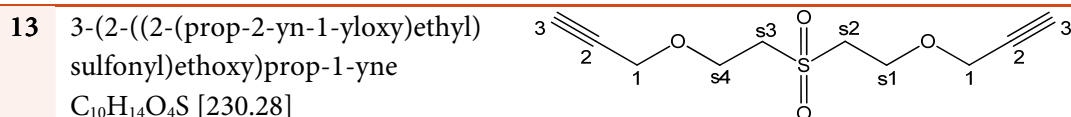
Propargyl alcohol (3.45 mL, 59.8 mmol, 3.0 eq) and DVS (2.00 mL, 19.9 mmol, 1 eq) were dissolved in dry DCM (40 mL) under inert conditions. PPh$_3$ (522.6 mg, 1.99 mmol, 0.1 eq) was added and the reaction solution was stirred at 23 °C until complete conversion of DVS was detected via ^{1}H NMR. The solution was concentrated under reduced pressure and the remaining yellowish oil was purified via column chromatography (CH/EE, 10:1 and 3:1, (v:v)) by sampling the spot with R$_f$ = 0.41 (CH/EE, 1:1, (v:v)). Yield: 4.095 g (17.8 mmol, 89.3 %) colorless oil. ^{1}H-NMR (300 MHz, CDCl$_3$, 25 °C): δ 4.19 (d, 4H, $^2J_{HH}$ = 1.91, CH_2^1), 3.97 (t, 4H, $^3J_{HH}$ = 5.56, C$H^{s4,s1}$), 3.34 (t, 4H, $^3J_{HH}$ = 5.56, C$H^{s2,s3}$), 2.48 (t, 2H, $^4J_{HH}$ = 2.19, CH^3) ppm. ^{13}C {^{1}H} NMR (75 MHz, CDCl$_3$, 25 °C): δ 78.7 (2C, C^2), 75.6 (2C, C^3), 63.4 (2C, C^{s1,s4}), 58.5 (2C, C^1), 54.9 (2C, C^{s2,s3}) ppm.

| 14 | 1-(2-((2-(but-2-yn-1-yloxy)ethyl)sulfonyl)ethoxy)but-2-yne C$_{12}$H$_{18}$O$_4$S [258.33] | |
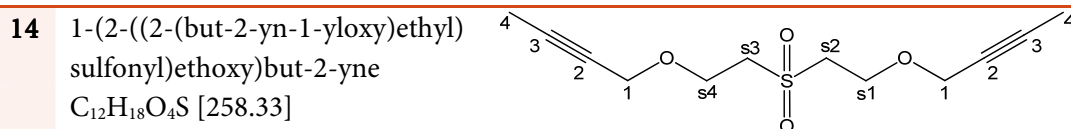
To a solution of 2-butyn-1-ol (768.1 mg, 10.96 mmol, 2.2 eq) and PPh$_3$ (130.6 mg, 0.498 mmol, 0.1 eq) in dry DCM (1.5 mL), DVS (588.5 mg, 4.981 mmol, 1.0 eq) was added (exothermic!) and stirred for 22 h (complete conversion of DVS detected by ^{1}H NMR) under inert atmosphere of N$_2$. Flash chromatography (CH/EA 20:1 (v:v), gradient to pure EA) of the reaction mixture yielded 689.3 mg (2.668 mmol, 53.8 %) white solid by sampling the spot with R$_f$ = 0.23 (C/EA 3:1 (v:v)). ^{1}H-NMR (300 MHz, CDCl$_3$, 25 °C): δ 4.15 (q, 4H, $^5J_{HH}$ = 2.18, CH_2^1), 3.95 (t, 4H, $^3J_{HH}$ = 5.80, C$H_2^{s1,s4}$), 3.35 (t, 4H, $^3J_{HH}$ = 5.58, C$H_2^{s2,s3}$), 1.86 (t, 6H, $^5J_{HH}$ = 2.13, CH_3^4) ppm. ^{13}C {^{1}H} NMR (75 MHz, CDCl$_3$, 25 °C): δ 83.66 (2C, C^2), 74.31 (2C, C^3), 63.12 (2C, C^{s1,s4}), 59.14 (2C, C^1), 54.95 (2C, C^{s2,s3}), 3.73 (2C, C^4) ppm.

| 15 | 4-methyl-3-(2-((2-((4-methylpent-1-yn-3-yl)oxy)ethyl)sulfonyl)ethoxy)pent-1-yne C$_{16}$H$_{26}$O$_4$S [314.44] | |
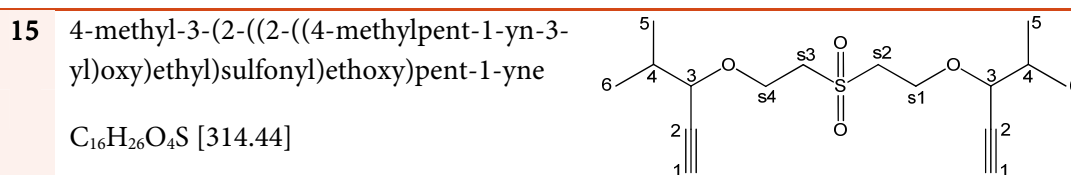
DVS (1.177 g, 9.962 mmol, 1.0 eq) was added (exothermic!) to a solution of 4-methyl-1-pentyn-3-ol (2.1509 g, 21.92 mmol, 2.2 eq) and PPh$_3$ (261.28 mg, 0.996 mmol, 0.1 eq) in dry DCM (2 mL). The mixture was stirred 24 h (complete conversion of DVS detected by ^{1}H NMR) at 23°C. Flash chromatography (silica gel, CH/EA 20:1 (v:v)) yielded 1.331 g (4.233 mmol, 42.5 %) pure product by sampling the spot with R$_f$ = 0.42 (CH/EA 3:1 (v:v)). ^{1}H-NMR (300 MHz, CDCl$_3$, 25 °C): δ 4.26–4.11 (m, 2H, CH^3), 3.95–3.74 (m, 4H, C$H_2^{s1,s4}$), 3.46–3.24 (m, 4H, C$H_2^{s2,s3}$), 2.45 (d, 2H, $^4J_{HH}$ = 1.98 Hz, CH^1), 1.95 (oct, 2H, $^3J_{HH}$ = 6.38, CH^4), 0.99 (t, 12H, $^3J_{HH}$ = 6.08, C$H_3^{5,6}$) ppm. ^{13}C {^{1}H} NMR (75 MHz, CDCl$_3$, 25 °C): δ 80.73 (2C, C^2), 75.82 and 75.79 (4C, C$^{3(R,S)}$), 75.38 (2C, C^1), 62.78 (2C, C^{s1,s4}), 54.97 and 54.94 (4C, C$^{s2,s3(R,S)}$), 33.00 (2C, C^4), 18.41 and 17.81 (4C, C^{5,6}) ppm.

| 16 | 3-methyl-3-(2-((2-((2-methylbut-3-yn-2-yl)oxy)ethyl)sulfonyl) ethoxy)but-1-yne C$_{14}$H$_{22}$O$_4$S [286.39] | |
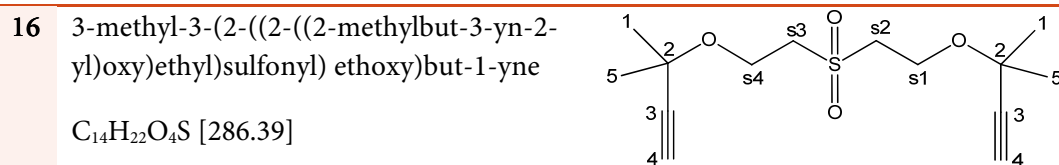
DVS (1.177 g, 9.96 mmol, 1.0 eq) was added (exothermic!) to a solution of 2-methyl-3-butyn-2-ol (2.124 mL, 21.92 mmol, 2.2 eq) and PPh$_3$ (261.3 mg; 0.996 mmol. 0.1 eq) in dry DCM (1 mL). The mixture was stirred 48 h at 23°C (>95% conversion of DVS detected via ^{1}H NMR). Column chromatography (silica gel, CH/EA 20:1 (v:v)) yielded 1.0986 g (3.836 mmol, 38.5 %) yellow liquid by sampling the spot with R$_f$ = 0.79 (TLC, C/EA 1:1 (v:v)). ^{1}H-NMR (300 MHz, CDCl$_3$, 25 °C): δ 4.00 (t, 4H, $^3J_{HH}$ = 5.84, C$H_2^{s1,s4}$), 3.33 (t, 4H, $^3J_{HH}$ = 5.84, C$H_2^{s2,s3}$), 2.47 (s, 2H, CH^4), 1.48 (2, 12H, C$H^{1,5}$) ppm. ^{13}C {^{1}H} NMR (75 MHz, CDCl$_3$, 25 °C): δ 85.19 (2C, C^3), 73.05 (2C, C^4), 70.84 (2C, C^2), 58.12 (2C, C^{s1,s4}), 55.42 (2C, C^{s2,s3}), 28.67 (4C, C^{1,5}) ppm.

| 17 | (((sulfonylbis(ethane-2,1-diyl)) bis(oxy))bis(prop-2-yne-1,1-diyl))dibenzene C$_{22}$H$_{22}$O$_4$S [382.47] | |
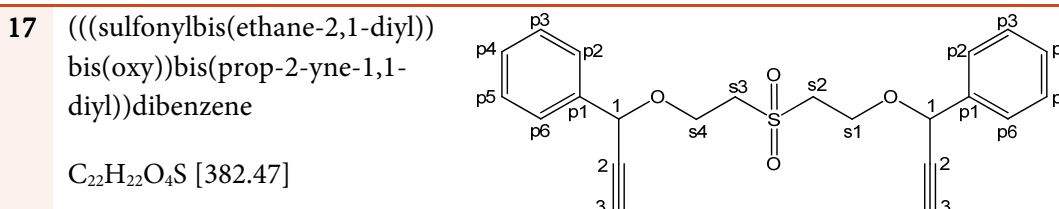
To a solution of 1-phenyl propargyl alcohol (1.817 mL, 14.94 mmol, 3 eq) and PPh$_3$ (130.6 mg, 0.498 mmol, 0.1 eq) in dry DCM (5 mL) DVS (588.5 mg, 4.981 mmol, 1.0 eq) was added and stirred at 23 °C. After complete conversion of DVS (1 h), flash chromatography (silica gel, CH/EA 20:1) yielded 1.727 g (4.516 mmol, 90.7 %) yellowish oil by sampling the spot with R$_f$ = 0.67 (CH/EA 1:1 (v:v)). ^{1}H-NMR (300 MHz, CDCl$_3$, 25 °C): δ 7.55–7.43 and 7.42–7.29 (m, 10H, CH^{p2-p6}), 5.21 (s, 2H, CH^1), 4.17–4.02 and 4.01–3.88 (m, 4H, C$H_2^{s1,s4}$), 3.47–3.25 (m, 4H, C$H_2^{s2,s3}$), 2.70–2.64 (m, 2H, CH^3) ppm. ^{13}C {^{1}H} NMR (75 MHz, CDCl$_3$, 25 °C): δ 137.31 (2C, C^{p1}), 128.94 (2C, C^{p4}), 128.76, 127.50 (8C, C$^{p2,6 \text{ and } p5,3}$), 80.61 and 80.59 (4C, C$^{2(R,S)}$), 76.79 (2C, C^3), 71.90 and 71.87 (4C, C$^{1(R,S)}$), 61.97 (2C, C^{s1,s4}), 54.95 and 54.92 (4C, C$^{s2,s3(R,S)}$) ppm.

NMR measurements after a few days storage under atmospheric conditions of the product indicated the decomposition of the compound.

| 18 | (((sulfonylbis(ethane-2,1-diyl))bis(oxy)) bis(prop-2-yne-1,1,1-triyl))tetrabenzene C$_{34}$H$_{30}$O$_4$S [534.66] | |
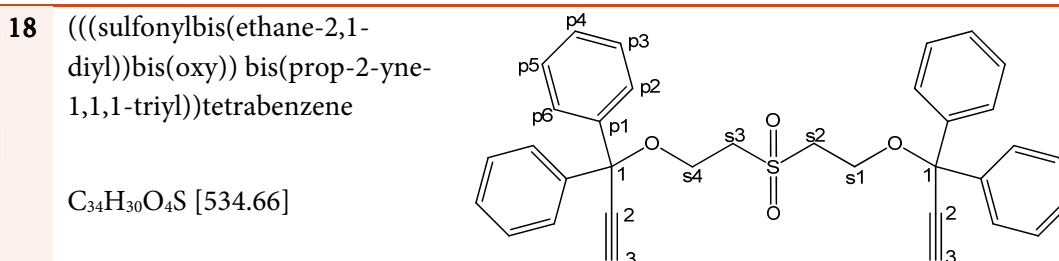
To a solution of DVS (100 μL, 0.996 mmol, 1.0 eq) and 1,1-diphenyl propargyl alcohol (778.0 mg, 2.989 mmol, 3.0 eq) in dry DCM (2 mL) PPh$_3$ (26.13 mg, 0.0996 mmol, 0.1 eq) was added and stirred at 40 °C. After 168 h 52.1 % monoadduct and 47.9 % (0.477 mmol, 255.1 mg)

diadduct were observed by ^{1}H NMR. The product was purified by flash chromatography (aluminium oxide, pH9–9.5, CH/EA 20:1 (v:v), with 10 ppm BHT in the eluent) and isolated by sampling the spot with R_f = (CH/EA 3:1 (v:v)). Yield: 82.5 mg (0.154 mmol, 15.5 %) white crystals. ^{1}H-NMR (300 MHz, CDCl$_3$, 25 °C): δ 7.60–7.48 and 7.36–7.26 (m, 20H, CH^{p2-p6}), 3.98 (t, 4H, $^3J_{HH}$ = 5.50, C$H_2^{s1,s4}$), 3.50 (t, 4H, $^3J_{HH}$ = 5.50, C$H_2^{s2,s3}$), 2.93 (s, 2H, CH^3) ppm. ^{13}C {^{1}H} NMR (75 MHz, CDCl$_3$, 25 °C): δ 142.29 (4C, C^{p1}), 128.52, 126.80 (16C, C^{p2,p3,p5,p6}), 128.20 (4C, C^{p4}), 82.56, 81.10 (4C, C^{1,2}), 78.74 (2C, C^3), 59.11 (2C, C^{s1,s4}), 55.13 (2C, C^{s2,s3}) ppm.

| 19 | ((sulfonylbis(ethane-2,1-diyl))bis(oxy))dibenzene
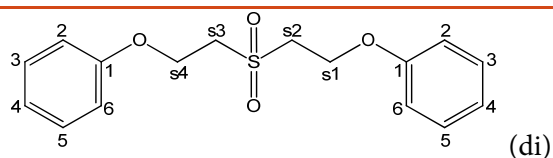
C$_{16}$H$_{18}$O$_4$S [306.38] | (di) |
| | (2-(vinylsulfonyl)ethoxy)benzene

C$_{10}$H$_{12}$O$_3$S [212.27] | (mono) |
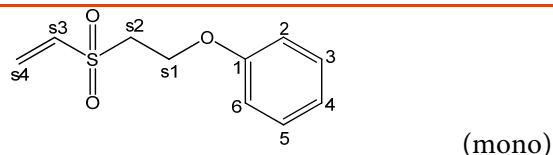
DVS (1.177 g, 9.962 mmol, 1.0 eq) and phenol (2.3438 g, 24.91 mmol, 2.5 eq) were dissolved in dry DCM (2 mL) and PPh$_3$ (261.3 mg, 0.996 mmol, 0.1 eq) was added. After 7d stirring at 23 °C a composition of 21.1 % DVS, 42.1 % monoadduct (0.419 mmol, 89.0 mg) and 36.8 % diadduct (0.367 mmol, 112.3 mg) was detected by ^{1}H NMR. The reaction mixture was purified by column chromatography (CH/EA 20:1 → 10:1 (v:v)), whereas 186.3 mg white solid were observed (mixture of mono- and diadduct ($R_{f(\text{mono})}$ = 0.29 and $R_{f(\text{di})}$ = 0.34 (C/EA 3:1 (v:v)). Diadduct: ^{1}H-NMR (300 MHz, CDCl$_3$, 25 °C): δ 7.30 (t, 4H, $^3J_{HH}$ = 8.07, C$H^{3,5}$), 7.01 (t, 2H, $^3J_{HH}$ = 7.36, CH^4), 6.89 (d, 4H, $^3J_{HH}$ = 8.07, C$H^{2,6}$), 4.48 (t, 4H, $^3J_{HH}$ = 5.65, C$H_2^{s1,s4}$), 3.61 (t, 4H, $^3J_{HH}$ = 5.65, C$H_2^{s2,s3}$) ppm. ^{13}C {^{1}H} NMR (75 MHz, CDCl$_3$, 25 °C): δ 157.76 (2C, C^1), 129.85 (4C, C^{3,5}), 122.01 (2C, C^4), 114.75 (4C, C^{2,6}), 61.89 (2C, C^{s1,s4}), 54.75 (2C, C^{s2,s3}) ppm. Monoadduct: ^{1}H-NMR (300 MHz, CDCl$_3$, 25 °C): δ 7.31 (t, 2H, $^3J_{HH}$ = 7.41, C$H^{3,5}$), 7.01 (t, 1H, $^3J_{HH}$ = 7.36, CH^4), 6.89 (d, 2H, $^3J_{HH}$ = 8.07, C$H^{2,6}$), 6.77 (dd, 1H, $^3J_{HH(Z)}$ = 10.0, $^3J_{HH(E)}$ = 16.8, CH^3), 6.45 (d, 1H, $^3J_{HH}$ = 16.8, C$H_2^{s4(Z)}$), 6.15 (d, 1H, $^3J_{HH}$ = 9.7, C$H_2^{s4(E)}$), 4.41 (t, 2H, $^3J_{HH}$ = 5.65, CH_2^{s1}), 3.47 (t, 2H, $^3J_{HH}$ = 5.65, CH_2^{s2}) ppm. ^{13}C {^{1}H} NMR (75 MHz, CDCl$_3$, 25 °C): δ 157.71 (1C, C^1), 137.52 (C^{s3}), 129.85 (2C, C^{3,5}), 129.71 (1C, C^{s4}), 122.01 (2C, C^4), 114.67 (2C, C^{2,6}) 61.82 (1C, C^{s1}), 54.64 (1C, C^{s2}) ppm.

I	3-(2-((2-(prop-2-yn-1-yloxy)ethyl)sulfonyl)ethoxy)prop-1-yne-$d_{1,2}$	
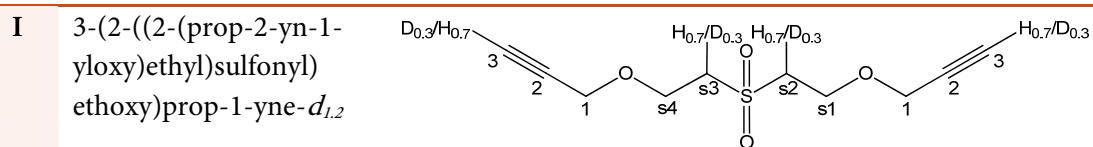
To a solution of DVS (50 µL, 0.498 mmol, 1.0 eq) and propargyl alcohol (86.2 µL, 1.494 mmol, 3.0 eq) in CDCl$_3$ (3.49 mL), PPh$_3$ (13.1 mh, 0.0498 mmol, 0.1 eq) was added and the mixture was stirred at 23 °C. After 24 h more than 99 % diadduct were formed and the product was isolated via column chromatography (silica gel, CH/EA 20:1 → 10:1 (v:v)). Sampling the spot with R$_f$ = 0.53 (CH/EA 1:1 (v:v)) yielded 67.0 mg (0.286 mmol, 57.4 %) colorless oil. H/D exchange was observed at positions s2 and s3 in approximately one third of the formed product and can be clearly evidenced by ^{13}C NMR spectroscopy via ^{13}C-^{2}D couplings. ^{1}H-NMR (300 MHz, CDCl$_3$, 25 °C): δ 4.22–4.15 (m, 4H, CH_2^1), 4.01–3.96 (m, 4H, C$H_2^{s1,s4}$), 3.39–3.27 (m, 2.67H, C$H_2^{s2,s3}$), 2.48 (t, 1.33H, $^4J_{HH}$ =2.31, CH^3) ppm. ^{13}C {^{1}H} NMR (75 MHz, CDCl$_3$, 25 °C): δ 78.7 (2C, C^2), 78.3 (t, 2C, $^2J_{CD}$ = 7.46, C^2), 75.5 (1.4C, C^3), 75.3 (t, 0.6C, $^1J_{CD}$ = 38.41, C^3), 63.4, 63.33 (2C, C^{s1,s4}), 58.5 (2C, C^1), 54.8 (1.4C, CH^{s2,s3}), 54.6 (t, 0.6C, $^1J_{CD}$ = 21.14, CD^{s2,s3}) ppm.

II	1,1-sulfonylbis[2-methoxy-ethane]-d_9	
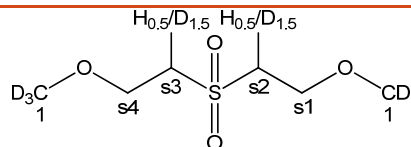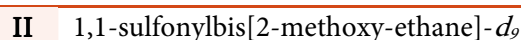
PPh$_3$ (2.61 mg, 0.00996 mmol 0.1 eq) was added to a solution of DVS (10 µL, 0.0996 mmol, 1.0 eq) in methanol-d_4 (600 µL, 18.73 mmol, 188 eq) in a NMR tube. The reaction was performed at 25°C and monitored via ^{1}H NMR kinetic measurements. The formed product was not isolated, but characterized via NMR spectroscopy. ^{1}H-NMR (300 MHz, CDCl$_3$, 25 °C): δ 3.83–3.77 (4H, C$H_2^{s4,s1}$), 3.35–3.23 (1H, C$H_2^{s2,s3}$) ppm. ^{13}C {^{1}H} NMR (75 MHz, CDCl$_3$, 25 °C): δ 66.06, 65.99 (2C, C^{s1,s4}), 58.26 (septet, 2C, $^1J_{CD}$ = 21.52, C^1), 54.73 (t, 2C, $^1J_{CD}$ = 21.04, C^{s2,s3}) ppm.
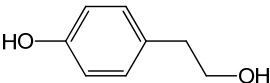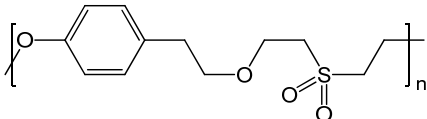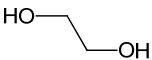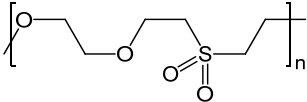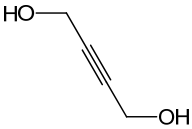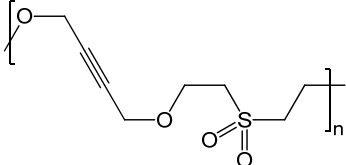
5.3 MICHAEL ADDITION POLYMERIZATION

Inspired by the recently established thiol-ene networks,[195,222] the Michael addition polymerization of divinyl sulfone and various alcohols was investigated. The use of di- and trifunctional alcohols as Michael donors in equimolar formulations with divinyl sulfone (one hydroxyl with respect to one double bond) allowed for the preparation of polymers. Linear macromolecules were accessible applying diols (Table 44), whereas triols resulted in crosslinked polymeric networks (Table 45). The Michael addition polymerization proceeded also in the presence of water, demonstrating the high reactivity of the system.
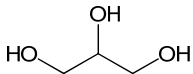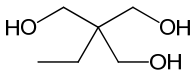
The formulations were prepared as follows: The alcohol was mixed with triphenylphosphine (0.1 eq from a stock solution in dichloromethane, 1 g·mL^{-1}), optionally diluted with H_2O deion. and stirred at least 10 minutes. DVS was added, the solution was shortly stirred vigorously and immediately placed on vitreous object carriers or in a teflon mold. For gelation, the mixtures were either placed at room temperature or in an oven at 80 °C.

An equimolar formulation of 4-(2-hydroxyethyl)phenol and divinyl sulfone in water was reacted at 23 °C upon adding triphenylphosphine (cp. substance Ia, section 5.3.1). A polymer featuring an average molar mass (M_n) of 780 g·mol^{-1} and a polydispersity index (PDI) of 1.6 was obtained. The use of ethane-1,2-diol or but-2-yne-1,4-diol (cp. substances II and III, section 5.3.1) gave polymers characterized by a M_n of 790 g·mol^{-1} (PDI 1.5) or 3200 g·mol^{-1} (PDI 1.9). In the case of but-2-yne-1,4-diol, a solution polymerization in THF / DCM 1:1 ([DVS] = 0.5 mol·L^{-1}) yielded a polymer with a M_n of 6400 g·mol^{-1} and a PDI of 1.7 in 70 % isolated yield after complete conversion of the monomers.

Table 44. Difunctional alcohols and according repeating units obtained via polyaddition reactions of equimolar formulations with DVS using PPh₃ (0.1 eq).

Alcohols	Repeating unit	Characteristics
4-(2-hydroxyethyl)phenol		M_n = 780 g·mol^{-1} PDI = 1.6
ethane-1,2-diol		M_n = 790 g·mol^{-1} PDI = 1.5
but-2-yne-1,4-diol		M_n = 3200 g·mol^{-1} PDI = 1.9 *under diluted conditions:* M_n = 6400 g·mol^{-1} PDI = 1.7

Table 45. Trifunctional alcohols used for polyaddition reactions with DVS (1 eq with respect to hydroxyl groups) promoted via DMAP (0.05 eq).

Alcohols	Characteristics
OH HO OH propane-1,2,3-triol	crosslinked polymer stiff, brittle
HO OH OH 2-ethyl-2-(hydroxymethyl)propane-1,3-diol	crosslinked polymer solid, T_g = 28 °C

Crosslinked and hence insoluble polymer networks were obtained using the multifunctional alcohols propane-1,2,3-triol or 2-ethyl-2(hydroxymethyl)propane-1,3-diol and divinyl sulfone. Curing of the formulations containing water (5 eq), both at room temperature and 80 °C, yielded solid glassy polymer films(cp. polymers IVa and Va, section 5.3.1). However, the curing at room temperature is notedly prolonged at RT (> 8 h) compared to 80 °C (~ 2 h). A polymerization under solvent-free conditions gave fast and exothermic reactions, additionally complicating the mixing of the three components as PPh₃ is poorly soluble in the neat alcohols. Ideally, the nucleophile should be dissolved in the alcohol and then DVS should be admixed.[221] Therefore, these reactions are preferably mediated with the alcohol-soluble dimethylaminopyridine (DMAP) in a reduced loading (0.05 eq). Mixing the alcohol / DMAP solution with DVS led to a slightly retarded polymerization with a pot life of approx. 30 s. The formulation was immediately transferred into Teflon molds (22 × 5 × 3 mm) and cured at 80 °C for 4 h. The obtained rectangular specimens were investigated by dynamic mechanical analysis (DMA) in a temperature range of −4 to 32 °C. The use of propane-1,2,3-triol gave stiff and brittle specimens which broke shortly after the measurement was started. The polymerization of 2-ethyl-2-(hydroxymethyl)-propane-1,3-diol and DVS resulted in specimens with a storage modulus of 3300 MPa (10 °C) and a T_g of 28 °C (maximum of the loss modulus curve) (Figure 53).
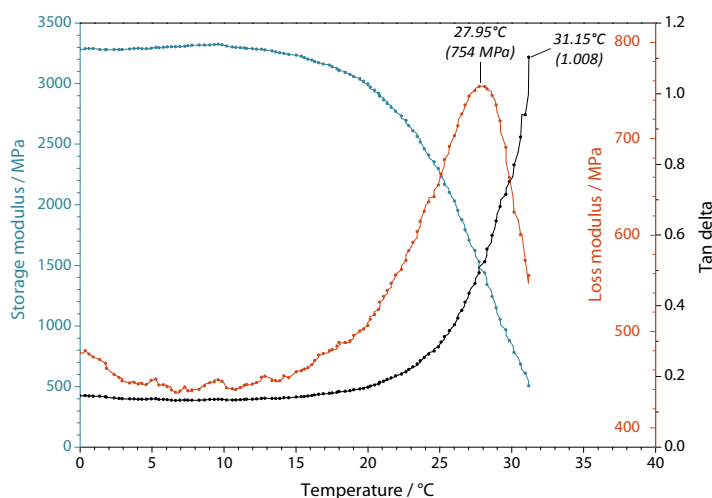
Figure 54. Dynamic mechanical analysis (DMA) of the DVS / 2-ethyl-2-(hydroxymethyl)propane-1,3-diol polymer.

LIGNIN + DVS

Successful Michael addition polymerizations were also performed utilizing lignin as alcoholic substrate. Especially the successful reaction of divinylfulfone and 4-(2-hydroxyethyl)phenol (cp. substance I, section 5.3.1) was of importance with regard to lignin. It could be shown that the phenolic hydroxyl group is involved in the Michael addition polymerization reaction (cp. ^{1}H NMR spectrum, Figure 56). Thus, it can accordingly be concluded that aliphatic as well as phenolic hydroxyl groups of lignin will serve as Michael donor for divinyl sulfone.

Annikki lignin was dissolved in divinyl sulfone (excess of 10 equivalents with regard to the hydroxyl groups) and stirred at room temperature (cp. substance VIa, section 5.3.1). Upon addition of PPh$_3$, the formulation solidified and foamed under heat generation. A piece of the friable solid (86.4 mg) was extracted with DCM, whereas 19 wt% (16.5 mg) extractives were observed. ^{1}H NMR spectroscopy revealed mainly triphenylphosphine species, traces of divinyl sulfone and undefined resonances, most likely originating from lignin moieties. Further extraction of the undissolved residue with DMSO showed no more soluble substances. Thus, it can be assumed that lignin is covalently bound into the polymeric network.

Using lignin as alcoholic Michael donor, also films could be obtained using base catalysis as well as nucleophilic initiation with triphenylphosphine (cp. substances VIb and c, section 5.3.1). Formulations with aqueous NaOH (1 mol·L^{-1}) cured only at higher temperatures (80 °C, 8 h). Using PPh$_3$, films were also observed at room temperature (8 h), but after notedly prolonged curing times compared to 80 °C, where 2 h are sufficient (Figure 55).

The films obtained from the base-catalyzed formulation were brittle and peeled up from the object carrier (Figure 55, left). This undesirable behavior is most likely due to the formation of sodium salts during the polymerization which are not removed. However, the organocatalyzed formulation exhibited better film forming properties.

These preliminary results showed that, depending on the composition of the monomer solution, films or even highly crosslinked materials are accessible by the organocatalyzed oxa-Michael addition polymerization of lignin and divinylsulfone.

lignin / DVS / NaOH
(80 °C)

lignin / DVS / PPh₃
(23 °C)   (80 °C)
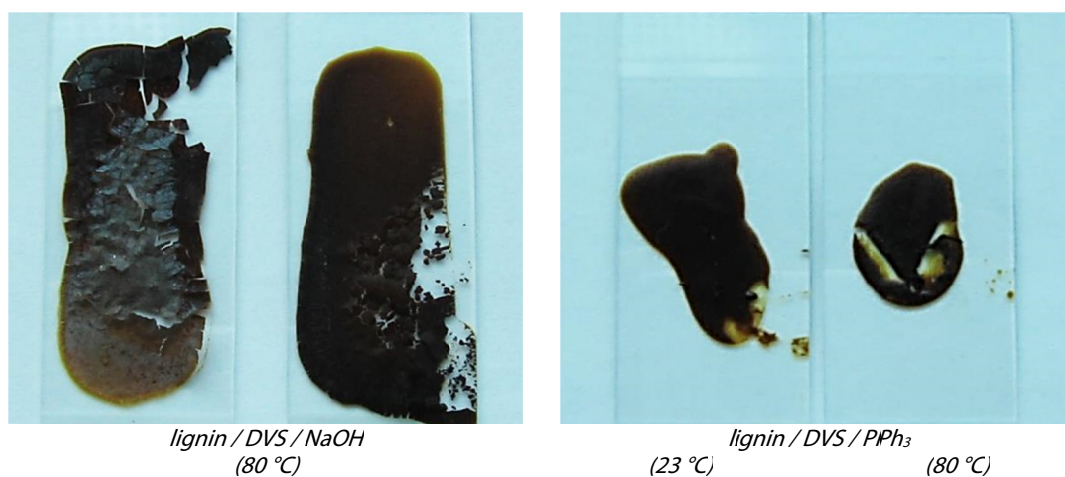
Figure 55. Lignin-DVS polymer films obtained using NaOH (left) or PPh$_3$ (right) as initiator.

5.3.1 Experimental details

(I) 4-(2-Hydroxyethyl)phenol + DVS

a) 4-(2-Hydroxyethyl)phenol (275.28 mg, 1.992 mmol, 1.0 eq) and H_2O (119.5 μL, 9.962 mmol, 5.0 eq) were mixed and heated until the alcohol melted. PPh_3 (52.26 mg, 0.199 mmol, 0.1 eq, dissolved in 52.3 μL DCM) was added and the mixture was stirred shortly. The Michael addition polymerization was started upon addition of DVS (200.0 μL, 1.992 mmol, 1.0 eq). The mixture was stirred vigorously for a few seconds and was then dropped onto a vitreous object carrier and cured 24 h at 23 °C and 4 h at 80 °C. SEC ($CHCl_3$ relative to PS): M_n = 630 g·mol^{-1}, M_w = 1130 g·mol^{-1}, PDI = 1.8 (cured at 23 °C) and M_n = 780 g·mol^{-1}, M_w = 1270 g·mol^{-1}, PDI = 1.6 (cured at 80 °C).

b) The Michael addition polymerization of 4-(2-hydroxyethyl)phenol (275.74 mg, 1.992 mmol, 1.0 eq) and DVS (200.0 μL, 1.992 mmol, 1.0 eq) in solution (DCM / THF 1:1 (v:v), 0.5 mL) at 23 °C promoted by PPh_3 (52.26 mg, 0.199 mmol, 0.1 eq) yielded 363.9 mg (71.3 %) yellowish soft solid after precipitation in cold MeOH. SEC ($CHCl_3$ relative to PS): M_n = 760 g·mol^{-1}, M_w = 1400 g·mol^{-1}, PDI = 1.8.

NMR spectra of the obtained polymers appear equally: ^{1}H-NMR (300 MHz, $CDCl_3$, 25 °C): δ 7.82–7.27 (m, P-containing species), 7.20–6.64 (m, CH^a) 6.64–5.86 (m, $CH^{\text{vinyl end group}}$), 4.50–4.00 (m, CH_2^g), 3.99–3.72 ($CH_2^{d,c}$), 3.71–3.45 (m, CH_2^f), 3.38–3.00 (m, CH_2^e), 2.99–2.51 (m, CH_2^b) ppm. ^{13}C {^{1}H} NMR (75 MHz, $CDCl_3$, 25 °C): δ 156.5, 156.4 (2C, $C^{a(\text{quarternary})}$), 132.1, 132.0 (P-containing species), 130.2 (2C, C^a), 115.4 (2C, C^a), 114.7 (2C, C^a), 72.4 (1C, C^c), 70.4 (2C, $C^{b,c}$), 64.6, 61.9 (2C, $C^{d,g}$), 63.8 (1C), 55.1, 54.7 (2C, $C^{e,f}$), 54.9 (1C), 38.4, 35.2 (2C, C^b) ppm.
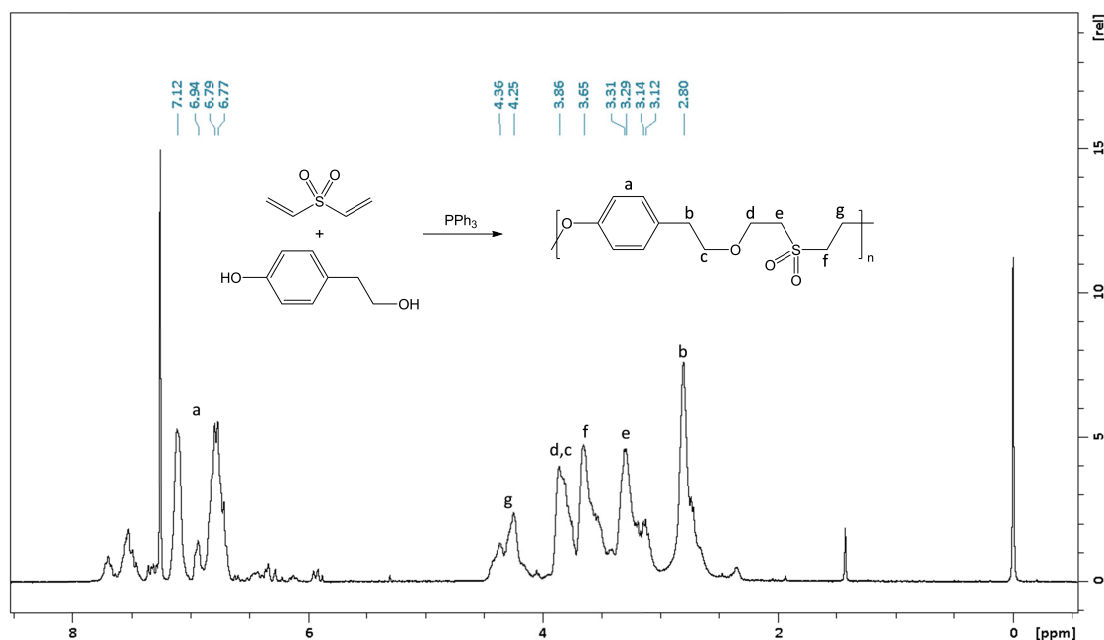
Figure 56. ^{1}H NMR spectrum of the Michael addition polymerization product of 4-(2-hydroxyethyl)phenol and DVS (25 °C, 300 MHz, $CDCl_3$).
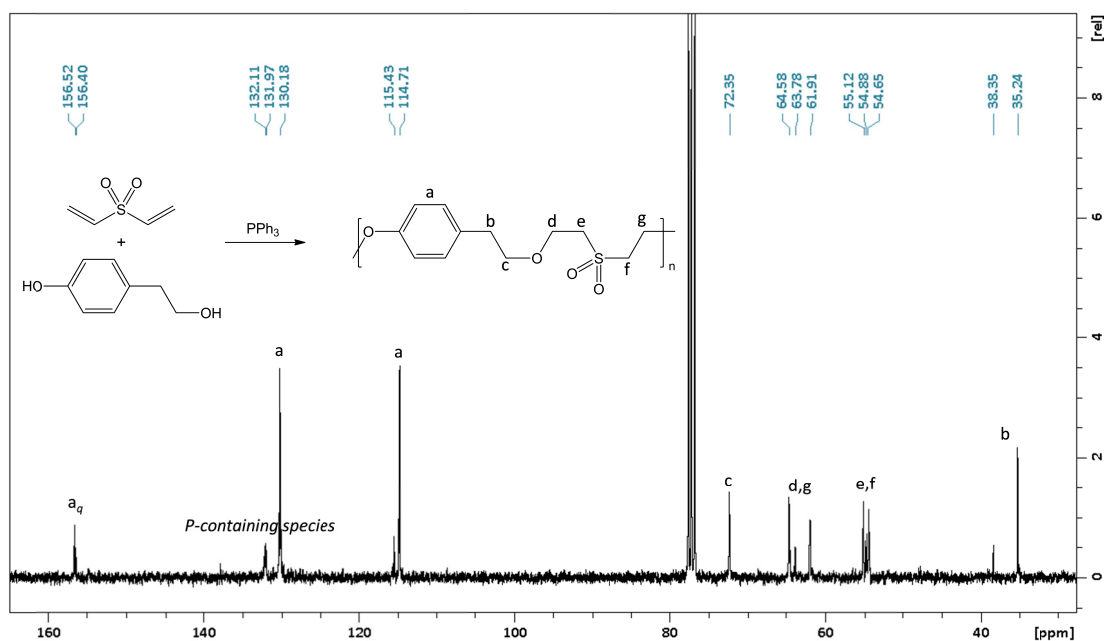
Figure 57. ^{13}C {^1H} NMR spectrum of Michael addition polymerization product of 4-(2-hydroxyethyl)phenol and DVS (25 °C, 75 MHz, CDCl$_3$).

(II) ETHANE-1,2-DIOL + DVS

Ethane-1,2-diol (123.67 mg, 1.992 mmol, 1.0 eq), H$_2$O (119.5 µL, 9.962 mmol, 5.0 eq) and PPh$_3$ (52.26 mg, 0.199 mmol, 0.1 eq, dissolved in 52.3 µL DCM) were mixed and stirred shortly. The Michael addition polymerisation was started upon addition of DVS (200.0 µL, 1.992 mmol, 1.0 eq). The mixture was dropped onto a vitreous object carrier and cured 8 h at 23°C and 4 h at 80°C. SEC (CHCl$_3$ relative to PS): M$_n$ = 830 g·mol^{-1}, M$_w$ = 1170 g·mol^{-1}, PDI = 1.4 (cured at 23°C) and M$_n$ = 790 g·mol^{-1}, M$_w$ = 1140 g·mol^{-1}, PDI = 1.5 (cured at 80 °C). ^1H-NMR (300 MHz, CDCl$_3$, 25 °C): δ 8.00–7.27 (m, 1.7H, P-containing species), 3.91 (m, 4.1H, C$H_2^{d,g}$), 3.78–3.52 (m, 5.5H, C$H_2^{b,c}$), 3.46–3.28 (m, 4H, C$H_2^{e,f}$) ppm. ^{13}C {^1H} NMR (75 MHz, CDCl$_3$, 25 °C): δ 134.0, 132.3, 132.2, 128.7, 128.6 (P-containing species), 72.7 (1C), 70.4 (2C, C^{b,c}), 64.7 (2C, C^{d,g}), 61.4 (1C), 55.0 (2C, C^{e,f}) ppm.

156
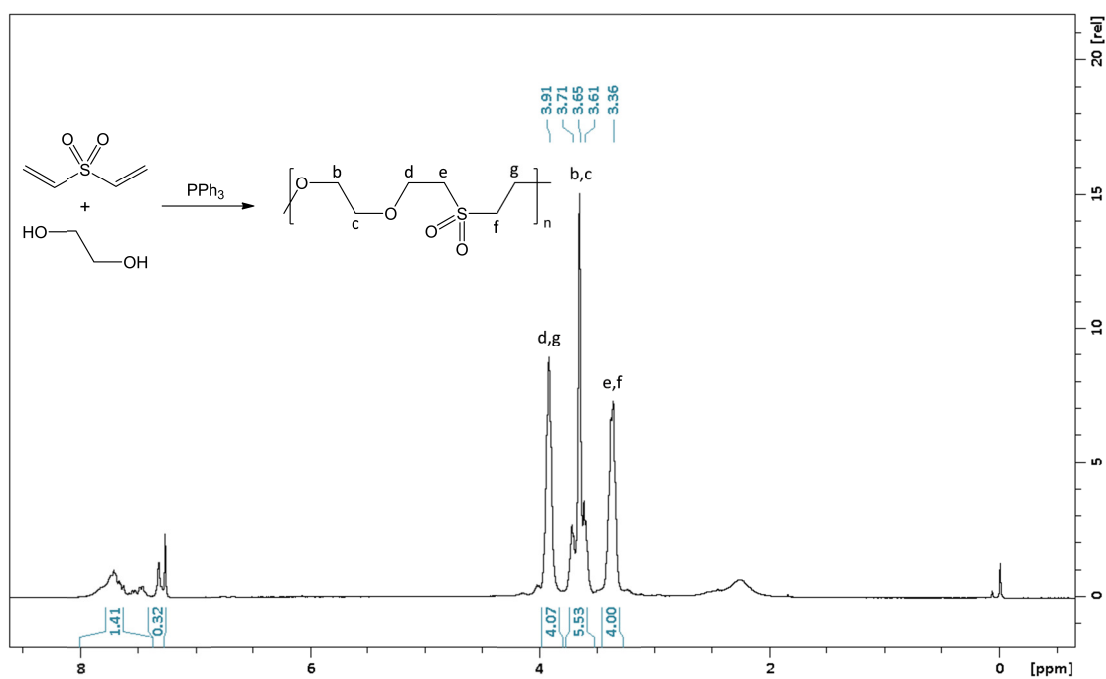
Figure 58. ¹H NMR spectrum of the Michael addition polymerization product of ethane-1,2-diol and DVS (25 °C, 300 MHz, CDCl₃).
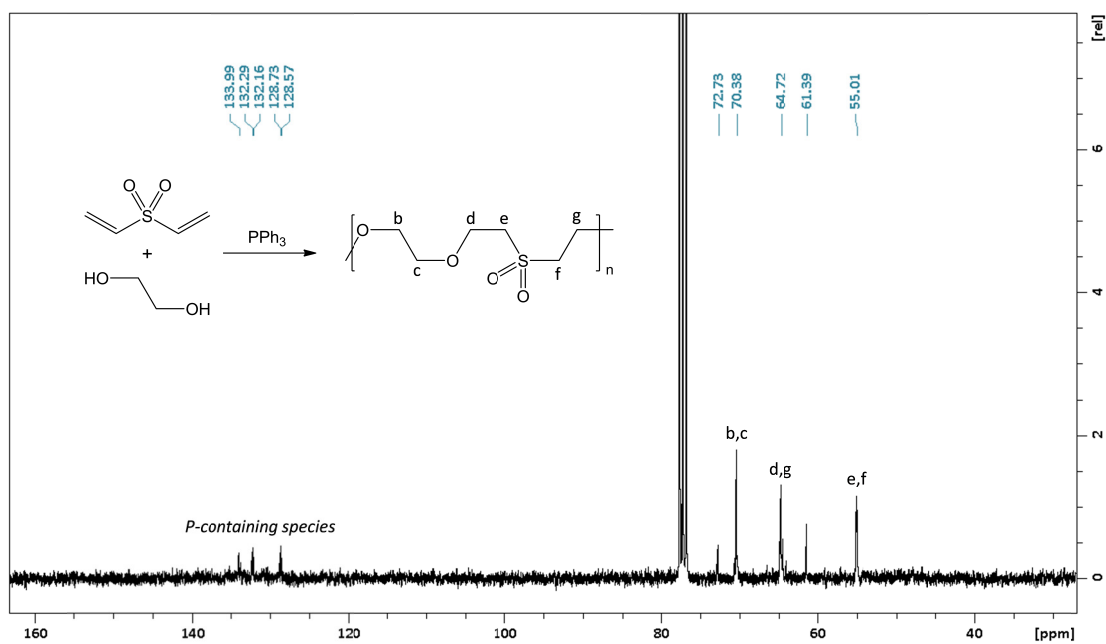
Figure 59. ¹³C {¹H} NMR spectrum of Michael addition polymerization product of ethane-1,2-diol and DVS (25 °C, 75 MHz, CDCl₃).

(III) B<small>UT</small>-2-<small>YNE</small>-1,4-<small>DIOL</small> + DVS

a) But-2-yne-1,4-diol (174.1 mg, 2.022 mmol, 1.015 eq) were dissolved in H_2O (119.5 µL, 9.962 mmmol, 5.0 eq) and PPh_3 (52.26 mg, 0.199 mmol, 0.1 eq, dissolved in 52.3 µL DCM) was added. DVS (200.0 µL, 1.992 mmol, 1.0 eq) was added and the mixture was transferred onto glass object carriers to cure 8 h at 23 °C (M_n = 3190, M_w = 6020, PDI = 1.9) and at 80 °C (M_n = 2420, M_w = 4480, PDI = 1.9).

b) To a solution of but-2-yne-1,4-diol (85.29 mg, 0.991 mmol) and DVS (100.20 µL, 0.998 mmol) in THF/CH_2Cl_2 = 1:1 (2 mL) PPh_3 (26.24 mg, 0.100 mmol) was added and the reaction mixture was stirred at 23 °C for 16 h. The reaction mixture turned yellow and a yellow precipitate formed, which was collected on a glass frit and washed with THF (2 times, 0.5 mL each) and dried in vacuum. Yield: 142.26 mg (70 %). SEC ($CHCl_3$ relative to PS): M_n = 6400 g·mol^{-1}, M_w = 11090 g·mol^{-1}, PDI = 1.7. A T_g of 6.0 °C was detected via DSC measurements.

After combining the reaction solution from the filtration described above with the corresponding washing-solutions, volatiles were removed in vacuum yielding 87 mg of an oily residue consisting of species with lower molecular mass and phosphorous containing species. ^{1}H NMR (300 MHz, $CDCl_3$, 25 °C): δ 7.95–7.27 (bm, 3.9H, aromatic protons), 6.73 (dd, $^3J_{HH}$ = 16.9, $^3J_{HH}$ = 10.7, 0.12H, SO_2-C*H*=CH_2), 6.42 (d, $^3J_{HH}$ = 16.9, 0.12H, SO_2-CH=C*H*$_{cis}$H$_{trans}$), 6.13 (d, $^3J_{HH}$ = 10.7, 0.12H, SO_2-CH=CH$_{cis}$*H*$_{trans}$), 4.29 (s, 0.37H, C≡C-C*H*$_2$-OH), 4.25 (s, 4H, C≡C-C*H*$_2$-O-), 3.97 (t, 4H, SO_2-CH_2-C*H*$_2$-O-), 3.36 (t, 3.75H, SO_2-C*H*$_2$-CH_2-O-), 3.29 (t, 0.25H, H_2C=CH-SO_2-C*H*$_2$-CH_2-O-) ppm.

NMR spectra of the obtained polymers appear equally: ^{1}H NMR (300 MHz, $CDCl_3$, 25 °C): δ 6.73 (dd, $^3J_{HH}$ = 16.9, $^3J_{HH}$ = 10.7, 0.01H, SO_2-C*H*=CH_2), 6.41 (d, $^3J_{HH}$ = 16.9, 0.01H, SO_2-CH=C*H*$_{cis}$H$_{trans}$), 6.12 (d, $^3J_{HH}$ = 10.7, 0.01H, SO_2-CH=CH$_{cis}$*H*$_{trans}$), 4.29 (s, 0.1H, C≡C-C*H*$_2$-OH), 4.25 (s, 4H, C*H*$_2$^{b,c}), 3.97 (t, 4H, C*H*$_2$^{d,g}), 3.36 (t, 4H, C*H*$_2$^{e,f}) ppm. ^{13}C {^{1}H} NMR (75 MHz, $CDCl_3$, 25 °C): δ 133.7, 128.6 (P-containing species), 82.5 (2C, C*), 63.5 (2C, C^{d,g}), 58.8 (2C, C^{b,c}), 54.9 (2C, C^{e,f}).
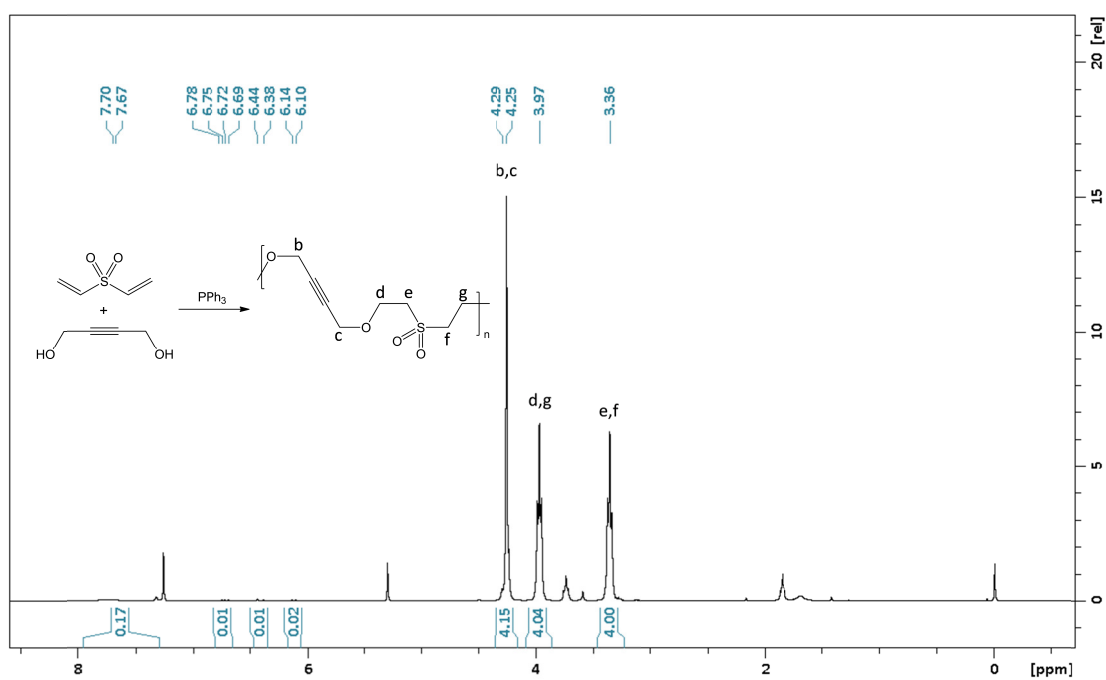
Figure 60. ^{1}H NMR spectrum of the Michael addition polymerization product of but-2-yne-1,4-diol and DVS (25 °C, 300 MHz, CDCl$_3$).
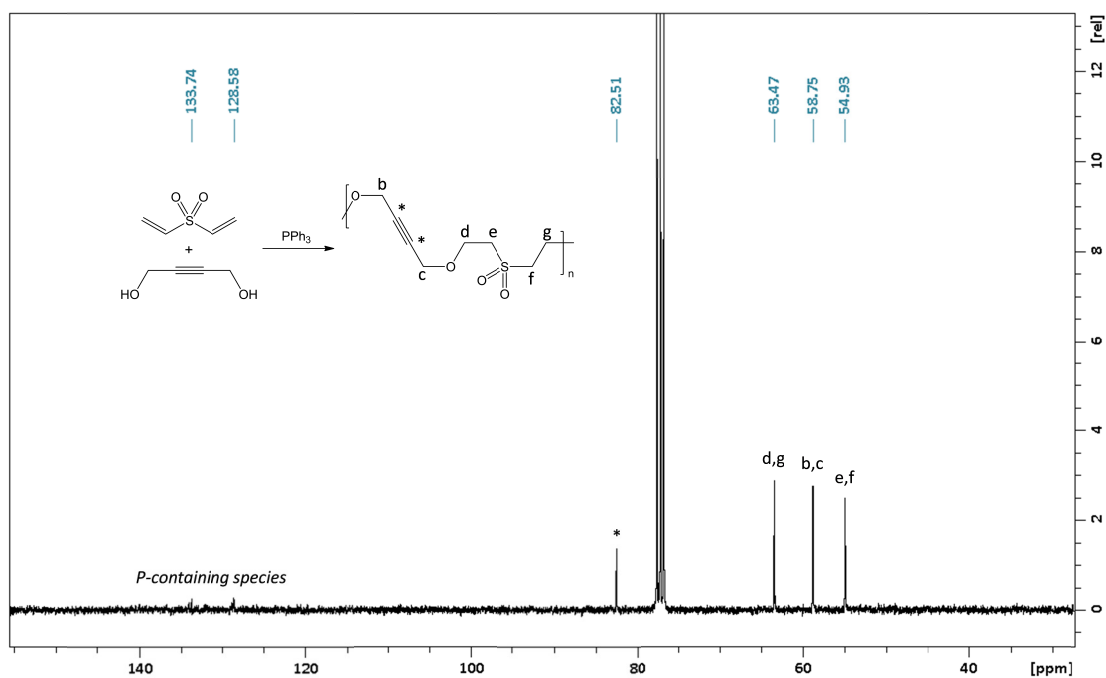
Figure 61. ^{13}C {^{1}H} NMR spectrum of Michael addition polymerization product of but-2-yne-1,4-diol and DVS (25 °C, 75 MHz, CDCl$_3$).

(IV) Propane-1,2,3-triol +DVS

a) Propane-1,2,3-triol (122.32 mg, 1.33 mmol, 2 eq) and PPh$_3$ (52.3 μL from a 1 mg·μL^{-1} DCM stock solution, 0.10 mmol, 0.1 eq) were dissolved in H$_2$O (119.5 μL, 3.32 mmol, 5 eq) and DVS (200 μL, 1.99 mmol, 3 eq) was added. The formulation was immediately placed on vitreous object carriers and placed at room temperature or in an oven at 80 °C to cure.

b) DMAP (40.55 mg, 0.498 mmol, 0.05 eq) was dissolved in propane-1,2,3-triol (611.60 mg, 6.641 mmol, 2.0 eq). DVS (1.0 mL, 9.962 mmol, 3.0 eq) was added and the mixture was placed in rectangular teflon molds (5 x 2 x 22 mm) to cure 4 h at 80 °C. DMA measurements of the sample failed due to sample rupture shortly after the start at −30 °C. A T_g of 64.8 °C was determined by DSC measurements.

(V) 2-Ethyl-2-(hydroxymethyl)propane-1,3-diol + DVS

a) 2-Ethyl-2-(hydroxymethyl)propane-1,3-diol (178.2 mg, 1.33 mmol, 2 eq) and PPh$_3$ (52.3 μL from a 1 mg·μL^{-1} DCM stock solution, 0.10 mmol, 0.1 eq) were dissolved in H$_2$O (119.5 μL, 3.32 mmol, 5 eq) and DVS (200 μL, 1.99 mmol, 3 eq) was added. The formulation was immediately placed on vitreous object carriers and placed at room temperature or in an oven at 80 °C to cure.

b) DMAP (40.55 mg, 0.498 mmol, 0.05 eq) was dissolved in 2-ethyl-2-(hydroxymethyl)-propane-1,3-diol (891.13 mg, 6.641 mmol, 2.0 eq). DVS (1.0 mL, 9.962 mmol, 3.0 eq) was added and the mixture was placed in rectangular teflon molds (5 x 3 x 22 mm) to cure 4 h at 80 °C. A T_g of 28 °C was determined by DMA measurements and evaluation of the loss modulus maximum (Figure 54). The T_g of 29.7 °C determined by DSC measurements is in good accordance with the DMA results.

(VI) Lignin + DVS

a) *Annikki* lignin (L_THF) (727.6 mg, 2.92 mmol OH, 1 eq) was dissolved in divinyl sulfone (3.0 mL, 3.531 g, 29.89 mmol, 10.24 eq) and stirred at 23 °C. Triphenylphosphine (392.1 mg, 1.50 mmol, 0.05 eq) was added and stirred. After a few minutes, the formulation solidified and foamed under heat generation. A piece of the friable solid (86.4 mg) was extracted with DCM (10 mL) at room temperature (20 h). 19 wt% (16.5 mg) extractives were observed and ^{1}H NMR spectroscopy revealed mainly triphenylphosphine species, traces of divinyl sulfone and undefined resonances, most likely originating from lignin moieties. The undissolved residue was further extracted with DMSO, where no soluble substances could be detected via ^{1}H NMR.

b) L_THF (209.8 mg, 0.841 mmol OH, 1 eq) was dissolved in aqueous sodium hydroxide (1 mL, 1 mol·L^{-1}) and DVS was added (84.45 μL, 99.4 mg, 1.68 mmol, 2 eq). The mixture was placed on an vitreous object carrier and cured at 23 °C (24 h). As no reaction progress was detected after 24 h (revealed via ATR-FTIR measurements), the samples were placed in an oven at 80 °C (8 h). Solid, but brittle films were obtained.

c) L_THF (200.1 mg, 0.80 mmol, 1 eq) was dissolved in divinyl sulfone (200 μL, 1.99 mmol, 4.97 eq). After complete dissolution of lignin, H$_2$O deion. (119.5 μL, 5 eq with respect to DVS) and PPh$_3$ (52.3 μL from a 1 g·mL^{-1} stock solution in DCM, 0.1 eq) were added. The formulation was placed on vitreous object carriers and cured at RT and 80 °C.

6 SUMMARY & CONCLUDING REMARKS

The wheat straw lignin provided by Annikki GmbH was thoroughly characterized using various analysis techniques. The amount of total hydroxyl groups was determined by quantitative ^{31}P NMR spectroscopy after phsophitylation. *Annikki* lignin features 3.9–4.8 mmol hydroxyl groups per gram, which is in the average range for non-wood lignins. The ratio of aliphatic and phenolic hydroxyl groups is approximately 3 to 1. Semiquantitative ^{13}C-^{1}H HSQC NMR spectroscopy revealed syringyl and guaiacyl units to be the main building blocks of *Annikki* lignin. The monomeric units are primarily connected via β-O-4' linkages. The number average molecular weight was determined via HPLC-SEC in DMF (relative to polystyrene standards) and is given with ~ 1250 g·mol^{-1} and a polydispersity of ~ 4, which are rather low values compared to most commercially available lignins. Especially when the molar mass distribution is investigated, the high propensity of lignin to form strong intermolecular aggregates comes into account. Lignin moieties are most likely tightly packed due to hydrogen bonding as well as π-stacking of aromatic units. The thermal properties were analyzed via STA as well as independent DSC measurements. Annikki wheat straw lignin is characterized by a T_g of 114 °C and ~ 60 % mass loss at 550 °C, which is in good accordance with reported values for wheat straw lignins.

Annikki lignin was esterified with carboxylic acid chlorides in DMF at 65 °C using Et$_3$N as base. Primarily long chain fatty acid chlorides (C$_{16}$ and C$_{18}$) were used, whereas a degree of substitution between 50 and 60 % was reached in most cases. The obtained ligninesters are well soluble (45–95 wt%) in non-polar dicyclopentadiene. Drawback of this modification method are the remaining free fatty acids (FFAs) in the final product in considerable amounts (8–43 wt%), which can only be removed via flash chromatography. FFAs in the product interfere further applications and thus the long chain ligninesters are considered as rather unattractive for large-scale or industrial applications.

A second approach towards organosoluble lignin derivatives was tested, namely the esterification / grafting reaction of lignin via ring opening polymerization (ROP) of β-butyrolactone (BBL), D,L-lactide (LA) and ε-caprolactone (CL). The organocatalyzed synthesis proceeds at elevated temperatures (100–150 °C) in bulk without any solvent. Using BBL only lignin / PHB blends were obtained instead of covalently grafted lignins. The characteristics of lignin-PCL grafts were far below the expectations, which may be reduced to catalyst deactivation under the applied reaction conditions. However, the grafting with LA gave satisfactory results with slightly higher degrees of substitution compared to the long chain ligninesters. The formation of homopolymers as side products, which can hardly be removed, has also to be considered using this protocol. Moreover, structural changes of lignin under the applied reaction conditions cannot be excluded. ^{31}P NMR as well as ^{13}C-^{1}H HSQC NMR measurements indicate the cleavage of β-O-4' bonds, involving H$_2$O elimination as well as condensation reactions. Nevertheless, this method provides a *green* and sustainable route towards renewable, organosoluble lignin derivatives.

Unmodified *Annikki* lignin as well as the obtained long chain ligninesters were applied as filler or reactive component in polydicyclopentadiene (PDCPD), a crosslinked thermoset synthesized via ring opening metathesis polymerization (ROMP) of dicyclopentadiene (DCPD). Shouldered test bars were produced by curing formulations of lignin and DCPD using a commercially available 2nd generation ROMP initiator. The mechanical properties were investigated via tensile strength tests. It was found that unmodified lignin, applied as insoluble filler for PDCPD, slightly enhances the elastic modulus at the expense of maximal loading capacity and strain. The soluble ligninester (palmitoyl lignin) acts as plasticizing agent and the mechanical properties were worse than PDCPD filled with the same amounts of unmodified lignin. A soluble and reactive filler is provided by the use of oleoyl lignin. However, the introduction of oleoyl lignin led to a drastic loss of the original material properties due to cross metathesis side reactions. In order to prevent the weakening of mechanical characteristics by the introduction of a lignin derivative, it was tried to functionalize lignin with a *ROMPable* moiety, namely a norbornene group (cp. section 5.1). Unfortunately, these approaches were not successful.

Palmitoyl lignin was suitable for the preparation of bicomponent thin films with trimethylsilyl cellulose (TMSC) in varying ratios. The blend films were fabricated by spin coating and regenerated to palmitoyl lignin / cellulose films upon exposure to HCl vapors. The ligninester was proven to be unaffected by the regeneration step. The wettability of the surfaces was determined via static water contact angle (SCA) measurements before (95–98°) and after (38–43°) regeneration. Contrary to our expectations, the SCA is only slightly altered by the introduction of palmitoyl lignin. Profilometric determination of the film thickness before (48–45 nm) and after (41–48 nm) regeneration revealed, that films containing more palmitoyl lignin shrink less upon converting TMSC into cellulose. The formation of bicontinuous phases as well as honeycomb-like cellulose structures were observed by AFM spectroscopy. The bicomponent surfaces were found to be resistant to unspecific protein adsorption as obtained from quartz crystal microbalance measurements with dissipation (QCM-D) with bovine serum albumin (BSA).

Finally, the oxa-Michael addition was extensively investigated as model reaction for lignin modification. The organocatalyzed addition reaction of electron-deficient olefins and hydroxyl groups provides a promising route towards the functionalization of lignin by the introduction of non-hydrolyzable ether bonds. Various primary, secondary and tertiary alcohols were screened with divinyl sulfone in order to learn more about the optimum reaction conditions for this conversion. Propargyl alcohol was found to exhibit an outstanding reactivity. By the use of multifunctional Michael donors and acceptors, such as lignin, polymeric materials are accessible. Preliminary experiments demonstrated that the oxa-Michael addition reaction, or polymerization respectively, is well suited to be applied to lignin chemistry. Coatings as well as a crosslinked polymeric network were obtained by reacting lignin with divinyl sulfone in the presence of triphenylphosphine.

7.1 ABBREVIATIONS

ATR-FTIR	attenuated total reflectance fourier transform infrared spectroscopy
BBL	β-butyrolactone
CH	cyclohexane
DCM	dichloromethane
DCPD	dicyclopentadiene
DMA	dynamic mechanical analysis
DSC	differential scanning calorimetry
DVS	divinyl sulfone
EA	ethyl acetate
FFA	free fatty acid
GL	*Annikki Gesamtlignin*
GPC	gel permeation chromatography
HPLC-SEC	high performance liquid chromatography-size exclusion chromatography
HSQC	heteronuclear single quantum coherence
M_n	number average molecular weight
M_w	weight average molecular weight
NML	low molecular weight *Annikki* lignin
NMR	nuclear magnetic resonance
PCL	poly(ε-caprolactone)
PDCPD	polydicyclopentadiene
PDI	polydispersity index
PHB	polyhydroxybutyrate
PLA	poly(lactic acid)
PS	polystyrene
*p*TSA	*p*-toluenesulfonic acid
ROMP	ring opening metathesis polymerization
ROP	ring opening polymerization
RT	room temperature
SEC	size exclusion chromatography
SEM	scanning electrom microscopy
STA	simultaneous thermal analysis
TA	tartaric acid
TBD	1,5,7-triazabicyclo[4.4.0]dec-5-ene
THF	tetrahydrofuran
TLC	thin layer chromatography
TMSC	trimethylsilyl cellulose

7.2 MATERIALS & INSTRUMENTS

All chemicals and substances for the syntheses in this contribution were purchased from commercial sources (Sigma Aldrich, Fluka, Alfa Aesar, Fisher Scientific, Umicore) or project partners and used without further purification if not stated otherwise (Table 46). Reactions were carried out either under atmospheric conditions or applying Schlenk technique under inert atmosphere of N_2 gas. Unless specified otherwise, solvents and auxiliary materials were used as purchased.

^{1}H NMR measurements were performed on a Bruker Avanze 300 MHz spectrometer (^{1}H 300.36 MHz, ^{13}C 75.53 MHz) at 25 °C. Chemical shifts are given in ppm relative to a tetramethylsilan (TMS) standard. Deuterated solvents were obtained from Cambridge Isotope laboratories Inc. and spectra were referenced against the residual proton signals according to literature.[236]

^{31}P NMR measurements were performed on a Varian Unity INOVA 500 MHz (^{1}H 499.894 MHz, ^{31}P 202.32 MHz) FT NMR instrument with a ^{1}H-^{19}F / ^{15}N-^{31}P 5 mm Switchable Probe, using at least 256 scans with a delay time of 25 s to accumulate spectra. 2-Chloro-4,4,5,5-tetramethyl-1,3,2-dioxaphospholane (TMDP) was used as phosphitylation reagent for lignin samples. The obtained ^{31}P chemical shifts are given relative to phosphoric acid and spectra are referenced to phosphitylated cyclohexanol as internal standard (145.2 ppm).

Two-dimensional ^{13}C-^{1}H heteronuclear single quantum coherence (HSQC) spectra were acquired at 35 °C on a Varian Unity INOVA 500 MHz (^{1}H 499.894 MHz, ^{13}C 125.687 MHz) FT NMR instrument with a ^{1}H {^{15}N-^{31}P} 5 mm PFG Indirect Detection Probe using a standard adiabatic gradient Varian pulse sequence implementation (gHSQCAD). The phase-sensitive HSQC spectra were conducted with an acquisition time of 150 ms with an $F2$ spectral width of 7998 Hz (16 ppm) in 2400 data points using 128 transients for each of 512 $t1$ increments of the $F1$ spectral width of 26393 Hz (210 ppm). Dummy scans (32) were used to establish equilibrium conditions at the start of the experiment. A coupling constant ($^1J_{CH}$) of 146 Hz was used and ^{13}C-decoupling during acquisition was performed by WALTZ40 composite pulse from the high-power output-decoupling channel. The 2D correlation peaks were integrated and compared using MestReNova NMR processing software.

Infrared spectra were recorded on a Bruker ALPHA-P FT-IR spectrometer equipped with ALPHA's Platinum single reflection diamond attenuated total reflection (ATR) module. The spectral range is from 7500–375 cm^{-1} with a resolution < 2 cm^{-1}. Fourier transformation (FT), processing and evaluation were done using an OPUS 6.5 software package.

Elemental analyses (CHNS) (double determination) were performed on an Vario EL III Element Analyzer from Elementar GmbH.

Simultaneous thermal analysis (STA) was performed with a Netzsch Simultaneous Thermal Analyzer STA 449C (crucibles: aluminum from Netzsch). A helium flow of 50 mL·min^{-1} was used in combination with a protective flow of 8 mL·min^{-1}.

Two set-ups are available at ICTM for gel permeation chromatographic (GPC) measurements, one system from WGE Dr. Bures operated with tetrahydrofuran, and one system from Shimadzu operated with chloroform. The SEC-3010 ENTRY-AS instrument from WGE Dr. Bures is equipped with a SEC-3010 SEC pump, featuring a "1 ½" piston principle of operation with active pulsation dampening, two MZ-Gel Sdplus Linear 5 µm separation columns from MZ Analysentechnik in line and a refractive-index as well as a UV detector (SEC-3010). The flow rate is adjustable from 0.001–5.00 mL·min^{-1} with a pressure limit up to 40 MPa. The LC-20 AD system from Shimadzu is equipped with the same separation columns and a refractive index (RD-20A) as well as a UV/VIS detector (SPD-20A). Polystyrene standards purchased from Polymer Standard Service were used for calibration and data was evaluated applying LabSolutions GPC software.

HPLC-SEC measurements in DMF were performed at Annikki GmbH (Graz) on an Agilent 1200 Infinity with three TOSOH TSK-GEL Alpha Series columns (TSKgel Alpha-2500; TSKgel Alpha-3000 and TSKgel Alpha-4000) in a row. Approximately 5 mg of sample material was dissolved in 1 mL of DMF + LiBr (1 g·L^{-1}). 20 µL of this solution were injected for analysis and eluted with a solution of lithium bromide in DMF (1 g·L^{-1} LiBr) at a column temperature of 50 °C (eluation time 90 min). Lignin was detected by UV absorption (280 nm) and measured against polystyrene standards (277000, 130000, 66000, 34800, 17600, 9130, 3250, 1250 and 682 g·mol^{-1}) purchased from PSS GmbH, Mainz. Integration was performed until the volume corresponding to the mass of 300 g·mol^{-1}.

Differential scanning calorimetry (DSC) analyses were measured on a DSC 8500 instrument from Perkin Elmer with nitrogen as purge gas. T_g values were retrieved from the second heating run. Lignin samples were investigated in a temperature range from −20 to 180 °C with a heating rate of 20 °C / min for the first run and with 30 °C / min in the second run. Michael addition step-growth polymers were measured in a temperature range from −20 to 100 °C with a heating rate of 20 °C / min for the first run and with 40 °C / min in the second run.

Tensile strength tests were performed on a Shimadzu Autograph AGS-X machine, with a force measuring range from 0.01–10 kN. The clamping length of the samples was 53 mm. An initial tension of 10.0 N was applied an tests were run at a constant speed rate of 1 mm/min. The hardness of the specimens was determined using a digital PCE-DD-D Shore D durometer (0-100 Shore D, resolution 0.5) from PCE Instruments UK Limited.

Dynamic mechanical analyses (DMA) were measured on a DMA Q 800 from TA Instruments Waters GmbH in the 3-point bending mode with a frequency of 1 Hz and amplitude of 25 µm in a temperature range from −4 to 31.2 °C (3 °C / min).

For spin coating, a Polos MCD wafer spinner (APT corporation, Germany) was operated at 4000 rpm for 60 s (acceleration 2500 rpm·s^{-1}).

Profilometric determination of the film thickness was performed with a DEKTAK 150 Stylus Profiler from Veeco (Plainview, NY, USA), whereas the profile was set to 'hills and valleys'. A set scan length of 1000 μm (for 3 s) was applied using a diamond stylus with a radius of 12.5 μm at 3 mg force with a resolution of 0.333 μm / sample and a measurement range of 6.5 μm. Contact angle measurements were conducted using the system OCA15+ (Dataphysics, Germany), applying the sessile drop method (drop volume of 3 μL, RT). The static contact angles (SCAs) were determined by analyzing the drop shape using the software provided by the manufacturer (SCA 20).

Atomic force microscopy (AFM) images were acquired on an 5500 AFM multimode scanning probe microscope (Agilent, Santa Barbara, CA) in tapping mode at RT after drying the samples in a nitrogen gas stream. Silicon cantilevers (ATEC-NC-20, Nanosensors, Germany) were used to scan the surfaces with a resonance frequency of 210–490 kHz and a force constant of 12–110 N·m^{-1}. The obtained images were processed using a Gwyddion software package.

Table 46. Basic information about the substances used in this contribution (alphabetic order).

	Molecular formula	Molecular weight / g·mol^{-1}	Density g·mL^{-1}	Purchased from, Purity
acetic acid	$C_2H_4O_2$	60.05	1.05	ABCR, 99 %
acetic anhydride	$C_4H_6O_3$	102.09	1.08	Sigma-Aldrich, 98 %
acetyl chloride	C_2H_3ClO	78.49	1.10	Fluka, 99 %
acryloyl chloride	C_3H_3ClO	90.51	1.114	Alfa Aesar, 96 %
allyl alcohol	C_3H_6O	58.08	0.85	Aldrich, 99 %
benzyl alcohol	C_7H_8O	108.14	1.04	Aldrich, 99 %
bicyclo[2.2.1]hept-5-ene-2-carbonyl chloride	C_8H_9ClO	156.61	1.256	manufactured in-house
cis-endo-bicyclo[2.2.1]hept-5-ene-2,3-dicarboxylic anhydride	$C_9H_8O_3$	164.16	–	manufactured in-house
endo,exo-bicyclo[2.2.1]hept-5-ene-2-yl(ethyl)-chlorodimethylsilane	$C_{11}H_{19}ClSi$	214.81	0.991	Sigma-Aldrich, 95 %
endo,exo-bicyclo[2.2.1]hept-5-ene-2-methanol	$C_8H_{12}O$	124.18	1.027	Sigma-Aldrich, 98 %
n-butanol	$C_4H_{10}O$	74.12	0.81	Fluka, 99.4 %
tert-butanol	$C_4H_{10}O$	74.12	0.79	Aldrich, 99.5 %
but-2-yne-1,4-diol	$C_4H_6O_2$	86.09	1.04	Alfa Aesar, 98 %
but-2-yn-1-ol	C_4H_6O	70.09	0.937	ABCR, 98 %
butyric anhydride	$C_8H_{14}O_3$	158.20	0.97	Aldrich, 99 %
β-butyrolactone	$C_4H_6O_2$	86.09	1.056	Sigma-Aldrich, 98 %
ε-caprolactone	$C_6H_{10}O_2$	114.14	1.08	Fluka, 99 %
chloroform-d_3	$CDCl_3$	120.38	1.50	Euriso Top, 99.8 %
2-chloro-4,4,5,5-tetramethyl-1,3,2-dioxaphospholane	$C_6H_{12}ClO_2P$	182.59	1.149	Aldrich, 95 %
chromium(III)acetylacetonate	$C_{15}H_{27}O_6Cr$	349.32	–	Adrich, 97 %
cyclohexanol	$C_6H_{11}O$	100.16	0.948	Sigma-Aldrich 99 %
cyclopentadiene	C_5H_6	66.10	0.80	freshly cracked and distilled from DCPD in-house
1,4-diazabicyclo[2.2.2]octane	$C_6H_{12}N_2$	112.17	1.14	Fluka, 97 %
1,8-diazabicyclo[5.4.0]-undec-7-ene	$C_9H_{16}N_2$	152.24	1.018	Sigma-Aldrich, 98 %
dicyclopentadiene	$C_{10}H_{12}$	132.20	0.98	ABCR, 97 %
4-dimethylaminopyridine	$C_7H_{10}N_2$	122.17	–	Fluka, 98 %
3,6-dimethyl-1,4-dioxan-2,5-dion (D,L-lactide)	$C_6H_8O_4$	144.13	–	Aldrich, 98 %
2-methylbut-3-yn-2-ol	C_5H_8O	84.12	0.868	ABCR, 98 %
1,1-diphenyl-2-propyn-1-ol	$C_{15}H_{12}O$	208.26	–	Sigma-Aldrich 99 %
divinyl sulfone	$C_4H_6SO_2$	118.15	1.177	Sigma-Aldrich 97 %
dodecanol	$C_{12}H_{26}O$	186.34	0.8309	Fluka 97 %
ethane-1,2-diol	$C_2H_6O_2$	62.07	1.11	Aldrich, 99.8 %
ethanol	C_2H_6O	46.07	0.7893	Sigma-Aldrich, 99 %
ethyl acetate	$C_4H_8O_2$	88.11	0.897	VWR, rectapur
2-ethyl-2-(hydroxymethyl)propane-1,3-diol (1,1,1-trimethylolpropane)	$C_6H_{14}O_3$	134.18	1.08	Fluka, 98 %
4-(2-hydroxyethyl)phenol	$C_8H_{10}O_2$	138.17	–	Aldrich, 98 %
lithium aluminium hydride	$LiAlH_4$	37.95	0.92	Aldrich, 95 %

Table 46 continued.

	Molecular formula	Molecular weight / g·mol^{-1}	Density g·mL^{-1}	Purchased from, Purity
maleic anhydride	C$_4$H$_2$O$_3$	98.06	1.48	Fluka, 98 %
methanol	CH$_4$O	32.04	0.79	VWR, normapur
methanol-d_4	CD$_3$OD	36.07	0.888	Euriso Top, 99.8 %
methacryloyl chloride	C$_4$H$_5$ClO	104.53	1.07	Alfa Aesar, 97 %
α-methyl benzyl alcohol	C$_8$H$_{10}$O	122.16	1.012	Aldrich, 98 %
1-methylimidazole	C$_4$H$_6$N$_2$	82.10	1.03	Sigma-Aldrich, 99 %
methyl oleate	C$_{19}$H$_{36}$O$_2$	296.49	0.874	Fluka, ≥ 60 %
methyl ricinoleate	C$_{19}$H$_{36}$O$_3$	312.49	0.925	ABCR, 75 %
oleic acid	C$_{18}$H$_{34}$O$_2$	282.46	0.89	Sigma-Aldrich, 90 %
oleoyl chloride	C$_{18}$H$_{33}$ClO	300.91	0.91	Sigma-Aldrich, ≥89%
(Z)-9-octadecenoic acid methyl ester (methyl oleate)	C$_{19}$H$_{36}$O$_2$	296.49	0.874	Sigma-Aldrich, 98 %
palmitoyl chloride	C$_{16}$H$_{31}$ClO	274.87	0.906	Sigma-Aldrich, 98%
phenol	C$_6$H$_6$O	94.11	1.07	Fluka, 99 %
1-phenylprop-2-en-1-ol (α-vinylbenzyl alcohol)	C$_9$H$_{10}$O	134.175	1.021	Sigma-Aldrich, 97 %
1-phenyl-2-propyn-1-ol (1-phenyl propargyl alcohol)	C$_9$H$_8$O	132.16	1.087	Sigma-Aldrich, 98 %
2-propanol	C$_3$H$_8$O	60.10	0.78	VWR, 98 %
propane-1,2,3-triol	C$_3$H$_8$O$_3$	92.09	1.261	Aldrich, 99.5 %
2-Propyn-1-ol (propargyl alcohol)	C$_3$H$_4$O	56.06	0.963	Fluka, 99 %
pyridine	C$_5$H$_5$N	79.10	0.982	Sigma-Aldrich, 99.9 %
sulfuric acid	H$_2$SO$_4$	98.079	1.84	VWR, 95 %
tartaric acid (TA)	C$_4$H$_6$O$_6$	150.09	1.788	Aldrich, 99 %
p-toluenesulfonic acid	C$_7$H$_8$SO$_3$	172.20	1.24	Merck, 99 %
1,5,7-triazabicyclo[4.4.0]dec-5-ene	C$_7$H$_{13}$N$_3$	139.20	–	Sigma-Aldrich, 98 %
triethylamine	C$_6$H$_{15}$N	101.19	0.726	Sigma-Aldrich, 99 %
trimethylsilyl cellulose	–	DS$_{TMS}$ = 2.8	–	Thüringisches Institut für Textil- und Kunststoffforschung (TITK)
triphenylphosphine	C$_{18}$H$_{15}$P	262.29	–	Sigma-Aldrich 95 %
undec-10-enoic acid	C$_{11}$H$_{20}$O$_2$	184.28	0.912	Schuchardt München
10-undecenoyl chloride	C$_{11}$H$_{19}$ClO	202.72	0.944	Sigma-Aldrich 97%
Umicore M2 ([1,3-Bis(2,4,6-trimethyl phenyl)-2-imidazolidinylidene] dichloro-(3-phenyl-1H-inden-1-ylidene) (tricyclohexylphosphine) ruthenium(II))	C$_{54}$H$_{69}$N$_2$Cl$_2$PRu	949.10	–	provided by Umicore
4-methylpentyn-3-ol	C$_6$H$_{10}$O	98.143	0.895	ABCR, 97 %

7.3 ADDITIONAL DATA

7.3.1 ^{13}C-^{1}H HSQC NMR

Table 47. Integrals used for the semi-quantitative determination of lignin substructures from the ^{13}C-^{1}H HSQC NMR spectrum of GL2.

Label	δ_C / δ_H Correlation / ppm	Integral	Hs	Integral normalized to 1 H	
OMe	55.6 / 3.75	set to 300	3	100	
A_α(G+S)	70.8 / 4.76 and 71.3 / 4.88 and 72.0 / 4.87	19.21	2	9.61	A / B / C 7
B_α	86.7 / 5.48 and 87.4 / 5.57	1.98	1	1.98	1.5
C_α	84.8 / 4.67	1.36	1	1.36	1.0
A_β (H)	83.7 / 4.29 and 84.4 / 4.24	4.95			A / B / C
A_β (G)	85.8 / 4.12	4.85	1	12.05	
A_β (S)	86.7 / 4.02 and 87.0 / 3.95	2.25			11
B_β	52.5 / 3.54	2.28	1	2.28	2
C_β	53.5 / 3.07	1.09	1	1.09	1.0
A_γ	60.4 / 3.38 59.4 / 3.41 and 3.72 59.8 / 3.24 and 3.62	60.90	2	20.3	A / B / C 18
B_γ	62.5 / 3.70	4.65	2	2.325	2
C_γ	71.0 / 3.83 and 4.19	2.28	2	1.14	1.0
$X1_\gamma$	61.3 / 4.09	2.03	2	1.015	
T_8	93.9 / 6.56	1.43	1	1.43	
T_6	98.7 / 6.22	1.12	1	1.12	average = 1.38
$T_{2',6'}$	104.1 / 7.33	3.53	2	1.765	
T_3	104.5 / 7.05	1.20	1	1.20	
$S'_{2,6}$	106.3 / 7.33 and 106.2 / 7.23	1.60	2	0.80	
$S_{2,6}$	103.7 / 6.67	24.40	2	12.20	
FA_2	110.9 / 7.27	6.44	1	6.44	
FA_6	121.9 / 7.11	5.87	1	5.87	average = 5.57
FA_β	116.4 / 6.40	4.39	1	4.39	
$H_{2,6}$	127.6 / 7.21 and 128.9 / 7.24	3.97	2	1.985	
G_2	110.7 / 6.95	17.68	1	17.68	
$PCA_{2,6}$	129.7 / 7.51	6.47	2	3.235	average = 3.54
PCA_β	115.2 / 6.32	3.84	1	3.84	
fatty acids (all)	33.38 / 2.19	22.50	2	11.25	
unsaturated fatty acids	129.32 / 5.33	1.88	1	1.88	
S+G+H				31.865	
X1+PCA+FA				10.125	
S+S'				13	
G+FA				23.25	
H+PCA				5.525	sum = 44.17
X1				1.015	
T				1.38	

Table 48. Integrals used for the semi-quantitative determination of lignin substructures from the ^{13}C-^1H HSQC NMR spectrum of sample 47.

Label	δ_C / δ_H Correlation / ppm	Integral	Hs	Integral normalized to 1 H	
OMe	55.6 / 3.75	set to 300	3	100	
A_α(G+S)	70.8 / 4.76 and 71.3 / 4.88 and 72.0 / 4.87	14.57	1	14.57	A / B / C 10.5
B_α	86.7 / 5.48 and 87.4 / 5.57	1.34	1	1.34	1.0
C_α	84.8 / 4.67	1.39	1	1.39	1.0
A_β (H)	83.7 / 4.29 and 84.4 / 4.24	4.87			A / B / C
A_β (G)	85.8 / 4.12	4.67	1	11.80	
A_β (S)	86.7 / 4.02 and 87.0 / 3.95	2.26			9.4
C_β	53.5 / 3.07	1.25	1	1.25	1.4
B_β	52.5 / 3.54	1.77	1	1.77	1.0
A_γ	60.4 / 3.38 59.4 / 3.41 and 3.72 59.8 / 3.24 and 3.62	51.51	2	25.76	A / B / C 15
B_γ	62.5 / 3.70	5.52	2	2.48	1.5
C_γ	71.0 / 3.83 and 4.19	3.34	2	1.67	1.0
X1$_\gamma$ (or N)	61.3 / 4.09	4.97	2	2.48	
T_8	93.9 / 6.56	0.92	1	0.92	
T_6	98.7 / 6.22	0.83	1	0.83	average = 0.93
$T_{2',6'}$	104.1 / 7.33	2.43	2	1.21	
T_3	104.5 / 7.05	0.76	1	0.76	
$S'_{2,6}$	106.3 / 7.33 and 106.2 / 7.23	1.90	2	0.95	
$S_{2,6}$	103.7 / 6.67	29.85	2	14.93	
FA_2	110.9 / 7.27	–	1	–	
FA_6	121.9 / 7.11	–	1	–	
FA_β	116.4 / 6.40	–	1	–	
$H_{2,6}$	127.6 / 7.21 and 128.9 / 7.24	5.30	2	1.70	
G_2	110.7 / 6.95	14.50	1	14.50	
$PCA_{2,6}$	129.7 / 7.51	–	2	–	
PCA_β	115.2 / 6.32	–	1	–	
new (N)	60.0 / 3.98	1.66			
N	110.9 / 7.24	5.96			
N	121.4 / 7.06	2.43			
N	129.9 / 7.54	0.38			
N	141.9 / 7.41	3.57			
N	127.2 / 7.28	4.52			
N	109.5 / 7.05 and 109.6 / 7.00	3.78			
N	118.7 / 6.38	2.83			
N	127.2 / 6.21, 6.17	1.07			
N	128.7 / 6.45, 6.42	1.67			
N	136.3 / 6.64, 6.61, 6.58	2.87			
S+G+H				31.13	
X1+PCA+FA				–	
S+S'				15.88	
G+FA				14.50	
H+PCA				1.70	sum = 33.01
X1				–	
T				0.93	

7.3.2 ^{31}P NMR

Table 49. Amount of functionalities present in all starting lignins, determined from quantitative ^{31}P NMR spectroscopy (average values from double determination).

Lignin sample	Total hydroxyls	Aliphatic OH	Total phenolics	Total uncondensed phenolics	Condensed phenolics			S/G/H ratio (phenol-terminated)	Total condensed phenolics	Uncondensed phenolics			Carboxyls
					S	G	H			Diphenyl-methane	4-O-5´	5-5´	
NML	4.02	2.97	1.05	0.91	0.09	0.53	0.29	1 / 5.3 / 2.9	0.14	0.00	0.12	0.02	1.09
GL1	3.86	3.28	0.58	0.47	0.09	0.14	0.24	1 / 1.6 / 2.6	0.10	0.02	0.04	0.04	1.21
GL2	4.32	3.35	0.97	0.86	0.05	0.56	0.24	1 / 10.5 / 4.5	0.11	0.02	0.04	0.05	1.24
GL2 *extracted*	4.28	3.28	1.00	0.90	0,07	0.58	0.25	1 / 8.1 / 3.4	0.10	0.01	0.05	0.03	1.18
GL3	4.38	3.41	0.97	0.83	0.06	0.55	0.23	1 / 10.0 / 4.1	0.14	0.02	0.05	0.06	1.29
GL4	4.80	3.72	1.07	0.92	0.06	0.62	0.24	1 / 9.6 / 3.6	0.15	0.05	0.05	0.05	1.12
GL5	4.26	3.23	1.03	0.89	0.07	0.58	0.24	1 / 7.9 / 3.2	0.14	0.02	0.06	0.06	1.23
L_HT (GL6)	4.11	2.72	1.39	1.21	0.27	0.73	0.22	1 / 2.7 / 0.8	0.18	0.02	0.12	0.04	0.92
L_THF (GL6)	4.01	3.01	1.00	0.86	0.07	0.58	0.22	1 / 8.5 / 3.2	0.14	0.04	0.05	0.06	1.07
KL2	5.24	2.47	2.77	2.05	0.06	1.87	0.11	1 / 30.4 /1.8	0.72	0.32	0.11	0.30	0.41

Content of functionalities / mmol·g^{-1}

Table 50. Corrected amount of total hydroxyls (mmol·g^{-1}) for the altered lignin contents (wt%) in samples of equimolar formulations of lignin and fatty acid chlorides (reference values for the determination of the DS from quantitative ^{31}P NMR results).

Lignin sample	Total hydroxyls	Palmitoyl-lignin	Oleoyl-lignin	1:1 (lignin / polyester)	1:2 (lignin / polyester)	1:3 (lignin / polyester)	1:5 (lignin / polyester)	1:10 (lignin / polyester)
NML	4.02	1.92	1.83	2.01	1.34	1.01	0.67	0.37
GL1	3.86	1.85	1.74	1.93	1.29	0.97	0.64	0.35
GL2	4.32	2.06	1.96	2.16	1.44	1.08	0.72	0.39
GL2 *extracted*	4.28	2.04	1.95	2.14	1.43	1.07	0.71	0.39
GL3	4.38	2.09	1.99	2.19	1.46	1.10	0.73	0.40
GL4	4.80	2.30	2.16	2.40	1.60	1.20	0.80	0.44
GL5	4.26	2.03	1.94	2.13	1.42	1.07	0.71	0.39
L_HT	4.11	1.96	1.87	2.06	1.37	1.03	0.69	0.37
L_THF	4.01	1.91	1.82	2.01	1.34	1.00	0.67	0.36
KL2	5.24	2.50	2.38	2.62	1.75	1.31	0.87	0.48

Table 51. ^{31}P NMR results and determined degree of substitution of investigated short chain and cyclic ligninesters (cp. Table 23) (25 °C, 200 MHz, CDCl₃).

| Lignin sample | Total hydroxyls in starting lignin | Content of functionalities / mmol·g⁻¹ | | | | | | | Degree of substitution / % |
		Total hydroxyls	Aliphatic OH	Total phenolics	Total uncondensed phenolics	S/G/H ratio (phenol-terminated)	Total condensed phenolics	Carboxyls	
	short chain								
9	4.02 (NML)	0.30	0.09	0.21	0.12	1 / 1.3 / 1.5	0.09	0.05	93
10	3.86 (GL1)	0.17	0.09	0.08	0.07	1 / 3.7 / 3.6	0.01	0.65	96
	cyclic								
19	3.86 (GL1)	0.53	0.16	0.37	0.34	1 / 3.7 / 1	0.03	0.35	86
20	1.33 (16*)	0.24	0.18	0.06	0.05	1 / 2.6 / 0.6	0.01	1.37	82
21	2.78 (39*)	1.55	1.31	0.24	0.21	1 / 5.2 / 1.7	0.03	0.47	44
22	1.23 (17*)	0.07	0.07	0.00	0.00	–	0.00	0.82	94

*Lignin grafts (samples 16, 17 (lignin-PLA) and 39 (lignin-PCL), cp. Table 31).

Table 52. ^{31}P NMR results and determined degree of substitution of investigated undecenoyl (samples 29 and 31) and palmitoyl lignins (cp. Table 23) (25 °C, 200 MHz, CDCl$_3$).

Lignin sample	Total hydroxyls in starting lignin (corrected amount)	Content of functionalities / mmol·g^{-1}							Degree of substitution / %	FFA / wt%
		Total hydroxyls	Aliphatic OH	Total phenolics	Total uncondensed phenolics	S/G/H ratio (phenol-terminated)	Total condensed phenolics	Carboxyls		
29	2.41 (NML)	1.52	1.23	0.29	0.25	1 / 2.8 / 0.8	0.04	1.58	37	nd
31	2.31 (GL1)	0.48	0.13	0.35	0.31	1 / 2.6 / 0.6	0.04	0.53	79	nd
33	2.41 (NML)	1.23	0.95	0.28	0.23	1 / 3.4 / 0.9	0.05	1.51	49	nd
35	1.85 (GL1)	0.13	0.06	0.07	0.06	1 / 1.9 / 0.8	0.01	1.38	93	nd
36	2.47 (L_THF (GL6))	0.88	0.71	0.17	0.15	1 / 3.6 / 1	0.02	1.45	64	nd
37	3.02 (KL2)	1.11	0.65	0.46	0.34	–	0.12	0.86	63	nd
39	3.02 (KL2)	1.34	0.68	0.66	0.51	1 / 47 / 3.3	0.15	1.08	56	nd
40	2.49 (L_HT (GL6))	1.29	0.97	0.32	0.29	1 / 1.6 / 0.3	0.03	1.12	48	nd
41	1.91 (L_THF (GL6))	0.66	0.60	0.06	0.03	1 / 2.5 / 0	0.03	0.93	65	nd
42_NS 42_ÜS	2.49 (GL2)	0.68 0.55	0.22 0.18	0.46 0.37	0.41 0.32	1 / 5.3 / 1.5 1 / 5.0 / 1.7	0.05 0.05	0.48 1.58	73 78	11 9
43	2.49 (GL3)	0.44	0.21	0.23	0.20	1 / 5.6 / 2.1	0.03	1.22	82	15
44	2.49 (GL3)	0.77	0.68	0.09	0.08	1 / 1.7 / 1.0	0.01	1.15	69	13
45	2.04 (GL2 extracted)	0.28	0.14	0.14	0.12	1 / 3.2 / 1.1	0.02	0.94	86	10
46	2.04 (GL2 extracted)	0.14	0.05	0.09	0.08	1 / 4.6 / 1.5	0.01	0.79	93	6
47	2.62 (NML)	1.54	1.11	0.43	0.35	1 / 4.4 / 1.2	0.08	1.58	41	nd
49	2.23 (NML)	1.07	0.71	0.36	0.30	1 / 3.8 / 1.2	0.06	1.48	52	nd
50	2.19 (NML)	0.98	0.55	0.43	0.38	1 / 5.0 / 1.5	0.05	1.24	55	nd

nd = not determined; 42_NS = precipitated in Et$_2$O; 42_ÜS = dissolved in Et$_2$O

Table 53. ^{31}P NMR results and determined degree of substitution of investigated oleoyl lignins (cp. Table 23) (25 °C, 200 MHz, CDCl$_3$).

Lignin sample	Total hydroxyls in starting lignin (corrected amount)	Content of functionalities / mmol·g^{-1}							Degree of substitution / %	FFA / wt%
		Total hydroxyls	Aliphatic OH	Total phenolics	Total uncondensed phenolics	S/G/H ratio (phenol-terminated)	Total condensed phenolics	Carboxyls		
57	1.83 (NML)	1.33	1.03	0.30	0.19	1 / 3.2 / 1.1	0.11	1.72	27	nd
59	3.35 (KL2)	1.33	0.61	0.72	0.58	1 / 27 / 1.9	0.14	1.36	60	nd
60	2.37 (NML)	1.37	0.98	0.39	0.34	1 / 5.8 / 1.9	0.05	1.27	42	nd
61	2.73 (NML)	1.95	1.54	0.41	0.35	1 / 6.2 / 1.9	0.06	1.15	29	nd
62	2.37 (NML)	1.74	1.32	0.42	0.37	1 /5.7 / 2.5	0.05	1.50	27	nd
63	2.73 (NML)	1.96	1.61	0.35	0.31	1 / 5.9 / 1.8	0.04	1.03	28	nd
64	1.83 (NML)	0.77	0.63	0.14	0.13	1 / 8.6 / 3.5	0.01	0.92	58	nd
65*	1.83 (NML)	0.69	0.55	0.14	0.12	1 / 4.4 / 1.4	0.02	0.91	62	nd
66*	1.83 (NML)	1.09	1.03	0.06	0.05	1 / 4.1 / 0.9	0.01	0.86	40	nd
67	2.13 (NML)	0.81	0.46	0.35	0.32	1 / 6.5 / 2.1	0.02	1.22	62	nd
68	2.13 (NML)	1.13	0.99	0.14	0.12	1 / 4.9 / 2.6	0.02	1.24	47	nd
69	2.07 (L_HT (GL6))	1.13	0.84	0.29	0.27	1 / 1.8 / 0.4	0.02	1.17	45	nd
71	2.26 (GL4)	0.59	0.32	0.27	0.24	1 / 4.0 / 0.8	0.03	1.08	74	14
72	2.26 (GL4)	0.64	0.46	0.18	0.16	1 / 4.1 / 0.9	0.02	0.94	72	11
73	2.26 (GL4)	0.61	0.60	0.01	0.00	–	0.01	0.89	73	10
74*	2.26 (GL4)	0.54	0.51	0.03	0.01	–	0.02	0.80	76	7
75	2.26 (GL4)	0.50	0.49	0.01	0.00	–	0.01	0.67	78	4
78	2.00 (GL5)	0.75	0.55	0.20	0.17	1 / 42 / 12	0.03	1.16	63	nd
79	2.00 (GL5)	0.76	0.70	0.06	0.04	1 / 3.0 / 1.1	0.02	1.27	62	nd
80	1.74 (GL1)	0.12	0.07	0.05	0.04	1 / 5.0 / 2.6	0.01	1.32	93	nd
81	1.74 (GL1)	1.17	0.72	0.45	0.39	1 / 6.1 / 2.0	0.06	1.00	33	nd
82	2.46 (KL2)	1.01	0.62	0.39	0.30	1 / 10 / 0.7	0.09	0.75	59	nd
83	2.05 (L_THF (GL6))	0.87	0.72	0.15	0.13	1 / 2.0 / 0.7	0.02	1.37	58	nd

*not completely dissolved; nd = not determined

Table 54. Amount of functionalities present in lignin /PHB blends and lignin-PLA grafts (Table 31), determined by quantitative ^{31}P NMR spectroscopy (25 °C, 200 MHz, CDCl$_3$).

Lignin sample	Total hydroxyls in starting lignin (*corrected amount*)	Total hydroxyls (*without end group*)	Aliphatic OH	Total phenolics	Total uncondensed phenolics	S/G/H ratio (phenol-terminated)	Total condensed phenolics	Carboxyls	Polyester end group	Degree of substitution / %
BBL									(146.6 ppm)	
1	0.35 (GL1) 1:10	0.33	0.22	0.11	0.09	1 / 6.8 / 2.7	0.02	0.70	0.08	–
2	0.35 (GL1) 1:10	0.28	0.21	0.07	0.06	1 / 7.2 / 2.8	0.01	0.79	0.12	–
3	0.97 (GL1) 1:3	1.12	0.81	0.31	0.26	1 / 4.5 / 1.7	0.05	1.14	0.22	–
4	0.97 (GL1) 1:3	0.96	0.71	0.26	0.22	1 / 7.9 / 2.3	0.04	2.13	0.22	–
LA									(146.6 ppm)	
6	0.55 (GL1) 1:6	1.14	0.87	0.27	0.24	1 / 5.5 / 2.1	0.03	0.96	3.96	–
7	0.64 (GL1) 1:5	0.13	0.03	0.10	0.09	1 / 2.3 / 0.5	0.01	1.53	1.81	80
8	0.97 (GL1) 1:3	0.25	0.05	0.20	0.18	1 / 3.2 / 0.8	0.02	0.23	0.93	74
11	1.93 (GL1) 1:1	0.96	0.62	0.34	0.31	1 / 6.9 / 2.6	0.03	0.42	1.22	50
13	1.29 (GL1) 1:2	0.69	0.37	0.32	0.27	1 / 5.6 / 1.7	0.05	0.59	1.19	47
14	1.29 (GL1) 1:2	0.44	0.14	0.30	0.27	1 / 3.8 / 1.3	0.03	0.64	1.18	66
14a	1.29 (GL1) 1:2	0.40	0.11	0.29	0.26	1 / 4.5 / 1.3	0.03	1.40	1.87	69
16	0.97 (GL1) 1:3	0.45	0.19	0.26	0.23	1 / 6.4 / 2.5	0.03	0.44	0.88	54
17	0.97 (GL1) 1:3	0.27	0.06	0.21	0.18	1 / 2.9 / 1.0	0.03	0.54	0.96	72
18	0.97 (GL1) 1:3	1.04	0.67	0.37	0.34	1 / 11 / 4.4	0.03	1.52	2.05	–
19	0.97 (GL1) 1:3	0.33	0.08	0.25	0.20	1 / 3.2 / 0.9	0.05	0.55	1.12	66
20	1.29 (GL1) 1:2	1.05	0.60	0.45	0.40	1 / 4.4 / 1.6	0.05	1.04	1.36	19
20_pure	1.29 (GL1) 1:2	0.86	0.41	0.45	0.39	1 / 4.5 / 1.6	0.06	0.99	1.31	33
21	1.29 (GL1) 1:2	0.28	0.02	0.26	0.24	1 / 2.8 / 0.8	0.02	1.16	1.45	78
22	1.93 (GL1) 1:1	0.81	0.43	0.38	0.34	1 / 2.9 / 0.8	0.04	1.13	150	58
23	1.93 (GL1) 1:1	0.70	0.34	0.36	0.32	1 / 3.0 / 0.7	0.04	1.18	1.34	64
24	3.04 (KL2) 1:0.7	0.52	0.10	0.42	0.34	1 / 72 / 4.4	0.08	0.93	1.36	83
25	2.15 (KL2) 1:1.4	0.93	0.15	0.78	0.63	1 / 52 / 2.4	0.15	1.25	1.76	57
26	1.68 (KL2) 1:2.2	0.45	0.08	0.37	0.29	1 / 43 / 1.7	0.08	0.80	1.18	73
27	3.04 (KL2) 1:0.7	0.53	0.05	0.48	0.40	1 / 28 / 1.5	0.08	0.50	1.06	83
28	2.15 (KL2) 1:1.4	0.82	0.17	0.65	0.57	1 / 55 / 3.2	0.08	0.43	1.03	62
29	1.68 (KL2) 1:2.2	1.28	0.26	1.02	0.90	1 / 55 / 2.6	0.12	1.36	1.82	24

Table 55. Amount of functionalities present in lignin-PCL grafts (Table 31), determined by quantitative ^{31}P NMR spectroscopy (25 °C, 200 MHz, CDCl$_3$).

Lignin sample	Total hydroxyls in starting lignin (corrected amount)	Total hydroxyls (without PCL end group)	Aliphatic OH	Total phenolics	Total uncondensed phenolics	S/G/H ratio (phenol-terminated)	Total condensed phenolics	Carboxyls	PCL end group	Degree of substitution / %
					Content of functionalities / mmol·g^{-1}					
CL									(147.2 ppm)	
33	1.29 (GL1) 1:2	1.11	0.72	0.39	0.33	1 / 8,6 / 3.4	0.06	0.64	0.91	14
34	0.97 (GL1) 1:3	0.76	0.48	0.28	0.24	1 / 9.3 / 4.4	0.04	0.50	0.65	22
36	0.64 (GL1) 1:5	1.15	0.95	0.20	0.17	1 / 7.3 / 3.1	0.03	0.45	1.35	–
37	0.35 (GL1) 1:10	0.54	0.25	0.29	0.26	1 / 6.8 / 2.0	0.03	0.95	1.82	–
38	1.29 (GL1) 1:2	1.41	0.93	0.48	0.42	1 / 7.2 / 2.3	0.06	0.62	1.13	–
39	0.97 (GL1) 1:3	1.77	0.91	0.86	0.80	1 / 0.6 / 0.2	0.06	0.50	1.01	–
39_pure	0.97 (GL1) 1:3	1.42	0.95	0.47	0.43	1 / 6.9 / 2.1	0.04	0.98	1.47	–
40	1.93 (GL1) 1:1	1.09	0.63	0.46	0.40	1 / 3.3 / 1.1	0.06	0.76	1.10	44
42	3.49 (KL2) 2:1	1.62	0.64	0.98	0.79	1 / 41 / 2.0	0.19	0.79	1.31	54
43	2.62 (KL2) 1:1	1.32	0.42	0.90	0.68	1 / 72 / 4.4	0.22	0.67	1.20	50
44	1.31 (KL2) 1:3	0.90	0.32	0.58	0.48	1 / 214 / 14	0.10	0.57	1.04	31
47	4.32 GL2 1:0	3.71	2.62	1.09	0.92	1 / 3.7 / 1.2	0.17	0.67	–	–

7.3.3 HPLC-SEC

FFA CONTENT

Table 56. Collected molar mass values of the synthesized ligninesters (Table 23), determined by HPLC-SEC (50 °C, DMF, relative to PS-standards).

Sample	M_n / g·mol^{-1}	M_w / g·mol^{-1}	D
20	3600	38400	11
37	2422	23330	9.6
38	5381	57630	10.7
39	2698	17200	6.4
40	2084	8974	4.3
41	1993	13870	7.0
42_NS	8265	88700	10.7
42_ÜS	2577	22380	8.7
43	4480	192600	43.0
44	3589	72350	20.2
45	3501	36660	10.5
46	3466	36120	10.4
50	2139	13100	6.1
59	2538	16970	6.7
60	2092	12130	5.8
61	2061	13950	6.8
62	1777	11600	6.5
63	1967	15550	7.9
64	2437	42910	17.6
65	2537	37830	14.9
66	2610	21320	8.2
67	2379	13990	5.9
68	2420	14200	5.9
69	2190	9705	4.4
71	3165	35400	11.2
72	3158	59450	18.8
73	4182	210500	50.3
74	3753	165500	44.1
75	4350	319600	73.5
76	4634	38910	8.4
78	3896	151000	38.8
79	3532	47820	13.5
82	3389	24900	7.3

42_NS = precipitated in Et$_2$O; 42_ÜS = dissolved in Et$_2$O

Table 57. Determination of the FFA content of various lignin esters (cp. Table 23) after calibration with palmitic and oleic acid.

Sample	Sample / mg	Integral fatty acid	Fatty acid / mg	FFA content / wt%
palmitoyl lignin				
37	10.91	42863.5	1.3	12
40	9.95	27987.3	0.8	8
41	10.18	27293.1	0.8	8
42	10.40	148816.3	4.5	43
43	10.45	96072.4	2.9	28
44	10.82	84149.5	2.5	23
45	10.81	75487	2.3	21
46	10.70	70540.3	2.1	20
palmitoyl / norbornenoyl lignin				
50	10.45	63628.4	1.91	18
oleoyl lignin				
39	10.16	63541.2	1.14	11
59	10.05	145613.5	2.62	26
60	9.55	117356.8	2.10	22
61	10.88	123647.5	2.22	20
62	10.79	158419.9	2.85	26
63	10.28	106451.2	1.91	19
64	10.68	81156.9	1.46	14
65	12.54	102038.9	1.83	15
66	10.37	79962.8	1.44	14
67	10.63	131361	2.36	22
68	10.82	125814	2.26	21
69	10.64	109915.6	1.97	19
71	10.19	172492.5	3.1	30
72	10.26	152622.6	2.7	27
73	10.69	115959.1	2.1	19
74	10.30	120392.9	2.2	21
75	10.30	128533.9	2.3	22
78	10.10	98531.1	1.77	18
79	10.32	125776.5	2.26	22
82	11.13	88550.5	1.59	14

Table 58. Collected molar mass values of the synthesized ligningrafts (Table 31), determined by HPLC-SEC (50 °C, DMF, relative to PS-standards).

Sample	M_n / g·mol^{-1}	M_w / g·mol^{-1}	D
3	1000	3300	3.1
4	1200	1300	11
5	1500	7500	5.0
6	17800	14400	8.0
7	5300	65000	12
8	12050	205400	17
11	8200	238500	29
12	3500	1500	4.2
12[a]	800	1700	2.2
13	3400	62200	18
16	2800	24200	8.6
16[a]	2900	24900	8.5
17	4600	90300	20
18	3660	53020	15
19	5590	78750	14
20	2600	103400	40
21	2910	34320	12
22	2400	61700	25
23	2070	48740	24
24	2440	45970	19
25	1960	42670	22
26	2530	44660	18
27	3080	66820	22
28	2430	79440	33
29	1390	28110	20
30	1600	9100	5.8
32	1800	9000	4.9
33	2960	23500	8.0
34	2970	21140	7.1
38	2760	20720	7.5
39	2620	16900	6.5
40	3500	225500	64
41	1730	24420	14
42	2560	55010	22
43	2770	49720	18
45	870	2630	3.0
46	980	4380	4.5

[a] *double determination*

7.3.4 ELEMENTAL ANALYSIS

Table 59. Elemental composition of the synthesized ligninesters listed in Table 23.

Sample	% C	% H	% N	% S	% O*
short chain					
2	57.5	5.3	1.7	nd	35.5
3	56.7	5.9	1.2	nd	36.2
9	60.6	5.7	1.4	nd	32.3
10	60.1	6.8	2.7	nd	30.4
14[a]	64.5	6.5	0.9	nd	28.1
16	54.5	5.8	4.6	0.8	34.3
cyclic					
19	61.8	6.0	1.2	0.4	30.6
20	59.6	7.7	0.6	0.6	31.5
21	58.7	8.0	0.5	nd	32.8
22	56.9	5.9	0.7	nd	36.5
long chain					
29	66.8	8.0	1.3	nd	23.9
33	69.3	9.5	1.1	nd	20.1
34	68.6	10.0	2.2	nd	19.1
34[a]	71.7	10.2	0.9	nd	17.2
35	71.2	10.2	1.0	nd	17.6
36	69.1	9.5	0.9	0.7	19.8
37	70.8	9.5	1.4	nd	18.3
38	55.5	7.3	2.7	nd	34.5
39	71.1	9.3	0.8	nd	18.8
40	68.8	8.8	0.8	nd	21.6
41	68.2	10.1	2.1	nd	19.6
42	67.7	8.3	1.4	0,2	22.4
42	70.3	10.3	1.0	0,2	18.1
43	66.9	10.2	3.0	0,2	19.7
44	67.3	10.0	2.5	0,2	20.0
45	61.4	10.3	2.9	0,4	25.0
46	59.1	9.9	2.5	0,6	27.9
47	66.8	8.3	1.2	nd	23.7
49	68.3	8.9	1.2	nd	21.6
50	66.7	8.5	2,1	nd	22.7
55	72.1	10.6	2.2	nd	15.1
57	69.7	9.3	1.4	nd	19.6
58	63.5	9.7	4.5	nd	22.3
58[a]	71.0	9.8	1.9	nd	17.3
59	71.8	9.2	0.7	nd	18.4
60	68.0	8.5	1.2	nd	22.3
61	67.0	8.2	1.4	nd	23.4
62	67.3	8.6	1.5	nd	22.5
63	66.5	8.3	1.9	nd	23.3

Table 59 continued.

Sample	% C	% H	% N	% S	% O*
64	68.4	9.4	1.9	nd	20.3
65	68.9	9.3	1.7	nd	20.1
66	69.2	8.8	1.1	nd	21.0
67	69.0	8.8	1.1	nd	21.1
68	69.6	8.9	1.1	nd	20.4
69	70.3	8.8	0.7	nd	20.1
71	68.0	9.8	2.7	0,2	19.3
72	67.6	10.0	2.7	0,2	19.5
73	67.4	10.1	3.2	0,2	19.0
74	67.5	10.0	2.7	0,2	19.6
75	65.5	10.2	4.0	0,2	20.1
76	33.6	4.8	0.4	nd	61.2
78	68.3	9.5	2.1	nd	20.1
79	68.9	9.8	1.9	nd	19.5
80	72.9	10.1	0.9	nd	16.1
82	70,9	9.4	1.5	nd	18.2
83	69.9	9.8	0.7	0.4	19.2

*calculated value; nd = not determined; [a] double determination

Table 60. Elemental composition of the synthesized lignin grafts listed in Table 31.

Sample	% C	% H	% N	% S	% O*
BBL					
1	54.8	6.8	0.3	nd	38.1
2	55.4	6.9	0.2	nd	37.5
3	57.5	7.0	0.6	0.2	34.7
4	57.1	6.9	0.6	0.3	35.1
5	53.7	6.3	0.3	0.9	38.8
LA					
6	50.6	6.4	0.5	0.8	41.7
7	50.2	5.8	0.2	0.2	43.6
8	52.1	5.5	0.7	0.5	41.2
9	47.2	5.7	0.0	0.2	46.9
11	56.1	6.0	1.5	0.7	35.7
13	54.0	6.0	0.8	0.2	39.0
14	53.3	5.7	0.7	1.1	39.2
16	54.4	6.0	0.9	0.2	38.5
17	52.2	5.9	0.5	0.2	41.2
18	58.3	6.2	1.3	0.3	33.9
19	53.9	6.1	0.8	0.4	38.8
20	55.4	6.2	0.8	0.2	37.4
21	52.5	6.1	0.6	0.5	40.3
22	55.3	6.4	0.9	0.2	37.2
23	55.2	6.3	1.0	0.5	37.0
24	53.0	5.7	0.3	nd	41.0
25	54.8	5.8	0.5	nd	38.9
26	52.2	5.7	0.3	nd	41.8
27	52.3	5.5	0.2	nd	42.0
28	56.1	5.8	0.3	nd	37.8
29	55.8	5.9	0.5	nd	37.8
CL					
31	61.1	8.1	0.1	nd	30.7
33	61.6	7.9	1.4	0.2	28.9
34	61.4	8.0	1.1	0.3	29.2
36	56.8	7.9	0.6	nd	34.8
37	60.5	7.9	0.9	nd	30.7
38	61.7	7.7	1.2	0.2	29.2
39	61.3	7.5	1.3	0.2	29.7
40	62.8	7.8	1.0	0.3	28.1
41	62.9	7.6	1.0	0.9	27.6
42	64.0	7.6	0.5	nd	27.9
43	63.6	7.5	0.4	nd	28.5
44	63.2	7.7	0.3	nd	28.8

*calculated value; nd = not determined
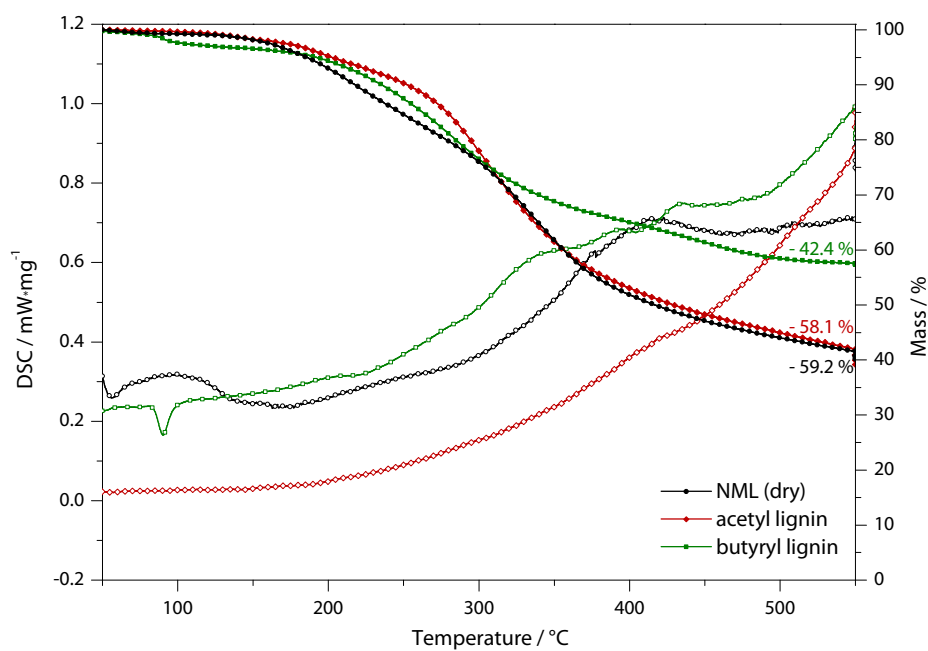
Figure 62. DSC and mass loss of short chain ligninesters (samples 2 and 3, cp. Table 23) and dry NML, determined by STA (5 °C / min).
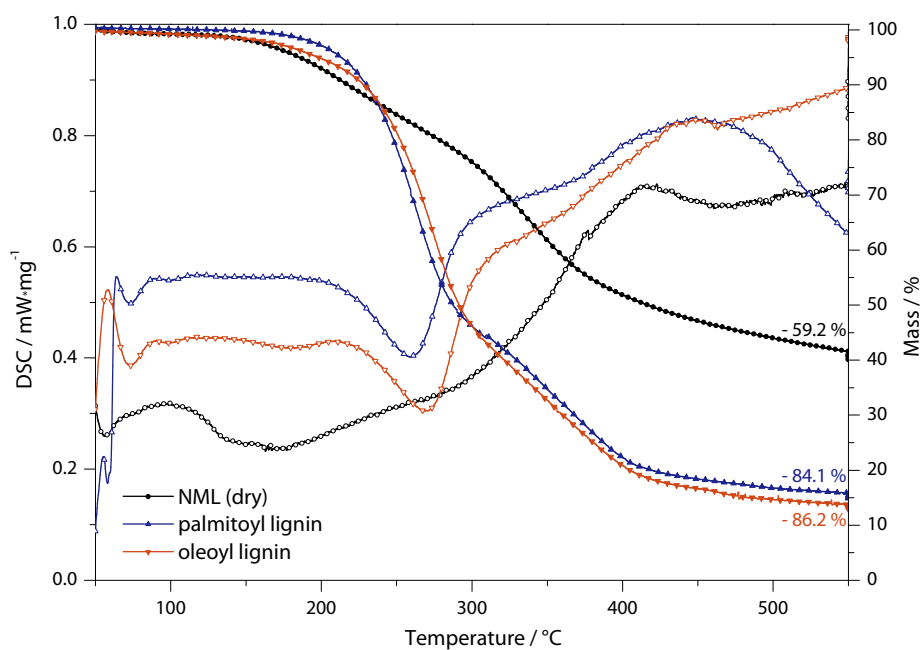
Figure 63. DSC and mass loss of long chain ligninesters (samples 34 and 58, cp. Table 23) and dry NML, determined by STA (5 °C / min).
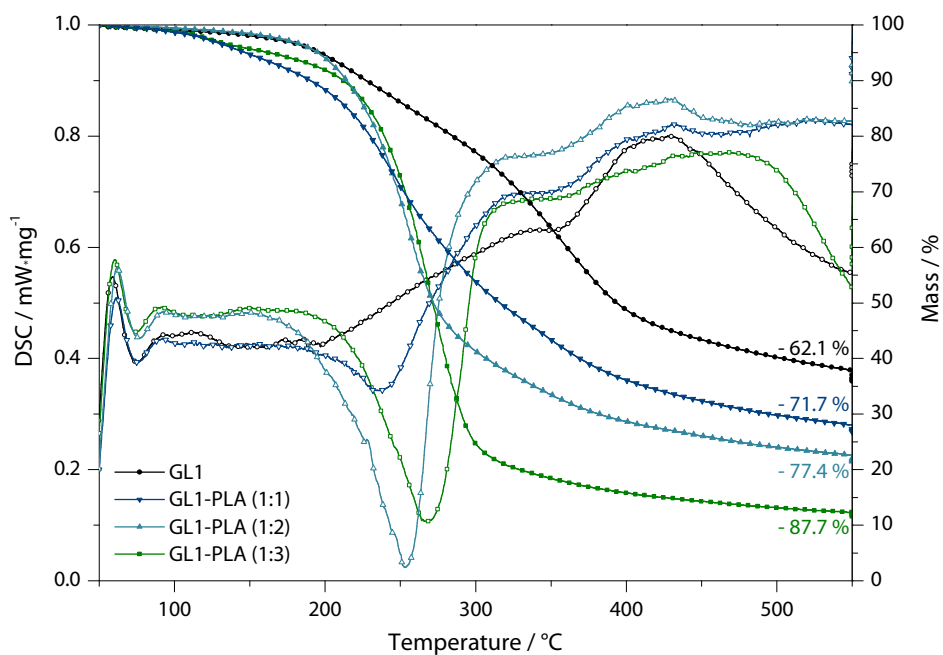
Figure 64. DSC and mass loss of lignin-PLA grafts in varying ratios (1:1 (sample 22), 1:2 (sample 20), 1:3 (sample 17), cp. Table 23) and GL1, determined by STA (5 °C / min).
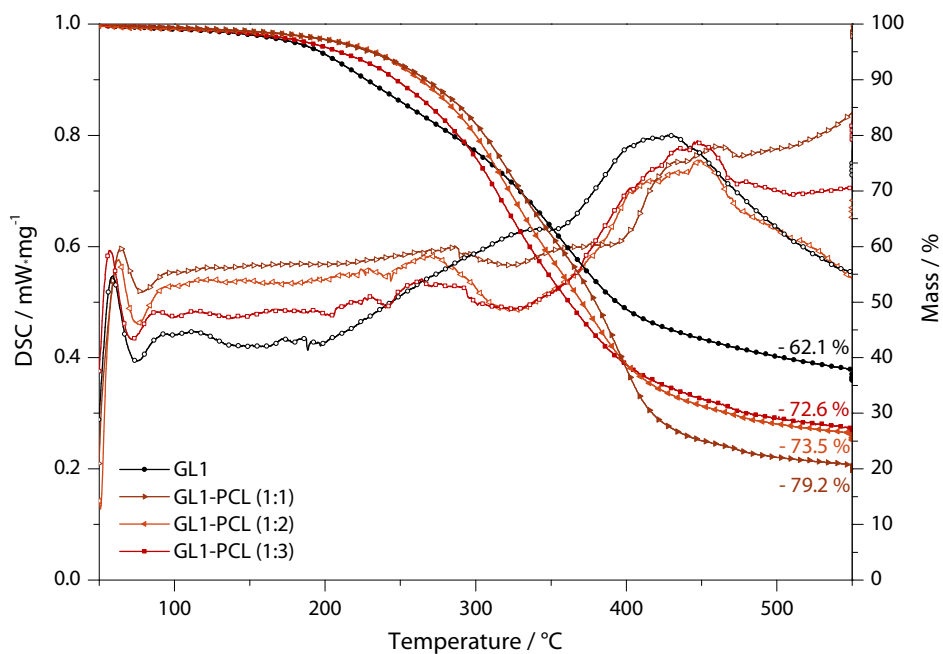
Figure 65. DSC and mass loss of lignin-PCL grafts in varying ratios (1:1 (sample 40), 1:2 (sample 38), 1:3 (sample 39), cp. Table 23) and GL1, determined by STA (5 °C / min).

7.4 References

[1] W. O. S Doherty, P. Mousavion, C. M. Fellows, *Industrial Crops and Products* **2011**, *33*, 259-276.
[2] W. Thielemans, R. P. Wool, *Biomacromolecules* **2005**, *6(4)*, 1895-1905.
[3] B. Saake, R. Lehnen, *Ullmann's Encyclopedia of Industrial Chemistry* **2012**, DOI: 10.1002/14356007.a15_305.pub3.
[4] E. Windeisen, G. Wegener, *Polymer Science* **2012**, *10*, 255-265.
[5] R. Vanholme, B. Demedts, K. Morreel, J. Ralph, W. Boerjan, *Plant Physiology* **2010**, *153*, 895-905.
[6] K. M. Herrmann, L. M. Weaver, *Annual Reviews of Plant Physiology and Plant Molecular Biology* **1999**, *50*, 473-503.
[7] J. C. del Río, J. Rencoret, P. Prinsen, A. T. Martínez, J. Ralph, A. Gutiérrez, *Journal of Agricultural and Food Chemistry* **2012**, *60*, 5922-5935.
[8] W. Thielemans, E. Can, S. S. Morye, R. P. Wool, *Journal of Applied Polymer Science* **2002**, *83*, 323-331.
[9] C. F. Dahl, US296935 A, **1884**, *Process of manufacturing cellulose from wood*.
[10] P. Tomani, *The 2nd Nordic Wood Biorefinery Conference*, Helsinki, FIN, **2009**, NWBC-2009, 181-188.
[11] B. C. Tilghman, USP 70.485, **1867**, *Improved Mode of Treating Vegetable Substances for Making Paper-Pulp*.
[12] H. Burgess, C. Watt, USP 11.343, **1854**, *Improvement in the Manufacture of Paper from Wood*.
[13] A. Abächerli, F. Doppenberg, US6239198 B1, WO 98/42912, **1998**, *Method for preparing alkaline solutions containing aromatic polymers*.
[14] J. H. Lora, C. Ricardo, J.-N. Cloutier, *TAPPI Engineering, Pulping and Environmental Conference* **2005**, Philadelphia, PA, USA.
[15] T. N. Kleinert, US 3585104 A, **1971**, *Organosolv pulping and recovery process*.
[16] a) E. K. Pye, J. H. Lora, *TAPPI* **1991**, *74(3)*, 113-118; b) C. Arato, E. K. Pye, G. Gjennestad, *Applied Biochemistry and Biotechnology* **2005**, *121(12)*, 871-882.
[17] a) K.-H. Brodersen, G. Dahlmann, H. Leopolc, DE4103572 A, **1992**, *Verfahren zum Delignifizieren von Pflanzenfasermaterial*; b) A. Lindner, G. Wegener, *Journal of Wood Chemistry and Technology* **1988**, *8(3)*, 323-340.
[18] E. van der Heide, X. Zhao, EP 2513150 A1, **2010**, *A process for the extraction of sugars and lignin from lignocellulose-comprising solid biomass*.
[19] J. Anttila, E. Rousu, P. Rousu, P. Rousu, WO2003006737 A1, **2002**, *Process for producing pulp*.
[20] W. H. Mason, US1578609, **1926**, *Process and apparatus for disintegration of wood and the like*.
[21] M. Fasching, P. Schroeder, R. P. Wollboldt, H. K. Weber, H. Sixta, *Holzforschung* **2007**, *62*, 15-23.
[22] A. Dybov, F. Boeck, Annikki GmbH, WO2013164234 A1, **2013**, *Method for producing pulp having low lignin content from lignocellulosic material*; O. Ertl, K. Fackler, K. Messner, T. Ters, Annikki GmbH, WO2012027767 A1, **2012**, *Method for lignin recovery*; K. Fackler, K. Messner, C. Krongtaew, O. Ertl, Annikki GmbH, WO2011014894 A2, **2011**, *Method for producing carbohydrate cleavage products from a lignocellulosic material*; K. Fackler, K. Messner, C. Krongtaew, O. Ertl, Annikki GmbH, WO2010124312 A2, **2010**, *Method for producing carbohydrate cleavage products from a lignocellulosic material*.
[23] S. Laurichesse, L. Avérous, *Progress in Polymer Science* **2014**, *39*, 1266-1290.
[24] J. H. Lora, W. G. Glasser, *Journal of Polymers and the Environment* **2002**, *10*, 39-48.
[25] A. Gandini, M. N. Belgacem, *Monomers, Polymers and Composites from Renewable Resources*, Chapter 11, 243-271, Copyright © **2015** Elsevier B. V.
[26] A. A. Morandim-Giannetti, J. M. M. Agnelli, B. Z. Lanças, R. Magnabosco, S. A. Casarin, S. H. P. Bettini, *Carbohydrate Polymers* **2012**, *87*, 2563-2568.
[27] R. R. N. Sailaja, M.V. Deepthi, *Materials and Design* **2010**, *31*, 4369-4379.
[28] P. Alexy, B. Košíková, G. Podstránska, *Polymer* **2000**, *41*, 4901-4908.
[29] Y. Li, S. Sarkanen, *Macromolecules* **2005**, *38*, 2296-2306.
[30] P. Mousavioun, G. A. George, W. O. S. Doherty, *Polymer Degradation and Stability* **2012**, *97*, 1114-1122.
[31] A. Campanella, J. J. La Scala, R. P. Wool, *Journal of Applied Polymer Science* **2002**, *119*, 1000-1010.
[32] Zhang, Y. Ma, C. Wang, S. Li, M. Zhang, F. Chu, *Industrial Crops and Products* **2013**, *43*, 326-333.
[33] Y. Park, W. O. S. Doherty, P. J. Halley, *Industrial Crops and Products* **2008**, *27*, 163-167.
[34] A. Pizzi, in *Handbook of Adhesive Technology*, Editors: A. Pizzi and K. L. Mittal, Marcel Dekker, New York, **2003**, 589.
[35] M. Turunen, L. Alvila, T. T. Pakkanen, J. Rainio, *Journal of Applied Polymer Science* **2003**, *88*, 582-588.
[36] A. Pizzi, *Journal of Adhesion Science and Technology* **2006**, *20(8)*, 829-846.
[37] a) D. Feldman, M. Lacasse, R. St. John Manley, *Journal of Applied Polymer Science* **1988**, *35*, 247-257; b) A. Natansohn, M. Lacasse, D. Ban, D. Feldman, *Journal of Applied Polymer Science* **1990**, *40*, 899-904.
[38] a) M. Detoisien, F. Pla, A. Gandini, H. Cheradame, *British Polymer Journal* **1985**, *17(3)*, 260-262; b) H. Cheradame, M. Destoisien, A. Gandini, F. Pla, G. Roux, *British Polymer Journal* **1989**, *21(3)*, 269-275.
[39] D. V. Evtuguin, J.-P. Andreolety, A. Gandini, *European Polymer Journal* **1998**, *34(8)*, 1163-1169.

40 H. Hatakeyama, T. Hatakeyama, *Journal of Renewable Materials* **2013**, *2(11)*, 113-123.

41 C. Bonini, M. D'Auria, L. Emanuele, R. Ferri, R. Pucciarello, A. R. Sabia, *Journal of Applied Polymer Science* **2005**, *98(3)*, 1451-1456.

42 G. Griffini, V. Passoni, R. Suriano, M. Levi, S. Turri, *ACS Sustainable Chemical Engeineering* **2015**, *3(6)*, 1145-1154.

43 a) W. G. Glasser, R. K. Jain, Final project report to IBM, **1996**, *The green card: development of a lignin-based epoxy resin for the use in printed circuit boards (PCB)*; b) J. M. Shaw, S. L. Buchwalter, J. C. Hedrick, S. K. Lang, L. L. Kosbar, J. D. Gelorme, D. A. Lewis, S. Purushothaman, R. Saraf, A. Viehbeck, *Printed Circuit Fabrication* **1996**, *19*, 38-44; c) L. L. Kosbar, J. D. Gelorme, R. M. Japp, W. T. Fotorny, *Journal of Industrial Ecology* **2001**, *4*, 93-105.

44 N. J. Nehez, WO 9714747, **1997**, *Lignin-based friction material*.

45 a) W. G. Glasser, S. Sarkanen, *ACS Symposium Series* **1989**, *397*, 546; b) J. H. Lora, A. W. Creamer, L. Wu, J. Ash, *Proc. Adh. Bonded Wood Symp. Forest Prod. Soc.* **1994**, 384-394.

46 A. Gregorová, Z. Cibulková, B. Kosíková, P. Simon, *Polymer Degradation and Stability* **2005**, *89(3)*, 553-558.

47 A. Gregorová, B. Kosíková, R. Moravcik, *Polymer Degradation and Stability* **2006**, *91(2)*, 229-233.

48 a) K. Toh, S. Nakano, H. Yokoyama, K. Ebe, K. Gotoh, H. Noda, *Polymer Journal* **2005**, *37(8)*, 633-635; b) R. J. A. Gosselink, M. H. B. Snijder, A. Kranenbarg, E. R. P. Keijsers, E. de Jong, L. L. Stigsson, *Industrial Crops and Products* **2004**, *20(2)*, 191-203.

49 D. Schorr, P. N. Diouf, T. Stevanovic, *Industrial Crops and Products* **2014**, *52*, 65-73.

50 B. Kosíková, A. Gregorová, *Journal of Applied Polymer Science* **2005**, *97*, 924-929.

51 T. Viswanathan, US 6977050 B1, **2005**, *Synthesis of lignosulfonic acid-doped polyaniline using transition metal ion catalysts*.

52 a) S. Lepitre, S. Baumberger, B. Pollet, F. Cazaux, X. Coqueret, C. Lapierre, *Industrial Crops and Products* **2004**, *20*, 219-230; b) S. Lepitre, M. Froment, F. Cazaux, S. Houot, D. Lourdin, X. Coqueret, C. Lapierre, S.Baumberger, *Biomacromolecules* **2004**, *5*, 1678-1686.

53 E. R. Inone-Kauffmann, *International Sugar Journal* **2009**, *11(1321)*, 10-11.

54 H. Nägele, J. Pfitzer, N. Eisenreich, P. Eyerer, P. Elsner, W. Eckl, WO 0027923, **1998**, *Plastic material made from a polymer blend*.

55 S. Kubo, J. F. Kadly, *Biomacromolecules* **2005**, *6*, 2815-2821.

56 a) S. Kubo, J. F. Kadla, *Macromolecules* **2003**, *36*, 7803-7811; b) S. Kubo, J. F. Kadla, *Journal of Applied Polymer Science* **2005**, *98*, 1437-1444; c) S. Kubo, J. F. Kadla, *Macromolecules* **2004**, *37*, 6904-6911; d) S. Kubo, J. F. Kadla, *Holzforschung* **2006**, *60*, 245-252.

57 Z. X. Guo, A. Gandini, *European Polymer Journal* **1991**, *27*, 1177-1180.

58 Y. Li, J. Mlinár, S. Sarkanen, *Journal of Polymer Science, Part B: Polymer Physics* **1997**, *35*, 1899-1910.

59 S. Kubo, J. F. Kadla, *Biomacromolecules* **2003**, *4*, 561-567.

60 E. Ten, W. Vermerris, *Polymers* **2013**, *5*, 600-642.

61 J. Oberkofler, WO 01/68530 A2, **2001**, *Sulphur-free lignin and derivatives thereof for reducing the formation of slime and deposits in industrial plants*.

62 Y. Ge, D. Li, Z. Li, *BioResources* **2014**, *9(4)*, 7119-7127.

63 M. N. Belgacem, A. Gandini, *Industrial Crops and Products* **2003**, *18*, 145-153.

64 D. Stewart, *Industrial Crops and Products* **2008**, *27*, 202-207.

65 C. Wang, CN 104609762 A, **2015**, *Lignin-based additive for increasing the crack resistance of concrete*.

66 X. Chen, J. Hong, T. Wei, S. Zhang, J. Lin, X. Zhu, G. Cai, CN 104311833 A, **2015**, *Preparation of lignin sulfonate-type emulsifier for cold regenerated asphalt*.

67 B. Li, H. Zhang, CN 104693450 A, **2015**, *A synthesis process of tetraethylenepentamine/formaldehyde modified lignin amine asphalt emulsifier*.

68 T. M. Slaghek, D. Van Vliet, C. Giezen, I. K. Haaksman, WO 2015137813 A1, **2015**, *Bitumen composition containing lignin compound*.

69 C.-G. Wan, Q.-T. Wang, B.-F. Ma, Y. Zhang, *Advanced Materials Research* **2014**, *912-914*, 188-193.

70 D. C. Olk, K. G. Cassman, K. Schmidt-Rohr, M. M. Anders, J.-D. Mao, J. L. Deenik, *Soil Biology and Biochemistry* **2006**, *38(11)*, 3303-3312.

71 Z. Zhu, C. Liu, Z Pang, Q Fan, C. Xia, CN10153320 A, **2009**, *Lignin nutritient medium additive for restoring vegetation on road slope and bare mountain*.

72 Z. Li, Y. Ge, *Journal of the Brazilian Chemical Society* **2011**, *22(10)*, 1866-1871.

73 S. Domenek, A. Louaifi, A. Guinault, S. J. Baumberger, *Journal of Polymer and the Environment* **2013**, *21*, 692-701.

74 K. Johansson, S. Winestrand, C. Johansson, L. Järnström, L. J. Jönsson, *Journal of Biotechnology* **2012**, *161*, 14-17.

75 M. P. Vinardell, V. Ugartondo, M. Mitjans, *Industrial Crops and Products* **2008**, *27*, 220-223.

76 J. Xu, CN 104434558, **2015**, *Cosmetic containing lignin*.

77 Y Qianm, X. Qiu, S, Zhu, *Green Chemistry* **2015**, *17(1)*, 320-324.

78 I. Norberg, Doctoral Thesis ,*Carbon fibres from Kraft lignin'*, KTH Stockholm, **2012**.

79   Q. Shen, T. Zhang, W.-X. Zhang, S. Chen, M. Mezgebe, *Journal of Applied Polymer Science* **2011**, *121(2)*, 989-994.

80   E. Ten, W. Vermerris, *Journal of Applied Polymer Science* **2015**, DOI: 10.1002/APP.42069.

81   W. E. Tenhaeff, O. Rios, K. More, M. A. McGuire, *Advanced Functional Materials* **2014**, *24(1)*, 86-94.

82   S. Chatterjee, T. Saito, O. Rios, A. Johs, *ACS Symposium Series* **2014**, *1186 (Green Technologies for the Environment)*, 203-2018.

83   S. Hu, S. Zhang, N. Pan, Y.-L. Hsieh, *Journal of Power Sources* **2014**, *270*, 106-112.

84   S. Leguizamon, K. P. Diaz Orellana, J. Velez, M. C. Thies, M. E. Roberts, *Abstract of Papers, 250th ACS National Meeting & Exposition*, Boston, MA, USA, **2015**, ENFL-142.

85   Q. Hu, J. Shao, H. Yang, D. Yao, X. Wang, H. Chen, *Applied Energy* **2015**, DOI:10.1016/j.apenergy.2015.05.019.

86   W. Sangchoom, R. Mokaya, *ACS Sustainable Chemical Engineering* **2015**, *3*, 1658-1667.

87   C.G. da Silva, S. Grelier, F. Pichavant, E. Frollini, A. Castellan, *Industrial Crops and Products* **2013**, *42*, 87-95.

88   T. D. H. Bugg, R. Rahmanpour, *Current Opinion in Chemical Biology* **2015**, *29*, 10-17.

89   S. J. Richter, D. L. Brink, C. G. Diddams, O. Peter, US2434626 A, **1945**, *Process for making vanillin*.

90   a) J. D. P. Araújo, C. A .Grande, A. E. Rodrigues, *Chemical Engineering Research and Design* **2010**, *88*, 1024-1032; b) J. C. villar, A. Caperos, F. García-Ochoa, *Wood Science and Technology* **2001**, *35*, 245-255; c) E. A. Silva, M. Zabkova, J. D. Araújo, C. A. Cateto, M. F. Barreiro, M. N. Belgacem, A. E. Rodrigues, *Chemical Engineering Research and Design* **2009**, *87*, 1276-1292.

91   S. van den Bosch, W. Schutyser, B. F. Sels, *Abstracts of Papers, 250th ACS National Meeting & Exposition*, Boston, USA, **2015**, CATL-391.

92   F. P. Bouxin, A. McVeigh, F. Tran, N. J. Westwood, M. C. Jarvis, S. D. Jackson, *Green Chemistry* **2015**, *17(2)*, 1235-1242.

93   A. Gandini, *Green Chemistry* **2011**, *13*, 1061-1083.

94   Phenol Derivatives/Cyclopentadiene and Cyclopentene. *Ullmann's Encyclopedia of Industrial Chemistry* (Online Version) DOI: 10.1002/14356007.

95   http://www.matweb.com/search/datasheettext.aspx?matid=78164, [11-09-2015].

96   a) D. S. Argyropoulos, *Journal of Wood Chemistry and Technology* **1994**, *14(1)*, 45-63 and 65-82. b) A. Granata, D. S. Argyropoulos, *Journal of Agricultural and Food Chemistry* **1995**, *43*, 1538-1544.

97   M. Aruni DeSilva, N. Shanaiah, G. A. N. Gowda, K. Rosa-Pérez, B. A. Hanson, D. Raftery, *Magnetic Resonance in Chemistry* **2009**, *47*, 74-80.

98   D. J. Yelle, P. Kaparaju, C. G. Hunt, K. Hirth, H. Kim, J. Ralph, *Bioenergy Research* **2013**, *6*, 211-221.

99   H. L. Trajano, N. L. Engle, M. Foston, A. J. Ragauskas, T. J. Tschaplinski, C. E. Wyman, *Biotechnology and Biofuels* **2013**, *6*, 110.

100   R. Samuel, S. Cao, B. K. Das, F. Hu, Y. Pu, A. J. Ragauskas, *RCS Advances* **2013**, *3*, 5305-5309.

101   J. C. del Río, J. Rencoret, P. Prinsen, Á. T. Martínez, J. Ralph, A. Gutiérrez, *Journal of Agricultural and Food Chemistry* **2012**, *60*, 5922-5935.

102   J.-L. Wen, S.-L. Sun, B.-L. Xue, R.-C. Sun, *Holzforschung* **2013**, *67(6)*, 613-627.

103   F. Zikeli, T. Ters, K. Fackler, E. Srebotnik, J. Li, *Industrial Crops and Products* **2014**, *61*, 249-257.

104   C. Crestini, F. Melone, M. Sette, R. Saladino, *Biomacromolecules* **2011**, *12*, 3928-3935.

105   E. Adler, *Wood Science and Technology* **1977**, *11*, 169-218.

106   F. Lu, J. Ralph, *Journal of Agricultural and Food Chemistry* **1998**, *46*, 547-552.

107   G. Delmas, B. Benjelloun-Mlayah, Y. Le Bigot, M. Delmas, *Journal of Applied Polymer Science* **2011**, *121*, 491-501.

108   N. Henry, D. Harper, M. Dadmun, *Macromolecular Chemistry and Physics* **2012**, *213*, 1196-1205.

109   S. Sarkanen, D. C. Teller, J. Hall, J. L .McCarthy, *Macromolecules* **1981**, *14*, 426-434.

110   A. Tolbert, H. Akinosho, R. Khunsupat, A. K. Naskar, A. J. Ragauskas, *Biofuels, Bioproducts and Biorefining* **2014**, DOI: 10.1002/bbb.

111   H. L. Chum, D. K. Johnson, M. P. Tucker, M. E. Himmel, *Holzforschung* **1987**, *41(2)*, 97-108.

112   S. Baumberger, A. Abaecherli, M. Fasching, G. Gellerstedt, R. Gosselink, B. Hortling, J. Li, B. Saake, E. de Jong, *Holzforschung*, **2007**, *61*, 459-468.

113   H. Yoshida, R. Morck, K. P. Kringstad, H. Hatakeyama, *Holzforschung* **1987**, *41*, 171-176.

114   H. Hatakeyama, T. Hatakeyama, *Lignin and Lignans* **2010**, CRC Press, Boca Raton, 301-319.

115   W. J. J. Huijgen, G. Telysheva, A. Arshanitsa, R. J. A. Gosselink, P. J. de Wild, *Industrial Crops and Products* **2014**, *59*, 85-95.

116   W. Fang, M. Alekhina, O. Ershova, S. Heikkinen, H. Sixta, *Holzforschung* **2015**, *69(8)*, 943-950.

117   D. A. Baker, N. C. Gallego, F. S. Baker, *Journal of Applied Polymer Science* **2012**, *124*, 227-234.

118   A. L. Horvath, *Journal of Physical and Chemical Reference Data* **2006**, *35(1)*, 77-92.

119   a) R. Pucciariello, V. Villani, C. Bonini, M. D'Auria, T. Vetere, *Polymer* **2004**, *45(12)*, 4159-4169 ; b) A. V. Madhure, J. D. Ekhe, E. Deenadayalan, *Journal of Applied Polymer Science* **2012**, *125(3)*, 1701-1712.

120   A.-P. Zhang, L. Mei, Z.-Z. Zhao, J. Xie, C.-F. Liu, R.-C. Sun, *BioResources* **2013**, *8(3)*, 4288-4297.

121 a) A. P. Gifford, J. A. Westland, A. N. Neogi, K. D. Ragan, US2010/0152428, **2010**, *Low T$_g$ lignin mixed esters.*;
b) Y. Teramoto, S.-H. Lee, T. Endo, *Polymer Journal* **2009**, *41*, 219-227; c) S. Siegle, K. Linkersdörfer, A. Ritter,
DE10057910A1, **2002**, *Verfahren zur Derivatisierung und Veredelung von technischem Lignin, veredeltes
technisches Lignin und Verwendung des derivatisierten Lignins.*

122 P. Dournel, E. Randrianalimanana, A. Deffieux, M. Fontanille, *European Polymer Journal* **1988**, *24(9)*, 843-
847.

123 a) L. C.-F. Wu, W. G. Glasser, *Journal of Applied Polymer Science* **1984**, *29*, 1111-1123; b) C. A. Cateto, M. F.
Barreiro, A. E. Rodrigues, M. N. Belgacem, *Industrial & Engineering Chemistry Research* **2009**, *48*, 2583-2589.

124 H. Nadji, C. Bruzzèse, M. N. Belgacem, A. Benaboura, A. Gandini, *Macromolecular Materials and Engineering*
2005, *290*, 1009-1016.

125 W. G. Glasser, C. A. Barnett, T. G. Rials, V. P. Saraf, *Journal of Applied Polymer Science* **1984**, *29*, 1815-1830.

126 H. Sadeghifar, C. Cui, D. S. Argyropoulos, *Industrial & Engineering Chemistry Research* **2012**, *51*, 16713-
16720.

127 Y. Li, A. J. Ragauskas, *Journal of Wood Chemistry and Technology* **2012**, *32*, 210-224.

128 H. Hatakeyama, A. Hirogaki, H. Matsumura, T. Hatakeyama, *Journal of Thermal Analysis and Calorimetry*
2013, *114(3)*, 1075-1082.

129 Zhang, Y. Ma, C. Wang, S. Li, M. Zhang, F. Chu, *Industrial Crops and Products* **2013**, *43*, 326-333.

130 a) S. S. Kelley, T. C. Ward, T. G. Rials, W. G. Glasser, *Journal of Applied Polymer Science* **1989**, *37*, 2961-2971;
b) S. S. Kelley, W. G. Glasser, T. C. Ward, *ACS Symposium Series* **1989**, 402; c) W. de Oliveira, W. G. Glasser,
ACS Symposium Series **1989**, 414; d) A. Toffey, W. G. Glasser, *Holzforschung* **1997**, *51(1)*, 71-78; e) S. S.
Kelley, T. C. Ward, W. G. Glasser W.G, *Journal of Applied Polymer Science* **1990**, *41*, 2813-2828; f) S. S. Kelley,
W. G. Glasser, T. C. Ward, *Polymer* **1989**, *30*, 2265-2268.

131 S. P. Huo, M. C. Nie, Z. W. Kong, G. M. Wu, J. Chen *Journal of Applied Polymer Science* **2012**, *125*, 152-157.

132 J. Huang, L. Zhang, *Polymer* **2002**, *43*, 2287-2294.

133 G. F. D'Alelio, US 3984363, **1975**, *Polymerizable lignin derivatives.*

134 a) K. Hofman, W. G. Glasser, *Journal of Wood Chemistry and Technology* **1993**, *13*, 73-95; b) *Journal of
Adhesion* **1993**, *40*, 229-241; c) *Macromolecular Chemistry and Physics* **1994**, *195*, 65-80.

135 a) B. Zhao, G. Chen, Y. Liu, K. Hu, R. Wu, *Journal of Materials Science Letters* **2001**, *20*, 859-862; b) G. Sun, H.
Sun, Y. Liu, B. Zhao, N. Zhu, K. Hu, *Polymer* **2007**, *48*, 330-337.

136 a) A. Campanella, J. J. La Scala, R. P. Wool, *Journal of Applied Polymer Science* **2002**, *119*, 1000-1010 ; b) W.
Thielemans, R. P. Wool, *Composites: Part A* **2004**, *35*, 327-338.

137 Y. S. Kim, J. F. Kadla, *Biomacromolecules* **2010**, *11*, 981-988.

138 H. P. Naveau, *Cellulose Chemistry and Technology* **1975**, *9*, 71-77.

139 a) L. Hu, H. Pan, Y. Zhou, M. Zhang, *BioResources* **2011**, *6*, 3515-3525; b) Y. B. Mu, C. P. Wang, L. W. Zhao, F.
X. Chu, *Chemistry and Industry of Forest Products* **2009**, *29*, 38-42.

140 A. Effendi, H. Gerhauser, A. V. Bridgewater, *Renewable and Sustainable Energy Reviews* **2008**, *12*, 2092-
2116.

141 Y. Liu, K. Li, *Journal of Adhesion* **2006**, 593-605.

142 X. Yue, F. Chen, X. Zhou, *BioResources* **2011**, *6*, 2022-2034.

143 a) Y. Li, S. Sarkanen, *Macromolecules* **2002**, *35*, 9707-9715; b) Y. Li, S. Sarkanen, *Macromolecules* **2005**, *38*,
2296-2306.

144 G. Cazacu, M. C. Pascu, L. Profire, M. Mihaes, C. Vasile, *Industrial Crops Procducts* **2004**, *20*, 261-273.

145 I. E. Raschip, R. P. Dumitriu, G. Cazacu, C. Vasile, *Proceedings of the 7th ILI Forum*, ES **2005**, 167.

146 G. Cazacu, C. Vasile, G. E: Agafitei, M. C. Pascu, *Proceedings of the 7th ILI Forum*, ES **2005**, 171.

147 D. M. Fernandes, A. A. Winkler Hechenleitner, A. E. Job, E. Radovanocic, E. A. Gómez Pineda, *Polymer
Degradation and Stability* **2006**, *91*, 1192-1201.

148 A. Gandini, M. N. Belgacem, Z. X. Guo, S. Montanari, *Chemical modification, properties, and usage of lignin.*
New York: Springer Sciences **2002**, 57-80.

149 I. Gosh, R. K. Jain, W. G. Glasser, *ACS Symposium Series 742*, **2000**, 331-350.

150 R. Bhardwaj, A. K. Mohanty, *Journal of Biobased Materials and Bioenergy* **2007**, *1*, 191-209.

151 S. Laurichesse, L. Avérous, *Polymer* **2013**, *54(15)*, 3882-3890.

152 Y.-L. Chung, J. V. Olsson, R. J. Li, C. W. Frank, R. M. Waymouth, S. L. Billington, E. S. Sattely, *ACS Sustainable
Chemical Engineering* **2013**, *1*, 1231-1238.

153 S. Xiao, J. Feng, J. Zhu, X. Wang, C. Yi, S. Su, *Journal of Applied Polymer Science* **2013**, *130*, 1308-1312.

154 P. Frigerio, L. Zoia, M. Orlandi, T. Hanel, L. Castellani, *Bioresources* **2014**, *9*, 1387-1400.

155 W. He, P. Fatehi, *RSC Advances* **2015**, *5*, 47031-47039.

156 M. Thunga, K. Chen, M. R. Kessler, US20140099505 A1, **2012**, *Compositions including esterified lignin and
poly(lactid acid) and carbon fibers produced therefrom.*

157 S. Chatterjee, A. Clingenpeel, A. McKenna, O. Rios, A. Johs, *RSC Advances* **2014**, *4*, 4743-4753.

158 I. E. Raschip, E. G. Hitruc, C. Vasile, *High Perfomance Polymers* **2011**, *23*, 219-229.

159 H. M. Caceido, L. A. Dempere, W. Vermerris, *Nanotechnology* **2012**, *23*, 105605/1-105605/12.

160 G. Socrates, *Infrared Characteristics Group Frequencies: Tables and Charts, Second Edition.* ©John Wiley & Sons Ltd., **1994**.

161 R. Sun, X. F. Sun, *Industrial Crops and Products* **2002**, *16(3)*, 225-235.

162 J. Hafrén, A. Córdova, *Macromolecular Rapid Communications* **2005**, *26*, 82-86.

163 S. M. Guillaume, *European Polymer Journal* **2013**, *49*, 768-779.

164 M. A. Rahman, C. De Santis, G. Spagnoli, G. Ramorino, M. Penco, V. T. Phuong, A. Lazzeri, *Journal of Applied Polymer Science* **2013**, *129(1)*, 202-214, DOI: 10.1002/APP.38705.

165 R. C. Pratt, B. G. Lohmeijer, D. A. Long, R. M. Waymouth, J. L. Hedrick, *Journal of the American Chemical Society* **2006**, *128(14)*, 4556-4557.

166 C. Thomas, F. Peruch, A. Deffieux, A. Milet, J.-P. Desvergne, B. Bibal, *Advanced Synthesis and Catalysis* **2011**, *353(7)*, 1049-1057.

167 A. Carlmark, E. Larsson, E. Malmström, *European Polymer Journal* **2012**, *48*, 1646-1659.

168 Y. Teramoto, S. Ama, T. Higeshiro, Y. Nishio, *Macromolecular Chemistry and Physics* **2004**, *205*, 1904-1915.

169 H. Lönnberg, L. Fogelström, M. A. S. Azizi Samir, L. Berglund, *European Polymer Journal* **2008**, *44*, 2991-2997.

170 W. de Oliveira, W. G. Glasser, *Macromolecules* **1994**, *27(1)*, 5-11.

171 C. G. Jaffredo, J.-F. Carpentier, S. M. Guillaume, *Macromolecular Rapid Communications* **2012**, *33*, 1938-1944.

172 P. Mousavioun, G. A. George, W. O. S. Doherty, *Polymer Degradation and Stability* **2012**, *97*, 1114-1122.

173 I. Cota, F. Medina, J. E. Sueiras, D. Tichit, *Tetrahedron Letters* **2011**, *52*, 385-387.

174 A. P. Dove, *ACS Macro Letters* **2012**, *1*, 1409-1412.

175 R Samuel, S. Cao, B. K. Das, F. Hu, Y. Pu A. J. Ragauskas, *RSC Advances* **2013**, *3(16)*, 5303-5309.

176 I. Cota, F. Medina, J. E. Sueiras, D. Tichit, *Tetrahedron Letters* **2011**, *52*, 385-387.

177 C. Slugovc, S. Strasser, EP2711396, **2012**; *Preparation of copolymerizable lignin derivatives for preparing plastic like fabrics.*

178 P. H. Henna, M. R. Kessler, R. C. Larock, *Macromolecular Materials and Engineering* **2008**, *293*, 979-990.

179 B. Pan, Y. Cheng, Y. Wang, Y. Feng, W. Ye, Y. Tian, X. Wang, *Polymer-Plastics Technology and Engineering* **2013**, *52*, 586-591.

180 F. Hu, J. Du, Y. Zheng, *Polymer Composites* **2014**, *35(10)*, 1918-1925.

181 a) R. Pucciariello, V. Villani, C. Bonini, M. D'Auria, T. Vetere, *Polymer* **2004**, *45*, 4159-4169; b) P. Alexy, B. Kosikova, G. Podstranka, *Polymer* **2000**, *41*, 4901-4908.

182 I. C. Hoeger, I. Filpponen, R. Martin-Sampedro, L.-S. Johansson, M. Österberg, J. Laine, S. Kelley, O. J. Rojas, *Biomacromolecules* **2012**, *13*, 3228-3240.

183 E. Kontturi, P. C. Thüne, J. W. Niemantsverdriet, *Langmuir* **2003**, *19*, 5735-5741.

184 a) H. M. A. Ehmann, O. Werzer, S. Pachmajer, T. Mohan, H. Amenitsch, R. Resel, A. Kornherr, K. Stana-Kleinschek, E. Kontturi, S. Spirk, *ACS Macro Letters* **2015**, *4*, 713-717; b) T. Mohan, S. Spirk, R. Kargl, A. Doliska, A. Vesel, I. Salzmann, R. Resel, V. Ribitsch, K. Stana-Kleinschek, *Soft Matter* **2012**, *8*, 9807-9815.

185 T. Mohan, R. Kargl, A. Doliska, A. Vesel, S. Koestler, V. Ribitsch, K. Stana-Kleinschek, *Journal of Colloid and Interface Science* **2011**, *358*, 604-610.

186 a) C. Salas, O. J. Rojas, L. A. Lucia, M. A. Hubbe, J. Genzer, *ACS Applied Materials & Interfaces* **2013**, *5(1)*, 199-206; b) R. Martín-Sampedro, J. L. Rahikainen, L.-S. Johansson, K. Marjamaa, J. Laine, K. Kruus, O. J. Rojas, *Biomacromolecules* **2013**, *14(4)*, 1231-1239; c) B. Yang, C. E. Wyman, *Biotechnology and Bioengineering*, **2006**, *94(4)*, 611-617; d) T. Mohan, K. Niegelhell, C. Zarth, R. Kargl, S. Köstler, V. Ribitsch, T. Heinze, S. Spirk, K. Stana-Kleinschek, *Biomacromolecules* **2014**, *15(11)*, 3931-3941; e) H. Orelma, I. Filpponen, L.-S. Johansson, J. Laine, O. J. Rojas, *Biomacromolecules* **2011**, *12(12)*, 4311-4318.

187 G. Sauerbrey, *Zeitschrift für Physik* **1959**, *155*, 206-222.

188 D. R. Kodali, US 6 420 322, **2002**, *Process for modifying unsaturated triacylglycerol oils: resulting products and uses thereof.*

189 P. H. Henna, R. C. Larock, *Macromolecular Materials and Engineering* **2007**, *292*, 1201-1209.

190 Y. Xia, Y. Lu, R. C. Larock, *Polymer* **2010**, *51(1)*, 53-61.

191 T. Tokoroyama, *European Journal of Organic Chemistry* **2010**, *10*, 2009-2016.

192 T. W. Schultz, J. W. Yarbrough, R. S. Hunter, A. O. Aptula, *Chemical Research in Toxicology* **2007**, *20*, 1359-1363.

193 A. V. Salin, A. R. Fatkhutdinov, A. V. Il'in, V. I. Galkin, F. G. Shamsutdinova, *Heteroatom Chemistry* **2014**, *25(3)*, 205-2016.

194 H. C. Kolb, M. G. Finn, K. B. Sharpless, *Angewandte Chemie International Edition* **2001**, *40(11)*, 2004-2021.

195 Y. Yu, Y. Chau, *Biomacromolecules* **2012**, *13*, 937-942.

196 F. Wang, H. Yang, H. Fu, Z. Pei, *Chemical Communications* **2013**, *49*, 517-519.

197 S. Senapati, S. Manna, S. Lindsay, P. Zhang, *Langmuir* **2013**, *29*, 14622-14630.

198 a) V. Rai, I. N. N. Namboothiri, *European Journal of Organic Chemistry* **2006**, *20*, 4693-4703; b) O. M. Berner, L. Tedeschi, D. Enders, *European Journal of Organic Chemistry* **2002**, *12*, 1877-1894.

199 S. Yamazaki, *Journal of Synthetic Organic Chemistry Japan* **2014**, *72(6)*, 666-679.
200 M. Shimizu, I. Hachiya, I. Mizota, *Chemical Communications* **2009**, *8*, 874-889.
201 S. Sulzer-Mossé, A. Alexakis, J. Mareda, G. Bollot, G. Bernardinelli, Y. Filinchuk, *European Journal of Chemistry* **2009**, *15(13)*, 3204-3220.
202 T. Janecki, J. Kedzia, T. Wasek, *Synthesis-Stuttgart* **2009**, *8*, 1227-1254.
203 F. F. Fleming, Q. Z. Wang, *Chemical Reviews* **2003**, *103(5)*, 2035-2077.
204 F. Wang, H. Yang, H. Fu, Z. Pei*, Chemical Communications* **2013**, *49*, 517.
205 D. Bhuniya, S. Mohan, S. Narayanan, *Synthesis* **2003**, *7*, 1018-1024.
206 D. Enders, K. Luettgen, A. A. Narine, *Synthesis Stuttgart* **2007**, *7*, 959-980.
207 M. Sánchez-Roselló, J. L. Aceña, A. Simón-Fuentes, C. del Pozo, *Chemical Society Reviews* **2014**, *43(21)*, 7430-7453.
208 C. F. Nising, S. Bräse, *Chemical Society Reviews* **2012**, *41*, 988-999.
209 K. Imai, T. Shiomi, Y. Tezuka, T. Tsukahara, *Polymer Journal* **1991**, *23(9)*, 1105-1109.
210 a) O. A. Stamm, *Helvetica Chimica Acta* **1963**, *46*, 3008-3019; b) S. P. Rowland, M. A. F. Brannan, *Journal of Applied   Polymer Science* **1970**, *14*, 441-452.
211 R. N. Ring, G. C. Tesoro, D. R. Moore, *Journal of Organic Chemistry* **1967**, *32(4)*, 1091-1094.
212 G. B. Cserép, Z. Baranyai, D. Komáromy, K. Horváti, S. Bősze, P. Kele, *Tetrahedron* **2014**, *70*, 5961-5965.
213 L. Wang, D. Menche, *Journal of Organic Chemistry* **2012**, *77(23)*, 10811-10823.
214 J. P. Schroeder, D. C. Schroeder, S. Jotikasthira, *Journal of Polymer Science Part A: Polymer Chemistry* **1972**, *10*, 2189-2195.
215 a) A. Sannino, M. Madaghiele, F. Conversano, G. Mele, A. Maffezzoli, P. A. Netti, L. Ambrosio, L. Nicolais, *Biomacromolecules* **2004**, *5*, 92-96; b) J.-Y. Lai, *Carbohydrate Polymers* **2014**, *101*, 203-212.
216 W. Xi, C. Wang, C. J. Kloxin, C. N. Bowman, *ACS Macro Letters* **2012**, *1*, 811-814.
217 H.-L. Liu, H.-F. Jiang, Y.-G. Wang, *Chinese Journal of Chemistry* **2007**, *25(7)*, 1023-1026.
218 S. Matsuoka, S. Namera, M. Suzuki, *Polymer Chemistry* **2014**, DOI: 10.1039/c4py01184h.
219 M. Hans, L. Delaude, J. Rodriguez, Y. Coquerel, *Journal of Organic Chemistry* **2014**, *79*, 2758-2764.
220 C. E. Hoyle, C. N. Bowman, *Angewandte Chemie International Edition* **2010**, *49*, 1540-1573.
221 S. Chatani, R. J. Sheridan, M. Podgórski, D. P. Nair, C. N. Bowman, *Chemistry of Materials* **2013**, *25*, 3897-3901.
222 S. Chatani, D. P. Nair, C. N. Bowman, *Polymer Chemistry* **2013**, *4*, 1048-1055.
223 I. C. Stewart, R. G. Bergman, F. D. Toste, *Journal of the American Chemical Society* **2003**, *125*, 8696-8697.
224 S. Chatani, T. Gong, B. A. Earle, M. Podgórski, C. N. Bowman, *ACS Macro Letters* **2014**, *3*, 315-318.
225 M. Podgórski, S. Chatani, C. N. Bowman, *Macromolecular Rapid Communications* **2014**, DOI: 10.1002/marc.201400260.
226 Y.-M. Jeon, T.-H. Lim, S.-H. Kim, J.-G. Kim, M.-S. Gong, *Macromolecular Research* **2007**, *15(1)*, 17-21.
227 S. Strasser, C. Slugovc, *Catalysis Science & Technology* **2015**, DOI: 10.1039/c5cy01527h.
228 a) I. Ugur, A. Marion, S. Parant, J. H. Jensen, G. Monard, *Journal of Chemical Information and Modeling* **2014**, *54*, 2200-2213; b) S. Takahashi, L. A. Cohen, H. K. Miller, E. G. Peake, *Journal of Organic Chemistry* **1971**, *36*, 1205-1209.
229 C. Lindner, R. Tandon, B. Maryasin, E. Larionov, H. Zipse, *Beilstein Journal of Organic Chemistry* **2012**, *8*, 1406-1442.
230 Y. C. Fan, O. Kwon, *Chemical Communications* **2013**, *49*, 11588-11619.
231 a) J. W. Chan, C. E. Hoyle, A. B. Lowe, M. Bowman, *Macromolecules* **2010**, *43*, 6381-6388; b) C. Wang, C. Qi, *Tetrahedron* **2013**, *69*, 5348-5354.
232 A. V. Salin, A. R. Faktkhutdinov, A. V. Il'in, V. I. Galkin, F. G. Shamsutdinova, *Heteroatom Chemistry* **2014**, *25*, 205-216.
233 T. A. Albright, W. J. Freeman, E. E. Schweizer, *Journal of the American Chemical Society* **1975**, *97*, 2942-2946.
234 M. V. Roux, M. Temprado, P. Jiménez, R. Notario, R. Guzmán-Mejía, E. Juaristi, *Journal of Organic Chemistry* **2007**, *72(4)*, 1143-1147.
235 N. A. Chernysheva, N. K. Gusarova, A. A. Tatarinova, M. L. Al'pert, B. A. Trofimov, *Zhurnal Organicheskoi Khimii* **1996**, *32(6)*, 832-835.
236 R. K. Harris, E. D. Becker, S. M. Cabral de Menezes, P. Granger, R. E. Hoffman, K. W. Zilm, *Pure and Applied Chemistry* **2008**, *80*, 59-84.